

**LOW VOC COATING SYSTEMS FROM NOVEL GLYCIDYL
CARBAMATE RESINS**

A Dissertation
Submitted to the Graduate Faculty
of the
North Dakota State University
of Agriculture and Applied Science

By

Umesh Deepak Harkal

In Partial Fulfillment of the Requirements
for the Degree of
DOCTOR OF PHILOSOPHY

Major Department:
Coatings and Polymeric Materials

September 2010

Fargo, North Dakota

North Dakota State University
Graduate School

Title

Low VOC coating systems from novel

glycidyl carbamate resins

By

Umesh Harkal

The Supervisory Committee certifies that this *disquisition* complies with North Dakota State University's regulations and meets the accepted standards for the degree of

DOCTOR OF PHILOSOPHY

North Dakota State University Libraries Addendum

To protect the privacy of individuals associated with the document, signatures have been removed from the digital version of this document.

ABSTRACT

Harkal, Umesh Deepak, Ph.D., Department of Coatings and Polymeric Materials, College of Science and Mathematics, North Dakota State University, September 2010. Low VOC Coating Systems From Novel Glycidyl Carbamate Resins. Major Professor: Dr. Dean C. Webster.

The goal of the research presented in this dissertation was to design and synthesize novel glycidyl carbamate (GC) resins for low VOC applications and study the structure property relationships of their coatings. Primarily GC resins are synthesized using aliphatic polyisocyanate resins such as biuret and isocyanurate of hexamethylene diisocyanate. Polyisocyanate based GC resins had extremely high viscosity. Biuret glycidyl carbamate (BGC) resin was modified by replacing part of the glycidol with alcohols. The alcohol composition and the extent of alcohol composition in the resin were systematically varied. The alcohol modification reduced the resin viscosity dramatically. Performance of amine and self-crosslinked GC coatings was studied.

GC resins were synthesized for binder systems for flexible primer applications using diisocyanates and combinations of linear diols and a triol. The diisocyanates, diols and triol were used to obtain GC resins. Flexibility and barrier properties of the amine crosslinked coatings were influenced by the composition of the GC resins.

Water dispersible GC resins were synthesized for low or zero VOC waterborne coating applications. Non-ionic hydrophilic group, methoxy poly(ethylene glycol) (mPEG), was incorporated into the resin structure. Molecular weight and mol % of mPEG in the resin was systematically varied. Waterborne GC coatings were prepared using water-based amine crosslinker and properties of the cured coatings were studied.

UV curable GC resins were made by reacting BGC, isocyanurate glycidyl carbamate (IGC), and alcohol modified IGC resins with acrylic acid. UV curable coating formulations were prepared using reactive diluents, a photoinitiator, and an amine co-initiator. Real-time FTIR (RTIR) was used to determine the degree of double bond conversion in UV curing. The performance of the UV cured coatings was studied.

Finally, air drying (autoxidizable) GC resin (BGC-LOFA) was obtained by reacting BGC resin with linseed oil fatty acid (LOFA). Air drying GC coatings were obtained using common driers used for alkyd-based coatings.

ACKNOWLEDGEMENTS

I take this opportunity to thank all the people who helped me to achieve this goal.

Dr. Dean C. Webster, for your guidance, support, and patience through the program; I am extremely fortunate to have a mentor like you. While working with you I got the opportunities and inspirations not only to explore the science but also to expand my capabilities. This experience will always give energy to me to continue the journey ahead. My committee members, Dr. Stuart Croll, Dr. Richard Roesler, Dr. Sanku Mallik, and Dr. Robert Littlefield for fruitful discussion and constructive criticism. I believe it will contribute to my growth as a scientist.

I would like to thank Andrew J. Muehlberg (AJ) for his great help to carry out many tasks such as resin synthesis, coating formulations, and numerous tests to get the job done. I am grateful to Heidi Docktor for her assistance in instrumentation and characterization required to accomplish this research. I am thankful to Dr. Bierwagen for his input on characterization of the coatings by electrochemical technique. I am also thankful to Vinod for his help to carry out EIS experiments and discussion to interpret the results. I would like to thank Partha Majumdar for his discussion on DryAdd software.

I would like to thank Carol, Jaci, and Kathy for making the place pleasant to work in every possible way. My thanks go to Neena for suggestions, Abdullah for cracking jokes around, Alex for sharing books, Ankit for many rides, Abhijit for being a good team member, and Stacy for delicious cookies and trip to Wisconsin. I would also like to thank my college friends; Yogesh for New York trip and Sudhir for sharing his experience. I am very thankful to all the Webster group members, former and present for being very cooperative; you are great and fun to work with. Thank you all.

DEDICATION

I would like to dedicate this dissertation to my parents, Mr. Deepak R. Harkal and Mrs. Sharayu D. Harkal, to my three sisters; Sonal, Shital, and Priyanka, and to my wife Ritu. Without your support, encouragement, patience, and faith, it was impossible for me to achieve this goal.

TABLE OF CONTENTS

ABSTRACT	iii
ACKNOWLEDGEMENTS	v
DEDICATION	vi
LIST OF TABLES	xiv
LIST OF FIGURES	xvi
CHAPTER 1. GENERAL INTRODUCTION	1
1.1. Introduction.....	1
1.2. Polyurethanes.....	3
1.3. Epoxies.....	8
1.4. Glycidyl carbamate (GC) resins.....	10
1.5. Environmentally friendly low or zero VOC coatings.....	14
1.5.1. Low viscosity resins.....	15
1.5.2. Water dispersible resins.....	17
1.6. Binder systems for highly flexible coatings.....	21
1.7. UV-curable coatings.....	23
1.8. Air-drying coatings.....	26
1.9. Objective.....	29
1.10. References.....	31
CHAPTER 2. STRUCTURAL MODIFICATION OF GLYCIDYL CARBAMATE RESINS	43
2.1. Introduction.....	43
2.2. Experimental.....	45

2.2.1. Materials.....	45
2.2.2. Synthesis of glycidyl carbamate functional compounds.....	46
2.2.3. FTIR measurements.....	47
2.2.4. NMR characterization.....	47
2.2.5. Gel permeation chromatography.....	47
2.2.6. Viscosity measurements.....	48
2.2.7. Epoxy titration.....	48
2.2.8. Coating preparation.....	48
2.2.9. Coating performance.....	50
2.2.10. Differential scanning calorimetry (DSC).....	50
2.2.11. Thermogravimetric analysis (TGA).....	51
2.2.12. Dynamic mechanical analysis (DMA).....	51
2.2.13. Tensile test.....	51
2.2.14. Electrochemical impedance spectroscopy (EIS).....	51
2.2.15. Salt spray test (ASTM B 117).....	53
2.3. Results and discussion.....	53
2.3.1. Modified GC resins and their coating performance.....	53
2.3.2. BGC-EP resin series and their coating performance.....	64
2.3.3. Thermal Stability of modified GC coatings.....	73
2.3.4. Electrochemical impedance spectroscopy (EIS).....	75
2.3.5 Salt spray test.....	80
2.4. Conclusions.....	81
2.5. References.....	83

CHAPTER 3. GLYCIDYL CARBAMATE RESIN SYSTEMS FOR HIGHLY

FLEXIBLE COATINGS	89
3.1. Introduction.....	89
3.2. Experimental.....	91
3.2.1. Materials.....	91
3.2.2. Synthesis of glycidyl carbamate functional resins for flexible coating applications.....	92
3.2.3. NCO titration.....	94
3.2.4. FTIR measurements.....	94
3.2.5. Epoxy titration.....	94
3.2.6. Determination of % solids.....	95
3.2.7. Coating preparation.....	95
3.2.8. Coating performance.....	97
3.2.9. Differential scanning calorimetry (DSC).....	97
3.2.10. Thermogravimetric analysis (TGA).....	98
3.2.11. Dynamic mechanical analysis (DMA).....	98
3.2.12. Tensile test.....	98
3.2.13. Electrochemical impedance spectroscopy (EIS).....	98
3.2.14. Salt spray test (ASTM B 117).....	100
3.3. Results and discussion.....	100
3.3.1. Synthesis of GC resins based on diisocyanates and diols.....	100
3.3.2. Performance of highly flexible GC coatings.....	102
3.4. Conclusions.....	120

3.5. References.....	121
----------------------	-----

CHAPTER 4. WATER DISPERSIBLE GLYCIDYL CARBAMATE

RESINS.....	127
4.1. Introduction.....	127
4.2. Experimental.....	130
4.2.1. Materials.....	130
4.2.2. Synthesis of mPEG-modified GC resins.....	130
4.2.3. FTIR measurements.....	131
4.2.4. NMR characterization.....	132
4.2.5. Epoxy titration.....	132
4.2.6. Particle size analysis.....	132
4.2.7. Coating formulation preparation.....	133
4.2.8. Coating performance.....	134
4.2.9. Differential scanning calorimetry (DSC).....	136
4.2.10. Thermogravimetric analysis (TGA).....	136
4.2.11. Dynamic mechanical analysis (DMA).....	136
4.2.12. Atomic Force Microscope (AFM).....	137
4.2.13. Barrier properties and corrosion resistance.....	137
4.3. Results and discussion.....	138
4.3.1. Synthesis of water dispersible GC resins.....	138
4.3.2. Dispersion stability.....	141
4.3.3. Coating formulations.....	144
4.3.4. Water and solvent resistance.....	145

4.3.5. Water contact angle.....	147
4.3.6. Other coating properties.....	148
4.3.7. Further analysis of the coating properties.....	150
4.3.8. Thermal stability.....	151
4.3.9. Barrier properties by EIS analysis.....	151
4.3.10. Salt spray test.....	156
4.4. Conclusions.....	156
4.5. References.....	157

CHAPTER 5. UV CURABLE GLYCIDYL CARBAMATE

RESINS.....	161
5.1. Introduction.....	161
5.2. Experimental.....	162
5.2.1. Materials.....	162
5.2.2. Synthesis of acrylated glycidyl carbamate resin.....	163
5.2.3. FTIR measurements.....	166
5.2.4. Epoxy titration.....	166
5.2.5. Acid value titration.....	167
5.2.6. Viscosity determination.....	167
5.2.7. UV curable formulation and coating preparation.....	167
5.2.8. Performance of coatings.....	169
5.2.9. Kinetic experiments using real-time FTIR (RTIR).....	170
5.2.10. Differential scanning calorimetry (DSC).....	170
5.2.11. Dynamic mechanical analysis (DMA).....	171

5.2.12. Tensile test.....	171
5.2.13. Thermogravimetric analysis (TGA).....	171
5.3. Results and discussion.....	172
5.3.1. Synthesis of acrylated GC resins.....	172
5.3.2. Viscosity of acrylated GC resins.....	174
5.3.3. Degree of conversion in UV curing.....	175
5.3.4. Coating properties.....	176
5.3.5. Thermal stability.....	180
5.4. Conclusions.....	180
5.5. References.....	181

CHAPTER 6. AIR DRYING GLYCIDYL CARBAMATE RESIN AND

COATINGS.....	185
6.1. Introduction.....	185
6.2. Experimental.....	186
6.2.1. Materials.....	186
6.2.2. Synthesis of air drying GC resin.....	187
6.2.3. FTIR measurements.....	189
6.2.4. Epoxy titration.....	189
6.2.5. Acid value titration.....	189
6.2.6. NMR characterization.....	190
6.2.7. Air drying coating formulations.....	190
6.2.8. Study of coating performance.....	191
6.2.9. Differential scanning calorimetry (DSC).....	192

6.2.10. Thermogravimetric analysis (TGA).....	192
6.3. Results and discussion.....	192
6.3.1. Synthesis of air drying GC resin.....	192
6.3.2. Performance of the coatings.....	193
6.3.3. Thermal stability.....	195
6.4. Conclusions.....	195
6.5. References.....	196
OVERALL CONCLUSIONS.....	199
FUTURE WORK.....	202

LIST OF TABLES

<u>Table</u>	<u>Page</u>
1.1. Composition of HDI isocyanurate polyisocyanates.....	5
2.1. Chemical structures of the materials used for the modification of GC resins and the epoxy equivalent weight (EEW) of the GC resins synthesized.....	55
2.2. Properties of BGC and modified GC coatings.....	63
2.3. Properties of the BGC-EP series coatings.....	72
2.4. Elongation at break and Young's modulus.....	73
3.1. Recipes for the synthesis of GC resins for flexible coating applications.....	103
3.2. Performance of PACM crosslinked GC coatings in screening study.....	104
3.3. Properties of highly flexible GC coatings.....	106
3.4. Wt.% non-polar hydrocarbon.....	114
3.5. % Decrease in T_g after wet condition.....	116
4.1. GC resins synthesized.....	139
4.2. Weight and number distribution of hydrophobic and hydrophilic molecules in the GC resin.....	141
4.3. Dispersion stability of GC resins.....	143
4.4. Coating formulations of the GC resins.....	145
4.5. Water and solvent resistance of the coatings.....	146
4.6. Performance of waterborne GC coatings.....	150
4.7. Tensile tes of the screened coatings.....	151
4.8. Extent of ether groups in the resin compositions.....	155
5.1. Recipe for the synthesis of acrylated GC resins.....	164
5.2. Recipe for UV curable coating formulation.....	168

5.3. UV-lamp intensity used for curing.....	169
5.4. RTIR UV-lamp intensity.....	170
5.5. Viscosity of acrylated GC resins.....	175
5.6. Degree of conversion of the acrylate double bonds in the UV cured coatings.....	176
5.7. Properties of the UV cured GC coatings.....	179
6.1. Recipe for the synthesis of air drying GC resin.....	190
6.2. Air drying coating formulations.....	191
6.3. Coating properties after two weeks of air drying.....	194
6.4. Hardness development in air drying GC-LOFA coatings.....	194
6.5. Hardness development in air drying UROTUF F48-M50 coatings.....	195
6.6. Hardness development in air drying UROTUF F77-M60 coatings.....	195

LIST OF FIGURES

<u>Figure</u>	<u>Page</u>
1.1. Schematic representation of the reaction of isocyanate with alcohol to obtain urethane.....	3
1.2. Schematic representation of the structures of isocyanurates, biurets, allophanates, and uretdiones.....	4
1.3. Schematic representation of the major higher oligomers present in HDI isocyanurate resins.....	5
1.4. Schematic representation of the types of hydrogen bonds.....	7
1.5. Schematic representation of the structures of epoxy resins and compounds.....	9
1.6. Schematic representation of the epoxy-amine reaction.....	10
1.7. Schematic representation of the synthesis of BGC resin.....	11
1.8. Schematic representation of the synthesis of IGC.....	12
1.9. Schematic representation of formation of crosslinked network in amine crosslinked GC coatings.....	12
1.10. Schematic representation of symmetric and asymmetric trimer.....	16
1.11. Schematic representation of generation 1, 2, and 3 water dispersible polyisocyanates.....	19
1.12. Schematic representation of a typical coating system for aircraft application.....	21
1.13. Illustration of the coating failure around riveted and joint area.....	22
1.14. Schematic representation of the formation of crosslinked network in acrylate based UV-cured coatings.....	24
1.15. Schematic representation of the formation of crosslinked network in air-drying (autoxidation) process.....	27
2.1. Schematic representation of EIS experiment performed using the conventional three-electrode system.....	52

2.2. Schematic representation of the synthesis of GC resins.....	53
2.3. Schematic representation of the synthesis of modified GC resins.....	54
2.4. FTIR spectra of BGC and modified GC resins.....	56
2.5. GPC Chromatograms for HDB-LV and BGC-EP resin.....	56
2.6. ¹³ C NMR spectra of BGC and modified GC resin, BGC-1BuOH.....	57
2.7. Structures of BGC, BGC-1BuOH and BGC-DB.....	58
2.8. Property trends for control BGC resin and alcohol modified GC resins and coatings. (a) Resin viscosities (neat resins), (b) Glass transition temperature (T _g), (c) König pendulum hardness, (d) Reverse impact strength of the coatings.....	59
2.9. Effect of the structural composition of EP on viscosity of the BGC-EP series resins (neat resins).....	65
2.10. Storage modulus (<i>E'</i>) and tan δ curves for the coatings crosslinked by (a) PACM and (b) A-2353.....	67
2.11. Property trends of control and EP-modified coatings as a function of EP content. (a) Crosslink density, (b) DSC T _g , (c) König pendulum hardness, (d) Reverse impact strength.....	68
2.12. TGA of the BGC and modified GC coatings crosslinked with PACM.....	73
2.13. TGA of the BGC and modified GC coatings crosslinked with A-2353.....	74
2.14. TGA of the BGC-EP series coatings crosslinked with PACM.....	75
2.15. TGA of the BGC-EP series coatings crosslinked with A-2353.....	75
2.16. Modulus Bode plot after (a) 2.5 hrs and (b) seven days for BGC, BGC-2EHA, BGC-EP, BGC-EP 15%, and BGC-DB coatings.....	78
2.17. Capacitance of BGC, BGC-2EHA, BGC-DB, BGC-EP 15%, and BGC-EP 33% coatings after seven days of immersion.....	78
2.18. Salt spray of BGC, BGC-2EHA, BGC-DB, BGC-EP 15%, and BGC-EP after 312 hours.....	80
3.1. Schematic representation of EIS experiment performed using the conventional three-electrode system.....	99

3.2. Schematic representation of the synthesis of GC resins using diisocyanate, diol, and glycidol.....	100
3.3. Structures of the diisocyanates, diols, triol, and glycidol used in the synthesis of various GC resins. Figure 3.4. Stress vs. strain plots for coatings F1, F2, F3, L1, and L2.....	101
3.4. Stress vs. strain plots for coatings F1, F2, F3, L1, and L2.....	107
3.5. (a) Storage modulus and (b) $\tan \delta$ curves for coatings F1, F2, F3, L1, L2, and L3.....	109
3.6. TGA of coatings F1, F2, F3, L1, L2, and L3.....	110
3.7. Bode plot of coatings L1, L2, and L3 steel substrate after (a) 2.5 hrs, and (b) 7 days of immersion.....	112
3.8. Capacitance of L1, L2, and L3 coatings after seven days of immersion.....	113
3.9. DSC first cycle for dry and wet coatings L1, L2, and L3.....	115
3.10. TGA of dry and wet samples of coatings L1, L2, and L3.....	116
3.11. Bode plot for coatings L1, L2, and L3 on aluminum substrate after (a) 2.5 hrs of and (b) seven days of immersion.....	117
3.12. Capacitance of L1, L2, and L3 coatings on aluminum substrate after seven days of immersion.....	118
3.13. Pictures of L1, L2, and L3 coatings on steel and aluminum substrates after 240 hrs of salt spray.....	119
4.1. Schematic representation of the synthesis of water dispersible GC resins.....	139
4.2. ¹³ C NMR spectrum of resin R1.....	140
4.3. Major (a) hydrophobic GC molecule and (b) hydrophilic GC molecule in the hydrophilic of GC resin.....	141
4.4. Schematic representation of a GC resin particle dispersed in water.....	144
4.5. Schematic representation of making a waterborne GC coating formulation.....	145
4.6. Water contact angle of the GC coatings.....	147

4.7. AFM images and reflection image of the waterborne GC coatings.....	149
4.8. (a) Storage modulus and (b) $\tan \delta$ curves of coatings F1, F2, F4, and F10 (control).....	152
4.9. TGA of coatings F1, F2, F4, and F10.....	153
4.10. Bode plot of the coatings on steel substrate after 2.5 hrs of immersion.....	153
4.11. Bode plots of the coatings on aluminum substrate after (a) 2.5 hrs and (b) seven days.....	154
4.12. Capacitance of the coatings on aluminum substrate after seven days of immersion.....	155
4.13. Salt spray on the coatings on aluminum substrate for ten days.....	156
5.1. Reactive diluents and photoinitiator used.....	168
5.2. Schematic representation of the synthesis of (a) ABGC, (b) AIGC, and (c) AIGC-EP 33%.....	173
5.3. FTIR spectra for the GC resins and the acrylated GC resins.....	174
5.4. Degree of conversion of the acrylate double bonds determined using RTIR.....	176
5.5. (a) Storage modulus and (b) $\tan \delta$ curves for coatings ABGC, AIGC, AIGC-EP 15%, AIGC-EP 33%, and CN929.....	178
5.6. TGA of coatings ABGC, AIGC, AIGC-EP 15%, AIGC-EP 33%, and CN929 in nitrogen atmosphere.....	180
6.1. Schematic representation of the synthesis of GC-LOFA.....	188
6.2. ^{13}C NMR spectra of the GC-LOFA resin.....	193
6.3. TGA of GC-LOFA coatings in nitrogen atmosphere.....	196
6.4. TGA of control coatings in nitrogen atmosphere.....	196

CHAPTER 1. GENERAL INTRODUCTION

1.1. Introduction

Many objects around us are coated for any one or more of three purposes: surface protection, decoration, and/or surface functionalization for specialty applications.^{1, 2} Organic coatings are complex materials composed of resins, volatile components, pigments and additives. The resins used in coating applications are often called binders. The resins or binders are natural materials, synthetic materials or polymers capable of forming a continuous film on a surface, adhering to surface, and binding together the other constituents of the coating. Resin is a major component of coatings and to a large extent, governs the properties of coating films. The volatile components are solvents used to make coating compositions fluid enough for application purpose. The volatile components evaporate during and after coating application and the binder turns to a solid continuous film due to chemical reaction (thermosetting resins) or as a consequence of solvent evaporation from high molecular weight polymers (thermoplastic resins) or due to coalescence between resin particles dispersed in water (latex). Pigments are finally divided insoluble inorganic or organic particles and are dispersed and stabilized in coating formulations. The pigments offer appearance, corrosion resistant or other specialty effects to coating films. Non-pigmented coatings are known as clear coatings. Additives such as flow aids, stabilizers, catalysts, etc. are generally used in small quantities to modify coating properties.¹⁻⁵

Solid coating films formed due to chemical reactions, known as crosslinking reactions, have good chemical resistance, thermal stability, and good mechanical properties. The crosslinking reaction connects resin molecules together through covalent

bonds. Due to crosslinking reactions, multifunctional reactive resins form a three dimensional crosslinked network which plays a vital role in determining properties of coatings. The fundamental chemical nature and molecular architecture of resins have a profound influence on crosslinked network and coating properties such as mechanical properties (flexibility, tensile strength, toughness, scratch resistance, hardness, adhesion, etc), glass transition temperature (T_g), thermal stability, and resistance to chemicals, corrosion, and weathering.⁶⁻¹³

Several combinations of resin and crosslinking chemistries are used to obtain high performance crosslinked coatings. Traditional resin systems based on many crosslinking chemistries used in coating industries are polyurethanes, epoxies, acrylics, drying oils, alkyds, polyesters, silicones, phenolics, and amino resins. In addition, several hybrid resin systems which combines the properties of both the resins and crosslinking chemistries such as urethane-acrylate, epoxy-acrylate, silane-acrylates, uralkyd, etc. are designed to meet specific requirements.^{1, 4, 5}

Modern coatings technology research is focused on the design novel resins, crosslinkers, and additives to meet functional, environmental, and economic objectives for specific applications. The reduction in volatile organic components harmful to environment and use of renewable raw materials has gained significant attention in coating industries. A challenging part is to develop environmentally friendly coating systems to meet increasing legislative regulations without compromising performance and economical aspects.¹⁴⁻²⁰

The goal of the research presented in this dissertation was to design novel thermosetting glycidyl carbamate (GC) functional resins and study the properties of their

coatings. GC resins contain both urethane and epoxy groups in their structures and thus, combine the performance of polyurethanes and the reactivity of epoxides. Urethane and epoxy systems are introduced in sections 1.2 and 1.3 of this chapter, respectively. A discussion on previous research on GC resins and their coatings is presented in section 2. Further, in context to the research presented in this dissertation, a general introduction of environmentally friendly coatings low or zero VOC coatings, highly flexible coatings, UV curable coatings, and air-drying coatings are presented in sections 3, 4, 5, and 6, respectively.

1.2. Polyurethanes

Polyurethanes and epoxy resins are commercially important systems widely used as binders for architectural, industrial, maintenance, and specialty coating applications. In addition to coating applications, polyurethane and epoxy resins are also used to produce adhesives, sealants, elastomers, foams, and composite materials.²¹⁻²⁷

Urethanes are most commonly obtained by reaction of isocyanate functional compound with alcohol catalyzed by bases or organometallic compounds. Figure 1.1 is a schematic representation of the reaction used to obtain urethanes, where R and R' can be aliphatic or aromatic. Aromatic isocyanates are more reactive compared to their aliphatic counterparts.¹

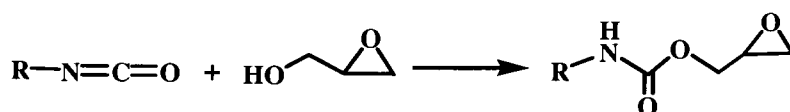


Figure 1.1. Schematic representation of the reaction of isocyanate with alcohol to obtain urethane.

The isocyanate functional compounds also react with other active hydrogen compounds such as water, amines, and carboxylic acids to produce ureas, and amides,

respectively. Reaction of isocyanates with primary and secondary amines to produce urea is very rapid and may take place at ambient temperature without catalyst. The commercially important multifunctional isocyanates such as isocyanurates, biurets, allophanates, and uretdiones used in polyurethane coatings are produced by reacting isocyanates with urethanes, ureas, or isocyanates, respectively. These reactions take place in special conditions (high temperature or specific catalysts).^{1, 13, 22} Figure 1.2 is a schematic representation of the structures of isocyanurates, biurets, allophanates, and uretdiones.²⁸

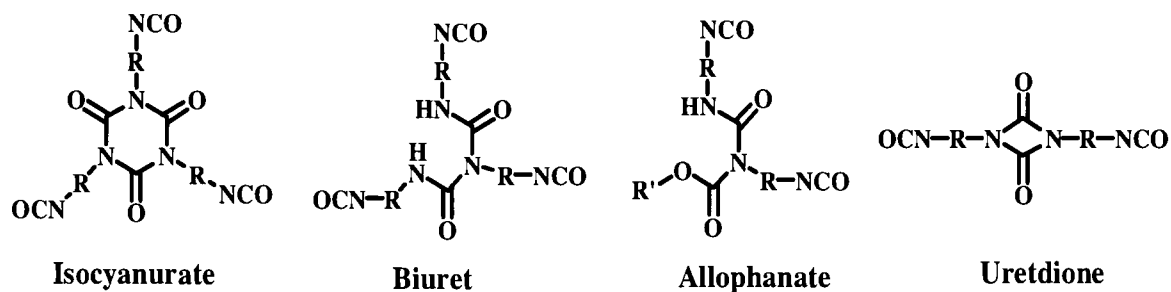


Figure 1.2. Schematic representation of the structures of isocyanurates, biurets, allophanates, and uretdiones.

Crosslinked polyurethane coatings are obtained by the reaction of polyisocyanates and polyols at ambient or slightly higher temperature. Biuret and isocyanurate resins based on hexamethylene diisocyanate (HDI), are widely used in 2K polyurethane coatings for automotive, maintenance, and aircraft coatings. Mundstock reports that commercial HDI biuret and isocyanurate resins contain trifunctional as well as higher functional oligomeric isocyanates and are polyisocyanates in nature with average NCO functionality more than 3. Figure 1.3 is a schematic representation of the major higher oligomers present in HDI isocyanurate. Higher amounts of the higher molecular weight oligomers results in higher viscosity polyisocyanates. Allophanates and

uretdiones are used as reactive diluents in 2K polyurethane coatings to reduce the viscosity.²⁹

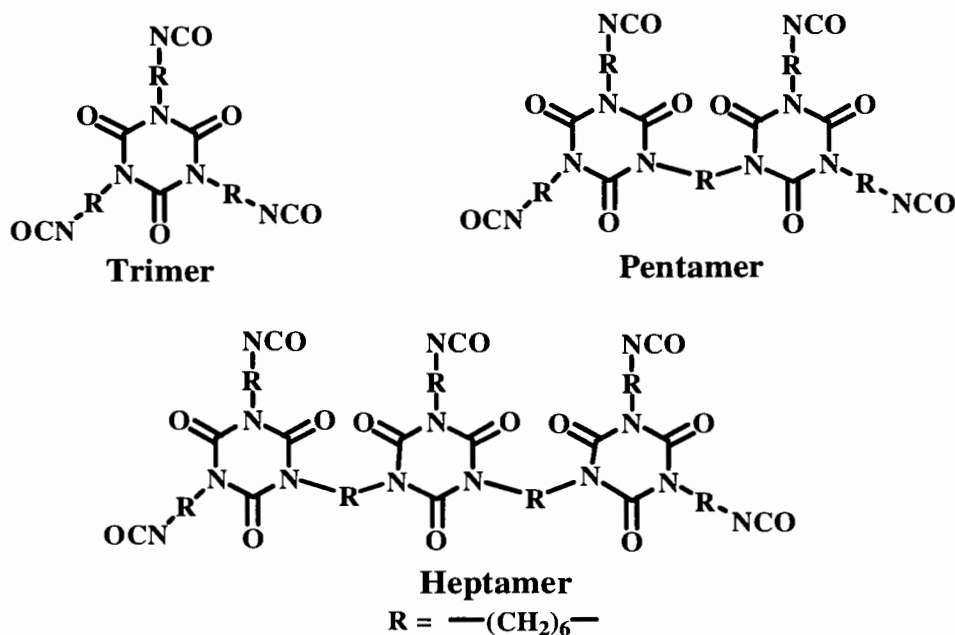


Figure 1.3. Schematic representation of the major higher oligomers present in HDI isocyanurate resins.

Table 1.1 shows influence of the composition of HDI isocyanurate polyisocyanate on their viscosity, NCO functionality, and drying rate of coatings.²⁹

Table 1.1. Composition of HDI isocyanurate polyisocyanates.²⁹

HDI Isocyanurate	Viscosity (mPas)	Functionality	Dry time	Oligomer distribution		
				n = 3	n = 5	n > 5
High viscous	15,000	~ 4.0	+++	~ 30 %	~ 20 %	~ 50 %
Standard	3,500	~ 3.5	++	~ 50 %	~ 20 %	~ 30 %
Low viscous	1,200	~ 3.1	+	~ 70 %	~ 15 %	~ 15 %

HDI biuret and isocyanurate resins due to their polyisocyanate nature, when crosslinked with polyols, produce polyurethane coatings with higher crosslink density and better properties compared to that of allophanate and uretdione based coatings.^{1, 28, 29}

The formation of hydrogen bonding in polyurethanes is an important characteristic which influences the viscosity of polyurethane based resins and their

coating properties. Hydrogen atom in the imine group of urethane forms a hydrogen bond with the carbonyl of another urethane group. The imine hydrogen atom can also form a bond with oxygen in the ether or carbonyl in the ester group.^{1, 30} Figure 1.4 is a schematic representation of the types of possible hydrogen bonds.³⁰ Hydrogen bonds having a double interaction between the carbonyl oxygen and hydrogen atoms are stable and strong compared to other type of hydrogen bonds in urethane groups. Thus, hydrogen bond energy (46.5 KJ/mol) of cis-cis hydrogen bond shown in Figure 1.4 is higher than that of trans-trans hydrogen bond energy (18.4 KJ/mol). In addition to strong hydrogen bonds, weaker bonds between hydrogen in imine group of urethane and oxygen in carbonyl of ester and oxygen in ether groups are formed with bond energy of 25.9 kJ/mol and 23.6 kJ/mol, respectively. Urea group is also capable of forming very strong hydrogen bond of energy 58.5 kJ/mol, as it contains two imine hydrogen atoms.^{30, 31}

Hydrogen bonds break under mechanical stress and reform after the removal of stress. Reversible breaking and reforming of hydrogen bonds results in energy absorption and reduces the possibility of irreversible breaking of covalent bonds and leads to the toughness and scratch resistance of polyurethane-based materials.¹ Li correlated properties of urethane, thiourethane, and dithiourethane based coatings with the extent of hydrogen bonding in coatings. Li found that extent of hydrogen bonding in urethane and thiourethane coatings was similar but higher than that in dithiourethane based coatings. Because of higher hydrogen bonding, urethane and thiourethane based coatings showed higher hardness and scratch resistance compared to that of dithiourethane based coatings.³²

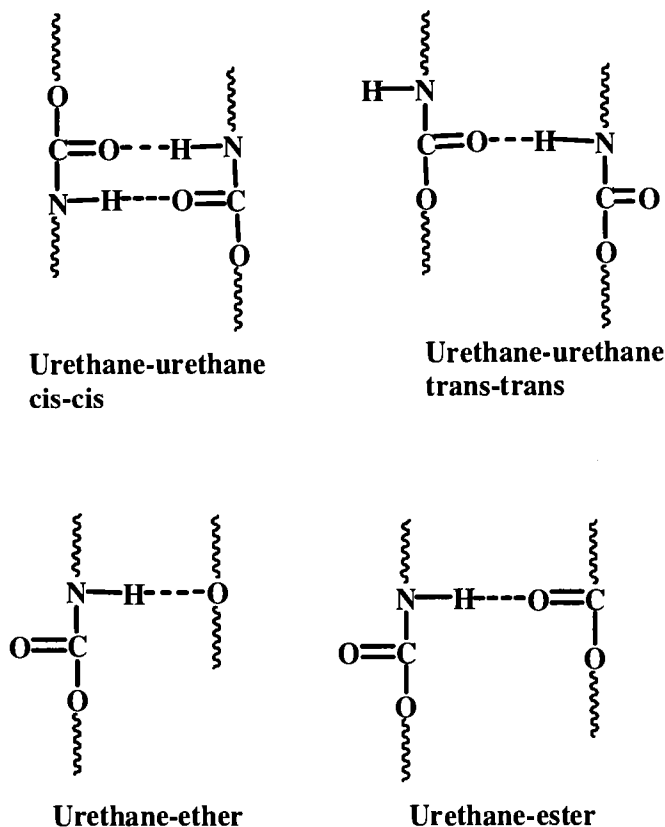


Figure 1.4. Schematic representation of the types of hydrogen bonds.

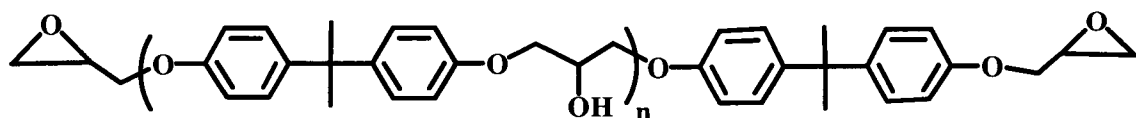
The performance of polyurethane coatings is also influenced by the type of isocyanate and alcohol. Dearth studied the mechanical properties and chemical resistance of crosslinked polyurethane coatings obtained from trimer polyisocyanates and allophanate polyisocyanates of HDI, bis(4-isocyanatocyclohexyl)methane (H_{12} MDI), and isophorone diisocyanate (IPDI). HDI based coatings in trimer and allophanates series showed excellent flexibility and toughness in tensile tests. Necking and yielding was observed for HDI based coatings. Due to the rigid molecular structure of H_{12} MDI and IPDI, their coatings showed very high strength, stiffness, and hardness.³³ Ni studied the influence of polyester diols on polyurethane coatings obtained using HDI isocyanurate. Several polyester diols were synthesized by systematic variation in their structures using combinations of 1,3 and 1,4 isomers of cyclohexane dicarboxylic acids (1,3 and 1,4

CHDA isomers), neopentyl glycol (NPG), 2-butyl-2-ethyl-1,3-propanediol (BEPD), 1,4-cyclohexanedimethanol (CHDM), 1,6 hexanediol (HD), hydroxypropyl hydroxyphenyl ether (HPHP). The polyesters had molecular weight between 800 to 1000 g/mol. Polyurethane coatings from BEPD and HPHP based polyester diols showed very high elongation at break. Due to the rigid structure of CHDM, polyurethane coatings based on CHDM polyester diols showed the highest T_g , tensile modulus, hardness, and fracture toughness.³⁴

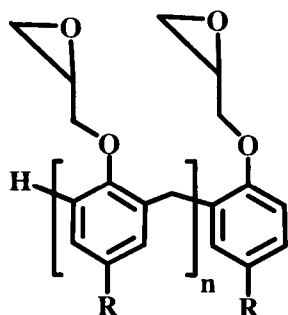
1.3. Epoxies

The most widely used epoxy resins are diglycidyl ether of bisphenol A (DGEBA) epoxy resins obtained by the reaction of bisphenol A (BPA) and epichlorohydrin. The coatings based on DGEBA epoxy resins and polyamide crosslinkers are state of the art technology for corrosion resistant protective applications. Other epoxy resins and epoxy functional compounds used in epoxy coating systems are epoxy novolac resins, triglycidylisocyanurate resins, glycidyl ester and ethers, cycloaliphatic compounds, and epoxidized plant oil based resins. Epoxy coatings show high modulus, good adhesion, hardness, thermal stability, and chemical resistance.^{1, 26, 35-37} Figure 1.5 is a schematic representation of the structures of selected epoxy resins and epoxy compounds.^{1, 26, 38}

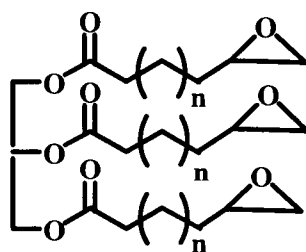
Epoxy resins are highly reactive due to the strained nature of the oxirane group and therefore can be crosslinked with numerous compounds to obtain crosslinked systems such as coatings, adhesives, sealants, and composites. Epoxy coatings with a diverse range of performance attributes or modified epoxy resins for specific applications can be obtained by crosslinking or reacting the oxirane ring with amines, carboxylic acids



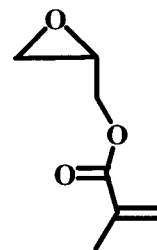
Diglycidyl ether of bisphenol A (DGEBA)



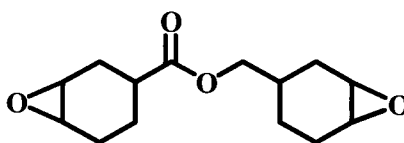
Epoxy novolac



Terminally epoxidized plant oil



Glycidyl methacrylate



Cyclohexyl diepoxy

Figure 1.5. Schematic representation of the structures of epoxy resins and compounds.

and anhydrides, hydroxy compounds, thiols, and amides. Epoxy groups can undergo anionic or cationic ring opening polymerization. Epoxy resins can also produce UV cured coatings by cationic photopolymerization mechanism in the presence of photoinitiators.^{26,}

36, 39

Nucleophilic ring opening of epoxy group by amines, a signature reaction, is widely used to obtain epoxy-amine crosslinked coatings at ambient conditions. Figure 1.6 is a schematic representation of the epoxy-amine reaction.²⁷ Shechter studied the influence of the structure of amines on epoxy-amine reaction. The reactivity of aliphatic amines was inherently high and depended on the steric factors. The reactivity of aromatic amines due to lower basicity was slower compared to aliphatic amines.⁴⁰ Reactivity of amines with oxirane ring decreases in following order: primary > secondary >> tertiary

amines. Also, reactivity of amines can also vary from aliphatic to aromatic in decreasing order: aliphatic > cycloaliphatic > aromatic amine.¹

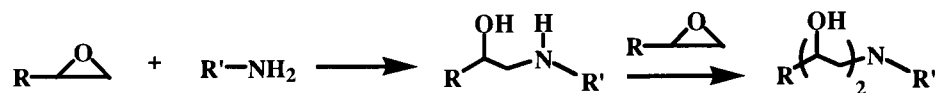


Figure 1.6. Schematic representation of the epoxy-amine reaction.

The development of epoxy-amine crosslinked networks plays a crucial role in the determination of coating properties. The properties of epoxy-amine crosslinked coatings can be influenced by type of resin, functionality of the resin, and type of amine crosslinker. Multifunctional epoxy resins can be used to tailor crosslinked network and coating performance. Crosslinked network of multifunctional epoxy resins has high crosslink density and T_g compared to that of bifunctional epoxy resins.⁴¹⁻⁴³ Flexibility of epoxy-amine crosslinked system was found to increase by increasing the spacer length between reactive amine groups in amine crosslinker.⁴⁴

1.4. Glycidyl carbamate (GC) resins

Glycidyl carbamate (GC) resins are obtained from the reaction of isocyanate functional compounds with glycidol. An unique property of GC resins is that the performance of urethane and the reactivity of epoxide is combined in single resin structure. In a previous study, Edwards synthesized biuret glycidyl carbamate (BGC) and isocyanurate glycidyl carbamate (IGC) resins by reacting aliphatic polyisocyanates based on hexamethylene diisocyanate (HDI) such as biuret and isocyanurate, respectively, with glycidol. The reaction was carried out in the presence of a catalyst, dibutyltin dilaurate (DBTDL) at the temperature between 35 – 60 °C.⁴⁵⁻⁴⁸ Figure 1.7 is a schematic

representation of the synthesis of biuret glycidyl carbamate (BGC) resin and Figure 1.8 is a schematic representation of the synthesis of IGC resin.⁴⁵

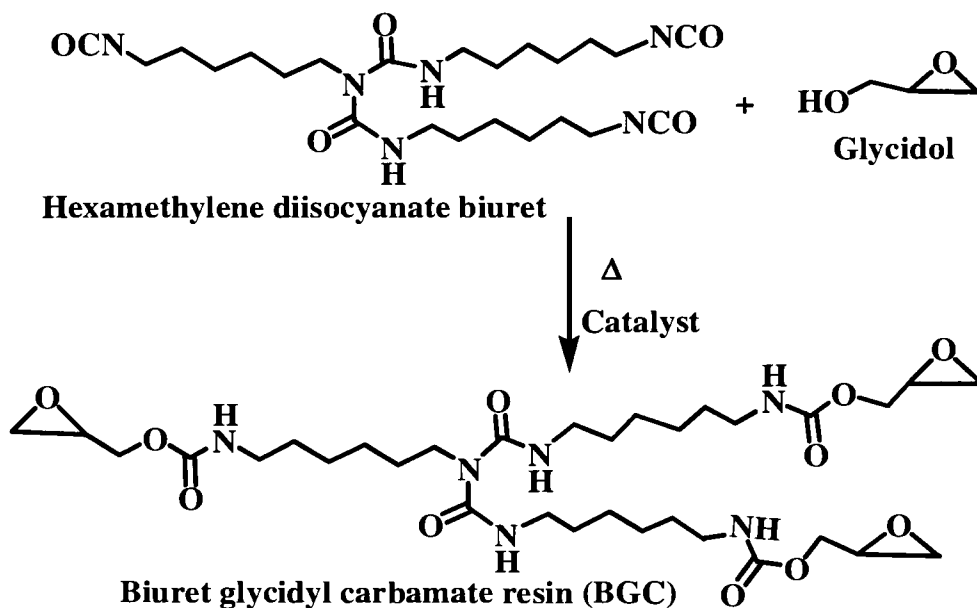


Figure 1.7. Schematic representation of the synthesis of BGC resin.

Edwards obtained GC coatings by crosslinking BGC and IGC resins with cycloaliphatic amine and polyamide. The GC coatings thus obtained had an excellent combination of properties such as high solvent resistance, impact resistance, adhesion and, hardness. The combination of excellent properties of GC coatings was attributed to the chemical nature and densely crosslinked network of GC coatings.⁴⁵ Figure 1.9 is a schematic representation of the formation of the crosslinked network in amine crosslinked GC coatings. Edwards and coauthors found that the reactivity of amines with oxirane group of GC resins followed the trend; aliphatic amine > cycloaliphatic amine > aromatic amine. This trend is consistent with general epoxy-amine reaction kinetics.³⁶ Also, another interesting feature of the reactivity of GC resins observed was the higher reactivity of the epoxy group of GC resins compared to that of the epoxy group of typical glycidyl ethers.^{45, 48}

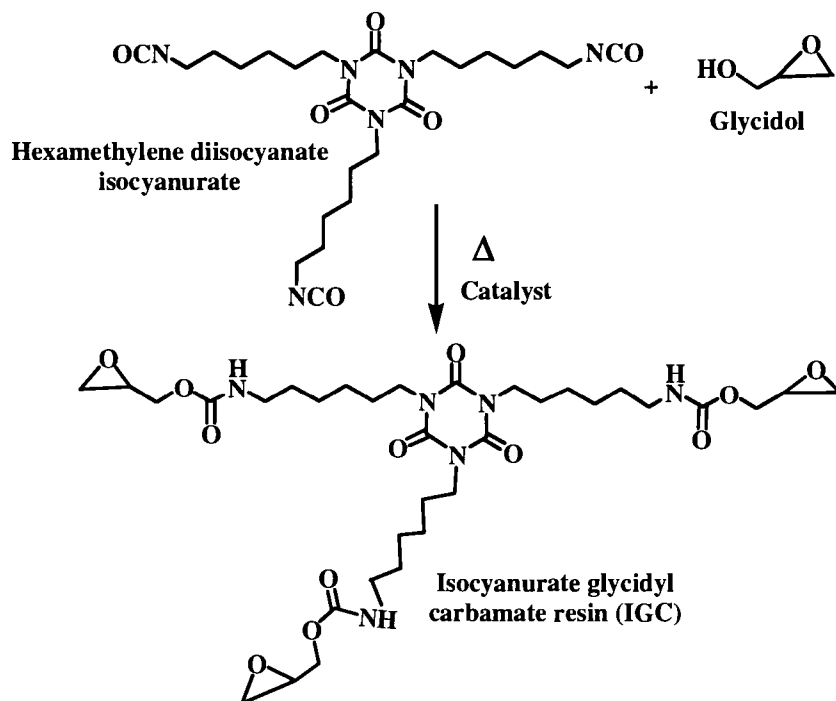


Figure 1.8. Schematic representation of the synthesis of IGC.

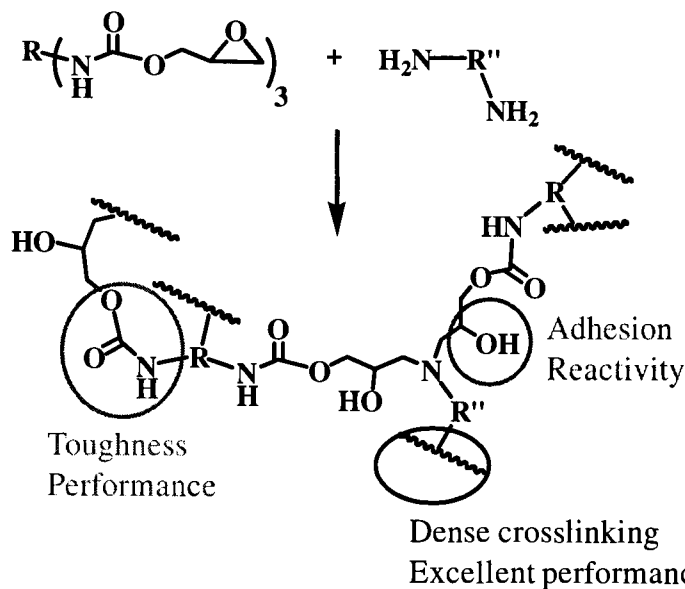


Figure 1.9. Schematic representation of formation of crosslinked network in amine crosslinked GC coatings.

In another study, Edwards obtained coatings by self-crosslinking of BGC and IGC resins at elevated temperature (typically 150 °C). Self-crosslinked GC coatings exhibited a good combination of properties. The study suggested that the self-

crosslinking reaction in GC resins can proceed by a combination of several intermolecular and intramolecular reactions. The primary mechanism suggested is the attack of the amino group of the carbamate on epoxide, followed by polyetherification.⁴⁸

49

Edwards also developed waterborne GC coatings using hydrophilically modified isocyanate and glycidol. The GC resin was dispersed in water using surfactant and crosslinked with waterborne amine crosslinker to obtain waterborne coatings with good cure development.⁴⁹

Coatings obtained from BGC and IGC resins showed an excellent combination of properties. However, the viscosity of the resins was very high (millions of mPa·s) probably due to extensive intermolecular hydrogen bonding. It was necessary to reduce the viscosity of the resins for low VOC applications. In a previous study, Suryanarayana approached this problem by using plasticizers and VOC exempt solvents. Suryanarayana also explored other diisocyanates (aliphatic and aromatic) instead of polyisocyanates (HDI biuret and isocyanurate) to obtain GC resins. Plasticizers (dioctyl phthalate, dibutyl phthalate and diisononyl phthalate) were mixed with BGC and IGC to reduce viscosity. The plasticizer approach did not reduce the viscosity significantly. VOC exempt solvents evaluated were tertiary butyl acetate (TBA), methyl acetate, acetone, oxsol, and acetone. TBA reduced the viscosity when added in high levels. Other isocyanates used to obtain low viscosity GC resins were aliphatic and aromatic diisocyanates. Amine crosslinked GC coatings made from aliphatic and aromatic diisocyanate had lower resistance to impact and solvent compared to that of BGC and IGC coatings.⁵⁰

Suryanarayana also found that amine crosslinked GC coatings obtained from blends of GC resins and BPA based epoxy resins exhibited excellent corrosion resistance when tested by salt spray method.^{50, 51}

Chattopadhyay developed organic-inorganic hybrid GC coatings. GC resins were functionalized by alkoxy silane and crosslinked by amine crosslinker and by moisture curing (sol-gel) technique using tetraethoxyorthosilicate. Optically transparent hybrid GC coatings thus obtained had an excellent combination of properties. Amine crosslinker and amine functional alkoxy silane compound can also be added to GC coating formulations to obtain hybrid GC coatings. The thermal stability of these coatings increased with the increase in the inorganic content in the coatings.⁵²⁻⁵⁴

1.5. Environmentally friendly low or zero VOC coatings

The demand for environmentally friendly products has increased significantly. Many industrial sectors such as construction, transportation, manufacturing, electronics, health care, and energy are seeking environmentally friendly products for next generation. Industrial and academic research on coatings is focused to reduce volatile organic compounds (VOC), mainly organic solvents that causes air pollution especially smog. To make coatings environmentally friendly, legislation for VOC reduction are becoming stringent. In recent years, industrial and academic research on development of low VOC coating systems has increased significantly. Low or zero VOC coatings can be obtained by reducing the resin viscosity (high solids coatings), using water as a solvent (waterborne coatings), or using 100% solid UV curable or powder coatings.^{1, 15-18, 55, 56}

1.5.1. Low viscosity resins

Resins with high molecular weight, large number of reactive functional groups, and high hydrogen bonding have high viscosity and require a large amount of solvent to achieve application viscosity. Low viscosity resins require reduced amount of solvent (low VOC and increased solids) to achieve application viscosity. Polymers with controlled molecular weight distribution show a reduction in viscosity. Recent advancements in designing polymer architecture, hyperbranched polymers, are promising in obtaining binder systems for low VOC and high solids coatings.^{12, 14, 15, 28, 57, 58}

Szewczyk synthesized low viscosity hyperbranched and star alkyd resins for low VOC application. Szewczyk showed that hyperbranched and star-shaped alkyd resins have narrower molecular weight distribution and lower viscosity than conventional alkyd resins with similar fatty acid content. Air drying coatings obtained from high molecular weight star-shaped alkyd resins showed increase in hardness over the period of one month.⁵⁹

Huybrechts synthesized low viscosity branched polyether polyol and obtained VOC compliant 2K polyurethane coatings with good properties using HDI and IPDI polyisocyanates.⁶⁰

Low VOC high solids 2K polyurethane coatings can also be obtained by using low viscosity starting polyisocyanates. The viscosity of starting polyisocyanates is reduced by removing higher molecular weight oligomeric fractions. This approach is limited by economic feasibility. Recently Bayer Inc. developed a novel low viscous asymmetric isocyanate trimer, iminooxadiazinedione, an isomer of HDI isocyanurate (symmetric trimer). In the asymmetric trimer, one NCO group is incorporated in the ring

structure by opening C=O bond rather than usual C=N bond as in the symmetric trimer. This is achieved through a special catalyst. The flat centrosymmetric isocyanurate ring changes to an asymmetric ring. The result is a dramatic reduction in viscosity. Figure 1.10 is a schematic representation of the structures of symmetric and asymmetric trimer.²⁹

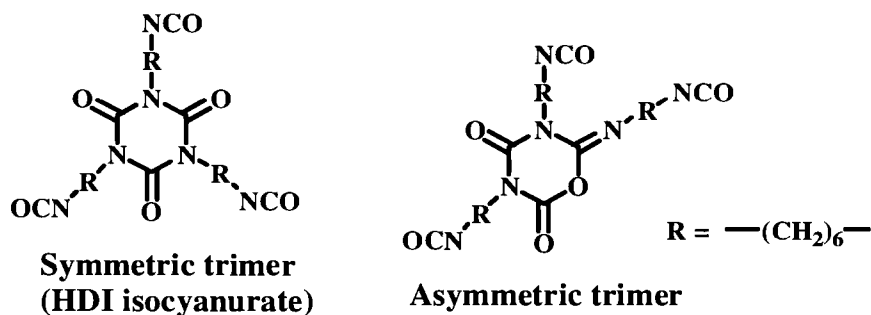


Figure 1.10. Schematic representation of symmetric and asymmetric trimer.

The viscosity of a low viscous symmetric trimer (HDI isocyanurate) grade is 1,200 mPa·s and the viscosity of an asymmetric trimer of comparable molecular weight is 700 mPa·s, maintaining high NCO functionality. The asymmetric trimer showed similar reactivity and produced 2K polyurethane coatings with comparable properties to that of conventional symmetric trimer.²⁹

A cooperative hydrogen bonding network is considered responsible for high viscosity in hydrogen bonding materials.^{61, 62} A disruption of the cooperative hydrogen bonding network can significantly reduce the viscosity. Sijbesma showed that supramolecular polymers can be formed due to unidirectional quadruple hydrogen bonding between difunctional ureidopyrimidone units. The viscosity of supramolecular polymers was dramatically reduced by the addition of a small amount of monofunctional ureidopyrimidone compound (chain stopper) which breaks the cooperative hydrogen bonding interactions.⁶³

1.5.2. Water dispersible resins

Waterborne polymers are an important class of materials for coatings due to increasing environmental regulations. Water as a solvent for coatings has a good potential in development of low or zero VOC coatings. While water may have certain limitations in coating applications due to its high heat capacity, high surface tension, and slow and humidity dependent evaporation rate, research on waterborne coatings has gained significant attention. In general, resins used as binders in coating applications are hydrophobic and are difficult to disperse in water. Common techniques to disperse resins in water are the use of the surfactants, incorporation of hydrophilic groups in the resin structure, or the synthesis of latex by emulsion polymerization.

The hydrophilic component in waterborne coating is an essential part but may cause multiple issues such as increased water sensitivity, low chemical resistance, phase separation, and poor appearance. Also, a current trend is to minimize or eliminate the use of surfactants (external emulsifiers) in waterborne coatings. Surfactants remain in coatings after film formation and over a period of time they can diffuse to the surface, cause phase separation, increase hydrophilicity and decrease the water resistance of coatings.⁶⁴ Resins for waterborne coatings should be designed considering the ease of applicability and performance attributes. It is highly desirable to incorporate appropriate level of hydrophilic groups in resin structures to obtain dispersion by minimal shear force (hand mixing) for mixing of resin and crosslinker at the time of application and to obtain coatings with good water and chemical resistance.^{5, 6, 15, 20, 29, 64-68}

Widely used coating binders such as polyurethanes, epoxies, polyesters, and alkyds are dispersed in water by incorporation of non-ionic hydrophilic groups, (e.g.

polyethers) or water reducible ionic (anionic and cationic) groups in resin structures. Film formation and final coating properties of waterborne coatings improve with coalescence between resin particles. A coalescing solvent, a volatile plasticizer, is usually used to increase coalescence of the particles. However, it may contribute to the VOC of coatings. Waterborne 2K polyurethane and epoxy coatings are obtained by crosslinking of water dispersible isocyanates and epoxy with waterborne polyols and amines, respectively.^{1, 15, 20, 65-68}

Waterborne polyurethane coatings are developed for automotive, construction, and wood coating applications. Bayer Inc. developed a series of water dispersible polyisocyanates. Shaffer and Melchior reviewed the focus of Bayer to develop water dispersible polyisocyanates with internal non-ionic and ionic emulsifying agents for 2K waterborne polyurethane coatings. The hydrophilic polyisocyanates can be dispersed in water and polyol by minimum shear force (hand mixing) to obtain polyurethane coatings with good hardness, solvent resistance, and appearance. Figure 1.11 is a schematic representation of generation 1, 2 and, 3 water dispersible polyisocyanates developed by Bayer Inc.

Bayer's generation 1 water dispersible polyisocyanate is an HDI (isocyanurate) polyisocyanate containing non-ionic hydrophilic polyether group through urethane linkage as the internal emulsifying agent. The generation 2 water dispersible hydrophilic polyisocyanate contains polyether group through allophanate linkage. The generation 2 hydrophilic polyisocyanate has higher NCO and lower hydrophilic content, and has water dispersibility compared to that of the generation 1 polyisocyanate.^{64, 66} Melchior reported the properties of 2K waterborne polyurethane clear coat for car refinish prepared from the

generations 1 and 2 polyisocyanates and a waterborne polyol. Both of the coatings showed a good balance of properties such as hardness, solvent resistance, low haze, and

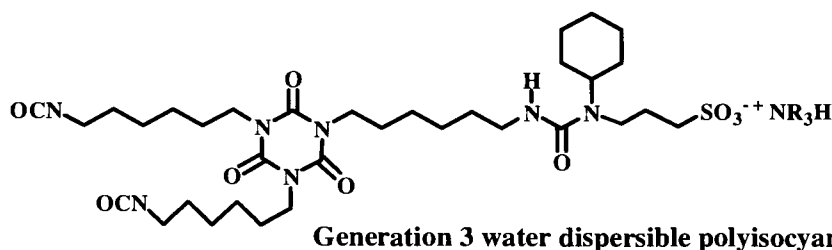
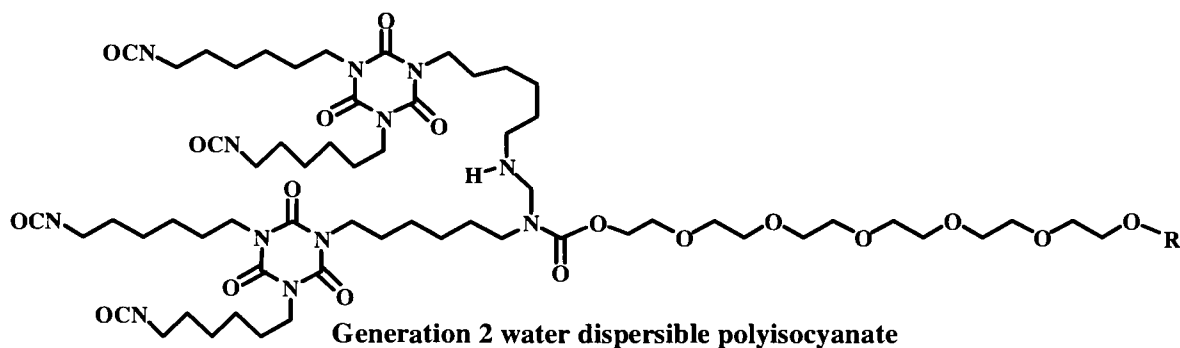
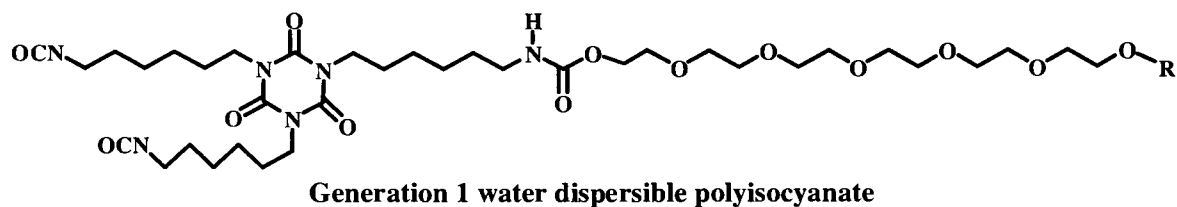


Figure 1.11. Schematic representation of generation 1, 2, and 3 water dispersible polyisocyanates.

good transparency. Due to high NCO and low hydrophilic content in second generation hydrophilic polyisocyanates, their coatings had higher crosslink density and showed higher hardness and solvent resistance compared to that of the coatings made from the first generation hydrophilic polyisocyanates.⁶⁶

In addition to non-ionic hydrophilic modification of polyisocyanate resins, Bayer developed the generation 3 hydrophilic polyisocyanate by ionic modification. The sulfonic acid group is incorporated in HDI (isocyanurate) polyisocyanate through a urea linkage. The urea linkage produced additional hydrogen bonding and improved coating

performance. Waterborne polyurethane coatings based on ionic polyisocyanate had lower water sensitivity and higher hardness compared to that of generation 1 and 2 isocyanate based coatings. The generation 3 polyisocyanate has improved water dispersibility.⁶⁴

While the waterborne 2K polyurethane coatings are used for low or zero VOC coatings, they have a disadvantage. During the preparation of waterborne 2K polyurethane coatings isocyanate functional resins react with polyols as well as water. Therefore excess stoichiometric amount of isocyanate resin with respect to polyol has to be used. The reaction of isocyanate with water produces urea linkages and also results in CO₂ evolution. The urea linkages may improve crosslink density and mechanical properties but their crystalline nature and relatively low compatibility may lead to turbidity in coatings. The evolution of CO₂ may cause film defects such as blistering and foaming.⁶⁷

Waterborne epoxy coating systems are developed for low or zero VOC applications by hydrophilic modification of epoxy resins and amine curing agents. Air Products and Chemicals Inc. and Resolution Performance Products (now part of Hexion Specialty Chemicals) developed waterborne epoxy resins and amine crosslinkers for high performance coating applications.⁶⁹⁻⁷³ Elmore reviewed the development of waterborne epoxy-amine coating systems. Epoxy resins and amine crosslinkers are modified with polyether groups to improve their water dispersibility. The amine crosslinkers are also modified with ionic groups for waterborne coating applications. An optimum amount of hydrophilic groups are incorporated in resins and crosslinkers to achieve good coalescence between resin and crosslinker particles, high crosslink density, and good film properties.⁶⁸

1.6. Binder systems for highly flexible coatings

Highly flexible coatings are used for many industries such as electronics, packaging, automotive, and aircraft.^{74, 75} A typical aircraft coating system consists of a chromate treated aluminum alloy surface, chromated epoxy-polyamide primer, and polyisocyanate-polyol urethane top coat.⁷⁶ Figure. 1.12 is a schematic representation of a typical coating system for aircraft application.

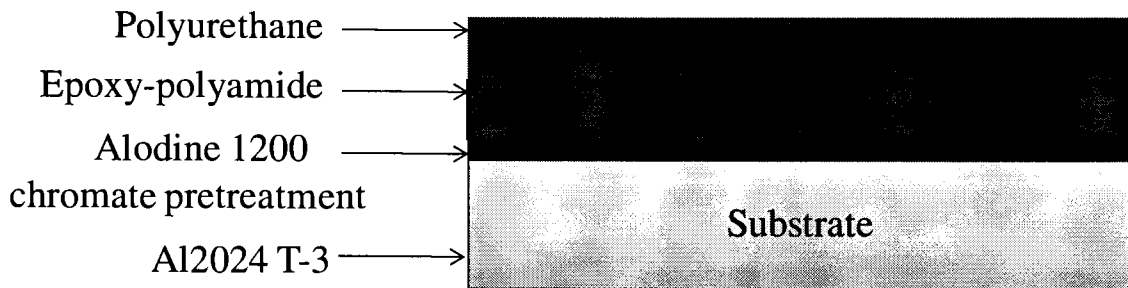


Figure 1.12. Schematic representation of a typical coating system for aircraft application.

The most commonly used aluminum alloys, Al2024 T-3 and Al7075 T-6, for aircraft are complex phase separated metal-in-metal composites and offer high strength and light weight characteristics. However, the alloy composition causes undesirable galvanic corrosion when exposed to a corrosive environment.⁷⁶

Aircraft are exposed to severe loading (extension and compression) due to pressurization, wing flexure and multiple landing and takeoff cycles. Corrosion resistant coatings made from a suitable binder provide barrier properties and protect the metal from corrosion. Damage to the coating exposes the metal surface to the corrosive environment and initiates electrochemical corrosion reactions. Corrosion inhibitors used in such coatings slow down the rate of corrosion reactions. Corrosion resistant primer is in direct contact with metallic parts of aircraft. It is desirable that a binder for corrosion

resistant primer should produce highly flexible coatings to accommodate the severe loading experienced by aircraft. Aircraft are made of thousands of joints and riveted parts which act as stress concentrators. Coating systems, due to lack of flexibility are prone to failure around fasteners.⁷⁷⁻⁷⁹ Figure 1.13 illustrates the failure of coatings around joints and riveted parts of aircraft.

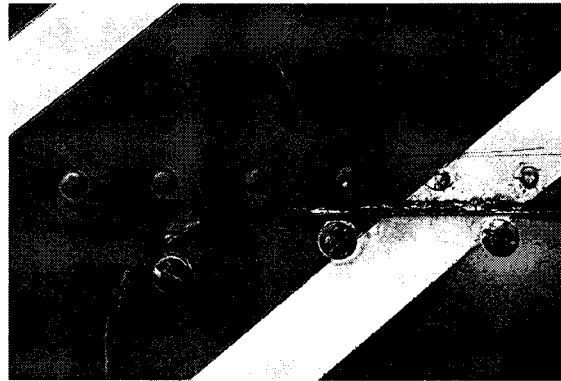


Figure 1.13. Illustration of the coating failure around riveted and joint area.

A coating system of DGEBA epoxy resin crosslinked with low molecular weight mercaptan-terminated polysulfide rubbers are used as flexible primers for aircraft.¹ PPG Industries developed flexible coating systems for flexible primer and flexible multilayer coating applications. The coatings were prepared by reacting isocyanate terminated polyurethane with phosphatized epoxy resins. The coating compositions were also prepared using polyester diol, phenolic resins, polyisocyanates, and phosphatized epoxy resins. PPG also prepared epoxy functional extended urethane and crosslinked with polyamide to obtain flexible primer. The primer had better impact resistance, flexibility, and chemical resistance compared to that of traditional DGEBA based epoxy-amine systems⁸⁰⁻⁸³

The U.S. Navy developed flexible sealant-prime compositions for fastener head patterns in high performance aircraft. The sealant-primer composition was prepared using

isocyanate terminated aromatic polyurethane, DGEBA epoxy resin, and aromatic ketamine crosslinker. In presence of moisture, aromatic ketamine released aromatic diamine and reacted with the resins to produce crosslinked coatings. The coating systems with corrosion inhibitor such as strontium chromate had good adhesion, flexibility, and corrosion resistance when tested on aluminum substrate.⁸⁴

1.7. UV-curable coatings

UV-curing or radiation curing has gained interest due to its unique economic and ecological advantages. These unique advantages are ultrafast curing at ambient temperatures or lower and 100 % solid coating formulations as in most cases solventless liquid monomers, oligomers or solid polymers are used.^{58, 85, 86}

Radiation curing or photocrosslinking produces densely crosslinked polymeric materials within a very short time (seconds) from multifunctional monomers, oligomers or telechelic polymers upon exposure to radiation such as ultraviolet light (UV) or electron beam (EB).⁸⁷⁻⁸⁹

For more than three decades radiation curing has been successfully used for many applications such as coatings, adhesives, inks, optical waveguides, and microelectronics. UV curable coatings are widely used for furniture, plastic substrates, optical fibers, compact discs, headlight lenses, and metal substrates.^{85, 90}

Two major types of UV-curable coatings are free radically and cationically cured coatings. Most commonly used UV-curable systems are acrylates based on the free radical mechanism.^{39, 88} Figure 1.14 is a schematic representation of the formation of crosslinked network in acrylate based UV-cured coatings.⁸⁸

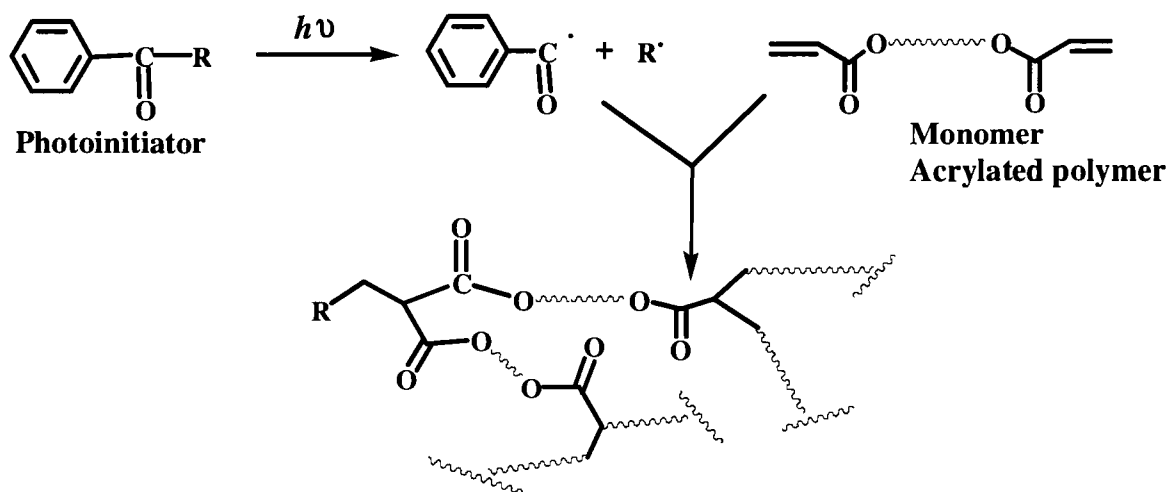


Figure 1.14. Schematic representation of the formation of crosslinked network in acrylate based UV-cured coatings.

A typical UV-curable system consists of a UV light source (most common is medium pressure mercury vapor lamp), photoinitiator which generates reactive species (such as radicals or cations) for polymerization upon exposure to a suitable UV radiation, functionalized oligomers (acrylated or epoxidized) and monomers also known as reactive diluents.⁹¹

Resins used for UV-curable coatings are hybrid resins obtained by acrylation of traditional resins. Typical UV curable resins developed are epoxy-acrylates, urethane-acrylates, polyester-acrylates, polyether-acrylates, and silicone-acrylates. Basic chemical structure of resin governs UV-curing process and bulk physical and chemical properties of UV cured coating films. Reactive diluents or monomers are used to reduce the viscosity and are low molecular weight acrylates or methacrylates with functionality ranging from one to six. Reactive diluents get incorporated into the crosslinked network of coating film after cure and their type and amount influence coating performance. Aromatic ketones are used as photoinitiators to generate free radicals, and initiate

polymerization and their type and amount influence rate and degree of cure, and coating performance.^{87, 92, 93}

DGEBA based epoxy-acrylate resins hold the biggest share in the UV curing market and are widely used in paper coatings, wood coatings, and inks. High cure speed and chemical resistance of cured coatings are characteristics of epoxy-acrylate systems. UV curable epoxy-acrylate resins are obtained by reacting the oxirane ring in the resins with acrylic acid. Acrylated epoxy resins thus obtained produce UV cured coatings by free radical photopolymerization mechanism in the presence of photoinitiators. Acrylated DGEBA based epoxy resins are highly reactive due to terminal acrylic group and participation of generated hydroxyl group in cure mechanism.^{36, 85, 93}

The composition of UV curable resins and coating formulations influence the resulting coating properties. Chattopadhyay synthesized acrylated and methacrylated DGEBA and epoxy novolac resins using acrylic acid and methacrylic acid. UV cured coatings were obtained using the acrylated resins, trimethylol propane triacrylate (TMPTA) as a reactive diluent, and photoinitiator. UV cured coatings based on novolac resins showed higher T_g compared to the coatings based on DGEBA based resins due to higher rigid aromatic groups in novolac based resins. Also, methacrylate based coatings had relatively higher T_g and strength compared to that of acrylate based coatings. Increase in TMPA content increased crosslink density, T_g , and hardness of the coatings.⁹⁴ Safranski studied influence of composition of monofunctional and multifunctional methacrylates on crosslinked network obtained by UV curing. Increase in the functionality of methacrylates increased the crosslink density and T_g .⁹⁵

1.8. Air-drying coatings

One of the oldest binders for coatings are drying oils such as linseed, tung, soybean, castor, safflower, etc. obtained from renewable sources (plants). Conventional binders used in air-drying coatings are based on alkyd resins and are widely used for exterior and interior coatings on wood, metal, and architectures. Alkyd resins are obtained by the polycondensation reaction of polycarboxylic acids, polyhydric alcohols, with oils or unsaturated fatty acids.^{1,96}

Drying oils, alkyd resins, and unsaturated fatty acids and their derivatives have regained significant attention due to their renewable origin. Drying oils, fatty acids and their derivatives are still being explored to obtain new coating binders such as uralkyd, epoxy esters of fatty acids, epoxidized oils and their derivatives, and fatty acid functional sucrose derivatives.^{96,97}

The unsaturation with reactive diallylic methylene group in fatty acids is responsible for air-drying i.e. reaction of oxygen with unsaturated fatty acid to produce crosslinked films. The air-drying process occurs through a lipid autoxidation mechanism.^{1,98,99}

The most commonly used oils and fatty acids in coatings systems are obtained from linseed (linseed oil and linseed oil fatty acid) and soybean (soybean oil and soy fatty acid). Linseed oil fatty acid has higher compositional amount of linolenic acid than soy fatty acid and has higher rate of autoxidation.^{1,98} Figure 1.15 is a schematic representation of the autoxidation process.⁹⁹

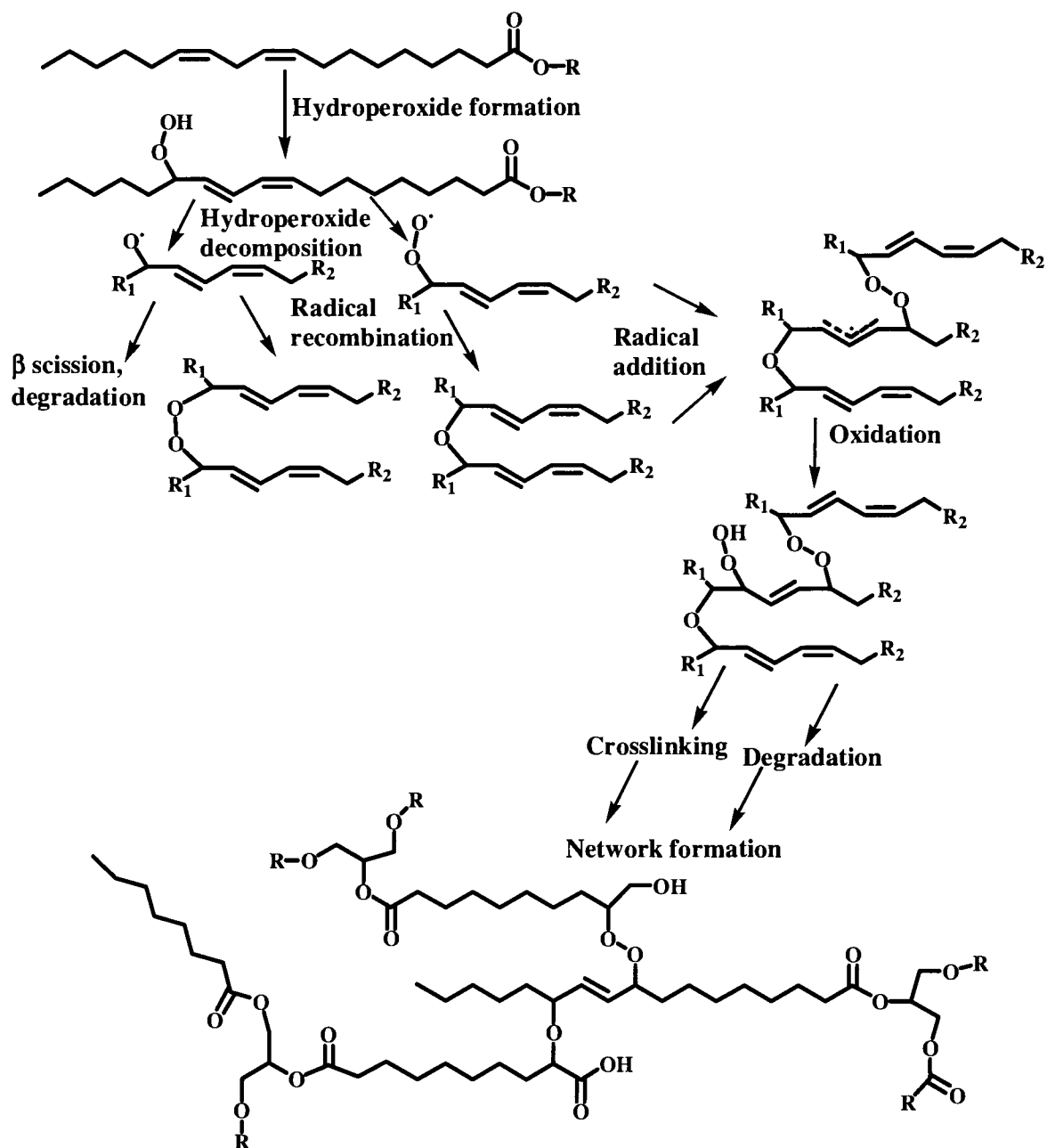


Figure 1.15. Schematic representation of the formation of crosslinked network in air-drying (autoxidation) process.

The development of a crosslinked network by autoxidation (air-drying) mechanism in air-drying coatings is a complex process. The distinct stages of autoxidation are; induction stage (natural antioxidants are destroyed), oxygen uptake and

weight gain, and polymerization, and crosslinking. Other side products such as ketones, epoxides, and aldehydes may form and further oxidize in this process. The autoxidation (and crosslinking) of the remaining double bonds continues for a long time and get reflected in an increase in coating hardness.^{97, 99}

Components of a typical air-drying coating formulation are air-drying binder, catalysts or driers, solvent, and additives such as antiskinning agent if required. Combination of several driers or catalysts are used in air-drying coatings to catalyze oxygen uptake and generation of free radicals required for crosslinking. Common driers are metal (cobalt, manganese, lead, zirconium, and calcium) salts of carboxylic acids and are classified as surface and through driers. In general, a combination of surface and through driers is used in air-drying coatings to ensure uniform curing.^{1, 97, 99}

Autoxidizable polyurethanes, commonly known as uralkyds, are prepared by reacting aromatic or aliphatic diisocyanate with hydroxyl group of transesterified linseed or soy oil. Uralkyd coatings show better hardness, adhesion, and hydrolysis and abrasion resistance compared to conventional alkyd coatings.¹⁰⁰ Xu studied water absorption and desorption showed that uralkyd coatings have higher barrier properties compared to the conventional alkyd coatings.¹⁰¹

Fatty acid functional source derivatives are also explored recently for air-drying applications. Linseed and soy fatty acid functional sucrose derivatives are used to obtain air-drying coatings. Sucrose octalinoleate is used as a reactive diluent to obtain high solid alkyd coating formulation.⁹⁶ Blends of sucrose soyate and acetoacetylated sucrose are used to obtain coatings by a combination of crosslinking mechanisms of air-drying and

enamine formation.¹⁰² In addition, epoxidized sucrose fatty acid derivatives are used to obtain cationic UV crosslinked coatings.¹⁰³

1.9. Objective

The overall goal the research presented in this dissertation was to design novel resin structures in order to obtain coatings having an optimum combination of properties.

In the previous research, biuret glycidyl carbamate (BGC) and isocyanurate glycidyl carbamate (IGC) resins were synthesized by reacting aliphatic polyisocyanates such as HDI biuret and HDI isocyanurate, respectively with glycidol. Amine and self-crosslinked BGC and IGC coatings showed an excellent combination of mechanical and chemical properties. However, the viscosity of the GC resins was extremely high (in the range of millions of mPas). The high viscosity the GC resins makes them less feasible for low VOC coating applications. The previous approaches to reduce the viscosity of GC resins were use of the external plasticizers and the VOC exempt solvents. The plasticizers did not reduce viscosity significantly while the solvent reduced viscosity at high level of addition. The objective of the research presented in Chapter 2 was to reduce the viscosity of GC resins by structural modification of the resins and to study the influence of the compositions of the GC resins on the coatings properties. The structure of HDI biuret based GC resin was modified by alcohols to obtain low viscosity GC resins. The structural composition of GC resin was varied by varying the amount of alcohol and the extent of alcohol in GC resin. GC coatings were prepared using two amine crosslinkers and by self-crosslinking. The influence of the type of alcohol and extent of alcohol modification of GC resin, type of amine crosslinker, and type of crosslinking technique on coating properties was studied. The structure- property relationships was established.

In the previous research, GC resins were obtained using polyisocyanates and glycidol or diisocyanates and glycidol. Amine and self-crosslinked GC coatings had a good combination of properties. The objective of the research presented in Chapter 3 was to design GC binders for highly flexible coating applications. The compositions of the GC resins were varied using linear diisocyanates, diols, triol, and glycidol and the properties of the amine crosslinked coatings were studied. Initial screening of the coatings for flexibility and chemical resistance was carried out by reverse impact test and MEK double rubs test, respectively. The screened coating systems were further characterized for flexibility using tensile test and for barrier properties using electrochemical impedance spectroscopy and salt spray tests.

The waterborne GC coating in the previous research was based on a water dispersible GC resin obtained from hydrophilic polyisocyanate and glycidol. The influence of the extent of hydrophilic group on waterborne GC coatings was not studied before. The objective of the research presented in Chapter 4 was to further explore water dispersible GC resins and their waterborne coatings by varying the extent of hydrophilic group in the resin structure for low or zero VOC coating applications. The water dispersible GC resins based on HDI isocyanurate were obtained by varying the amount of non-ionic hydrophilic groups, methoxy poly(ethylene glycol) (mPEG). The waterborne coating formulations were prepared by dispersing the hydrophilically modified GC resins in water and mixing it with water based amine crosslinker. No cosolvents and in most cases no surfactants were used during the preparation of the waterborne GC coatings. The influence of extent of hydrophilic groups on the properties of the cured coatings such as water resistance, chemical resistance, and barrier properties was studied. The

performance of the waterborne GC coatings was correlated to the composition of water dispersible GC resins.

With the realization that the GC resins produce coatings with an excellent combination of properties when crosslinked by amines, self-crosslinking, and by hybrid sol-gel crosslinking, the technology of GC resins and coatings was further explored for UV curing and traditional air-drying techniques. Thus, the objective of the research presented in Chapter 5 was to obtain UV curable GC resins and develop UV cured GC coatings. Acrylation of GC resins and modified GC resins was carried out by reacting epoxy groups in the resins with acrylic acid. UV curable coating formulations were prepared using common reactive diluents and the properties of UV cured GC coatings was studied.

The objective of the research presented in Chapter 6 was to develop GC resin for air-drying coatings. The epoxy groups in BGC resin was reacted with linseed oil fatty acid to obtain air-drying GC resin. The air-drying coating formulations were developed using common driers. The properties of air-drying GC coatings were studied.

1.10. References

1. Wicks (Jr), ZW, Jones, FN, Pappas, SP, Wicks, DA, Organic Coatings: Science and Technology. 3rd ed., John Wiley and Sons Inc., New Jersey (2007).
2. Ghosh, SK, Functional Coatings. WILEY-VCH Verlag GmbH & Co. KGaA, Weinheim (2006).
3. Fettis, G, Automotive Paints and Coatings. 1st ed., VCH Verlagsgesellschaft mbH, D-69451 Weinheim (Federal Republic of Germany), Weinheim (1995).

4. Lambourne, R, Strivens, TA, *Paint and Surface Coatings Theory and Practice*. 2nd ed., Woodhead Publishing Ltd., Cambridge (1999).
5. Marrion, AR, *The Chemistry and Physics of Coatings*. 2nd ed., The Royal Society of Chemistry, Cambridge (2004).
6. Taylor, JW, Winnik, MA, "Functional latex and thermoset latex films". *JCT Res.*, **1** (3) 163-190 (2004).
7. Dusek, K, Duskova-Smrckova, M, "Network structure formation during crosslinking of organic coating systems". *Prog. Polym. Sci.*, **25** (9) 1215-1260 (2000).
8. Tsige, M, Lorenz, CD, Stevens, MJ, "Role of Network Connectivity on the Mechanical Properties of Highly Crosslinked Polymers". *Macromolecules*, **37** (22) 8466-8472 (2004).
9. Scanlan, JC, Webster, DC, Crain, AL, "Correlation Between Network Mechanical Properties and Physical Properties in Polyester-Urethane Coatings". *ACS Symp. Ser. (Film Formation in Waterborne Coatings)*, **648** 222-234 (1996).
10. Koleske, JV, *Paint and Coating Testing Manual*. 14th ed., ASTM publication, (1995).
11. Schwalm, R, "Crosslinking Effect on Mechanical Properties of UV Curable Coatings". *PPCJ, Polym. Paint Colour J.*, **189** (4421) 18-20, 22 (1999).
12. Johansson, M, Glauser, T, Jansson, A, Hult, A, Malmstrom, E, Claesson, H, "Design of coating resins by changing the macromolecular architecture: solid and liquid coating systems". *Prog. Org. Coat.*, **48** (2-4) 194-200 (2003).
13. Chattopadhyay, DK, Raju, KVS, "Structural Engineering of Polyurethane Coatings for High Performance Applications". *Prog. Polym. Sci.*, **32** (3) 352-418 (2007)

14. Mijs, WJ, "A brief history of the Athens conference on organic coatings, science and technology". *Prog. Org. Coat.*, **40** (1-4) 1-5 (2000).
15. Schoff, CK, "Organic coatings: the paradoxical materials". *Prog. Org. Coat.*, **52** (1) 21-27 (2005).
16. Geurink, PJA, Scherer, T, Buter, R, Steenbergen, A, Henderiks, H, "A Complete New Design for Waterborne 2-Pack PUR Coatings With Robust Application Properties". *Prog. Org. Coat.*, **55** (2) 119-127 (2006).
17. Tanabe, H, Ohsugi, H, "A New Resin System for Super High Solids Coating". *Prog. Org. Coat.*, **32** (1-4) 197-203 (1997).
18. de Meijer, M, "Review on the Durability of Exterior Wood Coatings With Reduced VOC-content". *Prog. Org. Coat.*, **43** (4) 217-225 (2001).
19. Raquez, JM, Deleglise, M, Lacrampe, MF, Krawczak, P, "Thermosetting (bio)materials derived from renewable resources: A critical review". *Prog. Polym. Sci.*, **35** (4) 487-509 (2010).
20. Overbeek, A, "Polymer heterogeneity in waterborne coatings". *J. Coat. Technol. Res.*, **7** (1) 1-21 (2010).
21. Clemitson, IR, Castable Polyurethane Elastomers. CRC press, Florida (2008).
22. Lonescu, M, Chemistry and Technology of Polyols for Polyurethanes. Rapra Technology Ltd., Shropshire (2005).
23. Krol, P, Linear Polyurethanes - Synthesis Methods, Chemical Structures, Properties and Applications. Koninklijke Brill NV, Leiden, The Netherlands, Boston (2008).

24. Ashida, K, Polyurethanes and Related Foams - Chemistry and Technology. CRC press, Florida (2007).
25. Thomson, T, Polyurethanes as Specialty Chemicals Principles and Applications. CRC press, Florida (2005).
26. Pascault, J-P, Williams, RJJ, Epoxy Polymers - New Materials and Innovations. WILEY-VCH Verlag GmbH & Co. KGaA, Weinheim (2010).
27. Wehlack, C, Possart, W, Krueger, JK, Mueller, U, "Epoxy and Polyurethane Networks in Thin Films On Metals - Formation, Structure, Properties". *Soft Mater.*, **5** (2 & 3) 87-134 (2007).
28. Renz, H, Bruchmann, B, "Pathways targeting solvent-free PUR coatings". *Prog. Org. Coat.*, **43** (1-3) 32-40 (2001).
29. Mundstock, H, Pires, R, Richter, F, Schmitz, J, "New low viscous polyisocyanates for VOC compliant systems". *Macromol. Symp.*, **187** 281-292 (2002)
30. Krol, P, "Synthesis methods, chemical structures and phase structures of linear polyurethanes. Properties and applications of linear polyurethanes in polyurethane elastomers, copolymers and ionomers". *Prog. Mater. Sci.*, **52** (6) 915-1015 (2007)
31. Yilgor, I, Yilgor, E, "Structure-Morphology-Property Behavior of Segmented Thermoplastic Polyurethanes and Polyureas Prepared without Chain Extenders". *Polym. Rev. (Philadelphia, PA, U. S.)*, **47** (4) 487-510 (2007)
32. Li, Q, Zhou, H, Wicks, DA, Hoyle, CE, Magers, DH, McAlexander, HR, "Comparison of Small Molecule and Polymeric Urethanes, Thiourethanes, and Dithiourethanes: Hydrogen Bonding and Thermal, Physical, and Mechanical Properties". *Macromolecules (Washington, DC, U. S.)*, **42** (6) 1824-1833 (2009)

33. Dearth, RS, Mertes, H, Jacobs, PJ, "An overview of the structure/property relationship of coatings based on 4,4'-dicyclohexylmethane diisocyanate (H12MDI)". *Prog. Org. Coat.*, **29** (1-4) 73-79 (1996)
34. Ni, H, Daum, JL, Soucek, MD, Simonsick, WJ, Jr., "Cycloaliphatic polyester based high solids polyurethane coatings: I. The effect of difunctional alcohols". *J. Coat. Technol.*, **74** (928) 49-56 (2002)
35. Tarlas, HD, "Amine Cured Epoxy Resin Coatings for Resistance to Atmospheric Corrosion". *Mater. Prot.*, **9** (5) 37-42 (1970)
36. May, CA, *Epoxy Resins - Chemistry and Technology*. 2nd ed., Marcel Dekker, Inc., New York (1988)
37. Crivello, JV, Narayan, R, "Epoxidized triglycerides as renewable monomers in photoinitiated cationic polymerization". *Chem. Mater.*, **4** (3) 692-9 (1992)
38. Earls, JD, White, JE, Dettloff, ML, Null, MJ, "Development and evaluation of terminally epoxidized triglycerides for coatings applications". *JCT Res.*, **1** (3) 243-245 (2004)
39. Crivello, JV, Liu, S, "Photoinitiated Cationic Polymerization of Epoxy Alcohol Monomers". *J. Polym. Sci., Part A: Polym. Chem.*, **38** (3) 389-401 (2000)
40. Shechter, L, Wynstra, J, Kurkjy, RP, "Glycidyl ether reactions with amines". *J. Ind. Eng. Chem. (Washington, D. C.)*, **48** 94-7 (1956)
41. Mustata, F, Bicu, I, "Multifunctional epoxy resins: synthesis and characterization". *J. Appl. Polym. Sci.*, **77** (11) 2430-2436 (2000)
42. Maity, T, Samanta, BC, Dalai, S, Banthia, AK, "Synthesis, characterisation and curing studies of BCCOMB". *Pigm. Resin Technol.*, **36** (1) 30-38 (2007)

43. Cheng, J,Chen, J,Yang, WT, "Synthesis and characterization of novel multifunctional epoxy resin". *Chin. Chem. Lett.*, **18** (4) 469-472 (2007)
44. Yang, Y,Chen, G,Liew, KM, "Preparation and analysis of a flexible curing agent for epoxy resin". *J. Appl. Polym. Sci.*, **114** (5) 2706-2710 (2009)
45. Edwards, PA,Striemer, G,Webster, DC, "Novel Polyurethane Technology Through Glycidyl Carbamate Chemistry". *J. Coat. Technol. Res.*, **2** (7) 517-527 (2005)
46. Edwards, PA,Erickson, J,Webster, DC, "Synthesis and Self-crosslinking of Glycidyl Carbamate Functional Oligomers". *Polym. Prepr. (Am. Chem. Soc., Div. Polym. Chem.)*, **44** (1) 54-55 (2003)
47. Edwards, PA,Erickson, J,Webster, DC, "Synthesis and Characterization of Glycidyl Carbamate Functional Oligomers". *Polym. Prepr. (Am. Chem. Soc., Div. Polym. Chem.)*, **44** (1) 144-145 (2003)
48. Edwards, PA,Striemer, G,Webster, DC, "Synthesis, Characterization and Self-crosslinking of Glycidyl Carbamate Functional Resins". *Prog. Org. Coat.*, **57** (2) 128-139 (2006)
49. Edwards, PA. Glycidyl carbamate resins to achieve polyurethane properties and epoxide reactivity. Ph.D. Dissertation, North Dakota State University, Fargo, 2004.
50. Suryanarayana, R. Zero VOC binder system from glycidyl carbamate functional resins. M. S. Thesis, North Dakota State University, Fargo, 2006.
51. Webster, DC,Suryanarayana, R, "Glycidyl carbamate coatings having improved corrosion resistance." PCT/US2008/086616, 2008.
52. Chattopadhyay, DK,Webster, DC, "Hybrid coatings from novel silane-modified glycidyl carbamate resins and amine crosslinkers". *Prog. Org. Coat.*, **66** (1) 73-85 (2009)

53. Chattopadhyay, DK,Zakula, AD,Webster, DC, "Organic-inorganic hybrid coatings prepared from glycidyl carbamate resin, 3-aminopropyl trimethoxy silane and tetraethoxyorthosilicate". *Prog. Org. Coat.*, **64** (2-3) 128-137 (2009)
54. Chattopadhyay, DK,Muehlberg, AJ,Webster, DC, "Organic-inorganic hybrid coatings prepared from glycidyl carbamate resins and amino-functional silanes". *Prog. Org. Coat.*, **63** (4) 405-415 (2008)
55. Howarth, GA, "Legislation-compliant polyurethane and epoxy coatings". *Pigm. Resin Technol.*, **29** (6) 325-336 (2000)
56. Decker, C, "Photoinitiated crosslinking polymerization". *Prog. Polym. Sci.*, **21** (4) 593-650 (1996)
57. Irfan, M,Seiler, M, "Encapsulation Using Hyperbranched Polymers: From Research and Technologies to Emerging Applications". *Ind. Eng. Chem. Res.*, **49** (3) 1169-1196 (2010)
58. Yagci, Y,Jockusch, S,Turro, NJ, "Photoinitiated Polymerization: Advances, Challenges, and Opportunities". *Macromolecules (Washington, DC, U. S.)*, ACS ASAP (2010)
59. Manczyk, K,Szewczyk, P, "Highly branched high solids alkyd resins". *Prog. Org. Coat.*, **44** (2) 99-109 (2002)
60. Huybrechts, JT,Tanghe, LM, "2.1 VOC solvent borne 2K clear coats based on star oligoethers". *Prog. Org. Coat.*, **58** (2-3) 217-226 (2007)
61. De, GTFA,Smulders, MMJ,Wolffs, M,Schenning, APHJ,Sijbesma, RP,Meijer, EW, "Supramolecular Polymerization". *Chem. Rev. (Washington, DC, U. S.)*, **109** (11) 5687-5754 (2009)

62. Nair, KP, Breedveld, V, Weck, M, "Complementary Hydrogen-Bonded Thermoreversible Polymer Networks with Tunable Properties". *Macromolecules (Washington, DC, U. S.)*, **41** (10) 3429-3438 (2008)
63. Sijbesma, RP, Beijer, FH, Brunsveld, L, Folmer, BJB, Hirschberg, JHKK, Lange, RFM, Lowe, JKL, Meijer, EW, "Reversible polymers formed from self-complementary monomers using quadruple hydrogen bonding". *Science (Washington, D. C.)*, **278** (5343) 1601-1604 (1997)
64. Shaffer, M, Stewart, R, Allen, K, Wylie, A, Lockhart, A, Two component polyurethane coatings: High performance crosslinkers meet the needs of demanding applications. *Journal of Coatings Technology CoatingsTech* January 2009, 2009, pp 50-55.
65. Galgoci, EC, Komar, PC, Elmore, JD, "High performance waterborne coatings based on dispersions of a solid epoxy resin and an amine-functional curing agent". *J. Coat. Technol.*, **71** (891) 45-52 (1999)
66. Melchior, M, Sonntag, M, Kobusch, C, Jurgens, E, "Recent developments in aqueous two-component polyurethane (2K-PUR) coatings". *Prog. Org. Coat.*, **40** (1-4) 99-109 (2000)
67. Wicks, ZW, Wicks, DA, Rosthauser, JW, "Two package waterborne urethane systems". *Prog. Org. Coat.*, **44** (2) 161-183 (2002)
68. Elmore, JD, Kincaid, DS, Komar, PC, Nielsen, JE, "Waterborne epoxy protective coatings for metal". *J. Coat. Technol.*, **74** (931) 63-72 (2002)
69. Larry Steven Corley, Kincaid, DS, young, GC, "Amine-terminated polyamide in oil-in-water emulsion." US 5,962,269, 1999.

70. Larry Steven Corley, Kincaid, DS, young, GC, "Aqueous dispersion of polyamide-amine derived from aminoalkylpiperazine epoxy resin." US 5,998,508, 1999.
71. Stark, CJ, Elmore, JD, Back, GE, Wang, PC, Galgoci, EC, "Aqueous dispersion of epoxy resins." US 6,221,934, 2001.
72. Matthias, L, Cook, M, Klippstein, A, "Method of preparation of a water based epoxy curing agent." US 7,615,584 B2, 2009.
73. Back, GE, Wang, PC, Corley, LS, Elmore, KD, "Water dispersible epoxy resins." US 6,956,086 B2, 2005.
74. Lange, J, Stenroos, E, Johansson, M, Malmstrom, E, "Barrier coatings for flexible packaging based on hyperbranched resins". *Polymer*, **42** (17) 7403-7410 (2001)
75. Choi, M-C, Kim, Y, Ha, C-S, "Polymers for flexible displays: From material selection to device applications". *Prog. Polym. Sci.*, **33** (6) 581-630 (2008)
76. Bierwagen, G, Brown, R, Battocchi, D, Hayes, S, "Active metal-based corrosion protective coating systems for aircraft requiring no-chromate pretreatment". *Prog. Org. Coat.*, **68** (1-2) 48-61 (2010)
77. Bierwagen, G, "Next generation of aircraft coatings systems". *J. Coat. Technol.*, **73** (915) 45-52 (2001)
78. Bierwagen, GP, Tallman, DE, "Choice and measurement of crucial aircraft coatings system properties". *Prog. Org. Coat.*, **41** (4) 201-216 (2001)
79. Baboion, R, *Corrosion Tests and Standards Applications and Interpretations*. 2nd ed., ASTM International, West Conshohocken (2005)
80. Schmitt, RJ, Perez, LA, Montague, RA, Tetenbaum, MT, Van, BEJ, "Elastomeric coating compositions." US 4,692,382, 1987.

81. Carson, DW, Schmitt, RJ, Seneker, CA, Kuren, T, Av, Wallace, DR, "Flexible primer compositions and method of providing a substrate with a flexible multilayer coatings." US 4,680,346, 1987.
82. Carson, D, Schmitt, R, Seneker, C, Kuren, T, Wallace, D, "Flexible primer compositions and method of providing a substrate with a flexible multilayer coatings." US 4,720,405, 1988.
83. Morkunas, BT, Sawant, SG, Walker, JA, Omar, AA, "Flexible, impact-resistant two-component epoxy amine primer." US 2005/0288456 A1, 2005.
84. Charves, E, Pulley, DF, Stander, AO, "Sealant-primer coating." US 4,101,497, 1978.
85. Schwalm, R, UV Coatings - Basics, Recent Developments and New Applications. Elsevier Science (2006)
86. Decker, C, "Kinetic study and new applications of UV radiation curing". *Macromol. Rapid Commun.*, **23** (18) 1067-1093 (2002)
87. Mehnert, R, Pincus, A, Janorsky, I, Stowe, R, Berejka, A, UV and EB Curing Technology and Equipment. SITA Technology Ltd., London (1998) Vol. I,
88. Decker, C, "UV-radiation curing chemistry". *Pigm. Resin Technol.*, **30** (5) 278-286 (2001)
89. Decker, C, "Light-induced crosslinking polymerization". *Polym. Int.*, **51** (11) 1141-1150 (2002)
90. Rao, AV, Kanitkar, DS, Parab, AK, "Some specialty coatings from radiation curable poly(acrylic) combinations". *Prog. Org. Coat.*, **25** (3) 221-33 (1995)

91. Shukla, V, Bajpai, M, Singh, DK, Singh, M, Shukla, R, "Review of basic chemistry of UV-curing technology". *Pigm. Resin Technol.*, **33** (5) 272-279 (2004)
92. Crivello, JV, Dietliker, K, Bradley, G, Photoinitiators for Free Radical, Cationic and Anionic Photopolymerization. 2nd ed., SITA Technology Ltd., London (1998) Vol. III,
93. Webster, G, Prepolymers and Reactive Diluents - Chemistry and Technology of UV and EB Formulation for Coatings, Inks and Paints. SITA Technology Ltd., London (1996) Vol. II,
94. Chattopadhyay, DK, Panda, SS, Raju, KVS, "Thermal and mechanical properties of epoxy acrylate/methacrylates UV cured coatings". *Prog. Org. Coat.*, **54** (1) 10-19 (2005)
95. Safranski, DL, Gall, K, "Effect of chemical structure and crosslinking density on the thermo-mechanical properties and toughness of (meth)acrylate shape memory polymer networks". *Polymer*, **49** (20) 4446-4455 (2008)
96. van, HJ, Oostveen, EA, Micciche, F, Noordover, BAJ, Koning, CE, van, BRATM, Frissen, AE, Weijnen, JGJ, "Resins and additives for powder coatings and alkyd paints based on renewable resources". *J. Coat. Technol. Res.*, **4** (2) 177-186 (2007)
97. Lindeboom, J, "Air-drying high solids alkyd paints for decorative coatings". *Prog. Org. Coat.*, **34** (1-4) 147-151 (1998)
98. Samuelsson, J, Johansson, M, "A study of fatty acid methyl esters with epoxy or alkyne functionalities". *J. Amer. Oil Chem. Soc.*, **78** (12) 1191-1196 (2001)
99. van, GR, Bouwman, E, "The oxidative drying of alkyd paint catalysed by metal complexes". *Coord. Chem. Rev.*, **249** (17-18) 1709-1728 (2005)

100. Wicks, DA,Wicks, ZW, "Autoxidizable urethane resins". *Prog. Org. Coat.*, **54** (3) 141-149 (2005)
101. Xu, Y,Yan, C,Ding, J,Gao, Y,Cao, C, "Water vapor in the coatings of alkyd and polyurethane varnish". *Prog. Org. Coat.*, **45** (4) 331-339 (2002)
102. Pan, X,Nelson, TJ,Webster, DC, "Novel enamine formation (EF) and air-drying (AD) co-curable coating resins: miscible blends of sucrose esters". *PMSE Prepr.*, No pp. given (2010)
103. Sengupta, PP,Pan, X,Nelson, TJ,Paramarta, A,Webster, DC, "Cationic UV curing characteristics of epoxidized sucrose esters". *PMSE Prepr.*, No pp. given (2010)

CHAPTER 2. STRUCTURAL MODIFICATION OF GLYCIDYL

CARBAMATE RESINS

2.1. Introduction

Polyurethane and epoxy systems represent commercially important segments in the coatings industry and are widely used in many applications such as protective, industrial and architectural coatings, as well as being used in composites and adhesives. Urethane and epoxy coatings have their own distinct advantages. Polyurethane coatings show excellent mechanical properties (such as toughness and flexibility) and chemical resistance. The excellent toughness and flexibility of polyurethane coatings are due to intermolecular hydrogen bonding which undergoes reversible bond breakage and formation during the application of cyclic loading.^{1, 13} Epoxy coatings have excellent corrosion resistance, chemical resistance, adhesion and versatility in crosslinking chemistry.³⁵ Epoxy groups can react with nucleophiles such as amines, undergo ring opening polymerization at high temperature or react under cationic ring opening conditions to produce crosslinked networks.^{1, 39, 46, 104} Glycidyl carbamate functional resins are synthesized by the reaction of an isocyanate functional compound with glycidol to yield a carbamate (urethane) linkage (-NHCO-) and reactive epoxy group in the final product. Glycidyl carbamate chemistry results in a resin that contains both the urethane and the epoxy functionalities in its chemical structure. The combination of both functionalities in a single resin structure imparts excellent mechanical and chemical properties to the coatings.^{45, 47, 49} Glycidyl carbamate chemistry also reduces the hazards of isocyanates present in the end-use application of 2K urethane coating formulations. Previous studies showed that glycidyl carbamate (GC) resins based on hexamethylene

diisocyanate biuret (HDB) or hexamethylene diisocyanurate trimer (HDT) resins and glycidol could be synthesized. The corresponding GC resins obtained from biuret and isocyanurate polyisocyanate resins were designated “biuret glycidyl carbamate” (BGC) resin and “isocyanurate glycidyl carbamate” (IGC) resin, respectively. The coatings made from GC resins can be cured either using amine crosslinkers or by self-crosslinking at elevated temperature. An excellent combination of mechanical and chemical properties had been shown with GC coatings.^{45, 49} However, these GC resins have very high viscosity—in the range of millions of mPa·s—and a significant amount of organic solvent is required to achieve suitable application viscosity. In a previous study, Suryanarayana approached this problem by using plasticizers and VOC exempt solvents. Suryanarayana also explored using diisocyanates (aliphatic and aromatic) instead of polyisocyanates (HDI biuret and isocyanurate) to obtain GC resins. Plasticizers (dioctyl phthalate, dibutyl phthalate and diisononyl phthalate) were mixed with BGC and IGC to reduce viscosity. The plasticizer approach did not reduce the viscosity significantly. VOC exempt solvents used were tertiary butyl acetate (TBA), methyl acetate, acetone, oxsol, and acetone. TBA reduced the viscosity when added in high levels. Other isocyanates used to obtain low viscosity GC resins were aliphatic and aromatic diisocyanates. Amine crosslinked GC coatings made from aliphatic and aromatic diisocyanate had lower resistance to impact and solvent compared to that of BGC and IGC coatings.⁵⁰ Thus, it was of interest to determine if the BGC and IGC type resins could be modified to yield lower viscosity. Lower viscosity resins could also reduce the amount of volatile organic compounds (VOCs) required in the final coating formulation. Legislation regarding VOC content is very stringent and the coatings industry is focused on the development of coating systems

that contain minimal or zero VOC. Methods such as high solids coatings (low viscosity resins), UV curing, water borne and powder coating techniques are all viable approaches to reduce VOC.¹⁶⁻¹⁸

In the present study, GC resins based on BGC were synthesized by replacing part of the glycidol with aliphatic alcohols and ether alcohols to obtain lower viscosity resins. Since the resins are made using a multifunctional isocyanate, it is possible to react part of the isocyanate groups with alcohol and leave sufficient isocyanate to create resins having at least two glycidyl carbamate groups. The effect of the amount of modifier on resin viscosity was also investigated by making a series of BGC-EP resins where the amount of modification by ethyleneglycol monopropyl ether (EP) was systematically varied. The performance of BGC, modified GC and BGC-EP series resins in both amine-cured and self-crosslinked clear coatings was studied. A correlation between resin structures and their coating properties was obtained.

2.2. Experimental

2.2.1. *Materials*

Hexamethylene diisocyanate biuret (HDB), a biuret resin condensate derived from hexamethylene diisocyanate (Tolonate HDB-LV), was provided by Rhodia Inc. HDB-LV has an NCO equivalent weight of 175.44 g/eq. Glycidol was supplied by Dixie Chemical. Glycidol was stored refrigerated to minimize the formation of impurities. The modifiers, alcohols and ether alcohols, used were 2-ethyl hexanol (2EHA) (Alfa Aesar), isobutanol (IsoBuOH) (Alfa Aesar), 1-butanol (1BuOH) (J. T. Baker), ethylene glycol butyl ether (EB) (Aldrich), diethylene glycol butyl ether (DB) (Aldrich) and ethylene glycol propyl ether (EP) (Fluka-Aldrich). Dibutyltindilaurate (DBTDL), purchased from

Aldrich, was used to catalyze the isocyanate and hydroxyl reactions to form the glycidyl carbamate (GC) resins. All reagents were used as received without any further purification.

Solvents used for the coating formulations were ethyl 3-ethoxy propionate (EEP) and tertiary butyl acetate (TBA), obtained from Aldrich and Ashland, respectively. Air Products provided the two amine crosslinkers, para-aminocyclohexyl methane (PACM) and Ancamide-2353 (A-2353), having hydrogen equivalent weight (gm/H) of 52.5 and 114, respectively. Ancamide-2353 is a mixture of polyamides of different molecular weights.

2.2.2. Synthesis of glycidyl carbamate functional compounds

A 500 ml four neck reaction vessel was used for the synthesis of BGC, modified GC and BGC-EP series resins. The vessel was fitted with a condenser, nitrogen inlet and Model 210 J-KEM temperature controller and a mechanical stirrer. A water bath was used for heating and cooling the vessel. The stoichiometric equivalent amount of isocyanates and glycidol based on $-NCO$ and $-OH$ groups used for the synthesis of BGC resin was 1:1 (NCO:glycidol). The stoichiometric equivalent amount of NCO, glycidol and a modifier based on total $-NCO$ and $-OH$ groups used for the synthesis of modified GC resins was 1:0.66:0.33 (NCO:glycidol:modifier). In the synthesis of series of BGC-EP resins (BGC-EP 15 mol %, BGC-EP 25 mol %, BGC-EP 40 mol % and BGC-EP 45 mol %), the stoichiometric equivalent amounts of NCO, glycidol and EP used were 1:0.85:0.15, 1:0.75:0.25, 1:0.60:0.40 and 1:0.55:0.45, respectively.

During the synthesis of resins, the reaction vessel was charged with HDB-LV followed by addition of the required amounts of glycidol and modifier. The reaction

mixture was stirred for about 45 – 60 min. at 40 – 45 °C to ensure a homogeneous mixture. The catalyst (DBTDL), in the form of solution in tertiary butyl acetate (1 – 2 % by wt.), was added after the completion of mixing. The amount of catalyst added was 0.03 % by wt. (of the total reaction charge). After the addition of catalyst around at about 40 – 45 °C, all of the reactions showed an exotherm, bubble formation and an increase in viscosity. The reactions were continued until the –NCO peak in FTIR spectra disappeared completely. After the completion of the reactions, the resins were collected in glass jars.

2.2.3. FTIR measurements

The FTIR measurements were performed using a Nicolet Magna-850 FTIR spectrometer. Sample aliquots were taken and coated on a potassium bromide salt plate. Spectra acquisitions were based on 64 scans with a data spacing of 1.98 cm^{-1} . The FTIR was set for auto gain to monitor spectral range of $4000 - 500\text{ cm}^{-1}$. The change in band absorption of isocyanate (2272 cm^{-1}), -OH and -NH ($3750 - 3000\text{ cm}^{-1}$), amide (1244 cm^{-1}) and epoxide (910 cm^{-1}) bands were used to follow the reaction progress.

2.2.4. NMR characterization

^{13}C NMR was done for BGC and modified GC resins using a JEOL-ECA (400 MHz) NMR spectrometer coupled with an auto-sampler accessory. The spectra were run at 24 °C with 1000 scans. All the spectra were collected by dissolving 50 to 70 mg samples in 0.7 ml CDCl_3 . The spectra were analyzed using Delta NMR processing and control software (Version 4.3.5).

2.2.5. Gel permeation chromatography

Gel permeation chromatography (GPC) was conducted using a Waters GPC instrument with a Waters 2410 refractive index detector. The samples were dissolved in

tetrahydrofuran (THF) at 1 mg cm^{-3} concentration and were filtered with a $0.2 \text{ }\mu\text{m}$ PTFE filter. The flow rate and injection volume used were 1 ml min^{-1} and $200 \text{ }\mu\text{l}$, respectively. Polystyrene standards were used for calibration.

2.2.6. Viscosity measurements

A Brookfield DV-II+Pro viscometer was used for the viscosity measurements. Amount of the resins used for viscosity measurement was about 300 gm in glass jars. Spindle number 7 was used between 0.5 to 2 rpm. Six to eight readings of viscosity over a period of 10 minutes were averaged.

2.2.7. Epoxy titration

Epoxy equivalent weight of the resins was determined by titration with hydrogen bromide (HBr) according to ASTM D1652. The required amount of resin (0.06 to 0.8 gm) was dissolved in 5 – 10 ml of chloroform and was titrated against a standardized HBr solution prepared in glacial acetic acid. The indicator used was a solution of crystal violet in glacial acetic acid. End point of the titration was the appearance of permanent yellow-green color.

2.2.8. Coating preparation

Amine crosslinked and self-crosslinked coating formulations were made for the coating performance study. The solvents used for all the coating formulations were ethyl 3-ethoxy propionate (EEP) (20 % by wt.) and tertiary butyl acetate (TBA) (20 % by wt.). The amine crosslinkers used were para-aminocyclohexyl methane (PACM) and Ancamide-2353 (A-2353). Amine active hydrogen:epoxy equivalent ratio was 1:1 in all of the formulations. The formulations were warmed up using heating mantle to get good mixing and flow and were allowed to sit for 15 min before taking drawdowns. The films

were drawdown at a wet thickness of 8 mils using a drawdown bar on steel panels (smooth finished Q panels, type QD36, 0.5×76×152 mm) cleaned with *p*-xylene. Films were also applied to glass panels to obtain free films for tensile test, DMA, DSC, and TGA measurements. The coated panels were kept at ambient conditions overnight and the next day the coated panels were cured in an oven at 80 °C for an hour. All the panels were kept at ambient after curing and were tested after fourteen days. The free films were obtained for tensile test. The cured coatings on glass panels were kept under water overnight and the free coating films were removed the next day using razor blade. The free films were kept at ambient for a day for the removal of water before the tensile test.

The self-crosslinked coating formulations were made in the same way as above except that no amine crosslinkers were used. The coating films were applied as described above. The coated panels were cured at 150 °C for 1 hr and 45 min. The cured coatings were kept at ambient conditions for three days before their properties were evaluated.

The coating samples used for electrochemical impedance spectroscopy (EIS) and salt spray test were applied in two coats. Two coats of the same coatings were used to minimize the local defects in the coatings. The first coat was drawdown at 4 mils and kept at ambient for two days before curing at 80 °C for 1 hr. The second coat at 5 mils was drawdown on the previously coated and cured panels. After keeping the coatings at ambient for two days, the coatings were again cured at 80 °C for 1hr. Finally, all the coatings were kept at ambient for 8 - 9 days before they were characterized by electrochemical impedance spectroscopy (EIS) and by salt spray test. The coating thickness was 80 – 95 μm.

2.2.9. Coating performance

König pendulum hardness of the coatings was measured following ASTM D 4366. The hardness test results are reported in seconds (sec). Reverse impact strength of the coatings was determined following ASTM D 2794 using a Gardener impact tester. The maximum drop height was 43 inches and the drop weight was 4 pounds. Crazeing or loss of adhesion was noted and inch-pounds (in-lbs) were reported at film finish failure. Samples that did not fail were noted as having an impact strength of >172 in-lbs. The conical mandrel test was also used according to ASTM D 522 for the determination of flexibility of the coatings. The results of the flexibility test were reported as the length of a crack (cm) formed on the coating during the test. Methyl ethyl ketone (MEK) double rubs test was used according to ASTM D 5402 to assess the chemical resistance and development of cure. A 26-ounce hammer with three layers of cheesecloth wrapped around the hammerhead was soaked in MEK. The hammer head was rewet with MEK after 30 – 50 double rubs. Once mar was achieved, a number of double rubs was noted. Cross hatch adhesion of the coatings was evaluated using a Gardco cross hatch adhesion instrument following ASTM D 3359.

2.2.10. Differential scanning calorimetry (DSC)

A TA Instruments Q1000 differential scanning calorimeter (DSC) coupled with an auto sampler accessory was used to determine the glass transition temperature (T_g) of the coatings. DSC experiments were performed by placing a sample into the conventional aluminum pans. The samples were subjected to a heat-cool-heat cycle. The samples were heated to 200 °C and then cooled to -75 °C and held there for 5 min. DSC thermograms

were taken from -75 °C to 250 °C at a heating rate of 10 °C min⁻¹. Glass transition temperature was determined as the temperature of the inflection at the mid-point.

2.2.11. Thermogravimetric analysis (TGA)

TGA was performed using a TA Instruments Q500. Temperature was ramped from ambient to 800 °C with a ramp rate of 10 °C min⁻¹. A nitrogen atmosphere was used during the test. Weight retained was plotted as a function of temperature.

2.2.12. Dynamic mechanical analysis (DMA)

A TA Instruments Q800 Dynamic Mechanical Analysis system was used to determine the viscoelastic properties of the cured coating films. The dimensions of free films used were of 23 to 26 mm in length, 5 mm in width and 0.09 to 0.1 mm in thickness. Poisson's ratio was assumed to be 0.4 for all of the coating films. The experiments were carried out within a temperature range of -20 °C to 200 °C with a temperature ramp rate of 5 °C min⁻¹ at a frequency of 1 Hz. Crosslink density was calculated by measuring storage modulus (E') of the cured coatings in the rubbery plateau around 50 °C greater than T_g .

2.2.13. Tensile test

Tensile testing of the coatings was performed using an Instron 5542 instrument. The test specimen were prepared according to ASTM D 638-5 method. The test was carried out at 10 mm/min at ambient conditions. Elongation at break and Young's modulus of the coatings were recorded.

2.2.14. Electrochemical impedance spectroscopy (EIS)

Figure 2.1 is a schematic representation of EIS experiment performed using the conventional three-electrode system. The conventional EIS set up consists of metal

substrate as the working electrode (WE) with Platinum (Pt) and saturated calomel electrode (SCE) as counter and reference electrodes, respectively. A Gamry Instruments R 600 Potentiostat/Galvanostat/ZRA and Gamry Framework Version 5.20/EIS 300 software supplied by Gamry Instruments, Inc. of Willow Grove, PA were used for the experiments. The impedance response corresponding to the applied frequency of 100 kHz to 0.01 Hz was measured with an acquisition rate of 10 points per decade. A 10mV amplitude perturbation potential with respect to the open circuit potential was used during the measurement.

Perspex cylinder with a surface area of 7.07 cm^2 was mounted on the samples and was clamped with an O-ring insert for the electrochemical measurements. All the EIS measurements were performed under immersed condition using 5% NaCl solution as the electrolyte. Initially an EIS measurement at zero time was performed to check for any application defect. The samples were kept at immersed condition for seven days to facilitate electrolyte penetration through the coatings. EIS measurements were performed after 2.5 hrs and after seven days.

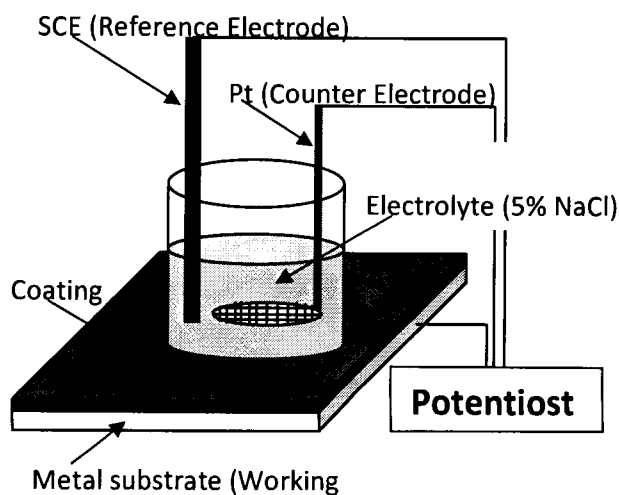


Figure 2.1. Schematic representation of EIS experiment performed using the conventional three-electrode system.

2.2.15. Salt spray test (ASTM B 117)

The coated panels were scribed and exposed to continuous salt spray (5 % NaCl in deionized water) fog at 35 °C for ten days. The images of the coatings were taken periodically by scanning.

2.3. Results and discussion

To study the effect of structural modification of GC resins and their coating performance, the experiments were carried out in two stages. First, a series of modified GC resins was obtained by replacing 33 mol % of glycidol equivalents with different alkyl alcohols and ether alcohols. Since the base polyisocyanate used to synthesize the resins has three or more isocyanate groups per molecule, reacting the polyisocyanate with 33 mole percent alcohol and the remainder with glycidol results in resins with a statistical average of at least two epoxy groups per molecule. In the second part of the study, to study the effect of the level of alcohol substitution on resin viscosity and coatings properties, a series of resins was prepared by replacing glycidol equivalents with EP in a series of 0, 15, 25, 33, 40 and 45 mole percent.

2.3.1. Modified GC resins and their coating performance

2.3.1.1. *Synthesis of BGC and modified GC resins*

The addition reaction of an isocyanate with the hydroxyl group of glycidol yields the glycidyl carbamate functional group. Figure 2.2 is a schematic representation of the reaction for the synthesis of GC resins.⁴⁵

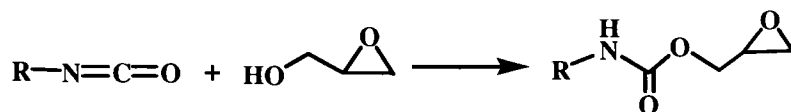


Figure 2.2. Schematic representation of the synthesis of GC resins.

The synthesis of glycidyl carbamate resins can be highly exothermic and can become uncontrolled if appropriate heat transfer techniques are not implemented. Beside this, the amount of catalyst added and the temperature at which the catalyst is added can influence the exothermic nature. Figure 2.3 is a schematic representation of the synthesis of the modified GC resins.

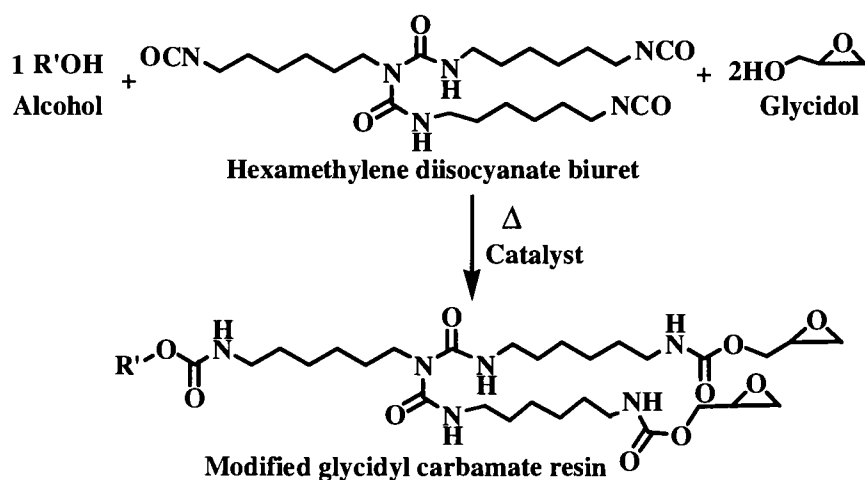


Figure 2.3. Schematic representation of the synthesis of modified GC resins.

If glycidol is the only alcohol used for the synthesis of the GC resin, the resin obtained is BGC. When 33 mol % of the glycidol is replaced with an alcohol or ether alcohol, the corresponding modified GC resin is obtained. Table 2.1 shows the alcohols used, the name of the corresponding modified GC resins formed, and epoxy equivalent weight (EEW) of the resins synthesized in this study. Compared with the synthesis reactions of the ether alcohol modified GC resins, the synthesis reactions of the BGC and alcohol modified GC resins were found to be more exothermic. The modified GC resins synthesized were characterized using FTIR, GPC, ^{13}C NMR and Brookfield viscometry.

2.3.1.2. Characterization of GC resins.

Figure 2.4 shows the FTIR spectra for BGC and the modified GC resins synthesized in this study. Compared to BGC, the modified GC resins showed FTIR spectra with corresponding peaks. The appearance of the amide (1244 cm^{-1}) and epoxide (910 cm^{-1}) peaks indicated the presence of urethane and epoxy functionalities in the resin structures.^{105, 106} A change in the band absorptions of isocyanate (2272 cm^{-1}), -OH and -NH ($3750\text{ to }3000\text{ cm}^{-1}$) was used to monitor the progress of the reaction. The synthesis of the BGC-EP series resins was also analyzed in a similar way.

Table 2.1. Chemical structures of the materials used for the modification of GC resins and the epoxy equivalent weight (EEW) of the GC resins synthesized.


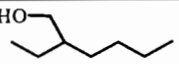
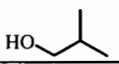
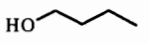
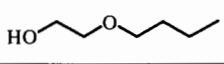
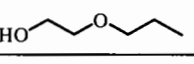
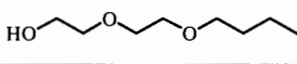
Name of R'OH	Structure of R'OH	Corresponding GC Resins	EEW (gm/eq)
Glycidol (Control)		BGC	255
2-Ethyl Hexanol (2EHA)		BGC-2EHA	450
Isobutanol (IsoBuOH)		BGC-IsoBuOH	405
1-Butanol (1BuOH)		BGC-1BuOH	391
Ethyleneglycol Butylether(EB)		BGC-EB	319
Ethyleneglycol Propylether(EP)		BGC-EP	355
Diethyleneglycol Butylether(DB)		BGC-DB	384

Figure 2.5 shows the GPC chromatograms of HDB-LV (biuret) and BGC-EP resins. The GPC of HDB-LV shows peaks for the various oligomers present in the resin. Compared with the elution pattern for the HDB-LV resin, the elution pattern for the BGC-EP resin is slightly shifted to a lower elution time. The lower elution time in GPC indicates an increase in the molecular weight.¹⁰⁷ The slight shift in the elution time

indicated that alcohol and glycidol were merely added to HDB-LV without any significant additional chain extension. GPC curves of the other resins were similar.

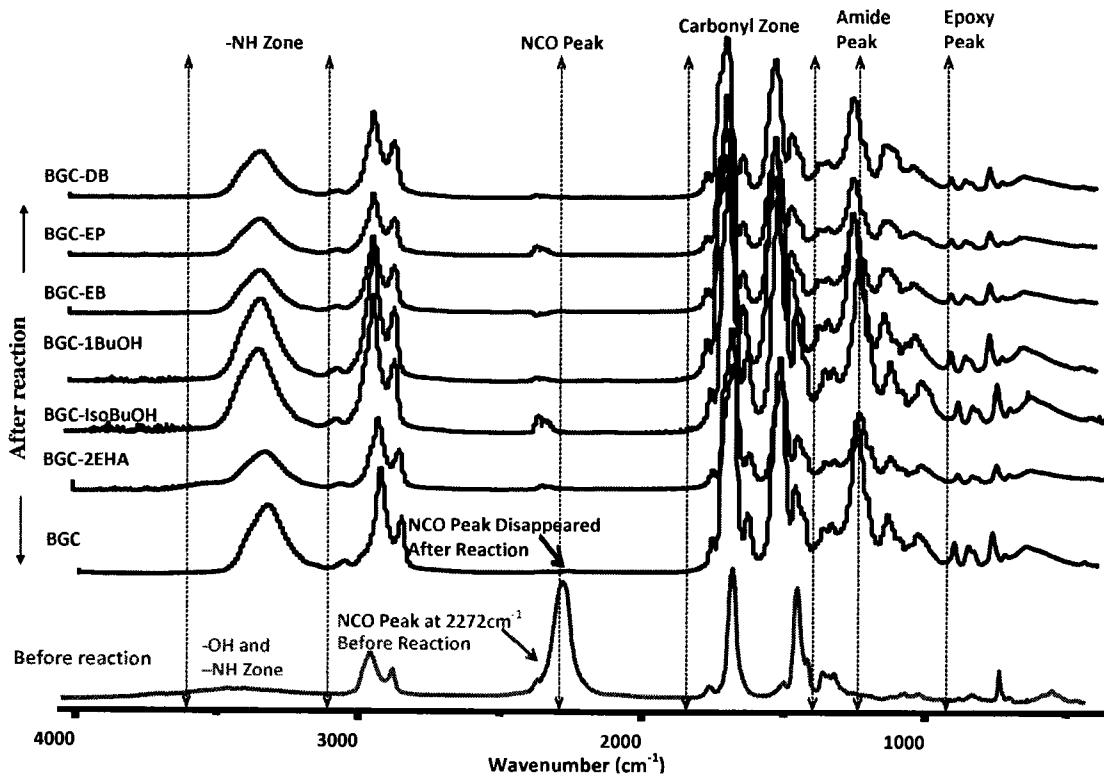


Figure 2.4. FTIR spectra of BGC and modified GC resins.

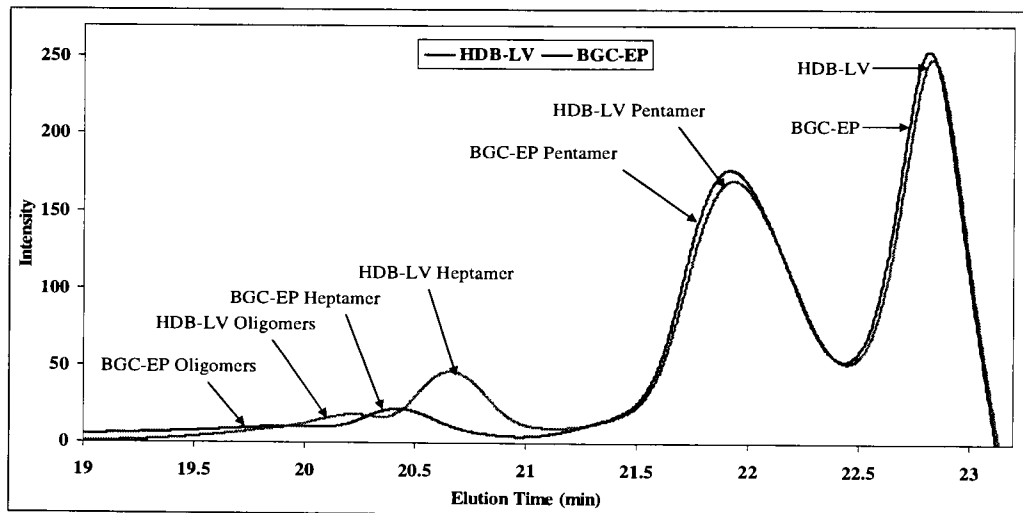


Figure 2.5. GPC Chromatograms for HDB-LV and BGC-EP resin.

^{13}C NMR was found to be a very useful technique for the analysis of the structures of the modified GC resins. The peak assignments of ^{13}C NMR spectra of BGC were found to be consistent with the previous findings.⁴⁸ Figure 2.6 shows the ^{13}C NMR spectra of the BGC and modified GC (BGC-1BuOH) resins. When the ^{13}C NMR spectra of modified GC resins were compared with BGC spectra, they showed a good correlation in carbon assignments. The ^{13}C NMR assignments of BGC and BGC-1BuOH resins were correlated to each other except the additional peaks appeared for BGC-1BuOH because of methyl and methylene group carbons in butanol. Similar results were observed when ^{13}C NMR spectra of the other modified GC resins were compared with that of BGC resin.

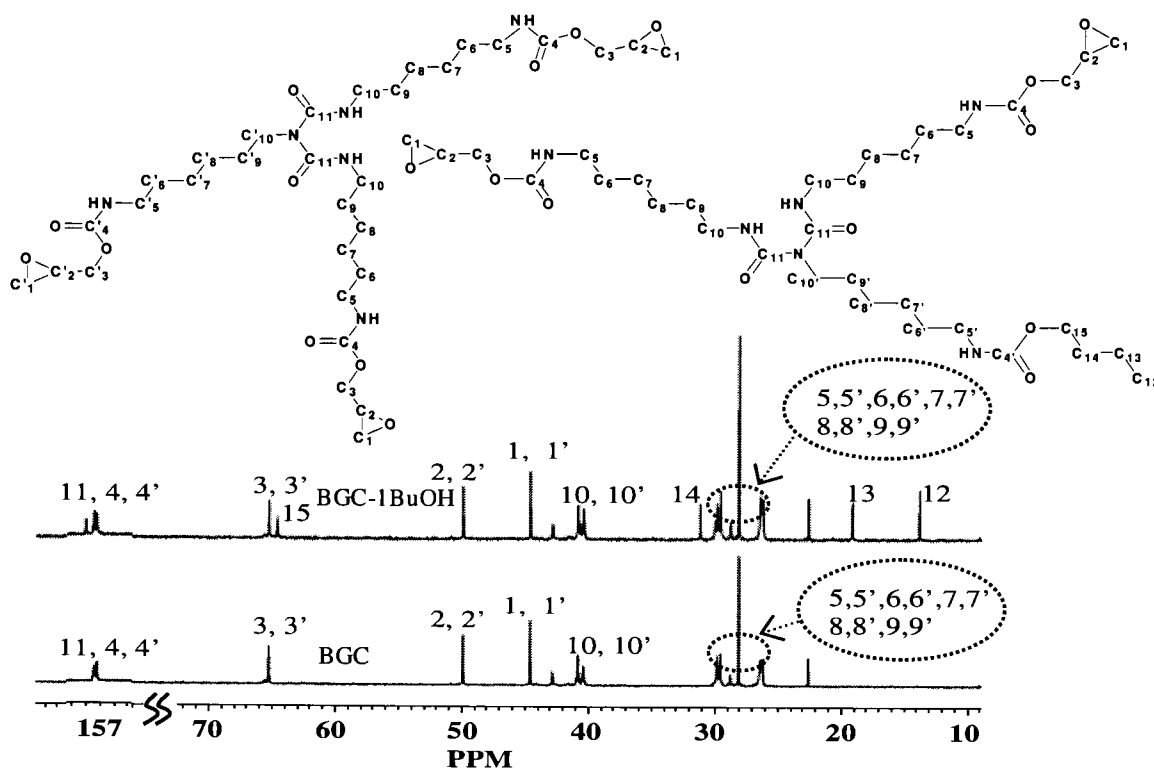


Figure 2.6. ^{13}C NMR spectra of BGC and modified GC resin, BGC-1BuOH.

2.3.1.3. Viscosity of modified GC resins

The base BGC resin consists of both the epoxy and urethane groups in its structure and coatings made from BGC show an excellent combination of mechanical properties.⁴⁵ However, BGC resin has a very high viscosity in the range of 3,210,000 to 3,680,000 mPa.s. The high viscosity of the resin is probably due to the large number of hydrogen bonding groups (-NH and -C=O) in the resin structure which could facilitate the formation of a dense network of inter chain hydrogen bonds. Figure 2.7 shows the proposed structures of BGC, BGC-1BuOH and BGC-DB. The work of Nair and coauthors and Stadler and coauthors showed that a high degree of interchain connectivity and network formation in the polymers could be produced due to hydrogen bonding, influencing their rheological properties.¹⁰⁸⁻¹¹⁰

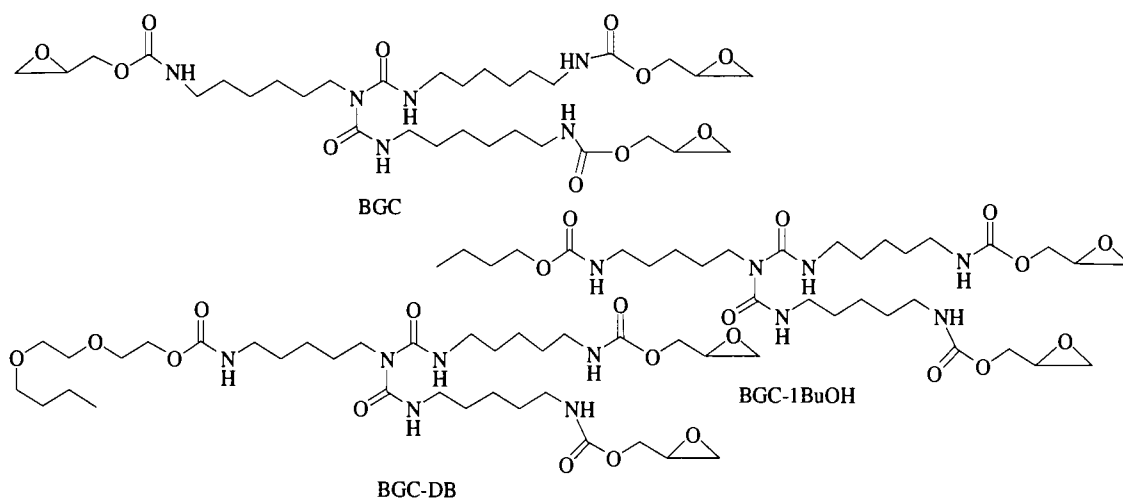


Figure 2.7. Structures of BGC, BGC-1BuOH and BGC-DB.

The viscosity of the resins was found to depend on the type of the alcohols and ether alcohols used for the modification of their structures. When one third of the glycidol was replaced by alcohols or ether alcohols, a dramatic reduction in viscosity compared with that of the base BGC resin was found. Figure 2.8(a) compares the viscosities of the

BGC and modified GC resins (neat resins). Figure 2.8(a) indicates that the type of modifier used, such as alcohol or ether alcohol, significantly influences the viscosity of the resins. The alcohol modification of BGC resins is able to reduce the viscosity up to about 90%. The primary effect is likely due to plasticization of the resin by the alkyl chains of the modifiers. Ether alcohols were found to be the most effective in viscosity reduction probably because of the ether bonds in their structure. Among the ether alcohols, diethyleneglycol butyl ether was found to be the most effective in viscosity reduction as it has two ether groups.

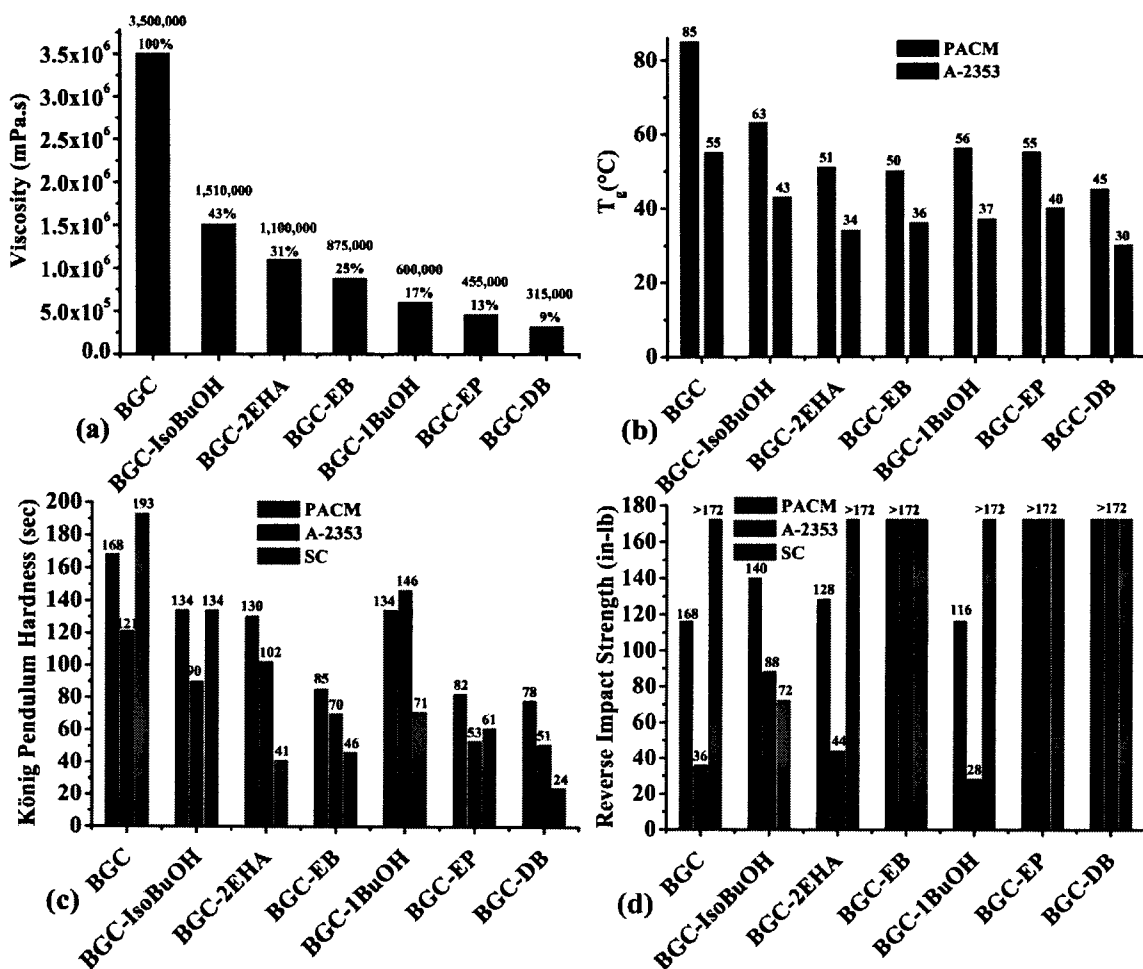


Figure 2.8. Property trends for control BGC resin and alcohol modified GC resins and coatings. (a) Resin viscosities (neat resins), (b) Glass transition temperature (T_g), (c) König pendulum hardness, (d) Reverse impact strength of the coatings.

2.3.1.4. Performance of coatings from modified GC resins.

While the viscosity reduction achieved with alcohol modified GC resins is significant, it is important to evaluate the effect of the modification on the properties of the coatings made from the modified resins. Both amine-crosslinked and self-crosslinked clear coatings were prepared from the modified GC resins and their key properties were determined.

The glass transition temperature of crosslinked networks is governed by many factors such as flexible units in the resin structure, the number of functional groups taking part in crosslinking, the extent of crosslinking, the mechanism of crosslinking, and the type and amount of the crosslinkers used.¹¹¹ Amine-cured BGC and modified GC coatings were made using PACM and A-2353 crosslinkers at a 1:1 epoxy:amine active hydrogen equivalent ratio. The values of glass transition temperature of the coatings were obtained using DSC. Figure 2.8(b) shows the T_g values for BGC and modified GC coatings crosslinked with PACM and A-2353. The T_g of the coatings shows a good correlation with the viscosity (Figure 2.8(a)). The coatings made from the trifunctional BGC resin shows the highest T_g and viscosity. The lowest T_g was shown by the coating made from a resin having the lowest viscosity i.e. BGC-DB. The T_g values of the coatings made from the modified GC resins were generally in a close range and only varied about 10 degrees from one another. The addition of the non-reactive flexible units such as alcohol or ether alcohol could have had a plasticizing effect in addition to interrupting the hydrogen bonding network. In addition, the extent of chemical crosslinking in the modified resins will be lower since the epoxy group functionality of the resins is lower than that of the BGC resin. This might have produced a softer and

more flexible network in the modified coatings resulting in lower T_g . The coatings crosslinked with A-2353 showed lower T_g values as compared with that of PACM crosslinked coatings which is consistent with the chemical structure of the crosslinkers. PACM has a relatively rigid cycloaliphatic and a low equivalent weight while A-2523 is a polyamide resin having a largely alkyl chain structure.

Figure 2.8 (c) shows a plot of the König pendulum hardness for the amine crosslinked and self-crosslinked coatings. The trifunctional BGC resin coatings crosslinked either with amines or by self-crosslinking show the highest hardness as compared with that of the other coatings. The hardness trend of the modified GC coatings closely follows the viscosity and T_g trends (Figures 2.8 (a) and 2.8 (b), respectively). The BGC coatings with the densely crosslinked network and the highest T_g were found to be more resistant towards the damping of the pendulum used in König hardness test. The soft and less crosslinked coating, BGC-DB, showed less resistance towards the damping and hence resulted in the lowest hardness values. A factor that influenced hardness in the modified GC coatings was the type of modifier used which also influenced the T_g of the coatings. Compared with the alcohol modified coatings, the ether alcohol modified coatings were softer. This might be because ether alcohol modified resins showed lower viscosity and produced lower T_g coatings compared with that of alcohol modified coatings. Thus, the hardness of the coatings was found to be a direct function of the types of modifiers used and was related to the T_g of the coatings.

Figure 2.8 (d) shows the reverse impact strength of the modified GC coatings. The impact strength showed the expected trends for the amine and self-crosslinked coatings. The viscosity and T_g trends also supported the impact strength study. The

coatings made from modified low viscosity resin with low T_g were expected to show high flexibility and impact strength. The flexibility or impact strength are related to crosslink density and T_g of the coatings.⁹ Modified GC coatings crosslinked with amines showed better impact strength as compared with that of the amine-crosslinked BGC coatings. It might be due to lower epoxy functionality (two) in the modified GC resins compared with that of BGC resin (three). Amine crosslinked low epoxy functional modified GC coatings would have formed a less densely crosslinked network than that of the BGC coating. Self-crosslinked coatings showed excellent impact strength. Impact strength of self-crosslinked coatings exceeded the maximum of the impact tester (172 in-lb). Self-crosslinked coatings did not use any external crosslinkers and hence might have produced an optimized crosslink density and crosslinked network resulting in excellent impact strength. Thus, reverse impact strength of the coatings was found to be a function of inter dependent factors such as resin functionality, crosslink density, T_g and the type of crosslinking used. An optimum crosslinked network was required to obtain good impact strength. The crosslinked network in GC coatings could be optimized by a combination of a number of reactive functional groups in resins and the techniques of crosslinking such as amine crosslinking or self-crosslinking.

Table 2.2 shows additional coating performance properties such as MEK resistance, flexibility and adhesion of the modified GC coatings. The amine crosslinked modified GC coatings showed excellent solvent resistance (> 400 MEK double rubs). The number of MEK double rubs is widely accepted as an indication of the extent of crosslink density and a high number of MEK double rubs are considered as an indication

of high cross-link density.¹¹² Amine crosslinked coatings showed higher MEK double rubs

Table 2.2. Properties of BGC and modified GC coatings.

BGC-EP series coatings	MEK double rubs			Conical mandrel (cm) (0 cm = Best)			Cross-hatch adhesion (5B = Best)		
	PACM	A-2353	SC	PACM	A-2353	SC	PACM	A-2353	SC
BGC	>400	>400	>400	0	0	0	5B	5B	5B
BGC-1BuOH	>400	>400	150	0	0	0	3B	4B	5B
BGC-IsoBuOH	>400	>400	100	0	0	0	3B	1B	5B
BGC-2EHA	>400	>400	95	0	0	0	4B	2B	5B
BGC-EB	>400	>400	150	0	0	0	5B	4B	5B
BGC-EP	>400	>400	120	0	0	0	5B	4B	5B
BGC-DB	>400	>400	110	0	0	0	5B	4B	5B

compared with that of the self-crosslinked coatings indicating higher crosslink density in the amine crosslinked coatings compared with that of the self-crosslinked coatings. The lower MEK double rubs observed for the self-crosslinked modified GC coatings compared with that of self-crosslinked BGC coatings confirmed the general correlation between MEK double rubs and crosslink density. The modified GC resins contain lower epoxy functionality (difunctional) implying lower crosslink density resulting in lower MEK double rubs compared with that of the trifunctional BGC coatings made from trifunctional BGC resin. All of the coating systems showed excellent flexibility in conical mandrel test consistent with that of the reverse impact strength. Adhesion of coatings was found to be comparable and dependent on the type of crosslinkers and mechanism of crosslinking used. PACM crosslinked and self-crosslinked coatings showed better adhesion compared with that of the A-2353 crosslinked coatings.

2.3.2. BGC-EP resin series and their coating performance

2.3.2.1. *Synthesis of BGC-EP resin series*

In order to further explore the effect of the degree of modification on the properties of the modified GC resins, a series of BGC-EP resins was made by replacing glycidol with varying amounts of ethylene glycol propyl ether (EP). The molar percent of EP used to replace glycidol was 15, 25, 33, 40 and 45 and the corresponding BGC-EP series resins obtained were labeled BGC-EP 15 mol %, BGC-EP 25 mol %, BGC-EP 33 mol % (BGC-EP), BGC-EP 40 mol % and BGC-EP 45 mol %, respectively. During the synthesis of the BGC-EP series resins, the amount of glycidol was varied to maintain the overall NCO:OH ratio as 1:1; thus, as the amount of EP increased, the amount of glycidol necessarily decreased. EEW (gm/eq) of BGC-EP 15 mol %, BGC-EP 25 mol %, BGC-EP 33 mol %, BGC-EP 40 mol %, and BGC-EP 45 mol % resins was 336, 330, 355, 380, and 465, respectively. The purpose of this study was to investigate the influence of the degree of modification on resin viscosity, cross-link density of the coatings, T_g and coating performance.

2.3.2.2. *Viscosity of series of BGC-EP resins*

Figure 2.9 shows the effect of composition on the viscosity of the BGC-EP series resins. The viscosity of the resins decreased as the amount of EP was increased, as expected. This could be attributed to the disruption of hydrogen bonding, hydrogen bond accepting oxygen atom in the ether and a plasticizing effect resulting from an increase in the amount of linear flexible chain in the resin structure. A substantial decrease in viscosity is obtained with just 15 mol % modification of the GC resin. Above 33 mol % modification the viscosity levels off.

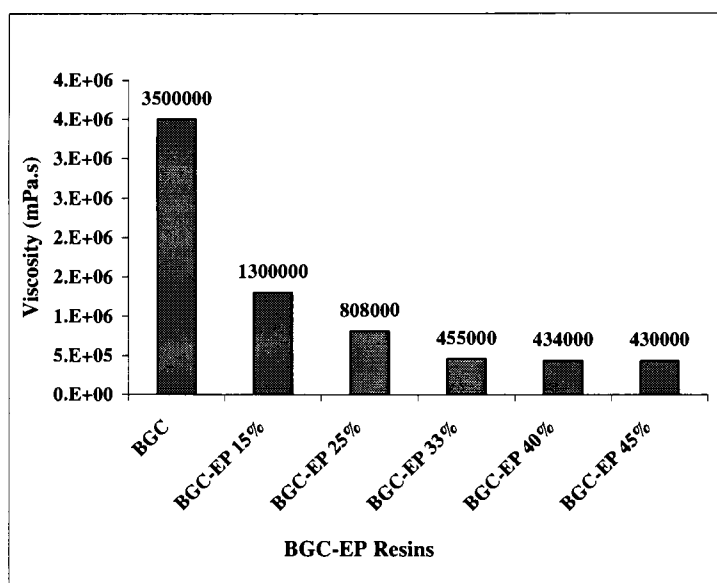


Figure 2.9. Effect of the structural composition of EP on viscosity of the BGC-EP series resins (neat resins).

2.3.2.3. Dynamic Mechanical Analysis (DMA)

The chemical and physical properties of coatings such as solvent resistance, network structure, crosslink density, T_g and mechanical properties are closely interdependent, as was seen in the first part of this study. To explain their correlation with each other, the effects of a systematic variation in the resin structures on their coating properties was studied. The series of BGC-EP resins was made to study the effects of variation in resin structure on coatings performance and network properties. The coatings made from these resins were expected to show a systematic variation in their $\tan \delta$ curves, crosslink density, glass transition temperature (T_g), hardness, impact strength, MEK double rubs, flexibility and adhesion.

DMA is a direct technique to study the viscoelastic properties of coatings and is well-suited for understanding influence of the systematic variation in the resin structures on coatings properties. The nature of $\tan \delta$ curves and extent of crosslink density calculated from storage modulus (E') of the coatings determines the viscoelastic

response and can be correlated to the physical properties of the coatings.^{9, 10, 113} DMA experiments were done on the PACM and A-2353 crosslinked coatings made from BGC-EP series resins. Figures 2.10 (a) and (b) are representative plots of storage modulus (E') and $\tan \delta$ versus temperature for BGC, BGC-EP 15 mol % and BGC-EP 25 mol % coatings crosslinked with PACM and A-2353, respectively.

The figures show that with the increase in the amount of EP in the resins, the values of $\tan \delta$ peak maximum increase and shift towards lower temperature, indicating lower T_g . The increasing amount of the unreactive pendant EP chains in the resin structures decreases the epoxy functionality and crosslink density. The unreactive pendant chains in the network can also act as mobile dangling chains producing a plasticizing effect.¹¹⁴⁻¹¹⁶ Thus, the increase in peak maximum value and shift towards lower temperature can be attributed to the lower crosslink density, as a result of the decreased epoxy functionality as well as a plasticizing effect from the alcohol modification of the resins.¹¹⁷⁻¹¹⁹

An interesting observation of the $\tan \delta$ curves is their broadening. Figures 2.10 (a) and (b) show that the increase in the compositional amount of EP increases the breadths of the $\tan \delta$ peaks. This could be because dangling chains (pendant EP chains) do not contribute to the elastically effective network chains and elastically active crosslink points. Increase in the weight fraction of dangling chains in a crosslinked network results in a lower amount of crosslinking, soft coatings with decreased T_g and results in broadening of $\tan \delta$ peaks.^{120, 121} The broadening of $\tan \delta$ peaks can also be related to an increase in the non-uniformity in network chain lengths.¹²² A comparison of Figures 2.10 (a) and (b) also show that, compared with the $\tan \delta$ peaks of PACM

crosslinked coatings, A-2353 coatings have broader tan δ peaks. This could be because of non-uniformity in the network of A-2353 crosslinked coatings as a result of the relatively broad molecular weight distribution of the A-2353 crosslinker.

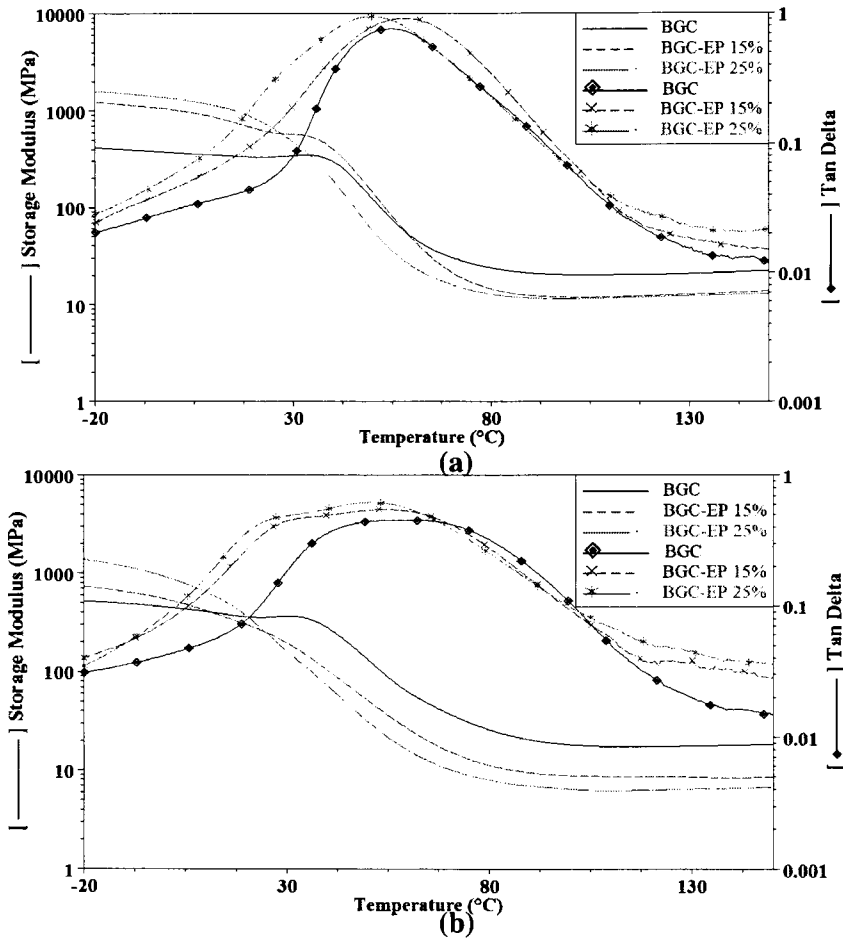


Figure 2.10. Storage modulus (E') and tan δ curves for the coatings crosslinked by (a) PACM and (b) A-2353.

The storage modulus values (E') in the rubbery plateau region (well above T_g) are used to calculate the crosslink density of the BGC and BGC-EP series coatings. Equation (2.1) was used to calculate cross-link density (ν_c) of the coatings:^{112, 121}

$$E' = 3\nu_c RT \quad (2.1)$$

where, E' = storage modulus (Pa); ν_c = crosslink density (mol/lit); R = gas constant (8.3 J/K/mol); and T = temperature (K). The calculated crosslink density of PACM and A-2353 crosslinked BGC-EP series coatings are shown in Figure 2.11(a).

The coatings made from BGC resin showed the highest crosslink density. BGC has three epoxy functional groups whereas, in the case of the BGC-EP series resins, the number of epoxy functional groups decreases with increasing replacement of glycidol with EP. The higher the number of active or effective crosslink points or junctions, the higher is the crosslink density.¹²³

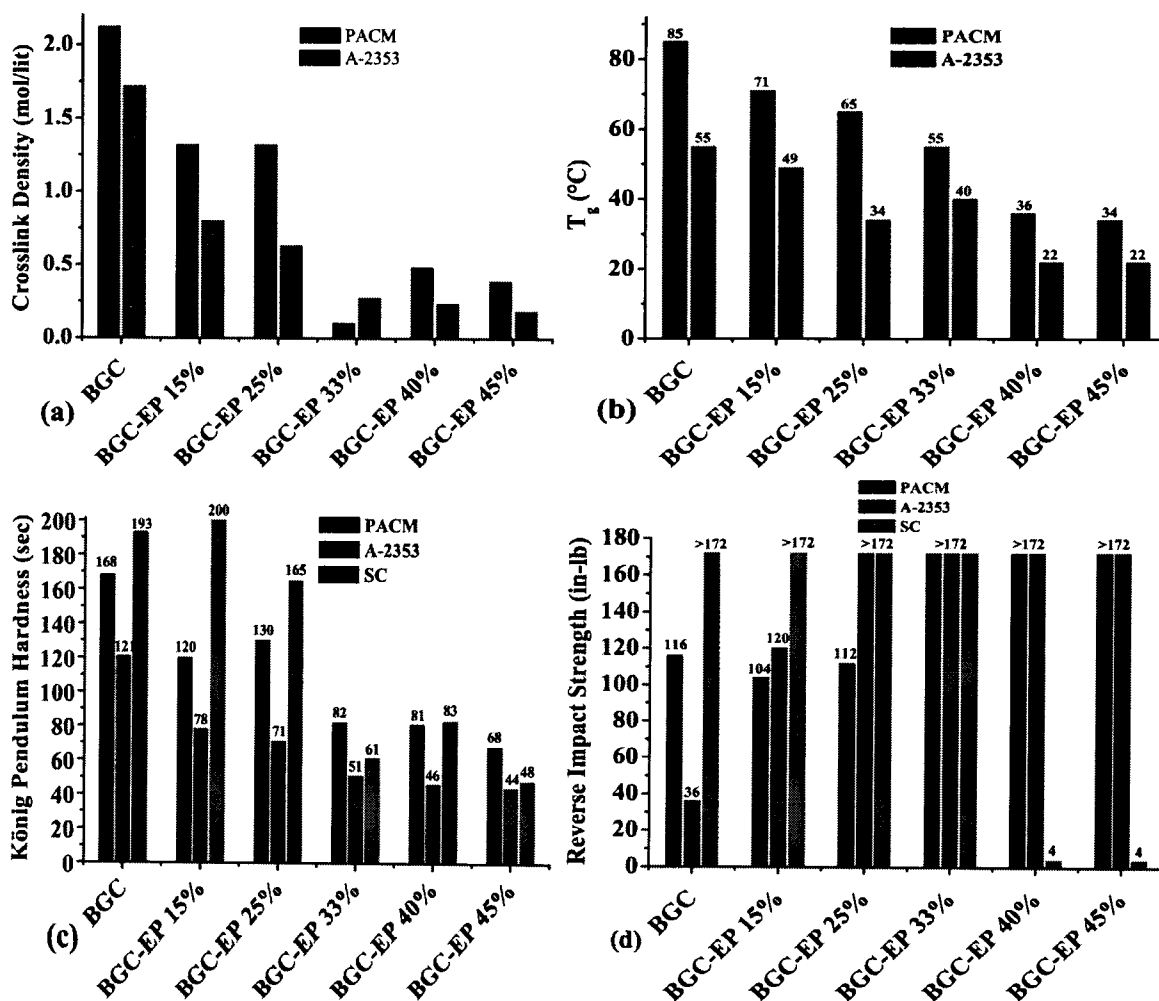


Figure 2.11. Property trends of control and EP-modified coatings as a function of EP content. (a) Crosslink density, (b) DSC T_g , (c) König pendulum hardness, (d) Reverse impact strength.

The higher amount of epoxy functional groups in BGC provides a higher number of active crosslink points and a more densely crosslinked network by reacting with the active hydrogen atoms of the amine crosslinkers. The increase in the content of non-reactive EP in the resins results in a decrease in the crosslink density.

PACM crosslinked BGC-EP series coatings showed a higher crosslink density compared with the A-2353 crosslinked coatings. The lower equivalent weight of PACM compared to the polyamide resin results in a higher crosslink density in the networks.

The crosslink density largely determines coating properties such as glass transition temperature (T_g), hardness, impact strength, solvent resistance, flexibility and adhesion of the coatings. The observations of the crosslink density trend, such as the highest crosslink density of trifunctional BGC and higher crosslink density of PACM crosslinked modified GC coatings compared with that of A-2353 crosslinked coatings can be correlated with the corresponding resin structures and their coating performance.

2.3.2.4. *Glass transition temperature (T_g) of series of BGC-EP coatings*

Figure 2.11 (b) shows the effect of the structural composition of the resins on the glass transition temperature of the series of BGC-EP coatings. An excellent correlation between crosslink density and glass transition temperature can be made by comparing this data to that of Figure 2.11 (a) (crosslink density). The T_g of the series of BGC-EP coatings also followed the trends observed for their viscosity, as well.

BGC resin contains the highest number of reactive epoxy functional groups, whereas BGC-EP 45 mol % resin contains the lowest number of the epoxy groups. BGC resin showed the highest viscosity and its coatings have the highest crosslink density and T_g . On the other hand, BGC-EP 45 mol % resin showed the lowest viscosity and its

coatings have the lowest crosslink density and T_g . The data is very consistent with the general rule that an increase in crosslink density increases the T_g of the coatings.^{11, 113} As the amounts of EP in the resins was increased, the non-reactive part increases and that decreases the crosslink density and T_g of the coatings. Figure 2.11 (b) shows that PACM crosslinked BGC-EP resins showed higher T_g compared with that of A-2353 crosslinked coatings due to their higher crosslink density.

2.3.2.5. *Hardness of series of BGC-EP coatings*

Figure 2.11 (c) shows the effect of the compositional amounts of EP on the hardness of the crosslinked coatings. The hardness of the coatings decreased as the amount of EP increased. The hardness trend for BGC-EP coatings consistently followed the trends seen for the viscosity, crosslink density and T_g . The viscosity of the BGC-EP series resins, crosslink density of the corresponding coatings, the T_g values and hardness all decreased as the amount of EP increased. Two closely interrelated factors, modulus and T_g , influence coating hardness. The swinging motion of the oscillating pendulum in König hardness test is strongly damped by the soft, low modulus and low T_g coatings resulting in low hardness.^{9, 10} High crosslink density and high T_g produces hard coating surfaces. Thus, the amount of alcohol modifier influences the hardness of the BGC-EP series coatings.

2.3.2.6. *Impact strength of series of BGC-EP coatings*

Figure 2.11 (d) shows the results obtained for impact strength of the BGC-EP series coatings. A correlation of the impact strength or flexibility with that of the crosslink density and T_g can be observed. As the amount of EP was increased, the impact strength of the amine crosslinked coatings increased and reached the maximum of the

impact tester. As seen before, the crosslink density and T_g of the coatings decreased with the increased amount of EP used. Thus, for the amine crosslinked coatings impact strength increased with the decrease in crosslink density. However, in case of the self-crosslinked coatings, the impact strength of BGC-EP 40 mol % and BGC-EP 45 mol % decreased abruptly to a low value. At this level of EP incorporation, the epoxy functionality is on average less than two per molecule and the resins do not contain enough reactive epoxy functional groups to provide sufficient crosslinking. This suggests that for self-crosslinked coatings, an optimum number of functional groups in the resins are needed to provide significant impact strength. The use of amine crosslinkers with low functionality resins provided the effective crosslink points in the coatings and improved crosslinked network to sustain mechanical deformation.

2.3.2.7. Solvent resistance, flexibility and adhesion of series of BGC-EP coatings

Table 2.3 shows the properties of the coatings made from the BGC-EP series resins. The MEK double rubs of amine crosslinked and self-crosslinked coatings decreased significantly after 33 mol % of EP in structural composition. This could be because at the higher percentages of EP there was not enough crosslinking to form a solvent resistant coating. Amine crosslinked coatings showed excellent flexibility as no crack was observed in any of the coatings made from the BGC-EP series resins. However, the flexibility of the self-crosslinked coating decreased above BGC-EP 33 mol % composition. During the conical mandrel test, the self-crosslinked BGC-EP 40 mol % and 45 mol % coatings were cracked by the lengths of 4.6 and 5 cm, respectively. The poor flexibility of the self-crosslinked BGC-EP 40 mol % and 45 mol % coatings in the mandrel bend test could be correlated to their poor performance in reverse impact

strength. This could be because of very low extent of crosslinking in the self-crosslinked BGC-EP 40 mol % and BGC-EP 45 mol % coatings which was unable to resist cracking. The low degree of crosslinking in the self-crosslinked coatings was also indicated by their extremely low MEK double rubs. Excellent adhesion was shown by the amine crosslinked as well as self-crosslinked coatings for the whole range of compositional variations in EP. Thus, MEK double rubs, flexibility and impact strength of the GC coatings could be correlated to each other through crosslink density. Optimum MEK resistance, flexibility and impact strength were produced by an optimum crosslinked network. Too low extent of crosslinking produced the lowest MEK resistance, flexibility and impact strength.

Table 2.3. Properties of the BGC-EP series coatings.

BGC-EP series coatings	MEK double rubs			Conical mandrel (cm) (0 cm = Best)			Cross-hatch adhesion (5B = Best)		
	PACM	A-2353	SC	PACM	A-2353	SC	PACM	A-2353	SC
BGC	>400	>400	>400	0	0	0	5B	5B	5B
BGC-EP 15%	>400	>400	55	0	0	0	5B	5B	5B
BGC-EP 25%	>400	280	15	0	0	0	5B	4B	5B
BGC-EP 33%	>400	>400	120	0	0	0	5B	4B	5B
BGC-EP 40%	80	50	2	0	0	4.6	5B	5B	5B
BGC-EP 45%	35	35	1	0	0	5	5B	5B	5B

2.3.2.8. Tensile test of series of BGC-EP coatings

Tensile testing of the coatings was carried out to determine the influence of the extent of modification of resins on elongation at break and Young's modulus of the coatings. The GC coatings selected for tensile test were based on BGC, BGC-EP 15%, and BGC-EP 33% resins and were crosslinked with PACM and A-2353. Table 2.4 shows the elongation at break and Young's modulus of the coatings crosslinked with PACM and A-2353. Elongation at break increased with increase in % modification while Young's

modulus decreased with increase in % modification. PACM crosslinked coatings had lower elongation at break and higher Young's modulus than that of the A-2353 coatings.

Table 2.4. Elongation at break and Young's modulus.

Coating	Elongation at break (mm)	Young's modulus (MPa)
PACM Crosslinked		
BGC	1.7	4290
BGC-EP 15%	2.3	4100
BGC-EP 33%	11.0	2000
A-2353 crosslinked		
BGC	6.9	2700
BGC-EP 15%	11.4	1200
BGC-EP 33%	19.0	581

2.3.3. *Thermal Stability of modified GC coatings*

The thermal stability of amine crosslinked BGC, modified GC and BGC-EP series coatings was studied using TGA. The TGA plots for PACM and A-2353 crosslinked BGC and modified GC coatings are shown in Figures 2.12 and 2.13, respectively.

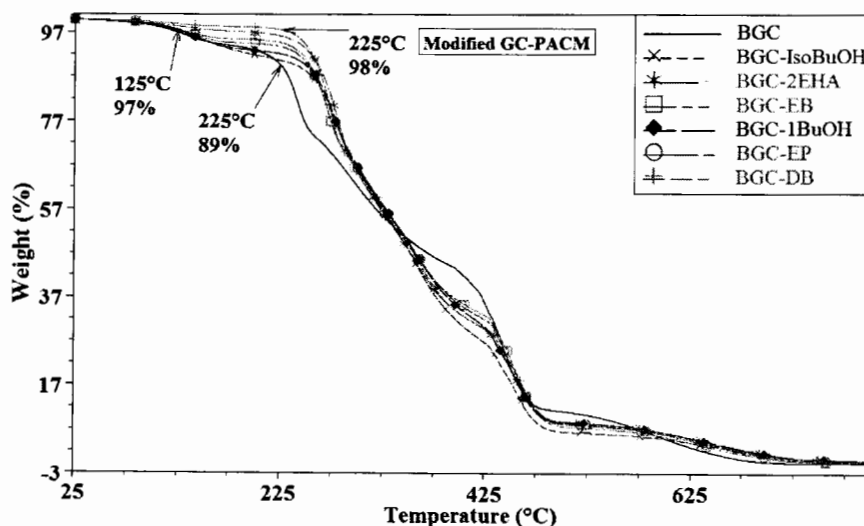


Figure 2.12. TGA of the BGC and modified GC coatings crosslinked with PACM.

The figures show that the coatings crosslinked with either of the crosslinkers were stable at 125 °C. The onset temperature of thermal degradation was found to be around 225 °C. A significant weight loss (11% and 12%) was observed at 225 °C for BGC coatings crosslinked with PACM and A-2353, respectively. Figures 2.12 and 2.13 also show that the modified coatings were relatively more stable at 225 °C as compared with that of the control BGC coatings. Coatings made from BGC-DB crosslinked with both the crosslinkers, PACM and A-2353, showed the highest thermal stability (2% weight loss) at 225 °C. PACM crosslinked coatings showed slightly higher thermal stability compared with that of the A-2353 crosslinked coatings.

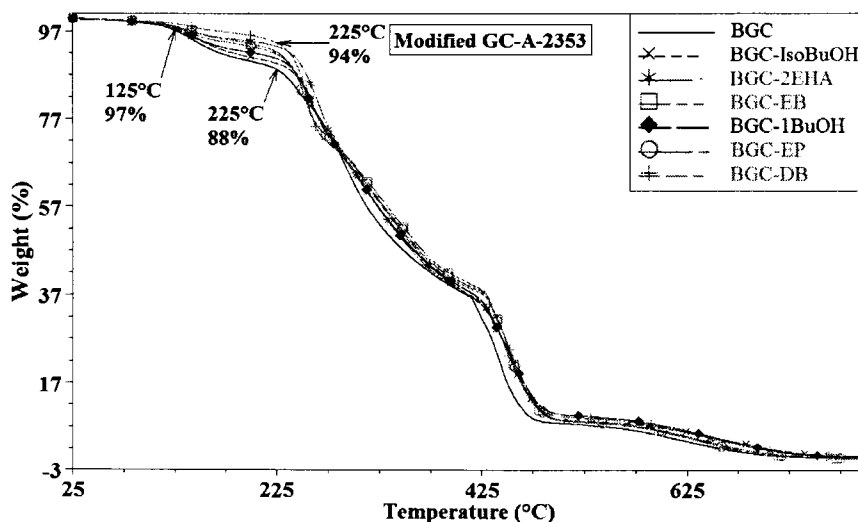


Figure 2.13. TGA of the BGC and modified GC coatings crosslinked with A-2353.

Figures 2.14 and 2.15 show the thermal stability of the coatings made from the series of BGC-EP resins crosslinked with PACM and A-2353. The figures show that the coatings were stable at 125°C (3% weight loss). The onset temperature for thermal decomposition was around 225 °C. PACM and A-2353 crosslinked coatings showed significant weight loss (10 and 14%) after 225 °C. However, the coatings made from the resins containing higher amounts of EP (40 and 45 mol %) showed slightly greater

thermal stability at 225 °C (4 and 7% weight loss for PACM and A-2353 crosslinked coatings) compared to the other coatings.

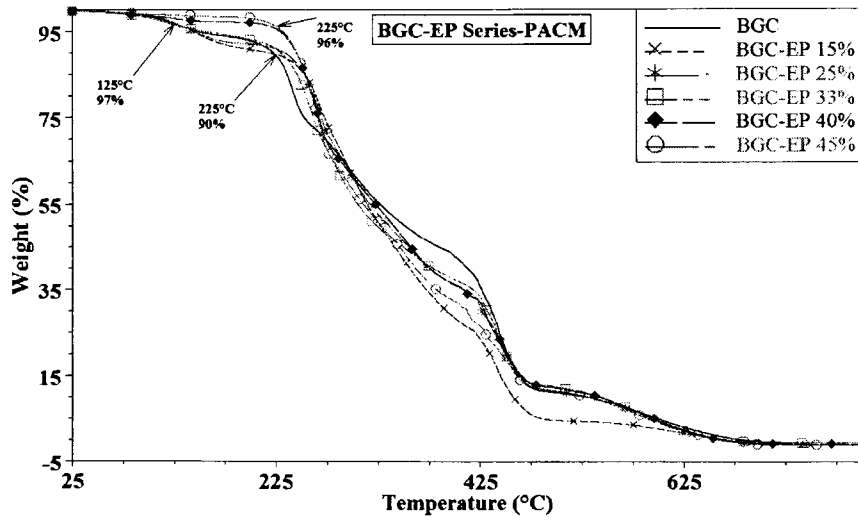


Figure 2.14. TGA of the BGC-EP series coatings crosslinked with PACM.

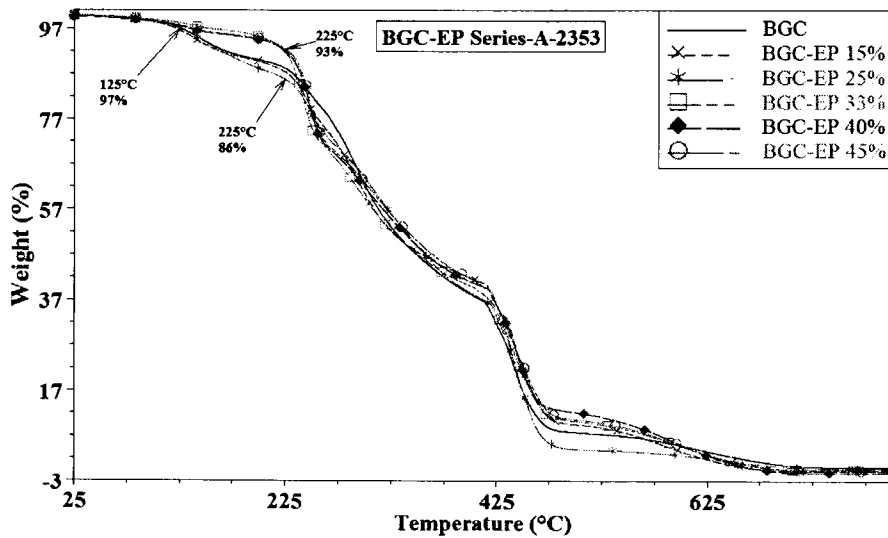


Figure 2.15. TGA of the BGC-EP series coatings crosslinked with A-2353.

2.3.4. Electrochemical impedance spectroscopy (EIS)

Coatings which have a high barrier to corrosive species and excellent adhesion to the metal substrate generally have very high corrosion resistance. The coatings act as a barrier against the penetration of corrosive species such as water, oxygen, and ions and

thus prevent the progress of corrosion at the metal-coating interface. The corrosive species diffuse and reach to a metal-coating interface through interconnected small pores or channels in crosslinked coatings.¹²⁴ The barrier of the coatings to the transportation of water and ions can be quantitatively determined by electrochemical impedance spectroscopy (EIS). EIS technique provides kinetic and mechanistic information related to the changes caused due to exposure to a corrosive environment in the bulk of coatings and across the metal-coating interface.¹²⁵⁻¹²⁷

The impedance is a tendency of a system to resist the flow of AC current. In the EIS experiments, a small AC voltage at varying frequency is applied across the coated metal substrate and a plot of the magnitude of impedance or modulus of impedance ($|Z|$) vs. frequency is obtained. A plot of change in phase angle between applied voltage and resulting current vs. frequency can also be obtained. The plots of $|Z|$ vs. frequency and phase angle vs. frequency are known as Bode plots. The magnitude of impedance ($|Z|$) of a coating changes with applied frequency depending upon capacitive and resistive components in the coating system and corrosion process. The $|Z|$ of coatings is widely measured as an indicator of the barrier properties of coatings. Typically, coatings having initial $|Z|$ of over $10^8 \Omega \text{ cm}^2$ in the low frequency region of Bode plot have excellent barrier properties and provide excellent corrosion resistance. Coatings with an initial $|Z|$ between $10^6 \Omega \text{ cm}^2$ - $10^8 \Omega \text{ cm}^2$ in the low frequency region of the Bode plot are considered to have good barrier properties and provide good corrosion performance.¹²⁷⁻¹²⁹ In the Bode plot, the coatings with very high impedance, very high barrier properties, and an excellent corrosion resistance show purely capacitive (frequency dependent) behavior with slope -1 over a wide range of frequencies.¹²⁹⁻¹³¹

In this research, EIS experiments were performed on the coatings to study the influence of structural composition of the resins on barrier properties of the coatings. EIS was performed on GC coatings obtained from GC resins with different compositions such as BGC, BGC-2EHA, BGC-EP, BGC-EP 15%, and BGC-DB crosslinked with A-2353 crosslinker. Figure 2.16 (a) and (b) show the impedance Bode plots of the coatings on steel substrate after 2.5 hrs and after seven days of immersion, respectively.

After 2.5 hrs of immersion BGC-2EHA coating showed the highest impedance compared to the other coatings while BGC-DB coating showed the lowest impedance. BGC-EP had higher impedance than BGC-EP 15% and BGC-EP 15% had higher impedance than BGC. This trend was continued after seven days of immersion except that the impedance of BGC-EP and BGC-EP 15% coatings became similar. After seven days of immersion the impedance of BGC-2EHA coating was between $10^7 - 10^8 \Omega \text{ cm}^2$. The impedance values of BGC-EP 15% and BGC-EP coatings were slightly above $10^6 \Omega \text{ cm}^2$ while the impedance of BGC and BGC-DB coatings was slightly below $10^6 \Omega \text{ cm}^2$. Impedance values of the GC coatings correlated to the composition of the GC resins. BGC-2EHA coatings had the highest impedance and indicated the least interaction with water and exhibited the highest protective behavior among the coatings tested in this experiment. 2EHA which does not contain any hydrophilic group can be considered as more hydrophobic than EP (containing one hydrophilic ether group) and DB (containing two hydrophilic ether groups). Thus, the lowest impedance of BGC-DB coating can be attributed to the hydrophilic DB in the resin structure.

Capacitance of the GC coatings after seven days of immersion was determined in EIS experiments at high frequency (10KHz). Capacitance of a coating can be related to

water uptake. Higher capacitance of coatings increases due to water uptake.¹²⁶ Capacitance of the GC coatings was influenced by the composition of the resins. Figure 2.17 shows the capacitance of the coatings characterized by EIS. The lowest capacitance of BGC-2EHA coating indicated the least water uptake while the highest capacitance of

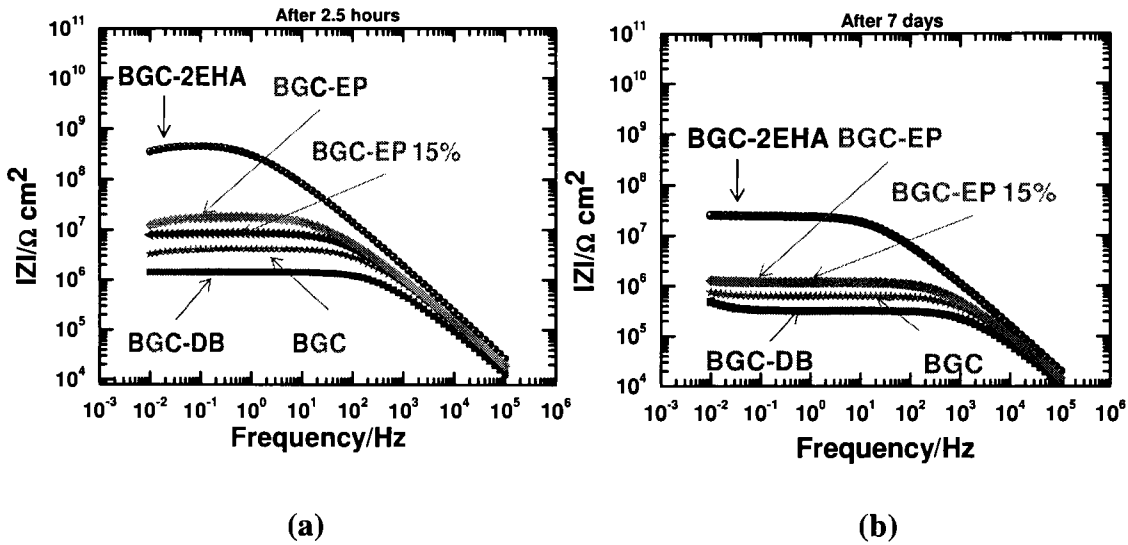


Figure 2.16. Modulus Bode plot after (a) 2.5 hrs and (b) seven days for BGC, BGC-2EHA, BGC-EP, BGC-EP 15%, and BGC-DB coatings.

BGC-DB coating indicated the highest water uptake. BGC coating had the second highest

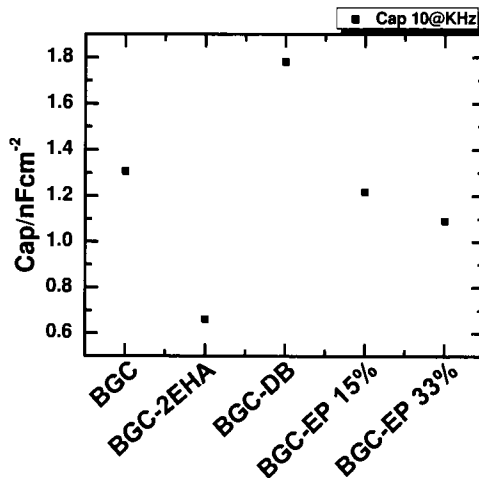


Figure 2.17. Capacitance of BGC, BGC-2EHA, BGC-DB, BGC-EP 15%, and BGC-EP 33% coatings after seven days of immersion.

capacitance value and indicated significant interaction with water. BGC-EP and BGC-EP 15% coatings had the capacitance values slightly lower than that for BGC coatings.

It has been shown that the interaction of epoxy based crosslinked systems with water is directly related to their chemical structure as well as physical morphology. The presence of polar hydrophilic groups such as hydroxyl, tertiary amines, and unreacted amine increases the concentration of water in the epoxy systems. Large proportion of water molecules in a polymer matrix are found to be in the vicinity of the polar hydrophilic groups. Also microscopic and macroscopic film defects, heterogeneous crosslinked network, film delamination (poor adhesion), and bubbles in the crosslinked film increases water absorption by the epoxy systems.^{68, 95, 132-136} Coatings based on BGC have the highest crosslink density and BGC resin has no modifier with a hydrophilic ether group. It was surprising then, that the impedance of BGC coating was lower than BGC-2EHA, BGC-EP 33%, and BGC-EP 15% coatings while its capacitance was higher than BGC-2EHA, BGC-EP, and BGC-EP 15% coatings. The second lowest impedance and the second highest impedance of BGC coating indicated a relatively high interaction with water. The probable reason for the reduced impedance and high capacitance of the BGC coatings could be related to the lower epoxy equivalent weight (EEW) of BGC resin due to its higher epoxy functionality compared to the other GC resins characterized in this experiment. The low EEW resin increases the concentration of amine crosslinker and generates a high amount of polar hydrophilic tertiary amines and hydroxyl groups during the crosslinking reaction. The high amount of polar hydrophilic groups generated in BGC coatings during crosslinking reaction might be responsible for high water uptake and reduced impedance of BGC coatings. It should be noted that in BGC-2EHA resins 33

mol % of glycidol is replaced by 2EHA and reduces EEW of the resin as well as introduces non-polar hydrocarbon (hydrophobic) units in the coating. The result is the highest impedance and the lowest capacitance which indicated the least interaction of water with BGC-2EHA coating and the highest protective behavior.

2.3.5. Salt spray test

The ASTM B 117 salt spray test is the oldest standard test used to compare corrosion resistance of coatings. The GC coatings used for salt spray test were BGC, BGC-2EHA, BGC-DB, BGC-EP15%, and BGC-EP. Figure 2.18 shows the scanned images of the coatings after 312 hrs of salt spray testing.

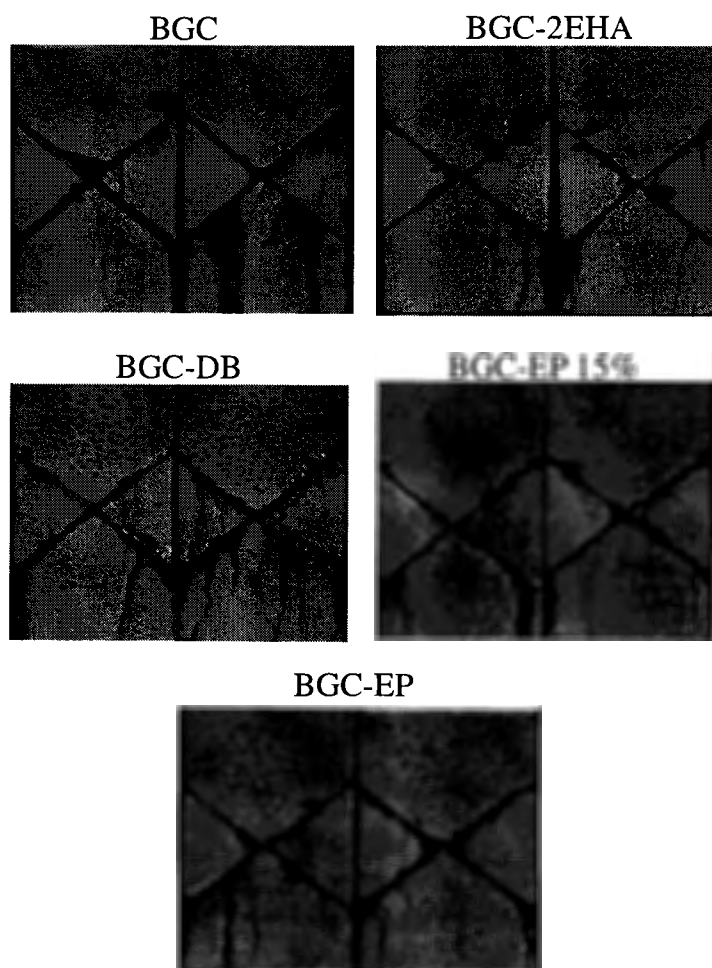


Figure 2.18. Salt spray of BGC, BGC-2EHA, BGC-DB, BGC-EP 15%, and BGC-EP after 312 hrs.

Two samples of each coating were used and the salt spray test was performed on scribed coatings on steel panels. The scribes on the coatings and panels result in physical damage to the coatings and the underlying substrate. The coatings were under continuous exposure to fog (5% NaCl solution) for 312 hrs. The composition of the GC resins influenced the behavior of the coatings in salt spray. The coatings showed the formation of small blisters above the scribed area due to the penetration of water. BGC-DB coating showed the highest extent of blisters. BGC-EP 33% coatings had a higher extent of blisters than BGC-EP 15%. BGC coating had lower extent of bubbles above the scribed area than that for BGC-EP 15% coating. BGC-2EHA had no blisters above the scribed area. One of the coating samples from BGC, BGC-EP 15%, and BGC-EP did not show large under film corrosion, delamination, or blisters along the scribed area. BGC-2EHA and BGC-DB coatings showed blisters along the scribed area.

2.4. Conclusions

Modification of the structures of GC resins based on polyisocyanates can be done by replacing a part of the glycidol in BGC resin by alcohols or ether alcohols. The modified GC resins showed a dramatic reduction in viscosity. The viscosity of the resins is lowest when the resin is modified with diethylene glycol butylether. The ether links in the modified GC resin structures are the most effective in decreasing the resin viscosity. The viscosity of a series of resins made with increasing levels of EP decreased as the amount of EP increased.

It was found that the viscosity of the resins, T_g and crosslink density of the respective coatings were strongly dependent on the corresponding resin structures. The types of crosslinkers, type and structural compositions of the modifier and technique of

crosslinking directly influenced the interrelated coatings properties such as crosslink density and T_g . PACM crosslinked coatings show higher crosslink density and T_g compared with that of the A-2353 crosslinked coatings. Higher extents of crosslinking led to higher T_g s. Increase in the amount of EP modification led to decreased viscosity, crosslink density and T_g of the coatings. The addition of crosslinkers produces a denser crosslinked network in coatings compared with the self-crosslinked coatings. The denser crosslinked network in amine crosslinked coatings is indicated by higher number of MEK double rubs compared with that of the self-crosslinked coatings.

The hardness of the coatings is influenced by their T_g . Higher T_g correlates to higher hardness. Amine crosslinked BGC, modified GC and BGC-EP series coatings showed good impact strength, flexibility and MEK resistance. Self-crosslinked BGC, modified GC and BGC-EP series coatings up to 33 mol % of compositional EP showed good impact strength, flexibility and MEK resistance. However, above 33 mol % of the structural composition of EP the self crosslinked BGC-EP series coatings showed an abrupt decrease in impact strength, flexibility and MEK resistance. At the high percentage of modification enough functional groups are not available to produce optimum crosslinking. A combination of a particular type of amine crosslinker, optimum number of functionality in resin and proper curing technique could produce optimized impact strength, flexibility and MEK resistance in the GC coatings.

The modified GC coatings were found to be slightly more thermally stable compared to the BGC coatings. PACM crosslinked coatings are thermally more stable compared to the A-2353 crosslinked coatings. The onset of decomposition for BGC coatings is around 225 °C.

The composition of GC resins such as hydrophilic or hydrophobic modifier in the resin and EEW of the resins influenced the barrier properties and corrosion resistance of the GC coatings. The coatings with hydrophilic DB had the lowest impedance and the highest capacitance and highest extent of the blisters over the scribed area. BGC coatings with the lowest EEW require the highest amount of crosslinker and can be assumed to generate the highest amount of polar hydrophilic groups such as hydroxyls and tertiary amines which reduces the impedance and increases the capacitance. Hydrophobic 2EHA groups in the resin reduced EEW and increased hydrophobic content in the resin and coating. Thus, BGC-2EHA coatings had the highest impedance, the lowest capacitance and no blisters over the scribed area in salt spray test. BGC-EP 15% coating had higher capacitance than BGC-EP coating although BGC-EP 15% resin contain less hydrophilic EP than BGC-EP 33% resin. This difference could be probably due to the higher amount of polar hydrophilic hydroxyl and tertiary amine groups generated in BGC-EP 15% coating than that in BGC-EP coating. As BGC-EP 15% resin had higher amount of reactive epoxy groups than that in BGC-EP resin it can be assumed that BGC-EP 15% coating contain more hydroxyl and tertiary amine groups generated during epoxy-amine crosslinking reaction than that in BGC-EP coating. The combined effect of hydrophilic EP, increased hydroxyl, and increased tertiary amine groups may result in increased capacitance due to water uptake in BGC-EP 15% coating.

2.5. References

1. Wicks (Jr), ZW, Jones, FN, Pappas, SP, Wicks, DA, Organic Coatings: Science and Technology. 3rd ed., John Wiley and Sons Inc., New Jersey (2007)

2. Chattopadhyay, DK,Raju, KVSN, "Structural Engineering of Polyurethane Coatings for High Performance Applications". *Prog. Polym. Sci.*, **32** (3) 352-418 (2007)
3. Tarlas, HD, "Amine Cured Epoxy Resin Coatings for Resistance to Atmospheric Corrosion". *Mater. Prot.*, **9** (5) 37-42 (1970)
4. Edwards, PA,Erickson, J,Webster, DC, "Synthesis and Self-crosslinking of Glycidyl Carbamate Functional Oligomers". *Polym. Prepr. (Am. Chem. Soc., Div. Polym. Chem.)*, **44** (1) 54-55 (2003)
5. Crivello, JV,Liu, S, "Photoinitiated Cationic Polymerization of Epoxy Alcohol Monomers". *J. Polym. Sci., Part A: Polym. Chem.*, **38** (3) 389-401 (2000)
6. Royappa, AT,Vogt, ML,Sharma, V, "Composition and long-term stability of polyglycidol prepared by cationic ring-opening polymerization". *J. Appl. Polym. Sci.*, **91** (2) 1344-1351 (2004)
7. Edwards, PA,Erickson, J,Webster, DC, "Synthesis and Characterization of Glycidyl Carbamate Functional Oligomers". *Polym. Prepr. (Am. Chem. Soc., Div. Polym. Chem.)*, **44** (1) 144-145 (2003)
8. Edwards, PA. Glycidyl carbamate resins to achieve polyurethane properties and epoxide reactivity. Ph.D. Dissertation, North Dakota State University, Fargo, 2004.
9. Edwards, PA,Striemer, G,Webster, DC, "Novel Polyurethane Technology Through Glycidyl Carbamate Chemistry". *J. Coat. Technol. Res.*, **2** (7) 517-527 (2005)
10. Suryanarayana, R. Zero VOC binder system from glycidyl carbamate functional resins. M. S. Thesis, North Dakota State University, Fargo, 2006.
11. de Meijer, M, "Review on the Durability of Exterior Wood Coatings With Reduced VOC-content". *Prog. Org. Coat.*, **43** (4) 217-225 (2001)

12. Geurink, PJA, Scherer, T, Buter, R, Steenbergen, A, Henderiks, H, "A Complete New Design for Waterborne 2-Pack PUR Coatings With Robust Application Properties". *Prog. Org. Coat.*, **55** (2) 119-127 (2006)
13. Tanabe, H, Ohsugi, H, "A New Resin System for Super High Solids Coating". *Prog. Org. Coat.*, **32** (1-4) 197-203 (1997)
14. Mishra, AK, Chattopadhyay, DK, Sreedhar, B, Raju, KVS, "FT-IR and XPS Studies of Polyurethane-Urea-Imide Coatings". *Prog. Org. Coat.*, **55** (3) 231-243 (2006)
15. Carrasco, F, Pagès, P, Lacorte, T, Briceño, K, "Fourier Transform IR and Differential Scanning Calorimetry Study of Curing of Trifunctional Amino-epoxy Resin". *J. Appl. Polym. Sci.*, **98** (4) 1524-1535 (2005)
16. Sperling, LH, Introduction to Physical Polymer Science. 4th ed., John Wiley and Sons Inc., New Jersey (2006)
17. Edwards, PA, Striemer, G, Webster, DC, "Synthesis, Characterization and Self-crosslinking of Glycidyl Carbamate Functional Resins". *Prog. Org. Coat.*, **57** (2) 128-139 (2006)
18. De Lucca Freitas, LL, Stadler, R, "Thermoplastic Elastomers by Hydrogen Bonding. 3. Interrelations Between Molecular Parameters and Rheological Properties". *Macromolecules*, **20** (10) 2478-85 (1987)
19. Hilger, C, Draeger, M, Stadler, R, "Molecular Origin of Supramolecular Self-assembling in Statistical Copolymers". *Macromolecules*, **25** (9) 2498-501 (1992)
20. Nair, KP, Breedveld, V, Weck, M, "Complementary Hydrogen-Bonded Thermoreversible Polymer Networks With Tunable Properties". *Macromolecules*, **41** (10) 3429-3438 (2008)

21. Hill, LW, "Structure/Property Relationships of Thermoset Coatings". *J. Coat. Technol.*, **64** (808) 29-42 (1992)
22. Scanlan, JC, Webster, DC, Crain, AL, "Correlation Between Network Mechanical Properties and Physical Properties in Polyester-Urethane Coatings". *ACS Symp. Ser. (Film Formation in Waterborne Coatings)*, **648** 222-234 (1996)
23. Hill, LW, "Determination of Crosslink Density in Thermoset Coatings". *Polym. Mater. Sci. Eng.*, **77** 387-388 (1997)
24. Koleske, JV, *Paint and Coating Testing Manual*. 14th ed., ASTM publication, (1995)
25. Masatsugu, O, Noriyuki, K, Tatsuo, K, "Effects of Crosslinking on Physical Properties of Phenol-Formaldehyde Novolac Cured Epoxy Resins". *J. Appl. Polym. Sci.*, **48** (4) 583-601 (1993)
26. Kong, X, Yue, J, Narine, SS, "Physical Properties of Canola Oil Based Polyurethane Networks". *Biomacromolecules*, **8** (11) 3584-3589 (2007)
27. Narine, SS, Kong, X, Bouzidi, L, Sporns, P, "Physical Properties of Polyurethanes Produced From Polyols From Seed Oils: I. Elastomers". *J. Amer. Oil Chem. Soc.*, **84** (1) 55-63 (2007)
28. Petrovic, ZS, Zhang, W, Javni, I, "Structure and Properties of Polyurethanes Prepared from Triglyceride Polyols by Ozonolysis". *Biomacromolecules*, **6** (2) 713-719 (2005)
29. Sorathia, UA, Yeager, WL, Dapp, TL, "Interpenetrating Polymer Network Acoustic Damping Material." US Patent 5,225,498, 1993.

30. Rodriguez, MT, Garcia, SJ, Cabello, R, Suay, JJ, Gracenea, JJ, "Effect of Plasticizer on the Thermal, Mechanical, and Anticorrosion Properties of an Epoxy Primer". *J. Coat. Technol. Res.*, **2** (7) 557-564 (2005)
31. Hill, LW, Lee, S-B, "Effect of Melamine-Formaldehyde Structure on Cure Response of Thermoset Coatings". *J. Coat. Technol.*, **71** (897) 127-133 (1999)
32. Dusek, K, Duscaronková-Smrcková, M, Fedderly, JJ, Lee, GF, Lee, JD, Hartmann, B, "Polyurethane Networks With Controlled Architecture of Dangling Chains". *Macromol. Chem. Phys.*, **203** (13) 1936-1948 (2002)
33. Skaja, A, Fernando, D, Croll, S, "Mechanical Property Changes and Degradation During Accelerated Weathering of Polyester-Urethane Coatings". *J. Coat. Technol. Res.*, **3** (1) 41-51 (2006)
34. Higginbottom, HP, Bowers, GR, Ferrell, PE, "Cure of Secondary Carbamate Groups by Melamine-Formaldehyde Resins". *J. Coat. Technol.*, **71** (894) 49-60 (1999)
35. Hill, LW, "Calculation of Crosslink Density in Short Chain Networks". *Prog. Org. Coat.*, **31** (3) 235-243 (1997)
36. Schwalm, R, "Crosslinking Effect on Mechanical Properties of UV Curable Coatings". *PPCJ, Polym. Paint Colour J.*, **189** (4421) 18-20, 22 (1999)
37. Grundmeier, G, Schmidt, W, Stratmann, M, "Corrosion protection by organic coatings: electrochemical mechanism and novel methods of investigation". *Electrochim. Acta*, **45** (15-16) 2515-2533 (2000)
38. Bierwagen, G, Tallman, D, Li, J, He, L, Jeffcoate, C, "EIS studies of coated metals in accelerated exposure". *Prog. Org. Coat.*, **46** (2) 148-157 (2003)

39. Le, TQ, Bierwagen, GP, Touzain, S, "EIS and ENM measurements for three different organic coatings on aluminum". *Prog. Org. Coat.*, **42** (3-4) 179-187 (2001)
40. McIntyre, JM, Pham, HQ, "Electrochemical impedance spectroscopy; a tool for organic coatings optimizations". *Prog. Org. Coat.*, **27** (1-4) 201-207 (1996)
41. Linda, GS, Appleman, BR, "EIS: Electrochemical impedance spectroscopy-A tool to predict remaining coating life?". *Journal of protective coatings and linings*, **February** 66-74 (2003)
42. Loveday, D, Peterson, P, Rodgers, B, "Evaluation of organic coatings with electrochemical impedance spectroscopy. Part 1: fundamentals of electrochemical impedance spectroscopy". *JCT CoatingsTech*, **1** (8) 46-52 (2004)
43. Loveday, D, Peterson, P, Rodgers, B, "Evaluation of organic coatings with electrochemical impedance spectroscopy. Part 2: Application of EIS to coatings". *JCT CoatingsTech*, **1** (10) 88-93 (2004)
44. Murray, JN, "Electrochemical test methods for evaluating organic coatings on metals: an update. Part III: Multiple test parameter measurements". *Prog. Org. Coat.*, **31** (4) 375-391 (1997)

CHAPTER 3. GLYCIDYL CARBAMATE RESIN SYSTEMS FOR HIGHLY FLEXIBLE COATINGS

3.1. Introduction

Glycidyl carbamate (GC) resins are obtained by the reaction of isocyanate functional compounds with glycidol. A unique property of GC resins is the combination of both urethane and epoxy functional groups in their structures and thus the performance of urethane and reactivity of epoxide are combined in a single resin structure. The primary research on GC resins and coatings was based on GC resins obtained from aliphatic polyisocyanates such as biuret and isocyanurate resins of hexamethylene diisocyanate. Thus, in previous studies Edwards and coauthors obtained biuret glycidyl carbamate (BGC) and isocyanurate glycidyl carbamate (IGC) resins by reacting biuret and isocyanurate polyisocyanate resin with glycidol, respectively. BGC and IGC coatings obtained by amine and self-crosslinking had an excellent combination of chemical and mechanical properties.^{45, 46, 48}

The reaction of an isocyanate functional compound with an alcohol produces urethane functionality. The formation of reversible hydrogen bonding between urethane groups improves scratch resistance and toughness. Polyurethane coatings with a diverse range of properties are obtained by varying the composition of diisocyanates and polyisocyanates with diols, and polyols. The fundamental chemical nature and molecular architecture of isocyanates and alcohols used to obtain urethanes have a profound influence on the crosslinked network and coating properties such as mechanical properties (elongation at break, modulus, scratch resistance, hardness, adhesion, etc), glass transition temperature (T_g), thermal stability, and resistance to chemicals, corrosion,

and weathering. For example, polyurethanes based on symmetric diisocyanates such as hexamethylene diisocyanate (HDI), 1,4-phenylene diisocyanate or 1,4-cyclohexyl diisocyanate results in flexible polymer films. High solids polyurethane coatings based on symmetric diisocyanates and linear diols show high elongation at break. Polyurethane coatings based on bis(4-isocyanatocyclohexyl)methane (H₁₂MDI), and isophorone diisocyanate (IPDI) exhibit high strength, stiffness, and hardness.^{31, 33, 34, 137, 138}

Highly flexible coatings are used in many industries such as electronics, packaging, automotive, and aircraft.^{74, 75} The motivation for the research presented in this chapter was the necessity of designing a novel binder for a highly flexible corrosion resistant primer for aircraft applications.

Aircraft are exposed to severe loading (extension and compression) due to pressurization, wing flexure and multiple landing and takeoff cycles. Corrosion resistant coatings made from suitable binders provide barrier properties and protect metal from corrosion. Damage to coatings exposes the metal surface to corrosive environment and initiates electrochemical corrosion reactions. Corrosion inhibitors used in such coatings slow down the rate of corrosion reactions. Corrosion resistant primer is in direct contact with a metallic parts of aircraft. It is desirable that a binder for corrosion resistant primer produce highly flexible coatings to accommodate the severe loading experienced by aircraft. Aircraft are made of thousands of joints and riveted parts which act as stress concentrators. Coating systems, due to lack of flexibility, are prone to fail around joints and riveted parts.^{1, 79}

There have been many efforts to develop highly flexible coating systems with good corrosion performance for aircraft applications. Traditional aircraft coatings are

based on epoxy-polyamide primer systems, or epoxy-polysulfide rubbers with a flexible polyurethane top coat.^{1, 76, 77, 80-84}

The goal of the research presented in this chapter was to develop novel highly flexible GC-based coatings by designing novel GC functional resins using diisocyanates, linear diols, and glycidol. Linear aliphatic diisocyanates were used in combination with linear diols, triol, and glycidol to obtain several GC resins and amine crosslinked coatings. Initially, the coating systems were screened based on their flexibility and solvent resistance using reverse impact test and MEK double rubs test, respectively. Flexibility of selected coatings was further studied by obtaining values for elongation at break in tensile tests. The coatings were then characterized by electrochemical impedance spectroscopy (EIS) and salt spray test to determine their relative barrier properties and resistance to corrosion. Differential scanning calorimetry (DSC), dynamic mechanical analysis (DMA), and thermo gravimetric analysis (TGA) on the selected coatings were performed to further understand the structure-property correlation.

3.2. Experimental

3.2.1. *Materials*

Diisocyanates used for the synthesis were hexamethylene diisocyanate (HDI), dicyclohexyl diisocyanate (H₁₂MDI), and trimethyl hexamethylene diisocyanate (TMDI). HDI, H₁₂MDI, and TMDI were Desmodur H, Desmodur W and Vestanat TMDI, respectively. Desmodur H, Desmodur W, and Vestanat TMDI were obtained from Bayer MaterialScience and Evonik, respectively. The diols and triol used were 2-butyl-2-ethyl-1,3 propane diol (BEPD) (Aldrich), neopentyl glycol (NPG) (Aldrich), and diethylene glycol (DG) (Sigma-Aldrich) and trimethylol propane (TMP) (Aldrich). Glycidol was

supplied by Dixie Chemical. Glycidol was stored refrigerated to minimize the formation of impurities. Dibutyltindilaurate (DBTDL), purchased from Aldrich, was used to catalyze the isocyanate and hydroxyl reactions to form the glycidyl carbamate (GC) resins. All reagents were used as received without any further purification.

Solvents were used during the resin synthesis to reduce viscosity and facilitate the synthesis reaction. The solvents used were MAK, ethyl 3-ethoxy propionate (EEP), and tertiary butyl acetate (TBA) obtained from Ashland and Aldrich, respectively. TBA and EEP were also used in coatings formulations. Air Products provided the two amine crosslinkers, para-aminocyclohexyl methane (PACM) and Ancamide-2353 (A-2353), having hydrogen equivalent weight (gm/H) of 52.5 and 114, respectively. Ancamide-2353 is a mixture of polyamides of different molecular weights.

3.2.2. Synthesis of glycidyl carbamate functional resins for flexible coating applications

The synthesis reaction of the GC resins was carried out in two steps. In the first step, isocyanate terminated urethane intermediate was synthesized using diisocyanates and combinations of diols. A small amount of triol was also used in selected resin composition to introduce higher functionality in resins. In the second step, GC resin was synthesized by end capping the isocyanate terminated urethane intermediate with glycidol. A 500 ml four neck reaction vessel was used for the synthesis of the GC resins. The vessel was fitted with a condenser, nitrogen inlet, Model 210 J-KEM temperature controller, heating mantle and mechanical stirrer. A water bath was used to maintain the reaction temperature. The stoichiometric equivalent amount of isocyanates and hydroxy group of diols and triol based on $-NCO$ and $-OH$ groups used for the synthesis of

isocyanate terminated urethane intermediate was 1:0.66 (NCO:diols). For the synthesis of GC resins, the stoichiometric equivalent amount of NCO and glycidol based on total –NCO and –OH groups was 1:1 (NCO:glycidol). A series of GC resins were obtained using linear aliphatic diisocyanates, and combinations of diols and triol.

During the synthesis of resins, the reaction vessel was charged with a required amounts of diols and triol. Solid diols and triol were heated to melt and mixed with solvents before addition of solvent mixture and diisocyanate. The reaction mixture was stirred for about 30 min. to ensure a homogeneous mixture. The catalyst (DBTDL), in the form of solution in TBA (1 – 2 % by wt.), was added after the completion of mixing. The amount of catalyst added was 0.03 % by wt. (of the total reaction charge). The reaction was carried out between 65 – 80 °C until the required value for % NCO was reached before addition of glycidol. Glycidol was added at 40 °C and reaction was further carried out between 45 – 55 °C for 3 – 4 hrs. The reaction temperature was increased in the range of 60 – 65 in the later stage of the reaction until the –NCO peak in FTIR spectra disappeared completely. After the completion of the reactions, the resins were collected in glass jars.

In addition to diisocyanate based GC resins, polyisocyanate based GC resins such as biuret glycidyl carbamate (BGC) and modified GC resins were synthesized for comparison. The modified GC resins were BGC-EP 15% and BGC-EP 25% where ethyleneglycol propylether (EP) is a modified at 15 and 25 mole %. The synthesis of the resins was carried out in a similar fashion as explained in Chapter 2 of this dissertation.

3.2.3. NCO titration

Isocyanate content (% NCO) of the isocyanate terminated urethane intermediate was determined by back titration method according to ASTM D 2572. A required amount (0.5 – 1.0 gm) of the NCO terminated urethane intermediate dissolved in 50 ml mixture of toluene and isopropyl alcohol (1:1 weight. ratio) was reacted with an excess (25 ml) of 0.1 N di-n-butyl amine solution. Unreacted di-n-butyl amine was titrated against 0.1 N HCl using solution of bromophenol blue as an indicator. End point of the titration was the appearance of a yellow color.

3.2.4. FTIR measurements

FTIR measurements were performed using a Nicolet Magna-850 and Nicolet 8700 FTIR spectrometers. Sample aliquots were taken and coated on a potassium bromide salt plate. Spectra acquisitions were based on 64 scans with a data spacing of 1.98 cm^{-1} . The FTIR was set for auto gain to monitor spectral range of $4000 - 500\text{ cm}^{-1}$. The change in band absorption of isocyanate (2272 cm^{-1}), -OH and -NH ($3750 - 3000\text{ cm}^{-1}$), amide (1244 cm^{-1}) and epoxide (910 cm^{-1}) bands were used to follow the reaction progress.

3.2.5. Epoxy titration

Epoxy equivalent weight of the resins was determined by titration with hydrogen bromide (HBr) according to ASTM D1652. A required amount of resin (0.06 to 0.8 gm) was dissolved in 5 – 10 ml of chloroform and was titrated against a standardized HBr solution prepared in glacial acetic acid. The indicator used was a solution of crystal violet in glacial acetic acid. End point of the titration was the appearance of permanent yellow-green color.

3.2.6. Determination of % solids

Percent solids of the resins were determined according to the procedure described in ASTM D 2369. About 1.00 gm sample of a resin taken in an aluminum boat and was dissolved in TBA. The aluminum boats were kept in an oven at 120 °C for one hour. The weights of the sample before and after heating in oven was used to determine the % solids of the resins.

3.2.7. Coating preparation

GC coatings were obtained from the GC resins using PACM and Ancamide 2353 crosslinkers. Amine active hydrogen:epoxy equivalent ratio was 1:1 in all of the formulations. The solvents used for the coating formulations were ethyl 3-ethoxy propionate (EEP) (20 % by wt. of total resin) and tertiary butyl acetate (TBA) (20 % by wt. of total resin). The formulations were warmed around 50 °C to 60 °C using a heating mantle to ensure homogeneous mixing. The formulations were allowed to sit for 15 min before taking drawdowns. The films were drawdown at a wet thickness of 6 mils using a drawdown bar on steel panels (smooth finished Q panels, type QD36, 0.5×76×152 mm) cleaned with *p*-xylene. Films were also drawdown on Alodine 5700 treated aluminum panels (aluminum alloy-Al2024 T0, 0.032") to study their impact resistance and adhesion. Films were applied to glass panels to obtain free films for dynamic mechanical analysis (DMA) and tensile test measurements. The coated panels were kept at ambient conditions overnight and the next day the coated panels were cured in an oven at 80 °C for 1hr. All the coated panels were kept at ambient after curing and were tested after fourteen days. The coatings obtained in this manner were used for reverse impact, MEK double rubs, conical mandrel, König hardness, cross-hatch adhesion, dry DSC and dry TGA tests.

Differential scanning calorimetry (DSC) and thermogravimetric analysis (TGA) were performed on dry and wet coatings samples. Wet coating samples were obtained from the coatings on glass panels cured by above method and kept under water overnight. DSC and TGA experiments were performed on the wet coating samples as soon as they were removed from the water.

The free coating films for DMA and tensile test were obtained by immersing the coated glass panels in water for overnight and removing the films next day. The free films were tested the following day after drying them at ambient overnight.

The coating samples used for electrochemical impedance spectroscopy (EIS) and salt spray test were two coat systems on steel and treated aluminum panels. Two coats of the same coatings were used to minimize the local defects in the coatings. The steel panels were wiped with *p*-xylene for degreasing before applying coatings on them. The aluminum panels used in this experiments were cleaned using MEK for degreasing and Brulin Cleaner (Formula 815MX) with abrasive pad. The aluminum panels were further treated with deoxidizer solution (35 % butanol, 25 % isopropanol, 18 % orthophosphoric acid, and 22 % volume deionized water) and Alodine 5700 (chromate free conversion coating). The treated aluminum panels were kept at ambient over night before applying coatings on them. The first coat was drawn at 4 mils and kept at ambient for two days before curing at 80 °C for 1 hr. The second coat at 5 mils was drawn on the previously coated and cured panels. After keeping the coatings at ambient for two days, the coatings were again cured at 80 °C for 1hr. Finally, all the coatings were kept at ambient for 8 – 9 days before they were characterized by electrochemical impedance spectroscopy (EIS) and by salt spray test.

3.2.8. Coating performance

König pendulum hardness of the coatings was measured following ASTM D 4366. The hardness test results are reported in seconds (sec). Reverse impact strength of the coatings was determined following ASTM D 2794 using a Gardener impact tester. The maximum drop height was 43 inches and the drop weight was 4 pounds. Crazeing or loss of adhesion was noted and inch-pounds (in-lbs) were reported at film finish failure. Samples that did not fail were noted as having an impact strength of >172 in-lbs. Flexibility of the coatings was determined using GE flexibility impact tester according to ASTM D 6905. The conical mandrel test was also used according to ASTM D 522 for the determination of flexibility the coatings. The results of flexibility test were reported as the length of a crack (cm) formed on the coating during the test. Methyl ethyl ketone (MEK) double rubs test was used according to ASTM D 5402 to assess the chemical resistance and development of cure. A 26-ounce hammer with three layers of cheesecloth wrapped around the hammerhead was soaked in MEK. The hammer head was rewet with MEK after 30 – 50 double rubs. Once mar was achieved, a number of double rubs was noted. Cross hatch adhesion of the coatings was evaluated using a Gardco cross hatch adhesion instrument following ASTM D 3359.

3.2.9. Differential scanning calorimetry (DSC)

A TA Instruments Q 1000 differential scanning calorimeter (DSC) coupled with an auto sampler accessory was used to determine the glass transition temperature (T_g) of the coatings. DSC experiments were performed by placing a sample into conventional aluminum pans. The samples were subjected to a heat-cool-heat cycle. The samples were heated to 200 °C and then cooled to -75 °C and held there for 5 min. DSC thermogram

were taken from -75 °C to 250 °C. A heating rate of 10 °C min⁻¹ was used during the experiments. Glass transition temperature of dry and wet coating samples was determined as the temperature of the inflection at the mid-point of the thermogram in the first DSC cycle.

3.2.10. Thermogravimetric analysis (TGA)

TGA was performed using a TA Instruments Q 500. Temperature was ramped from ambient to 800 °C with a ramp rate of 10 °C min⁻¹. A nitrogen atmosphere was used during the test. Weight retained was plotted as a function of temperature.

3.2.11. Dynamic mechanical analysis (DMA)

A TA Instruments Q 800 Dynamic Mechanical Analysis system was used to determine viscoelastic properties of the cured coating films. The dimensions of free films used were of 23 to 26 mm in length, 5 mm in width and 0.09 to 0.1 mm in thickness. Poisson's ratio was assumed to be 0.4 for all of the coating films. The experiments were carried out within a temperature range of -20 °C to 200 °C with a temperature ramp rate of 5 °C min⁻¹ at a frequency of 1 Hz.

3.2.12. Tensile test

Tensile testing of the coatings was performed using Instron 5542 instrument. The test specimen were prepared according to ASTM D 638-5 method. The test was carried out at 10 mm/min at ambient conditions. Elongation at break and Young's modulus of the coatings were determined.

3.2.13. Electrochemical impedance spectroscopy (EIS)

Figure 3.1 is a schematic representation of the EIS experiment performed using the conventional three-electrode system. Conventional EIS set up consists of metal

substrate as the working electrode (WE) with Platinum (Pt) and saturated calomel electrode (SCE) as counter and reference electrodes, respectively. A Gamry Instruments R 600 Potentiostat/Galvanostat/ZRA and Gamry Framework Version 5.20/EIS 300 software supplied by Gamry Instruments, Inc. of Willow Grove, PA were used for the experiments. The impedance response corresponding to the applied frequency of 100 kHz to 0.01 Hz was measured with an acquisition rate of 10 points per decade. A 10mV amplitude perturbation potential with respect to the open circuit potential was used during the measurement.

Perspex cylinder with a surface area of 7.07 cm^2 was mounted on the samples and was clamped with an O-ring insert for the electrochemical measurements. All the EIS measurements were performed under immersed condition using 5% NaCl solution as the electrolyte. Initially an EIS measurement at zero time was performed to check for any application defect. The samples were kept at immersed condition for seven days to facilitate electrolyte penetration through the coatings. EIS measurements were performed after 2.5 hrs and after seven days.

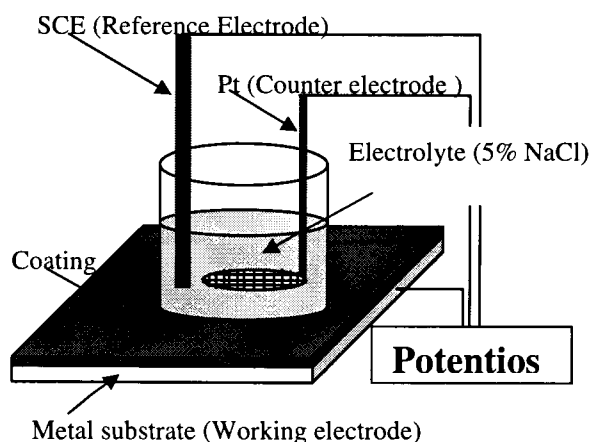


Figure 3.1. Schematic representation of EIS experiment performed using the conventional three-electrode system.

3.2.14. Salt spray test (ASTM B 117)

The coated panels were scribed and exposed to continuous salt spray (5 % NaCl in deionized water) fog at 35 °C for ten days. The pictures of the coatings were taken periodically by scanning.

3.3. Results and discussion

3.3.1. Synthesis of GC resins based on diisocyanates and diols

The synthesis of GC resins was a two step reaction. The first step of the reaction was the synthesis of isocyanate terminated urethane intermediate and the second step was end capping of the intermediate with glycidol. A schematic of the synthesis reaction is shown in Figure 3.2.

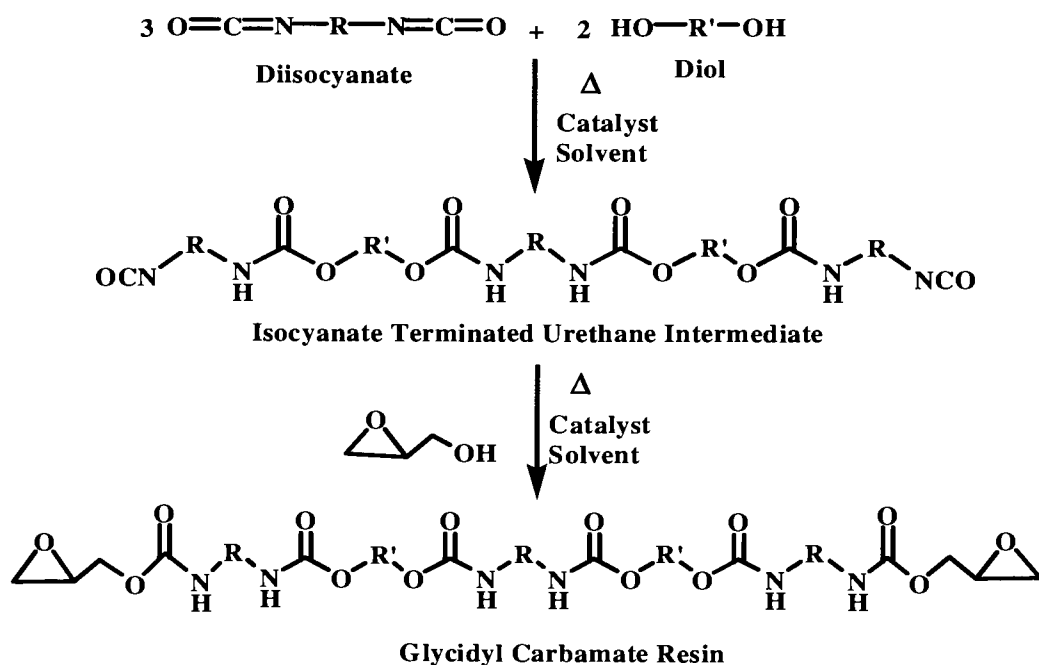


Figure 3.2. Schematic representation of the synthesis of GC resins using diisocyanate, diol, and glycidol.

The stoichiometric equivalent of isocyanates and hydroxy group of diols and triol based on -NCO and -OH groups used for the synthesis of isocyanate functional urethane intermediate was 1:0.66 (NCO:diols). For the synthesis of GC resins, the

stoichiometric equivalent amount of NCO and glycidol based on total –NCO and –OH groups was 1:1 (NCO:glycidol).

Thus, eight GC resins were obtained based on three diisocyanates and by varying the stoichiometric amount of diols and triol during the synthesis. Figure 3.3 shows the structures of the diisocyanates, diols, and triol used for the synthesis of GC resins.

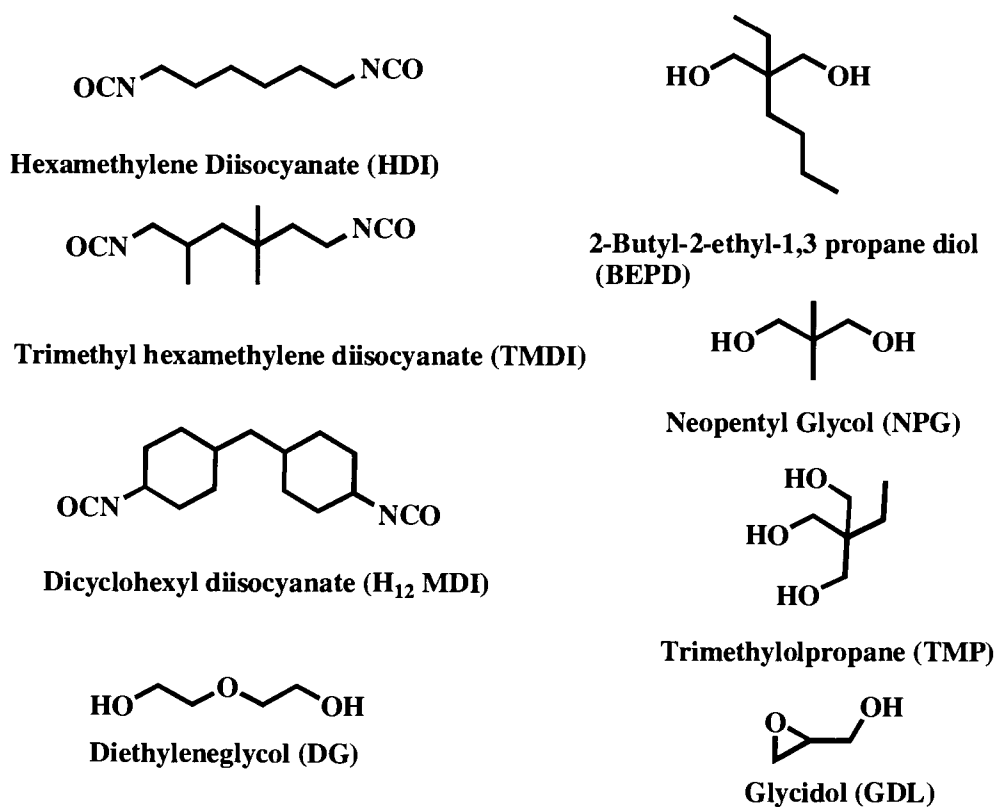


Figure 3.3. Structures of the diisocyanates, diols, triol, and glycidol used in the synthesis of various GC resins.

The synthesis of the isocyanate functional urethane intermediate was characterized by % NCO determination by back titration method using di-n-butyl amine and HCl solutions. The reaction was continued until the % NCO value was close to the theoretical expected value. The end capping reaction was continued until the NCO peak in FTIR at 2272 cm^{-1} had disappeared completely. Epoxy equivalent weight (gm/eq.) of

the synthesized GC resins was determined by titrating the resins with HBr solution. Table 3.1 shows the recipes of the GC resins synthesized in this research work.

It was thought that the coatings based on the GC resins obtained from linear diisocyanates and linear diols may exhibit low solvent resistance. A small amount (≤ 0.03 mol) of triol was used in selected resin composition to increase the functionality in the resins and solvent resistance of the coatings.

3.3.2. Performance of highly flexible GC coatings

3.3.2.1. *Initial screening of coating based on impact and solvent resistance*

The first phase of this research involved screening of the coatings to indentify the coatings with a combination of good flexibility and solvent resistance. For the screening study, PACM crosslinked GC coatings were prepared using GC resins R1 to R7, BGC, and modified GC resins (BGC-EP 15% and BGC-EP 25%). The GC coatings prepared from polyisocyanate based GC resins (BGC and modified GC resins) were used to compare their flexibility with the coatings prepared from diisocyanate based GC resins. Resin R8 was prepared in the second phase of the study and coatings based on resin R8 were characterized along with the screened coatings. The coatings based on resin R8 were included in the second phase of study to examine the influence of rigid cycloaliphatic structure of H₁₂MDI on the coatings properties. For the initial screening coatings were prepared on aluminum and steel substrates. Reverse impact test was carried out on the coatings prepared on aluminum substrate. MEK double rubs test was carried out on the coatings prepared on steel substrates. Table 3.2 shows the results of reverse impact and MEK double rubs tests.

Table 3.1. Recipes for the synthesis of GC resins for flexible coating applications.

Resin	Isocyanate terminated urethane intermediate				End capping by glycidol					Solvents (gm)			Solids (%)
	Composition	Weight (gm)	Mole (mol)	% NCO		Weight (gm)	Mole (mol)	EEW (g/eq.)		TBA	MAK	EEP	
				Theo.	Act.			Theo.	Act.				
R1	HDI BEPD NPG	150.00 47.80 30.90	0.89 0.30 0.30	10.93	10.47	42.18	0.57	458	510	None	25.00	None	90
R2	HDI BEPD	150.00 95.37	0.89 0.59	10.75	10.39	44.96	0.61	486	502	None	35.00	None	91
R3	TMDI BEPD	100.40 50.88	0.48 0.32	9.71	9.00	23.00	0.31	475	403	17.00	None	None	91
R4	TMDI BEPD NPG	100.17 25.54 16.52	0.48 0.16 0.16	9.39	8.67	20.92	0.28	521	566	15.00	None	None	91
R5	HDI BEPD TMP	100.00 56.95 3.55	0.60 0.36 0.03	10.44	10.66	28.00	0.38	483	450	20.00	None	None	94
R6	HDI DG BEPD TMP	100.30 29.27 12.72 3.54	0.60 0.28 0.08 0.03	11.50	9.00	22.20	0.30	446	418	35.00	None	None	95
R7	TMDI DG BEPD TMP	101.6 23.40 10.05 2.82	0.48 0.22 0.06 0.02	9.33	9.00	21.05	0.28	486	466	15.00	None	None	94
R8	H ₁₂ MDI BEPD	150.00 60.26	0.57 0.38	7.82	7.32	27.10	0.37	627	681	30	20	10	82

Table 3.2. Performance of PACM crosslinked GC coatings in screening study.

GC Coatings	Reverse Impact* (in.ib)	MEK Double Rubs
BGC	28	>400
BGC-EP 15%	96	>400
BGC-EP 25%	132	>400
R1	>172	>400
R2	>172	325
R3	44	100
R4	>172	50
R5	>172	100
R6	>172	80
R7	>172	46

BGC and modified GC coatings showed relatively low impact resistance compared to most of the GC coatings obtained from linear diisocyanate, diols and triol based GC resins. Solvent resistance of BGC, modified GC, R1, and R2 coatings was higher compared to that of the other GC coatings. Coatings obtained from resins R1 and R2 showed high impact strength and high solvent resistance. The compositions of HDI, BEPD and NPG in resin R1 and HDI and BEPD in resin R2 produced the coatings with a combination of high impact strength and high solvent resistance. Based on this study, coatings based on R1 and R2 resins were selected for further characterization. GC coatings obtained from resin R3 based on TMDI and BEPD showed low impact strength and solvent resistance. Addition of NPG and DG and TMP in the composition of TMDI based resins R4 and R7, respectively improved impact strength but did not improve solvent resistance. The coatings obtained from resins R5 and R6 had high impact strength

but low solvent resistance. Addition of higher functionality through TMP in resins R5, R6, and R7 did not result in improved solvent resistance.

3.3.2.2. Further analysis of properties of the screened coatings

Six GC coatings were prepared from the screened GC resins, R1, R2 and, R8, in combination with two amine crosslinkers. The crosslinkers used were PACM and Ancamide 2353. PACM crosslinked GC coatings from resins R1, R2 and, R8 were labeled F1, F2 and, F3, respectively. Ancamide 2353 crosslinked coatings from resins R1, R2, and, R8 were labeled L1, L2 and, L3, respectively. Table 3.3 shows the GC coatings properties such as crosslink density, adhesion, flexibility, solvent resistance, hardness, glass transition (T_g) temperature, elongation at break, and Young's modulus. The crosslink density of the coatings was calculated from the storage modulus values (well above T_g) obtained in DMA experiments. The equation 3.1 was used to calculate the crosslink density of the coatings^{112,121}

$$E' = 3\nu_e RT \quad (3.1)$$

where E' is the storage modulus (Pa), ν_e the crosslink density (mol/L), R the gas constant (8.3 J/K/mol), and T is the temperature (K).

The coatings had high hardness, good adhesion, and high chemical resistance. The flexibility of coatings F1, F2, L1, and L2 was higher compared to that of the coatings F3 and L3 as indicated by their highest impact strength, 60% elongation in GE impact test, no crack in conical mandrel test, and high elongation at break in tensile test. F3 and L3 coatings are obtained from GC resin R8 composed of cycloaliphatic diisocyanate, H₁₂MDI, whereas the other GC coatings F1, F2, L1, and L2 were obtained from resins R1

Table 3.3. Properties of highly flexible GC coatings.

GC coating	Reverse impact (in.lb)*	Elongation in GE impact test (% elongation)	Cross-link density (mol/L)	Conical mandrel (cm) (0cm=Best)	Elongation at break (mm)	Young's modulus (MPa)	Cross-hatch adhesion* (5B=Best)	MEK double rubs	König pendulum hardness (sec)	T _g DSC first dry cycle
PACM crosslinked										
F1	>172	60	0.660	0	34	2600	5B	>400	156	25
F2	>172	60	0.575	0	23	3176	5B	>400	153	25
F3	14	<10	0.172	1	1	5400	5B	>400	223	55 endotherm
Ancamide 2353 crosslinked										
L1	>172	60	0.549	0	22	2000	5B	190	100	20
L2	>172	60	0.394	0	26	1445	5B	170	81	18
L3	<8	<10	0.259	1	Films too brittle for sampling	Films too brittle for sampling	5B	300	208	57 endotherm

*Tests performed on aluminum substrate (Al2024-T0)

and R2 composed of aliphatic diisocyanate, HDI. Cycloaliphatic structure of H₁₂MDI is considered highly rigid and responsible for very low flexibility compared to non-rigid aliphatic diisocyanate, HDI.^{31, 33, 138, 139} Thus, high flexibility of coatings F1, F2, L1, and L2 obtained from resins R1 and R2 can be attributed to the resin composition containing non-rigid aliphatic diisocyanate(HDI). The influence of rigid H₁₂MDI was also reflected in higher hardness values for coatings F3 and L3 compared to that of the other coatings. While coatings F3 and L3 had lower crosslink density compared to that of the others, their transition temperature was higher than the others due to rigid H₁₂MDI. Figure 3.4 shows stress vs. strain plots for F1, F2, F3, L1, and L2 coatings. Highly brittle nature of L3 coatings did not produce intact samples for the tensile test. F1 coating based on resin R1 composed of HDI, BEPD and NPG, and crosslinked with PACM exhibited the highest elongation at break. However, the similar composition in F2 except no NPG showed lower elongation at break compared to that of F1.

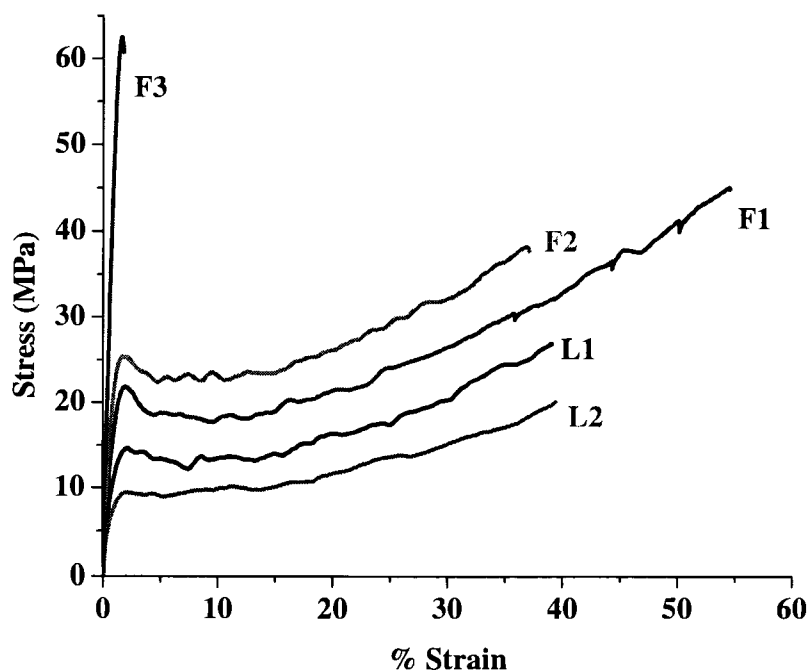


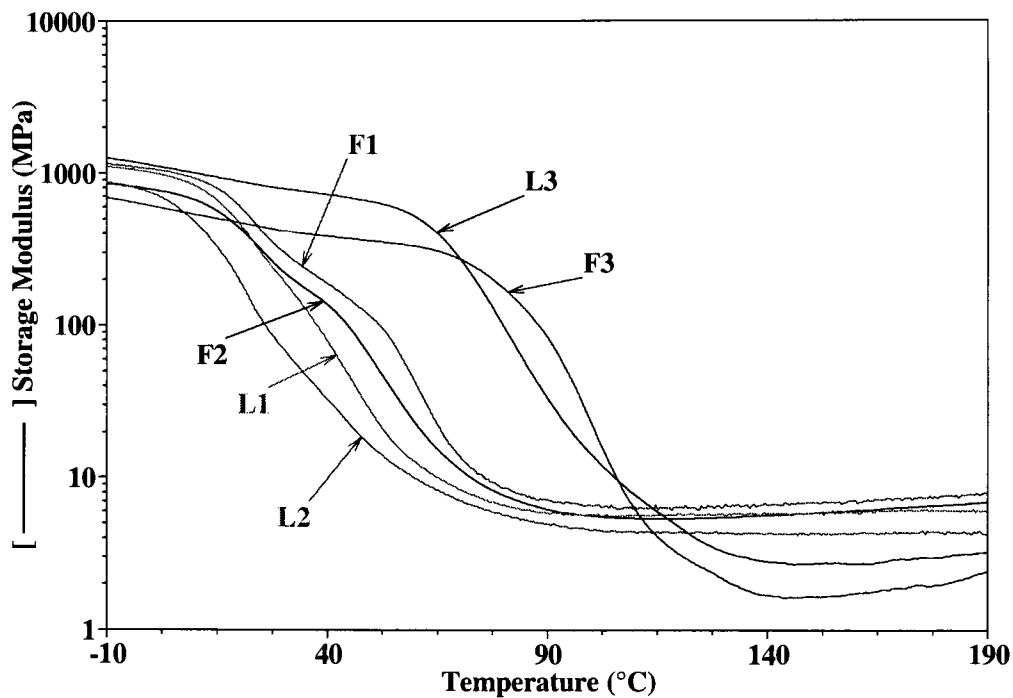
Figure 3.4. Stress vs. strain plots for coatings F1, F2, F3, L1, and L2.

Influence of the type of amine crosslinker was prominent on solvent resistance (MEK double rubs) and hardness. PACM crosslinked GC coatings had higher hardness and solvent resistance compared to that of Ancamide 2353 crosslinked coatings.

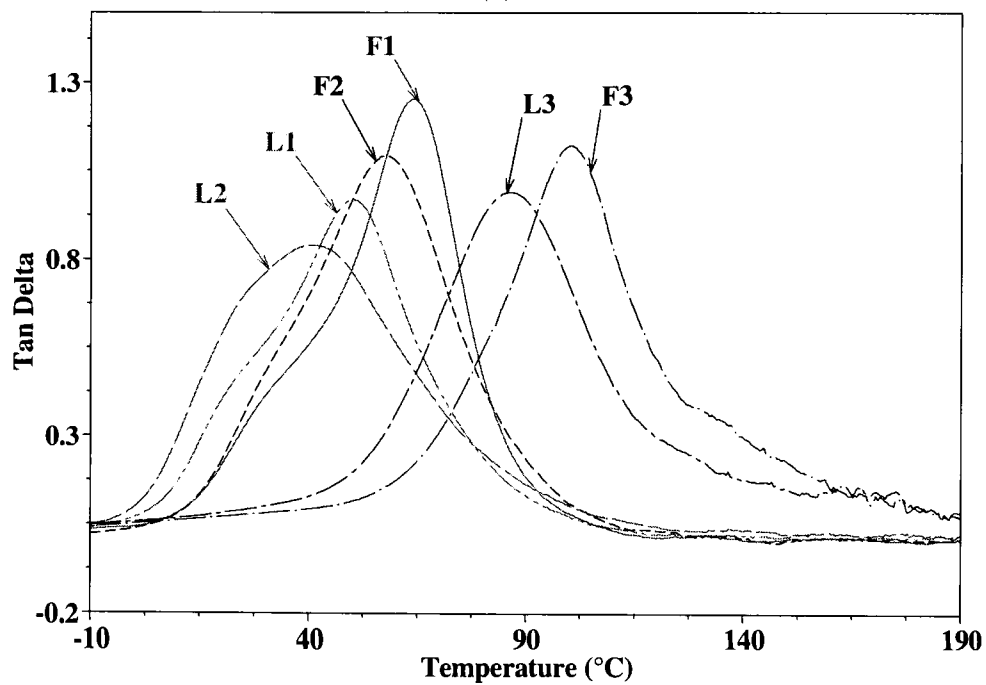
3.3.2.3. *Dynamic mechanical analysis*

Dynamic mechanical analysis correlated the influence of the composition of GC resins and type of amine crosslinker with the coating properties. Figure 3.5 shows (a) storage modulus and (b) $\tan \delta$ curves for the GC coatings. Storage modulus of coatings indicates the stiffness (rigidity) of coatings and it decreases in the transition region making coatings more flexible.¹⁴⁰ Transition temperatures for F1, F2, L1, and L2 coatings were much lower than that for F3 and L3 coatings. This indicated lower stiffness and higher flexibility of F1, F2, L1 and, L2 coatings compared to that of F3 and L3 coatings. F1, F2, L1, and L2 coatings are obtained from GC resins (R1 and R2) based on non-rigid aliphatic diisocyanate (HDI). On the other hand, F3 and L3 coatings are obtained from GC resins based on rigid cycloaliphatic diisocyanate (H_{12} MDI). The transition region and $\tan \delta$ curves for H_{12} MDI based GC coatings (F3 and L3) appear well above room temperature. High flexibility of HDI based GC coatings (F1, F2, L1 and, L2) can be correlated to the appearance of their transition region near room temperature. The type of crosslinker influenced the breadth of the $\tan \delta$ curves. For all the GC coatings, Ancamide 2353 crosslinked coatings showed broader $\tan \delta$ peaks compared to the corresponding PACM crosslinked GC coatings. The broadening of $\tan \delta$ peaks indicates non-uniformity in the crosslinked network.¹²² Also, a comparison of $\tan \delta$ peaks for H_{12} MDI based coatings (F3 and L3) with that of the other coatings shows that F3 and L3 coatings have relatively more symmetric and narrow $\tan \delta$ peaks compared to that of the other coatings.

Thus, H₁₂MDI based L3 coating had more uniform crosslinked network compared to that of HDI based L1 and L2 coatings.



(a)



(b)

Figure 3.5. (a) Storage modulus and (b) tan δ curves for coatings F1, F2, F3, L1, L2, and L3.

3.3.2.4. Thermal stability

The thermal stability of the amine crosslinked GC coatings was studied using TGA. TGA plots for the GC coatings are shown in Figure 3.6. GC coatings show stability around 125 °C. The onset temperature for thermal degradation was found to be between 240 and 260 °C and weight loss in this temperature range was between 7 to 16 %.

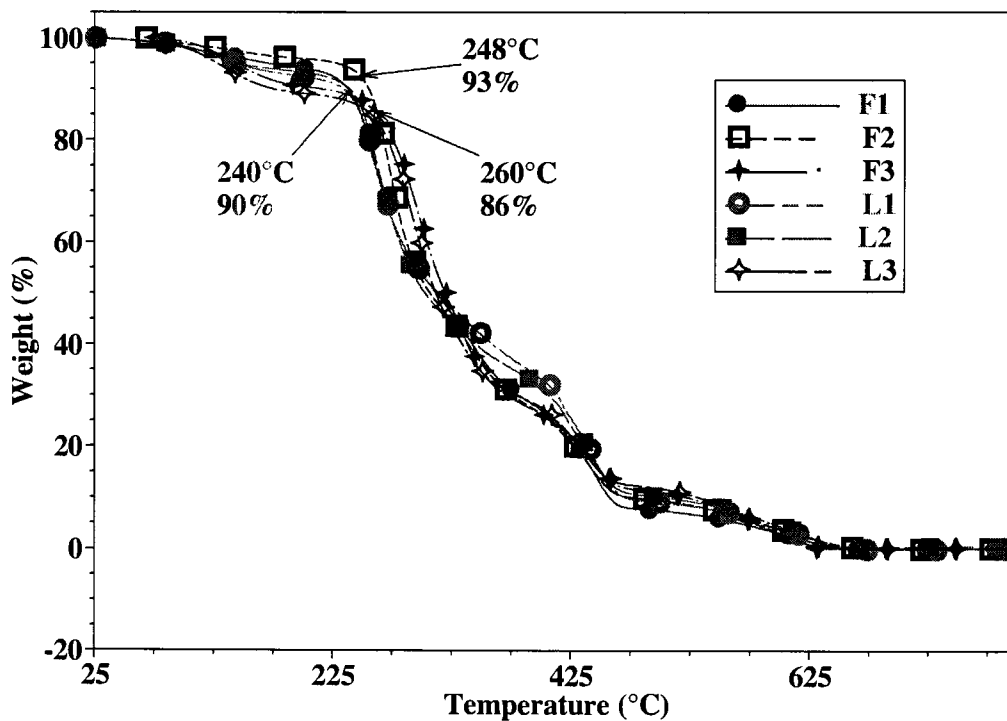


Figure 3.6. TGA of coatings F1, F2, F3, L1, L2, and L3.

3.3.2.5. Barrier properties of GC coatings

Coatings which have a high barrier to corrosive species and excellent adhesion to the metal substrate have very high corrosion resistance. The coatings act as barrier against the penetration of corrosive species such as water, oxygen, and ions and thus prevent progress of corrosion at the metal-coating interface. The corrosive species diffuse and reach the metal-coating interface through interconnected small pores or channels in

crosslinked coatings.¹²⁴ The barrier of the coatings to the transportation of water and ions can be quantitatively determined by electrochemical impedance spectroscopy (EIS). EIS technique provides kinetic and mechanistic information related to the changes caused due to exposure to corrosive environment in the bulk of coatings and across the metal-coating interface.¹²⁵⁻¹²⁷

The impedance is the tendency of a system to resist the flow of AC current. In the EIS experiments, a small AC voltage at varying frequency is applied across the coated metal substrate and a plot of the magnitude of impedance or modulus of impedance ($|Z|$) vs. frequency is obtained. A plot of change in phase angle between applied voltage and resulting current vs. frequency can also be obtained. The plots of $|Z|$ vs. frequency and phase angle vs. frequency are known as Bode plots. The magnitude of impedance ($|Z|$) of a coating changes with applied frequency depending upon capacitive and resistive components in the coating system and the corrosion process. The $|Z|$ of coatings is widely measured as an indicator of the barrier properties of coatings. Typically, initial $|Z|$ of coatings over $10^8 \Omega \text{ cm}^2$ in low frequency region (LF) of Bode plot have very high barrier properties and provide excellent corrosion resistance. The coatings with initial $|Z|$ between $10^6 \Omega \text{ cm}^2$ - $10^8 \Omega \text{ cm}^2$ in LF region of Bode plot have high barrier properties and provide reasonable corrosion performance.¹²⁷⁻¹²⁹ In the Bode plot, the coatings with very high impedance, very high barrier properties, and an excellent corrosion resistance show purely capacitive (frequency dependent) behavior with slope -1 over a wide range of frequencies.¹²⁹⁻¹³¹

In this experiment, the influence of structural composition of the GC resins on barrier properties of the coatings was studied. GC resins R1, R2, and R8 were crosslinked

with Ancamide 2353 crosslinker to obtain coatings L1, L2, and L3, respectively on cold rolled steel (QD) and aluminum (Al2024-T3) substrates. Bode plots of the coatings L1, L2, and L3 for 2.5 hrs and 7 days of immersion conditions were obtained. Figure 3.7 (a) and (b) show the $|Z|$ Bode plot for L1, L2, and L3 coatings on steel substrate after 2.5 hrs and seven days of immersion, respectively.

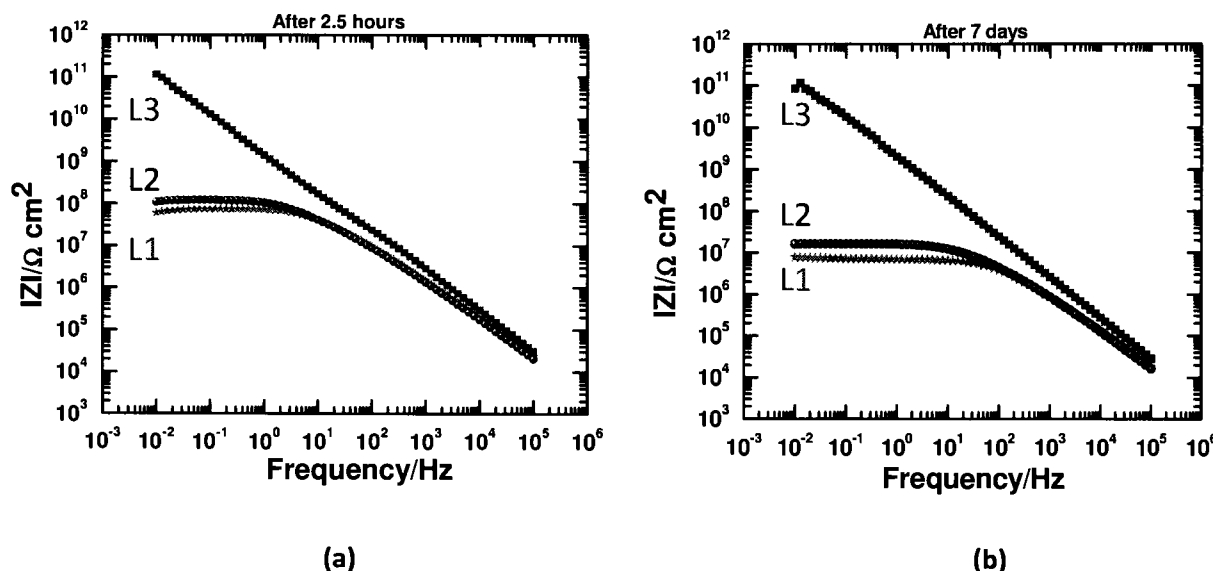


Figure 3.7. Bode plot of coatings L1, L2, and L3 steel substrate after (a) 2.5 hrs, and (b) 7 days of immersion.

The Bode plot after 2.5 hrs of immersion shows high impedance ($|Z|$) for all the coatings. The $|Z|$ value for coating L1 is slightly below $10^8 \Omega \text{ cm}^2$, for coating L2 slightly above $10^8 \Omega \text{ cm}^2$, and for coating L3 the impedance is very high and is slightly above $10^{11} \Omega \text{ cm}^2$. Thus, the increasing trend of impedance is in the order of $L3 \gg L2 > L1$. After seven days of immersion, the impedance of coatings L1 and L2 decreased by almost an order of magnitude, while coating L3 maintained its very high impedance value slightly above $10^{11} \Omega \text{ cm}^2$. After seven days of immersion, the decrease in impedance values of coatings L1 and L2 can be attributed to the uptake of water. The impedance values of all

the coatings above $10^6 \Omega \text{ cm}^2$ after seven days of immersion indicated good barrier properties. Noticeably, L3 coating maintained its capacitive character and exhibited very high barrier to penetration of water.

EIS experiments provide the capacitance of coatings in the high frequency (10 KHz) region of modulus Bode plot. Increase in water uptake increases the capacitance of the coatings and decreases the impedance.^{125, 126} Figure 3.8 shows the capacitance of the coatings after seven days of immersion. Coating L3 showed the lowest capacitance and indicated the least water uptake. Coatings L1 and L2 showed very small difference in their capacitance values.

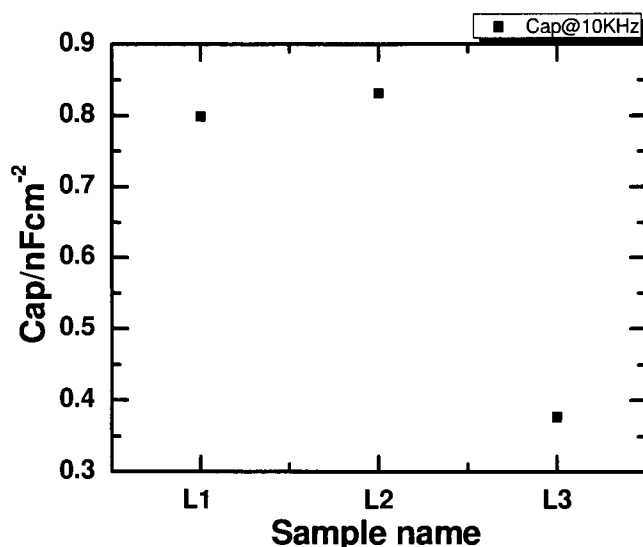


Figure 3.8. Capacitance of L1, L2, and L3 coatings after seven days of immersion.

The significant difference in barrier properties and capacitance of the coatings L1 and L2, and L3 can be explained with the help of composition of GC resins R1, R2, and R8. L1 and L2 coatings are obtained from resins R1 and R2 containing non-rigid aliphatic diisocyanate (HDI) whereas L3 coatings are obtained from resin R8 containing cycloaliphatic rigid diisocyanate (H₁₂MDI). Water uptake of polymeric network is found

to be directly proportional to the extent of polar and hydrophilic groups in the network.^{95,}
¹³⁴⁻¹³⁶ Thus, coatings based on GC resins with a high amount of non-polar hydrocarbon or low amount of polar groups can be expected to show low water uptake. The crosslinked GC coatings contain polar groups as well as non-polar hydrophobic groups. The highly polar groups in the GC coating system would be urethane groups present in the resin structure, and hydroxyl groups and tertiary amine groups generated during crosslinking. The non-polar hydrophobic portion in the crosslinked GC coatings is the hydrocarbon backbone of the GC resins. In the structure of HDI, the amount of non-polar hydrocarbon (6 carbon atoms from aliphatic chain) is lower than that in H₁₂MDI (13 carbon atoms from cycloaliphatic rings). The estimated weight % non-polar groups in the structure of GC resins based on HDI (resins R1 and R2) and H₁₂MDI (resin R8) are shown in Table 3.4.

Table 3.4. Wt. % non-polar hydrocarbon.

GC resin	Wt. % non-polar hydrocarbon
R1	58.0
R2	57.8
R8	65.0

Table 3.4 shows that resins R1 and R2 have a lower amount of non-polar groups, while resin R8 has the highest amount of non-polar groups. The capacitance of coating L3 was lower than that for L1 and L2 coatings which indicated lower water uptake by L3 coatings than L1 and L2 coatings. It was also interesting to note that EEW of the R8 resin was the highest and resin R8 required a relatively lower amount of polar polyamide crosslinker compared to that of the other resins to obtain coatings. Thus, the lower

amount of crosslinker in L3 coatings compared to the other coatings may have also contributed to its lower water uptake and hence higher capacitance.

The water uptake in coatings influence T_g of coatings. The large decrease in T_g of the coatings after immersion indicates a plasticization effect and resin/water interaction as water penetrates into the coatings and disrupts interchain interaction leading to a decrease in barrier properties of the coatings.^{125, 141-144} Dry and wet transition temperature values of L1, L2, and L3 were recorded in the first DSC cycle. Figure 3.9 shows the difference in the transition temperature in dry and wet coating samples. coating L3 had higher dry and wet first endotherm peak transition compared to that of T_g of L1 and L2 coatings. The broad endotherm seen after immersion indicates the interaction of water with the coatings.¹⁴⁵

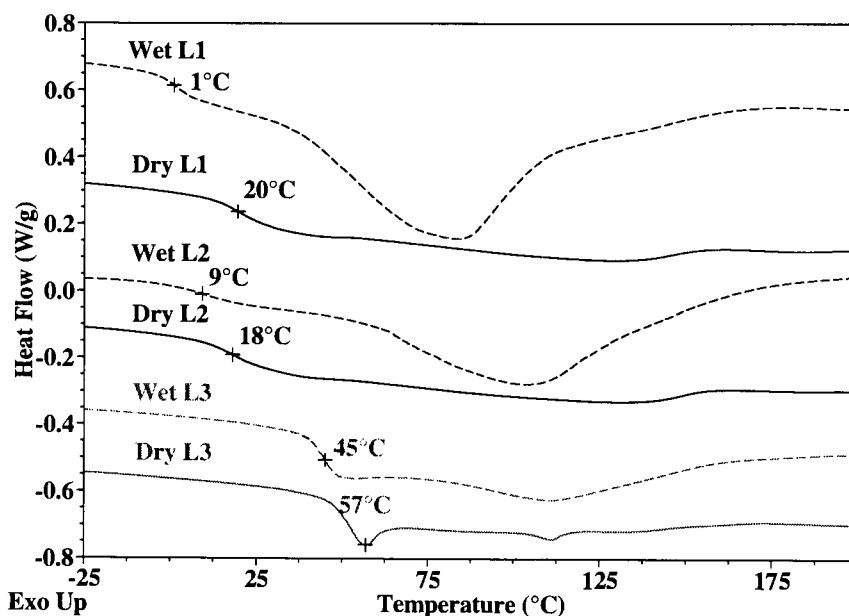


Figure 3.9. DSC first cycle for dry and wet coatings L1, L2, and L3.

The decrease in T_g or the change in transition temperature of the coatings due to immersion was in the order of $L1 \gg L2 > L3$ and correlated to their increasing impedance

and barrier trend of L3>>L2>L1. Table 3.5 shows the dry and wet T_g measured in first DSC cycle for L1, L2, and L3 coatings.

Table 3.5. % Decrease in T_g after wet condition.

Coatings	Dry T _g (°C) from cycle 1 in DSC	Wet T _g (°C) from cycle 1 in DSC	% decrease in T _g
L1	20	1	95
L2	18	9	50
L3	57 (endotherm peak)	45	21

TGA was also performed on the wet and dry coating samples to examine the influence of water on the coatings. Figure 3.10 shows TGA of dry and wet L1, L2, and L3 coating samples. In TGA experiments, dry and wet samples of L1 and L2 coatings

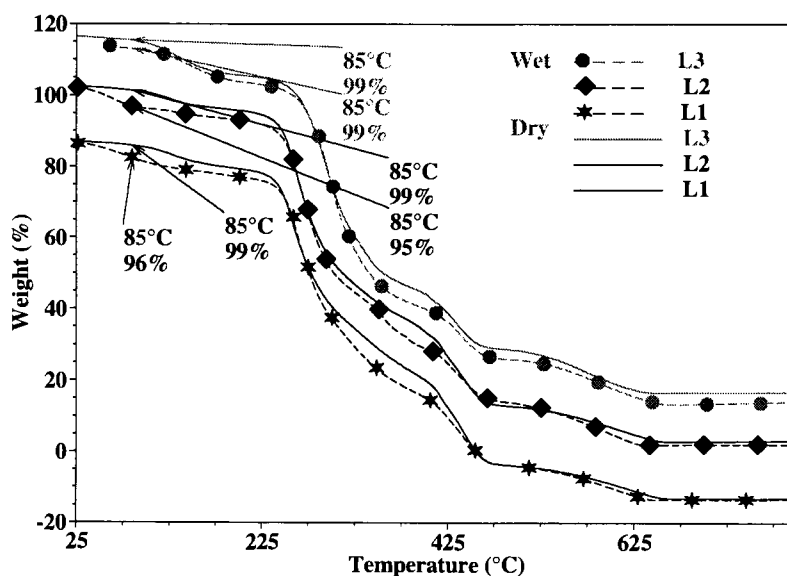


Figure 3.10. TGA of dry and wet samples of coatings L1, L2, and L3.

showed higher weight loss after immersion. For example, at 85 °C L1 and L2 coatings after immersion showed a weight loss of 3 and 4 % compared to that of dry condition samples. L3 coating did not show any difference in weight change before and after immersion condition at 85 °C.

L1, L2, and L3 coatings had high impedance (low frequency), low capacitance (high frequency) and exhibited good barrier properties after seven days of immersion condition. The significant difference in the impedance values and barrier properties of L1 and L2, and L3 coatings can be correlated to the composition of GC resins. A very high impedance value (above $10^{11} \Omega \text{ cm}^2$) and excellent barrier properties of L3 coating after seven days of immersion condition observed in EIS experiments can be correlated to low extent of polar group in the resin structure, high EEW which reduces equivalent amount of crosslinker, and high dry and wet T_g arising from the rigid molecular structure of H_{12} MDI.

EIS experiments were also performed on the coatings on aluminum substrate treated with Alodine 5700. Figure 3.11 show the modulus Bode plot for coatings L1, L2, and L3 after 2.5 hrs and seven days of immersion.

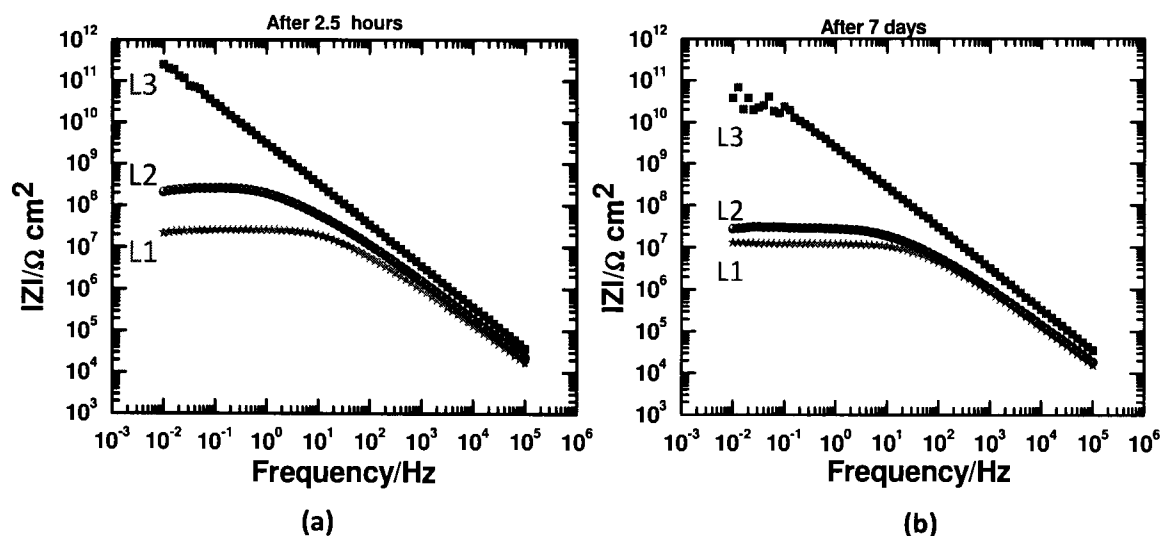


Figure 3.11. Bode plot for coatings L1, L2, and L3 on aluminum substrate after (a) 2.5 hrs of and (b) seven days of immersion

Figure 3.11 shows that all the coatings after seven days of immersion had high impedance and indicated protective behavior. Figure 3.11 shows that coating L1

maintained impedance value close to $10^7 \Omega \text{ cm}^2$ after seven days of immersion. Coating L2 had a reduction in impedance value about one order of magnitude after seven days but was still close to $10^7 \Omega \text{ cm}^2$. Coating L3 had the highest impedance after 2.5 hrs as well as after seven days of immersion and indicated excellent protective behavior. The scatter of the data at high impedance for coating L3 may appear due to its very high impedance value reaching the measuring limit of the EIS instrument.

Figure 3.12 shows the capacitance of the coatings on aluminum substrate after seven days of immersion. The capacitance of coatings L1 and L2 was higher than that for coating L3 which indicated higher water uptake in L1 and L2 coatings compared to that in coating L3.

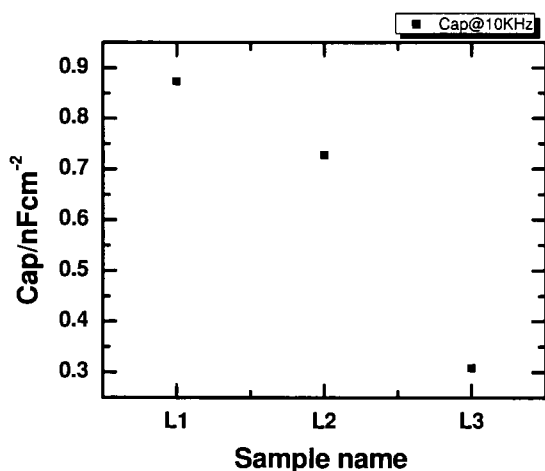


Figure 3.12. Capacitance of L1, L2, and L3 coatings on aluminum substrate after seven days of immersion.

3.3.2.6. Salt spray test

ASTM B 117 Salt spray test is the oldest standard test to compare corrosion resistance of the coatings. The salt spray test was performed on the coatings on scribed steel and aluminum panels. The scribe on the coatings and panels results in a physical damage to the coatings and underlying substrate. Performance of the coatings on steel

and aluminum panels was studied under continuous exposure to the fog (5% NaCl solution) over 240 hrs. Figure 3.13 shows the pictures of coatings L1, L2, and L3 two of each on steel panels and one of each on aluminum panel after 240 hrs of salt spray test.

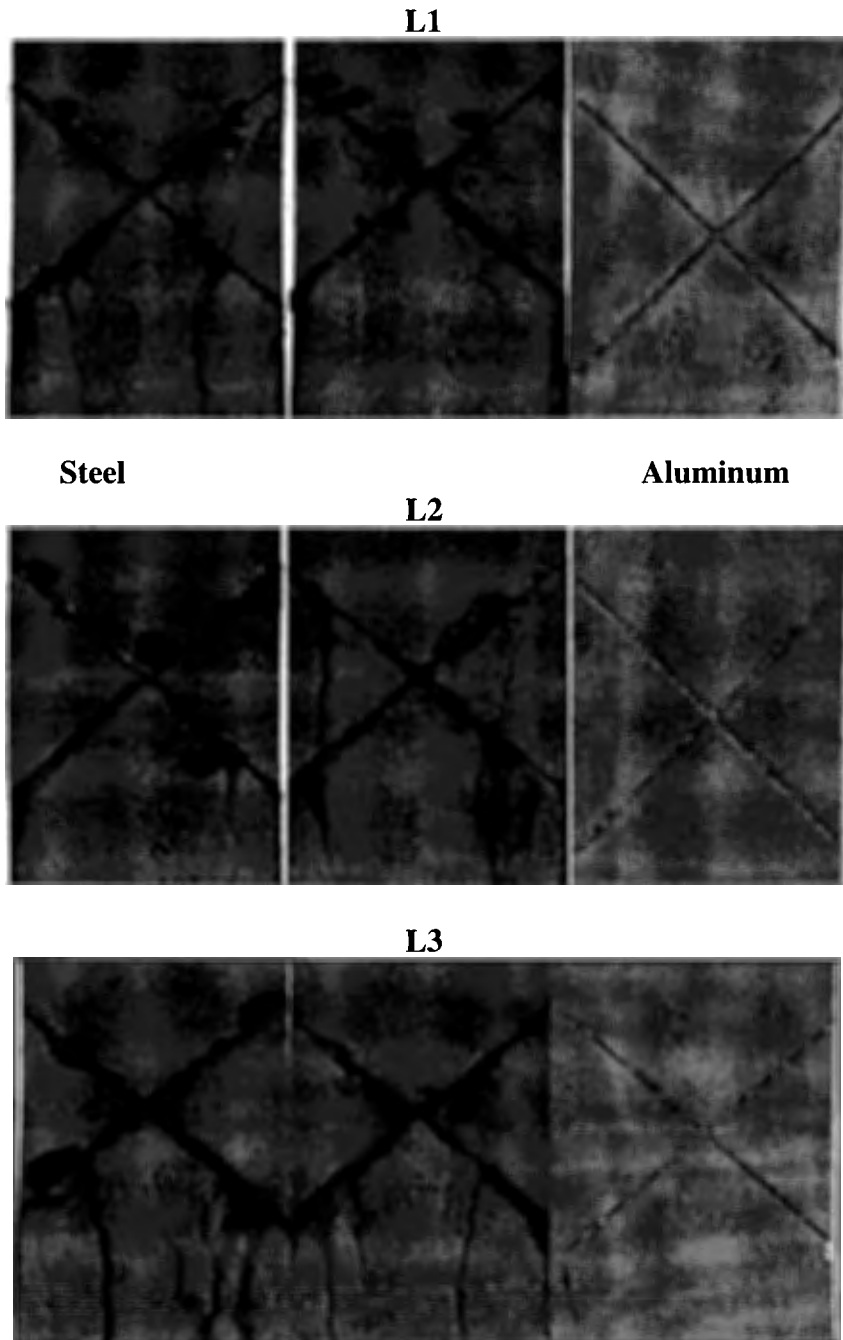


Figure 3.13. Pictures of L1, L2, and L3 coatings on steel and aluminum substrates after 240 hrs of salt spray.

After 240 hrs of salt spray, coating L1 on one steel panel showed under film corrosion while the coating on the second steel panel showed blister formation. Coatings L2 on both the steel panels had blisters after 240 hrs of salt spray. Coating L3 on one of the still panels did not show any blister, film delamination, or under-film corrosion. Coating L3 on the other steel panel showed under film corrosion but no blisters.

All the coatings on aluminum panels were intact after 240 hrs of salt spray with no signs of blister, delamination, or creep. Aluminum panels were treated with Alodine 5700. The Alodine treatment improved adhesion and corrosion performance of the coatings on aluminum substrate.

3.4. Conclusions

The composition of GC resins based on diisocyanate influenced coating performance. The GC coating based on resins R1 and R2 with the compositions of HDI, BEPD, and NPG, and HDI and BEPD, respectively had a good combination of properties such as high flexibility and high solvent resistance. The coatings obtained from the resin R1 with the composition of HDI, BEPD, and NPG had the highest flexibility. The composition of HDI and TMDI based resins with NPG showed improved flexibility. TMDI based GC resins and their coatings showed good flexibility but reduced solvent resistance. A small amount of TMP in the resin composition did not show a significant influence on solvent resistance. Coatings based on GC resin R8 with a composition of H₁₂MDI and BEPD had the least flexibility, the highest modulus and T_g, and high solvent resistance, the highest barrier exhibited through the highest impedance and the lowest capacitance, and high corrosion resistance compared the other coatings characterized in this research work. Thus, the structure of diisocyanate and diol influenced the flexibility

and T_g of the coatings. Linear HDI based coatings had higher flexibility and lower T_g than the H_{12} MDI based coatings. The resin compositions with NPG improved flexibility.

The coatings properties such as solvent resistance, hardness, and T_g was also influenced by the type of crosslinker used. PACM crosslinked coatings exhibited higher solvent resistance, hardness, and T_g compared to that of the A-2353 crosslinked coatings.

HDI and H_{12} MDI based GC coatings examined in this work showed high barrier and good corrosion resistance. Barrier properties and corrosion resistance of the coatings showed a good correlation with the composition of the GC resins examined in this research. The barrier of coatings was influenced by structure of diisocyanate, polar groups in resins, EEW, and T_g of the coatings. The resin R8 with the rigid diisocyanate structure of H_{12} MDI, with the least extent of polar groups, and with the highest EEW produced the coatings with the highest dry and wet T_g , the highest barrier represented by the highest impedance value, the least water uptake represented by the least capacitance values. Salt spray test showed that the coatings based on H_{12} MDI had better corrosion resistance than HDI based coatings. The substrate treatment also had the influence on the corrosion performance. The coatings on Alodine treated aluminum substrate had better corrosion performance in salt spray test compared to that of the coatings untreated steel substrate. The coatings on the treated aluminum substrate did not show any blisters or delamination.

3.5. References

1. Edwards, PA, Erickson, J, Webster, DC, "Synthesis and Self-crosslinking of Glycidyl Carbamate Functional Oligomers". *Polym. Prepr. (Am. Chem. Soc., Div. Polym. Chem.)*, **44** (1) 54-55 (2003)

2. Edwards, PA, Striemer, G, Webster, DC, "Novel Polyurethane Technology Through Glycidyl Carbamate Chemistry". *J. Coat. Technol. Res.*, **2** (7) 517-527 (2005)
3. Edwards, PA, Striemer, G, Webster, DC, "Synthesis, Characterization and Self-crosslinking of Glycidyl Carbamate Functional Resins". *Prog. Org. Coat.*, **57** (2) 128-139 (2006)
4. Wingborg, N, "Increasing the tensile strength of HTPB with different isocyanates and chain extenders". *Polym. Test.*, **21** (3) 283-287 (2002)
5. Ni, H, Daum, JL, Soucek, MD, Simonsick, WJ, Jr., "Cycloaliphatic polyester based high solids polyurethane coatings: I. The effect of difunctional alcohols". *J. Coat. Technol.*, **74** (928) 49-56 (2002)
6. Yilgor, I, Yilgor, E, "Structure-Morphology-Property Behavior of Segmented Thermoplastic Polyurethanes and Polyureas Prepared without Chain Extenders". *Polym. Rev. (Philadelphia, PA, U. S.)*, **47** (4) 487-510 (2007)
7. Dearth, RS, Mertes, H, Jacobs, PJ, "An overview of the structure/property relationship of coatings based on 4,4'-dicyclohexylmethane diisocyanate (H12MDI)". *Prog. Org. Coat.*, **29** (1-4) 73-79 (1996)
8. Yoo, H-J, Lee, Y-H, Kwon, J-Y, Kim, H-D, "Comparison of the properties of UV-cured polyurethane acrylates containing different diisocyanates and low molecular weight diols". *Fibers Polym.*, **2** (3) 122-128 (2001)
9. Lange, J, Stenroos, E, Johansson, M, Malmstrom, E, "Barrier coatings for flexible packaging based on hyperbranched resins". *Polymer*, **42** (17) 7403-7410 (2001)
10. Choi, M-C, Kim, Y, Ha, C-S, "Polymers for flexible displays: From material selection to device applications". *Prog. Polym. Sci.*, **33** (6) 581-630 (2008)

11. Wicks (Jr), ZW, Jones, FN, Pappas, SP, Wicks, DA, *Organic Coatings: Science and Technology*. 3rd ed., John Wiley and Sons Inc., New Jersey (2007)
12. Baboion, R, *Corrosion Tests and Standards Applications and Interpretations*. 2nd ed., ASTM International, West Conshohocken (2005)
13. Bierwagen, G, Brown, R, Battocchi, D, Hayes, S, "Active metal-based corrosion protective coating systems for aircraft requiring no-chromate pretreatment". *Prog. Org. Coat.*, **68** (1-2) 48-61 (2010)
14. Carson, D, Schmitt, R, Seneker, C, Kuren, T, Wallace, D, "Flexible primer compositions and method of providing a substrate with a flexible multilayer coatings." US 4,720,405, 1988.
15. Carson, DW, Schmitt, RJ, Seneker, CA, Kuren, T, Wallace, DR, "Flexible primer compositions and method of providing a substrate with a flexible multilayer coatings." US 4,680,346, 1987.
16. Charves, E, Pulley, DF, Stander, AO, "Sealant-primer coating." US 4,101,497, 1978.
17. Morkunas, BT, Sawant, SG, Walker, JA, Omar, AA, "Flexible, impact-resistant two-component epoxy amine primer." US 2005/0288456 A1, 2005.
18. Schmitt, RJ, Perez, LA, Montague, RA, Tetenbaum, MT, Van, BEJ, "Elastomeric coating compositions." US 4,692,382, 1987.
19. Bierwagen, G, "Next generation of aircraft coatings systems". *J. Coat. Technol.*, **73** (915) 45-52 (2001)
20. Hill, LW, "Determination of Crosslink Density in Thermoset Coatings". *Polym. Mater. Sci. Eng.*, **77** 387-388 (1997)

21. Skaja, A, Fernando, D, Croll, S, "Mechanical Property Changes and Degradation During Accelerated Weathering of Polyester-Urethane Coatings". *J. Coat. Technol. Res.*, **3** (1) 41-51 (2006)
22. Adhikari, R, Gunatillake, PA, Meijs, GF, McCarthy, SJ, "The effect of diisocyanate isomer composition on properties and morphology of polyurethanes based on 4,4'-dicyclohexyl methane diisocyanate and mixed macrodiols (PDMS-PHMO)". *J. Appl. Polym. Sci.*, **73** (4) 573-582 (1999)
23. Menczel, JD, Prime, RB, Thermal Analysis of Polymers Fundamentals and Applications. John Wiley & Sons, Inc., New Jersey (2009)
24. Higginbottom, HP, Bowers, GR, Ferrell, PE, "Cure of Secondary Carbamate Groups by Melamine-Formaldehyde Resins". *J. Coat. Technol.*, **71** (894) 49-60 (1999)
25. Grundmeier, G, Schmidt, W, Stratmann, M, "Corrosion protection by organic coatings: electrochemical mechanism and novel methods of investigation". *Electrochim. Acta*, **45** (15-16) 2515-2533 (2000)
26. McIntyre, JM, Pham, HQ, "Electrochemical impedance spectroscopy; a tool for organic coatings optimizations". *Prog. Org. Coat.*, **27** (1-4) 201-207 (1996)
27. Le, TQ, Bierwagen, GP, Touzain, S, "EIS and ENM measurements for three different organic coatings on aluminum". *Prog. Org. Coat.*, **42** (3-4) 179-187 (2001)
28. Bierwagen, G, Tallman, D, Li, J, He, L, Jeffcoate, C, "EIS studies of coated metals in accelerated exposure". *Prog. Org. Coat.*, **46** (2) 148-157 (2003)
29. Linda, GS, Appleman, BR, "EIS: Electrochemical impedance spectroscopy-A tool to predict remaining coating life?". *Journal of protective coatings and linings*, **February** 66-74 (2003)

30. Loveday, D, Peterson, P, Rodgers, B, "Evaluation of organic coatings with electrochemical impedance spectroscopy. Part 1: fundamentals of electrochemical impedance spectroscopy". *JCT CoatingsTech*, **1** (8) 46-52 (2004)
31. Murray, JN, "Electrochemical test methods for evaluating organic coatings on metals: an update. Part III: Multiple test parameter measurements". *Prog. Org. Coat.*, **31** (4) 375-391 (1997)
32. Loveday, D, Peterson, P, Rodgers, B, "Evaluation of organic coatings with electrochemical impedance spectroscopy. Part 2: Application of EIS to coatings". *JCT CoatingsTech*, **1** (10) 88-93 (2004)
33. Safranski, DL, Gall, K, "Effect of chemical structure and crosslinking density on the thermo-mechanical properties and toughness of (meth)acrylate shape memory polymer networks". *Polymer*, **49** (20) 4446-4455 (2008)
34. Mijovic, J, Zhang, H, "Molecular Dynamics Simulation Study of Motions and Interactions of Water in a Polymer Network". *J. Phys. Chem. B*, **108** (8) 2557-2563 (2004)
35. Kanapitsas, A, Pissis, P, Gomez, RJL, Monleon, PM, Privalko, EG, Privalko, VP, "Molecular mobility and hydration properties of segmented polyurethanes with varying structure of soft- and hard-chain segments". *J. Appl. Polym. Sci.*, **71** (8) 1209-1221 (1999)
36. Ito, S, Hashimoto, M, Wadgaonkar, B, Svizero, N, Carvalho, RM, Yiu, C, Rueggeberg, FA, Foulger, S, Saito, T, Nishitani, Y, Yoshiyama, M, Tay, FR, Pashley, DH, "Effects of resin hydrophilicity on water sorption and changes in modulus of elasticity". *Biomaterials*, **26** (33) 6449-6459 (2005)

37. Ji, W-G,Hu, J-M,Liu, L,Zhang, J-Q,Cao, C-N, "Enhancement of corrosion performance of epoxy coatings by chemical modification with GPTMS silane monomer". *J. Adhes. Sci. Technol.*, **22** (1) 77-92 (2008)
38. Zhou, J,Lucas, JP, "Hygrothermal effects of epoxy resin. Part I: the nature of water in epoxy". *Polymer*, **40** (20) 5505-5512 (1999)
39. Zhou, J,Lucas, JP, "Hygrothermal effects of epoxy resin. Part II: variations of glass transition temperature". *Polymer*, **40** (20) 5513-5522 (1999)
40. Li, J,Jeffcoate, CS,Bierwagen, GP,Mills, DJ,Tallman, DE, "Thermal transition effects and electrochemical properties in organic coatings: part 1 - initial studies on corrosion protective organic coatings". *Corrosion (Houston)*, **54** (10) 763-771 (1998)
41. Leventis, N,Vassilaras, P,Fabrizio, EF,Dass, A, "Polymer nanoencapsulated rare earth aerogels: chemically complex but stoichiometrically similar core-shell superstructures with skeletal properties of pure compounds". *J. Mater. Chem.*, **17** (15) 1502-1508 (2007)

CHAPTER 4. WATER DISPERSIBLE GLYCIDYL CARBAMATE

RESINS

4.1. Introduction

Glycidyl carbamate (GC) resins are produced by reaction of an isocyanate functional resin with glycidol. GC resins contain urethane (-NHCO-) and epoxy functional groups in their structure.⁴⁵ Polyurethane and epoxy resins are widely used in numerous commercial applications such as coatings, composites, high performance polymers, etc. Polyurethane coatings offer excellent toughness, adhesion, flexibility and chemical resistance. Epoxy coatings offer excellent corrosion and solvent resistance, adhesion and versatility in crosslinking (curing) mechanisms.^{13, 35} The combination of urethane and epoxy functional groups in GC resins imparts an excellent set of properties to GC-based coatings. GC resins can be crosslinked using amines or by self-crosslinking to produce high performance coating systems.^{45, 48} GC resins have also been used to produce hybrid sol-gel coatings with an excellent combination of properties.^{52, 53} GC resins show a very high viscosity due to intermolecular hydrogen bonding. GC resins were modified with several alcohols which could reduce their viscosity up to 90 %, and structure-property relationship of the coatings was studied. Most of the GC coatings developed in the past were solvent-based coatings.

Environmental concerns have led to stringent regulations and a demand for reduction in volatile organic compound (VOC) emission. Methods such as waterborne coatings, UV curing, high solids and powder coating techniques are all viable approaches to reduce VOCs.¹⁶⁻¹⁸

Waterborne polymers are an important class of materials for coatings due to increasing environmental regulations. Water as a solvent for coatings has good potential as a carrier or the solvent in the development of low or zero VOC environmentally friendly coatings. While water may have certain limitations in coating applications due to its high heat capacity, high surface tension, and slow and humidity dependent evaporation rate, research on waterborne coatings has gained significant attention. In general, resins used as binders in coating applications are hydrophobic and are difficult to disperse in water. Common techniques to disperse resins in water are the use of the surfactants, incorporation of hydrophilic groups in the resin structure, or the synthesis of latex by emulsion polymerization. The hydrophilic component in waterborne coatings is an essential part but may cause multiple issues such as increased water sensitivity, low chemical resistance, phase separation, and poor appearance. Resins for waterborne coatings should be designed considering the ease of applicability and performance attributes. It is highly desirable to incorporate appropriate level of hydrophilic groups in the resin structures to obtain dispersion by a minimal shear force (hand mixing).^{5, 6, 15, 20, 29, 65-68, 146} Film formation and final coating properties of waterborne coatings improve with coalescence between dispersed resin particles. A coalescing solvent, a volatile plasticizer, is usually used to increase coalescence of the particles. However, it may contribute to the VOC of coatings.¹ Also, a current trend is to minimize or eliminate the use of surfactants (external emulsifiers) in waterborne coatings. Surfactants remain in coatings after film formation and over a period of time they can diffuse to the surface, cause phase separation, increase hydrophilicity and decrease the water resistance of coatings.¹⁴⁶

There have been significant efforts in the development of waterborne resin and crosslinker systems to meet environmental regulations and demanding coating applications. Widely used coating binders such as polyurethanes, epoxies, polyesters, and alkyds are dispersed in water by incorporation of non-ionic hydrophilic groups, (e.g. polyethers) or water reducible ionic (anionic and cationic) groups in resin structures.¹ Bayer Inc. has developed water dispersible polyisocyanates for waterborne 2K polyurethane coatings.^{66, 67, 146} Air Products and Chemicals Inc., and Resolution Performance Products (now part of Hexion Specialty Chemicals) developed waterborne epoxy resins and crosslinkers by incorporating hydrophilic non-ionic or ionic groups in epoxy resins or amine crosslinkers.^{65, 68, 71-73, 147, 148}

Edwards developed a water dispersible GC resin using Bayer's hydrophilic polyisocyanate. The hydrophilic GC resin could be dispersed in water with the help of a surfactant. The coatings crosslinked with a waterborne amine crosslinker had good properties.⁴⁹

The influence of the extent of hydrophilic group modification in GC resins on their coating properties was not studied before. The goal of the research presented in this chapter was to synthesize water dispersible GC resins by incorporating non-ionic hydrophilic groups in the resin structure and study the influence of the extent of hydrophilic groups on coating properties. A non-ionic hydrophilic group incorporated in GC resin was methoxy poly(ethylene glycol) (mPEG). The hydrophilic group in the resin was varied by incorporating mPEG with varying chain length and molar ratio in the GC resin. The influence of the extent of hydrophilic group on coating properties was studied.

4.2. Experimental

4.2.1. *Materials*

Two polyisocyanates used were hexamethylene diisocyanate isocyanurate (Desmodur N 3600 with % NCO of 23) and hydrophilic isocyanate (Bayhydur XP 7165 with % NCO of 18.3) provided by Bayer MaterialScience. The NCO equivalent weight of Desmodur N 3600 is 180 g/eq and that of Bayhydur XP 7165 is 245 g/eq. Glycidol was supplied by Dixie Chemical. Glycidol was stored refrigerated to minimize the formation of impurities. Methoxy poly(ethylene glycol) (mPEG) of number average molecular weights 350, 550 and 750, were obtained from Aldrich. K-KAT 6212, a zirconium chelate complex, provided by King industries, was used to catalyze the isocyanate and hydroxyl reactions to form the glycidyl carbamate (GC) resins. All reagents were used as received without any further purification. Amine crosslinkers, Anquamine 731 and Anquamine 419 provided by Air Products, has hydrogen equivalent weights (gm/H) of 200 and 284, respectively. Anquamine 731 is water-based curing agent reportedly designed to emulsify and crosslink liquid epoxy resin without the use of any surfactants. Anquamine 419, waterborne curing agent, is a modified aliphatic amine used in waterborne epoxy dispersions. Surfactant, Triton GR-7M (anionic surfactant based on dioctyl sulfosuccinates) obtained from Dow chemical was used in selected coating formulations.

4.2.2. *Synthesis of mPEG-modified GC resins*

A 500 ml four neck reaction vessel was used for the synthesis of the GC resins. The vessel was fitted with a condenser, nitrogen inlet and Model 210 J-KEM temperature controller and mechanical stirrer. A water bath was used for heating and cooling the

vessel. The synthesis was done in two steps. The first step involved the reaction of the isocyanate with mPEG and the second step involved the reaction of glycidol with the remaining isocyanate groups. The stoichiometric equivalent amounts (% by mol) of mPEG based on isocyanate groups used to react with isocyanate were 5 %, 10 % and 15 %. The overall stoichiometric equivalent amount of isocyanate, mPEG and glycidol based on –NCO and –OH groups during the synthesis was maintained at 1:1. The catalyst K-KAT 6212, in the form of solution in tertiary butyl acetate (1 – 2 % by wt.) was used for the reaction of isocyanate and hydroxyl groups.

The reaction vessel was charged with Desmodur N 3600 followed by the addition of the required amount of mPEG. The reaction mixture was stirred at 50 – 60 °C for about 45 – 60 min. to ensure a homogeneous mixture. The catalyst (K-KAT 6212) amount added after the mixing time was 0.03 % by wt. (of the total reaction mass). The reaction was continued for 4 – 5 hrs at about 70 – 85 °C before the addition of glycidol. The amount of glycidol added was divided over 3 – 4 intervals over 4 – 5 hrs. Glycidol addition in the first interval was done at 45 °C. The subsequent addition of glycidol was done at the temperature about 55 – 60 °C and this temperature was maintained until the isocyanate peak (at 2271 cm⁻¹) had disappeared in FTIR. A GC resin was also synthesized by reacting hydrophilic isocyanate, Bayhydur XP 7165, with glycidol. The reaction of Bayhydur XP 7165 with glycidol was done using K-KAT 6212 as a catalyst.

4.2.3. FTIR measurements

The FTIR measurements were performed using a Nicolet 8700 FTIR spectrometer from Thermo Scientific. Sample aliquots were taken and coated on a potassium bromide salt plate. Spectra acquisitions were based on 64 scans with a data

spacing of 1.98 cm^{-1} . The FTIR was set for auto gain to monitor spectral range of $4000 - 500\text{ cm}^{-1}$. The change in band absorption of isocyanate (2272 cm^{-1}), -OH and -NH ($3750 - 3000\text{ cm}^{-1}$), amide (1244 cm^{-1}) and epoxide (910 cm^{-1}) bands were used to follow the reaction progress.

4.2.4. NMR characterization

^{13}C NMR was carried out for characterization of resins using a JEOL-ECA (400 MHz) NMR spectrometer coupled with an auto-sampler accessory. The spectra were run at $24\text{ }^\circ\text{C}$ with 1000 scans. All the spectra were collected by dissolving 50 to 70 mg samples in 0.7 ml CDCl_3 . The spectra were analyzed using Delta NMR processing and control software (Version 4.3.5).

4.2.5. Epoxy titration

Epoxy equivalent weight (EEW) of the resins was determined by titration with hydrogen bromide (HBr) according to ASTM D1652. A required amount of resin (0.8 – 1.0 gm) was dissolved in 5 – 10 ml of chloroform and was titrated against a standardized HBr solution prepared in glacial acetic acid. The indicator used was a solution of crystal violet in glacial acetic acid. End point of the titration was the appearance of a permanent yellow-green color.

4.2.6. Particle size analysis

The samples for particle size analysis were prepared by dispersing the GC resins into the water (30 % solids) using high speed laboratory homogenizer (5000 rpm) with six probes (each 35 mm in diameter). The Particle size was determined using dynamic light scattering (DLS) technique with a Nicomp 380 Submicron Particle Sizer (Particle Sizing Systems, SantaBarbara, CA). The experiments were carried out at room

temperature. The particle size was determined periodically for the samples that did not show permanent agglomeration and settlement.

4.2.7. Coating formulation preparation

Waterborne coating formulations were made in plastic cups by dispersing the required amount of resin in water (deionized water) using a tongue depressor. Surfactant, Triton GR-7M, was used in selected formulations to disperse GC resins in the water. To the dispersed resins, the required amount of amine crosslinker was added and the resulting formulations were kept at ambient for about 5 min. to stabilize the formulations. After the stabilization time, the coating formulations containing crosslinker were mixed by hand using a tongue depressor for about 5 min. and kept at ambient for about 10 – 20 min. (induction time) before taking drawdowns. The films were drawdown at 8 mils wet thickness on steel panels (smooth finished Q panels, type QD 36, 0.5×76×152 mm) cleaned with *p*-xylene. The coatings were cured at ambient conditions for about two weeks before determining their water resistance, solvent resistance, and other coating properties. Dry film thickness of the coatings was between 65 – 70 μm. The free films for tensile test were obtained by removing carefully the cured coating films from the steel substrate using a razor blade.

The three coat system was used on steel and treated aluminum panels for the EIS and salt spray experiments. The coating formulations were prepared as explained before. The steel panels were wiped with *p*-xylene for degreasing before applying coatings on them. The aluminum panels used in this experiments were cleaned using MEK for degreasing and Brulin Cleaner (Formula 815MX) with abrasive pad. The aluminum panels were further treated with deoxidizer solution (35 % butanol, 25 % isopropanol, 18

% orthophosphoric acid, and 22 % volume deionized water) and Alodine 5700 (chromate free conversion coating). The treated aluminum panels were kept at ambient over night before applying coatings on them. The first coat was taken at 3 mils on steel (QD) and aluminum (Al2024-T0) substrates and the coatings were kept at ambient for two days. The second coat was taken at 4 mils and the coatings were kept at ambient for two days. The third and final coat was taken at 6 mils and the coatings were cured at 80 °C for 1hr. The coatings were kept at ambient for 8 – 9 days before EIS and salt spray experiments. Dry film thickness of the coatings was between 85 – 95 µm. The free films for DMA were obtained by removing carefully the cured coating films from the steel substrate using razor blade.

4.2.8. Coating performance

Initially all of the coatings were characterized for water resistance, solvent resistance, flexibility, hardness, contact angle, and adhesion. The coatings which had good water and solvent resistance were selected for further characterization. The selected coatings were characterized to determine their tensile properties (elongation at break and Young's modulus), glass transition temperature, dynamic mechanical properties, thermal stability, barrier properties, and corrosion resistance.

Water resistance of the coatings was determined by water drop test and water double rubs test. The water drop test was carried out by placing a drop of water (approximate weight~ 0.05 gm) on the coating surface. The water drop was covered with a glass slide (of size 2 cm x 2 cm) to avoid evaporation of water. The glass slide was removed from coating surface after 1 hr. The surface of coating was examined for defects, bubble formation, film delamination and any permanent marks. Six replicates of

each coating formulation were tested. The number of coatings that did not show any surface defects, bubble formation, delamination and permanent marks was reported. Thus, water resistance test result reported as 6 indicates that all the six replicates passed the test (no surface defects, bubble formation, delamination or permanent marks) and the water resistance was the best. MEK double rubs test was used according to ASTM D 5402 to assess the solvent resistance and development of cure. A 26-ounce hammer with three layers of cheesecloth wrapped around the hammerhead was soaked in MEK. The hammer head was rewet with MEK after 30 – 50 double rubs. The number of double rubs was noted once the metal surface of the panel was visible due to removal of the coating layer during the test. The water double rub test was carried out in similar way as that of methyl ethyl ketone (MEK) double rub test by replacing MEK with deionized water. For the water double rub test, the number of double rubs was noted once the formation of bubble, film delamination, permanent mark or appearance of metal surface due to the removal of coating was observed. To determine relative hydrophilicity/hydrophobicity of the coatings, water contact angle was measured using First Ten Ångstroms FTA 100 series instrument.

König pendulum hardness of the coatings was measured following ASTM D 4366. The hardness test results are reported in seconds (sec). Reverse impact strength of the coatings was determined following ASTM D 2794 using a Gardener impact tester. The maximum drop height was 43 inches and the drop weight was 4 pounds. Crazeing or loss of adhesion was noted and inch-pounds (in-lbs) were reported at film finish failure. Samples that did not fail were noted as having an impact strength of >172 in-lbs. The conical mandrel test was also used according to ASTM D 522 for the determination of

flexibility the coatings. The results of flexibility test were reported as the length of a crack (cm) formed on the coating during the test. Cross hatch adhesion of the coatings was evaluated using a Gardco cross hatch adhesion instrument following ASTM D 3359. Tensile testing of the coatings was performed using Instron 5542 instrument. The test specimen were prepared according to ASTM D 638-5 method. The test was carried out at 10 mm/min at ambient conditions. Elongation at break and Young's modulus of the coatings were recorded. An average of three samples is reported.

4.2.9. Differential scanning calorimetry (DSC)

A TA Instruments Q1000 differential scanning calorimeter (DSC) coupled with an auto sampler accessory was used to determine the glass transition temperature (T_g) of the coatings. DSC experiments were performed by placing a sample into the conventional aluminum pans. The samples were subjected to a heat-cool-heat cycle. The samples were heated to 200 °C and then cooled to -75 °C and held there for 5 min. DSC thermogram were taken from -75 °C to 250 °C at a heating rate of 10 °C min⁻¹. Glass transition temperature was determined as the temperature of the inflection at the mid-point.

4.2.10. Thermogravimetric analysis (TGA)

TGA was performed using a TA Instruments Q500. Temperature was ramped from ambient to 800 °C with a ramp rate of 10 °C min⁻¹. A nitrogen atmosphere was used during the test. Weight retained was plotted as a function of temperature.

4.2.11. Dynamic mechanical analysis (DMA)

A TA Instruments Q800 Dynamic Mechanical Analysis system was used to determine the viscoelastic properties of the cured coating films. The dimensions of free films used were of 23 to 26 mm in length, 5 mm in width and 0.09 to 0.1 mm in

thickness. Poisson's ratio was assumed to be 0.4 for all of the coating films. The experiments were carried out within a temperature range of -20 °C to 200 °C with a temperature ramp rate of 5 °C min⁻¹ at a frequency of 1 Hz. The storage modulus values (E') in the rubbery plateau region (well above T_g) are used to calculate the crosslink density of the coatings. Equation (4.1) was used to calculate cross-link density (ν_e) of the coatings:^{112, 121}

$$E' = 3\nu_e RT \quad (4.1)$$

where, E' = storage modulus (Pa); ν_e = crosslink density (mol/L); R = gas constant (8.3 J/K/mol); and T = temperature (K).

4.2.12. Atomic force microscope (AFM)

The atomic force microscope (AFM) used in the present study was a Dimension 3100® microscope with a Nanoscope IIIa controller (Digital Instruments, Inc., California). Experiments were performed using tapping mode in air at laboratory conditions using silicon probes with force constant 2.8 N/m and nominal resonant frequency 17 kHz. A sample area of 20 μm \times 20 μm was scanned.

4.2.13. Barrier properties and corrosion resistance

Barrier properties and corrosion resistance of the coatings was evaluated by electrochemical impedance spectroscopy (EIS) and salt spray (ASTM B 117) tests. The conventional EIS set up used consisted of metal substrate as the working electrode (WE) with counter Platinum (Pt) and reference Standard calomel electrode (SCE) electrodes. A Gamry Instruments R 600 Potentiostat/Galvanostat/ZRA and Gamry Framework Version 5.20/EIS 300 software supplied by Gamry Instruments, Inc. of Willow Grove, PA were used for the experiments. The impedance response corresponding to the applied

frequency of 100 kHz to 0.01 Hz was measured with an acquisition rate of 10 points per decade. A 10mV amplitude perturbation potential with respect to the open circuit potential was used during the measurement. In the salt spray test, the coatings were exposed to a continuous salt spray (5 % NaCl in deionized water) at 35 °C for ten days. The pictures of the coatings were taken periodically by scanning.

4.3. Results and Discussion

4.3.1. *Synthesis of water dispersible GC resins*

The synthesis of the water dispersible GC resins was carried out by first incorporating a desired amount of mPEG in HDI polyisocyanate and then reacting the remaining isocyanate functional groups with glycidol. The molecular weight and mole % of mPEG reacted with isocyanate groups varied from 350, 550 and 750 and 5%, 10% and 15%, respectively. Figure 4.1 is a schematic representation of the reaction for the synthesis of the water dispersible GC resins.

A control GC resin was synthesized by reacting glycidol with a commercial hydrophilic isocyanate (Bayhydur XP 7165), described as an isocyanurate resin condensate derived from hexamethylene diisocyanate containing a polyether chain (the exact molecular weight and mol % of polyether chain are a trade secret of Bayer MaterialScience). Table 4.1 shows the GC resins synthesized in this study.

Characterization of the structures of the synthesized GC resins was done using ¹³C NMR. Figure 4.2 shows the NMR spectrum of the resin R1. The peaks at 45 and 50 ppm for epoxy group and at 59, 70 and 72 ppm for mPEG molecule indicated that epoxy group and mPEG were incorporated in the structure of GC resins. Since only a fraction of

the initial isocyanate groups are reacted with mPEG, the synthesized resins consist of a mixture of hydrophilic molecules containing mPEG and hydrophobic molecules

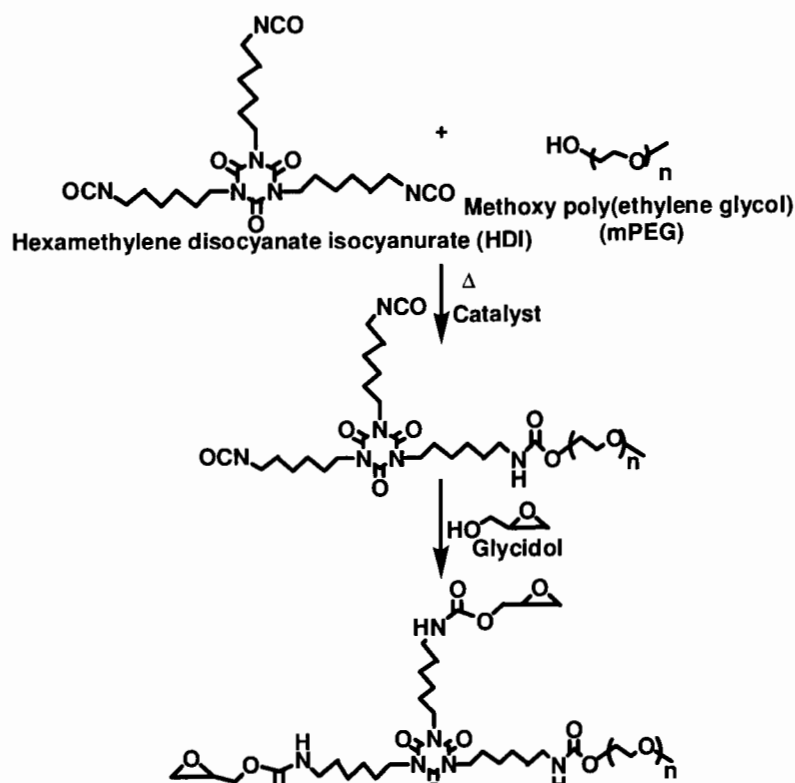


Figure 4.1. Schematic representation of the synthesis of water dispersible GC resins.

Table 4.1. GC resins synthesized.

Resin	mPEG Molecular weight (\bar{M}_n)	Mol % of mPEG	EEW (g/eq)
R1	350	5%	416
R2	550	5%	369
R3	750	5%	391
R4	350	10%	324
R5	550	10%	373
R6	750	10%	304
R7	350	15%	485
R8	550	15%	417
R9	750	15%	500
R10 (Control)	Made from commercial hydrophilic isocyanate		358

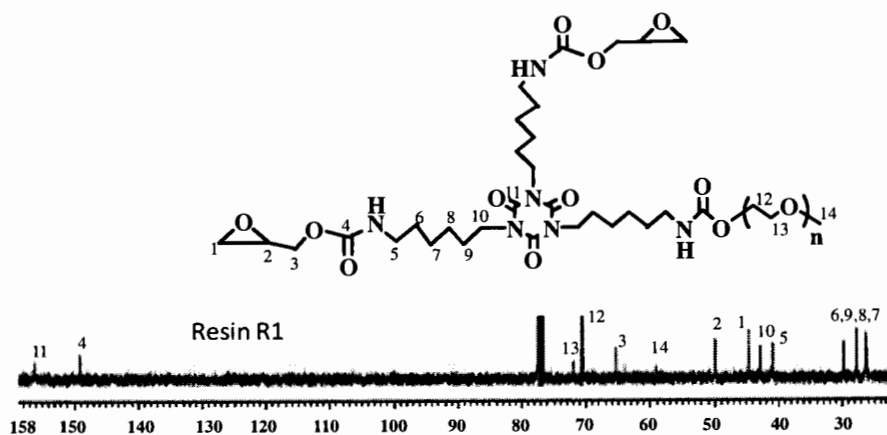


Figure 4.2. ^{13}C NMR spectrum of resin R1.

containing no mPEG. It should also be noted that while the polyisocyanurate is illustrated as being a trifunctional molecule, the commercial material is composed of trimer (~ 70 %), pentamer (< 20 %), heptamer, and higher molecular weight oligomers (< 15 %). A Monte Carlo simulation was performed to understand the possible distribution of hydrophilic and hydrophobic molecules in GC resins. A commercial software package, DryAdd-Pro+ v 4.33, was used for the simulation. The simulation software creates a distribution of the reactive sites and lets these sites react according to user specified information and thereby simulates the individual random reaction events of a real time reaction. For the simulation purpose, the composition of commercial isocyanurate used in this study was considered to be 70 % by wt. of trimer, 15 % by wt. of pentamer, and 15 % by wt. of heptamer. Water dispersible resin selected for the simulation was R2, IGC-mPEG550-5%. The simulation was carried out by specifying the two steps during the synthesis. The first step was the reaction of mPEG with the fraction of isocyanate groups in the isocyanurate and the second step was the reaction of glycidol with the remaining isocyanate groups in the isocyanurate. The simulation provided the % number and % weight distribution of the hydrophilic (containing mPEG) and hydrophobic (no mPEG)

molecules in the resin composition. The weight and number distribution of the hydrophilic and hydrophobic molecules in the resin with a significant amount of percentages is shown in Table 4.2. In the possible composition of the resin, trimer constituted to the highest weight and number % for hydrophobic molecules as well as hydrophilic molecules. The largest extent of the hydrophilic molecules were based on the reaction trimer with one mPEG and two glycidol molecules.

Table 4.2. Weight and number distribution of hydrophobic and hydrophilic molecules in the GC resin.

Composition of resin	% by wt.	% by number
Hydrophobic molecules		
T-3GDL	54.9	68.5
P-4GDL	10.5	8.4
H-5GDL	9.5	5.5
Total	74.9	82.4
Hydrophilic molecules		
T-1mPEG-2GDL	14.3	10.8
T-2mPEG-1GDL	1.1	0.6
P-1mPEG-3GDL	3.1	1.7
H-1mPEG-4GDL	3.4	1.5
Total	21.9	14.6

Where, T= trimer, P= pentamer, H=heptamer, GDL=glycidol

Based on the simulation data, the hydrophobic and hydrophilic molecules which constituted to the major fraction of the resin composition are shown in Figure 4.3.

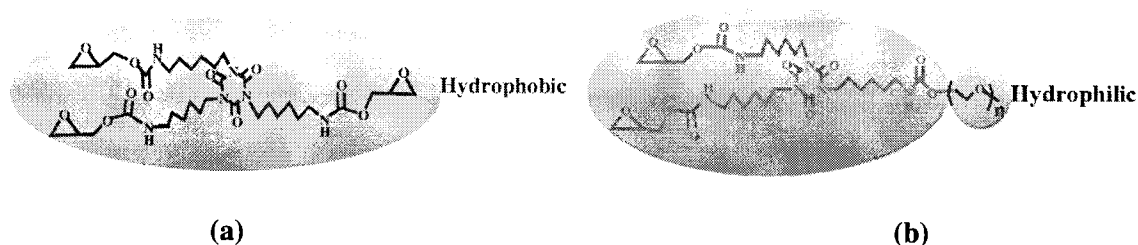


Figure 4.3. Major (a) hydrophobic GC molecule and (b) hydrophilic GC molecule in the hydrophilic of GC resin.

4.3.2. Dispersion stability

Dispersions of the synthesized GC resins were made at 30% solids using high speed homogenizer. The dispersions were kept at ambient conditions and their dispersion

stability after one, six and fourteen days was evaluated. Dispersion stability was determined by visual examination to determine if phase separation (settlement) occurred in the test samples. In general, dispersions of relatively low hydrophilic content resins showed phase separation (settlement), while dispersions of highly hydrophilic resins were stable and showed no phase separation. Particle size analysis was performed on the dispersions that did not show any phase separation. The results of dispersion stability study are shown in Table 4.3. Dispersion stability was found to be strongly dependent upon mPEG chain length and its mol % in the GC resins. Resin R1, being the most hydrophobic resin as it contains the smallest mPEG chain length (M_n of 350) in the smallest mol % (5 mol %) could not be dispersed in water using HSD and remained phase separated all the time. Control GC resin, R10, showed similar behavior to that of R1. Resin R10 did not go into water by HSD and remained phase separated. Resin R2 containing mPEG of molecular weight of 550 at 5 mol % showed better dispersibility compared to that of R1. Dispersion made with R2 showed formation of agglomerates at the bottom of the container. However, the agglomerates could be redispersed with hand mixing resulting in a good dispersion. Resin R4 showed some phase separation after six days but formed a good dispersion following hand mixing. On the fourteenth day, R4 had resulted in a viscous non-flowable dispersion that upon further dilution with water to obtain a flowable dispersion contained no agglomerates. Resin R7 dispersion was similar to that of R4 dispersion except R7 formed large agglomerates after diluting with water. Dispersion of resin R5 did not phase separate on the sixth day. The dispersion of resin R5 was found to be slightly phase separated on the fourteenth day but could be redispersed well by hand mixing. Dispersions of resins R3, R6, R8 and R9 showed no phase

separation after fourteen days. Particle size analysis of these dispersions did not indicate the formation of large agglomerates over fourteen days. Resins R3, R6 and R9 contained mPEG of 750 molecular weight in 5, 10 and 15 mol %. Resin R8 contained mPEG of molecular weight 550 in 15 mol %. Thus, chain length as well as mol % modification influenced the dispersion stability.

Table 4.3. Dispersion stability of GC resins.

Resin	One day		Six days		Fourteen days	
	Dispersion stability	Particle size (nm)	Dispersion stability	Particle size (nm)	Dispersion stability	Particle size (nm)
R1	C	---	C	---	C	---
R2	B	---	B	---	B	---
R3	A	25	A	11	A	23
R4	B	---	B	---	D	---
R5	A	24	A	31	B	---
R6	A	15	A	11	A	4
R7	B	---	B	---	E	---
R8	A	15	A	9	A	13
R9	A	4	A	9	A	3
R10 (control)	C	---	C	---	C	---

A = no phase separation, B = partial phase separation redispersable by hand, C = did not disperse in water by HSD and remained phase separated, D = non-flowable viscous dispersion became flowable after addition of water and hand mixing, no agglomeration, E = non-flowable viscous dispersion, showed large agglomerates after addition of water and hand mixing, --- = particle size experiments not performed because dispersions showed phase separation.

The Monte Carlo simulation performed to determine the distribution of the hydrophilic and hydrophobic molecules in hydrophilic GC resins showed that the major fraction of the hydrophilic molecules is trimer with one mPEG and two glycidol molecules. Based on this information a schematic representation of the dispersed particle of GC resin in water is shown in Figure 4.4. Figure 4.4. shows that the particle consists of hydrophobic GC molecules (containing no mPEG) at the core surrounded by hydrophilic

GC molecules with mPEG chains extending out into the aqueous medium. GC resins contain strong hydrogen bonding groups such as urethane (-NHCO-) and carbonyl (-CO) responsible for their high viscosity. The high viscosity resulting from hydrogen bonding indicates the strong interaction among GC molecules which make them less favorable to interact with water molecules. Modification of GC resin by non-ionic hydrophilic mPEG chain might have disrupted the hydrogen bonding interaction among GC molecules and made them hydrophilic.

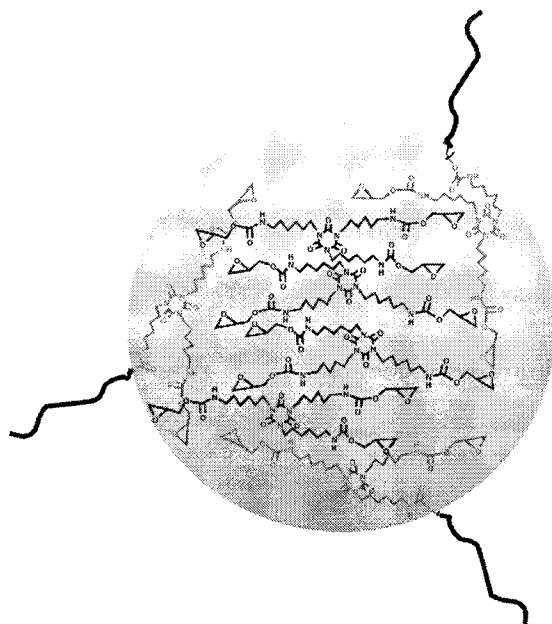


Figure 4.4. Schematic representation of a GC resin particle dispersed in water.

4.3.3. Coating formulations

Waterborne coating formulations from the GC resins were made by mixing the components in water by hand. Amine crosslinker was then added to the dispersion of GC resin in water made with hand mixing. Figure 4.5 is a schematic representation of the process employed in making the waterborne GC coating formulations. GC resins (except R1 and R10) were dispersed in water without using any surfactant. Surfactant was used to disperse resins R1 and R10, because these resins could not be dispersed in water by hand

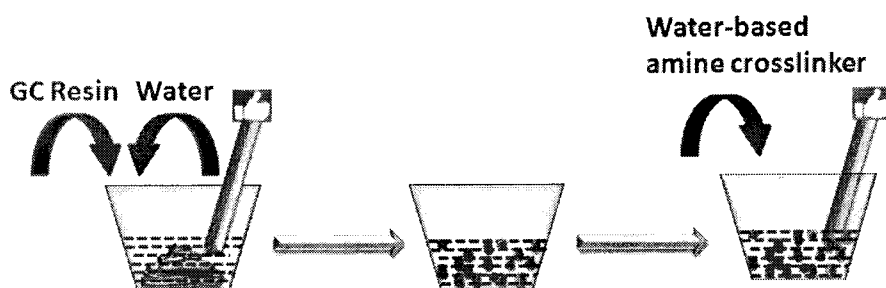


Figure 4.5. Schematic representation of making a waterborne GC coating formulation.

without surfactant. Table 4.4 shows the coating formulations of the GC resins used in this study. Films were drawdown on steel panels and were cured under ambient laboratory conditions for about two weeks before evaluating their water resistance and other coating properties.

Table 4.4. Coating formulations of the GC resins.

Coating formulation	Resin	Resin (wt. %)	Water (wt. %)	Surfactant (wt. %)	Crosslinker (E:A)
F1	R1	62	37.3	0.7	1:1
F2	R2	66	34	0	1:1
F3	R3	63	37	0	1:1
F4	R4	66	34	0	1:1
F5	R5	67	33	0	1:1
F6	R6	67	33	0	1:1
F7	R7	67	33	0	1:1
F8	R8	66	34	0	1:1
F9	R9	66	34	0	1:1
F10 (Control)	R10 (Control)	63	36.3	0.7	1:1

4.3.4. Water and solvent resistance

Water resistance of the waterborne GC coatings was determined by water drop and water double rubs tests. Table 4.5 shows the water and solvent resistance of the coatings. Water resistance of GC coatings was found to depend on the molecular weight and mol % of mPEG used in the resin synthesis. Coatings made from formulations F1, F2

and F4 exhibited excellent water resistance. The formulations F1, F2, and F4 were made from the resins R1, R2, and R4, respectively. Resins R1 and R2 contained 5 mol % mPEG having molecular weight of 350 and 550, respectively. Resin R4 contained 10 mol % mPEG having molecular weight of 350. The water resistance of the coating by water drop test made from control GC resin, R10 (formulation F10) was inferior to that of the coatings made from the resins R1, R2 and R4 (formulations F1, F2 and F4). Addition of a small amount of surfactant (0.7 % by wt.) in coating formulation F1 to disperse GC resin R1, made with low extent of hydrophilic portion (mPEG molecular weight of 350 at 5 mol %), did not appear to affect the water resistance of its coating.

Table 4.5. Water and solvent resistance of the coatings.

Coating	Water drop test (6 = Best)	Water double rubs	MEK double rubs
F1	6	>400	>400
F2	6	>400	>400
F3	3	>400	>400
F4	5	>400	>400
F5	2	>400	>400
F6	0	>400	>400
F7	2	>400	>400
F8	0	325	>400
F9	0	245	>400
F10 (Control)	4	>400	>400

Coatings became more hydrophilic with increase in mPEG molecular weight and mol % which resulted in a decrease of their water resistance. Coatings made from formulations F8 and F9 showed poor water resistance compared to that of the other coatings. The formulations F8 and F9 were made from the resins R8 and R9 and contained the large extent of hydrophilic part, 15 mol % mPEG having molecular weight of 550 and 750, respectively.

All of the GC coatings made in this study exhibited excellent solvent resistance through MEK double rubs values reaching above 400. The modification of GC resins by mPEG carried out in this experiment did not affect the solvent resistance of the coatings.

4.3.5. Water contact angle

The water contact angle of GC coatings was determined to understand the relative hydrophilicity/hydrophobicity of the coatings surfaces. Results of the contact angle measurements correlated well the results of the water resistance of the coatings. Figure 4.6 shows a plot of water contact angle of the GC coating. Increase in molecular weight and mol % of mPEG in GC resins decreased the water contact angle indicating the increase in hydrophilicity of the coatings. Water resistance of the coatings shown in Table 4 followed a similar trend. Increase in hydrophilicity of the coatings resulted in a

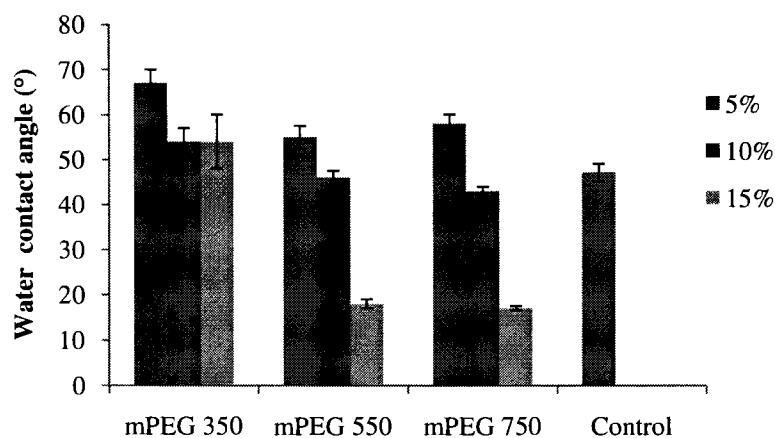


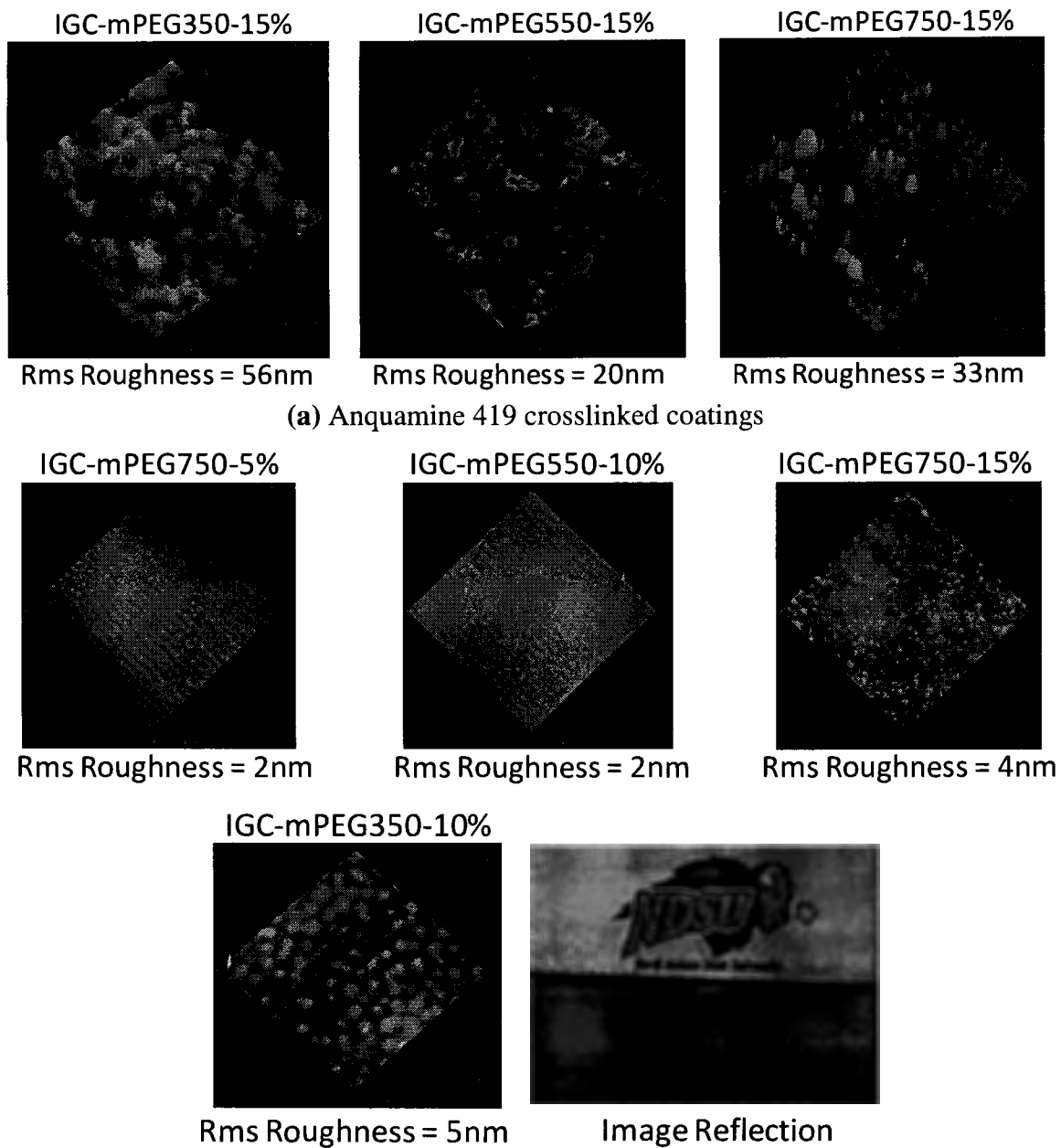
Figure 4.6. Water contact angle of the GC coatings.

decrease of water resistance of the coatings. Water resistance evaluated through the water drop test and water double rubs of the coatings made from resins R8 and R9 (formulations F8 and F9, respectively) was lower compared with that of the other coatings. Coatings made from resins R8 and R9 showed relatively lower water contact angle (18 and 17°, respectively) compared with that of the coatings made from the other

resins. Resins R8 and R9 contained a large amount of the hydrophilic portion, 550 and 750 molecular weight mPEG at 15 mol %. The results of water resistance and contact angle experiments suggested that the chain length as well as the mol % of mPEG in GC resins influenced the relative hydrophilicity of the coatings.

4.3.6. Other coating properties

Initially, waterborne GC coatings were prepared using Anquamine 419 crosslinker. However, the coatings crosslinked with Anquamine 419 had poor solvent and water double rubs (< 10), and a hazy or opaque appearance. On the other hand, waterborne GC coating crosslinked with Anquamine 731 crosslinker had a good solvent and water double rubs (> 245), and transparent and glossy appearance. AFM analysis on Anquamine 419 and Anquamine 731 crosslinked coatings was performed. Figure 4.7 (a) and (b) show the AFM images of the GC coatings crosslinked with the two crosslinkers. Figure 4.7 (b) also shows the reflection image over GC coating crosslinked with Anquamine 731. The AFM images in Figure 4.7 (a) show valleys, hills, and holes on the GC coatings crosslinked with Anquamine 419. The images in Figure 4.7 (a) indicated incompatibility between GC resin and the crosslinker and poor coalescence between the resin and crosslinker particles. The AFM images in Figure 4.7 (b) show no valleys, hills, and holes on the surface of the coatings crosslinked with Anquamine 731. The images in Figure 4.7 (b) indicated good compatibility and coalescence between resin and crosslinker particles. Figure 4.7 (a) and (b) also show the rms roughness of the coatings and indicate that the GC coatings based on Anquamine 731 were smoother compared to that of the GC coatings based on Anquamine 419.



(b) Anquamine 731 crosslinked coatings and image reflection

Figure 4.7. AFM images and reflection image of the waterborne GC coatings.

Table 4.6 shows the performance of the GC coatings crosslinked using Anquamine 731. All of the GC coatings showed no cracks in conical mandrel bend test indicating excellent flexibility. Reverse impact test showed excellent resistance of the

coatings to rapid deformation. The impact resistance value of most of the coatings reached the maximum (172 in.lb) of the instrument.

Table 4.6. Performance of waterborne GC coatings.

Coating	Conical mandrel (0cm = Best)	Reverse impact (in.lb)	König pendulum hardness (sec)	Cross-hatch adhesion (5B = Best)
F1	0	>172	44	5B
F2	0	128	97	4B
F3	0	112	90	0B
F4	0	>172	60	1B
F5	0	>172	59	1B
F6	0	>172	30	4B
F7	0	>172	23	5B
F8	0	>172	19	5B
F9	0	>172	24	5B
F10 (Control)	0	>172	39	5B

For further analysis of coating properties, coatings were selected from the results presented in Table 4.5 that show good water and solvent resistance determined by water drop test, water double rubs test, and MEK double rubs test. Thus coatings F1, F2, F4, and F10 (control) based on resins R1, R2, R4, and R10 (control) were selected for further analysis.

4.3.7. *Further analysis of the coating properties*

Table 4.7 shows the elongation at break and Young's modulus determined by tensile test, T_g determined by DSC, and crosslink density determined from DMA for F1, F2, F4, and F10 coatings. The coatings showed low elongation at break. Young's modulus, T_g , and crosslink density of the coatings decreased as the extent of mPEG increased in the respective GC resins.

Figure 4.8 shows the (a) storage modulus and (b) $\tan \delta$ curves for F1, F2, F4, and F10 coatings. Crosslink density of the coatings was determined from the values of storage

modulus well above T_g . Decrease in $\tan \delta$ peak height indicates increase in crosslink density.¹⁴⁹

Table 4.7. Tensile tes of the screened coatings.

Coatings	Elongation at break (mm)	Young's modulus (MPa)	T_g (°C) from DSC	Crosslink density (mol/L)
F1	6	3135	37	1.22
F2	4	2931	35	0.95
F4	11	978	27	0.61
F10 (control)	15	819	34	0.94

F1, F2, and F10 coatings had $\tan \delta$ peak at similar heights and also had crosslink density values very close to each other. Coating F4 had the lowest crosslink density determined from its storage modulus curve and also had the highest $\tan \delta$ peak. An increase in the amount of mPEG in the resins decreased the reactive epoxy group content in the coatings and decreased the crosslink density.

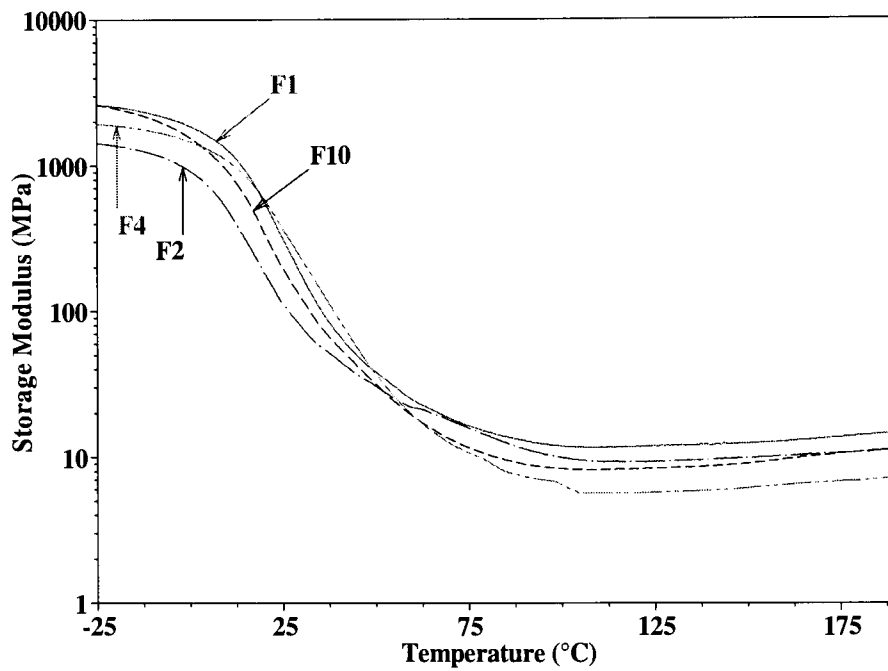
4.3.8. Thermal stability

TGA was performed on the coatings to determine their thermal stability. Results of TGA analysis are shown in Figure 4.9. The coating showed good thermal stability. The onset temperature for the degradation of the coatings was around 225 °C.

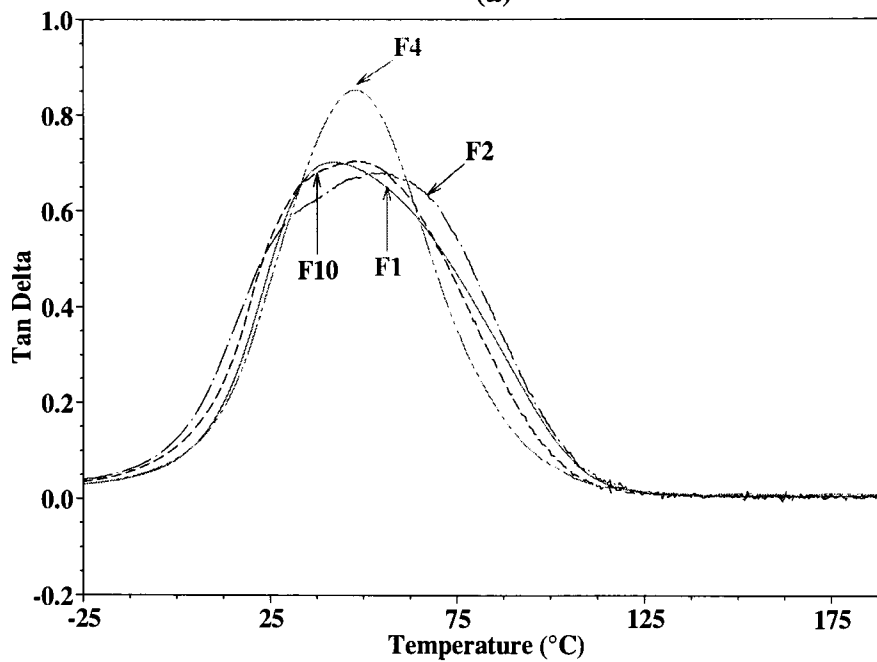
4.3.9. Barrier properties by EIS analysis

The waterborne GC coatings which exhibited high performance in water drop, and wtaer dorble rubs tests, and high solvent resistance in MEK double rubs were also screened for EIS experiments. The screened coatings were F1, F2, F4, and F10 based on resins R1, R2, R4, and R10, respectively. The coatings were prepared on steel and aluminum substrates and EIS expperiments were performed after 2.5 hrs and seven days of immersion. All of the coatings on steel substrate showed visible underfilm corrosion

within four days of immersion and hence EIS experiments after seven days were not performed. Figure 4.10 shows modulus Bode plot for the coatings on steel substrate after



(a)



(b)

Figure 4.8. (a) Storage modulus and (b) $\tan \delta$ curves of coatings F1, F2, F4, and F10 (control).

2.5 hrs of immersion. All the coatings showed capacitive, resistive, and capacitive behavior over the range of the test frequency used in the experiment. Coatings F1 and F2

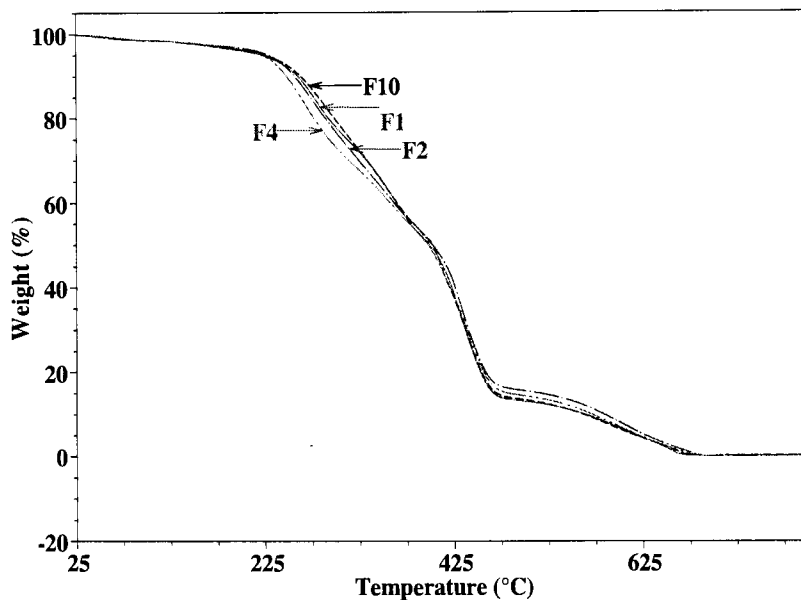


Figure 4.9. TGA of coatings F1, F2, F4, and F10.

showed relatively higher resistance compared to that of coatings F4 and F10. The capacitive behavior of the coatings at low frequency may indicate high interaction of water with the coatings.

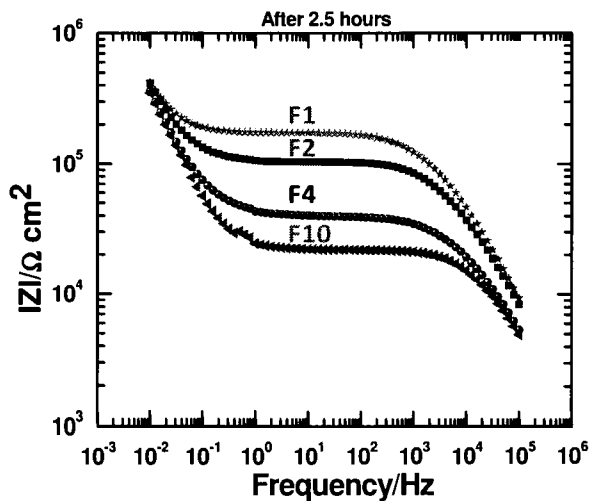


Figure 4.10. Bode plot of the coatings on steel substrate after 2.5 hrs of immersion.

EIS modulus Bode plots of the coatings on aluminum substrates after 2.5 hrs and seven days of immersion are shown in Figure 4.11 (a) and (b), respectively. The Bode plots showed that coatings F1, F2, and F10 had higher resistance than coating F10. The Bode plots showed capacitive behavior in high frequency region, resistive behavior in mid-frequency region, and capacitive behavior in low frequency region and indicated interaction of the coatings with water. Coatings F1 and F2 showed higher resistive values after seven days of immersion compared to that of coatings F4 and F10 and indicated relatively higher resistance to water compared to that of coatings F4 and F10.

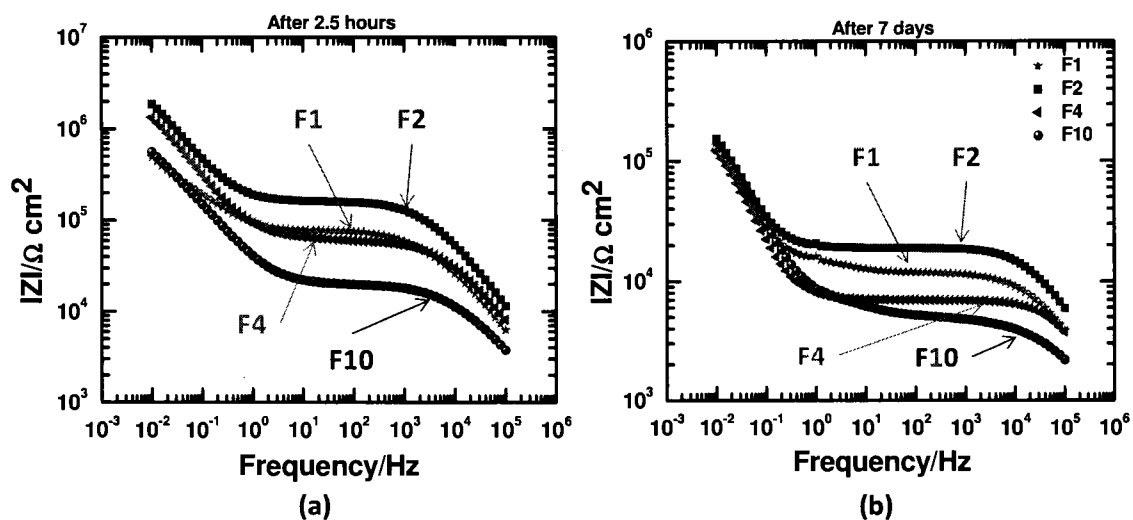


Figure 4.11. Bode plots of the coatings on aluminum substrate after (a) 2.5 hrs and (b) seven days.

Capacitance of the coatings on aluminum substrate after seven days of immersion was also obtained in EIS experiment. Figure 4.12 shows the capacitance of the coatings on aluminum substrate after seven day of immersion. Coatings F1 and F2 had lower capacitance compared to that of coatings F4 and F10. A comparison of the capacitance values for coatings F1 and F2 with that of coatings F4 and F10 indicates that coatings F1 and F2 had relatively less water uptake compared to that of coatings F4 and F10.

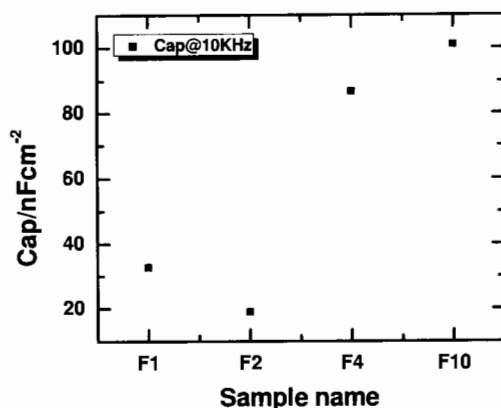


Figure 4.12. Capacitance of the coatings on aluminum substrate after seven days of immersion.

The water uptake of the coatings can be directly related to the extent of hydrophilic groups in the coatings. Higher amount of hydrophilic group increases water uptake.¹⁵⁰ Extent of hydrophilic ether group in R1, R2, and R4 GC resins are shown in Table 4.8. The capacitance values of F4 and F10 were close to each other and were significantly higher than coatings F1 and F2. Higher water uptake indicated by higher

Table 4.8. Extent of ether groups in the resin compositions.

Coatings	Resin composition	Moles of ether group per mole of GC resin
F1	IGC-mPEG350-5% (R1)	0.361
F2	IGC-mPEG550-5% (R2)	0.588
F4	IGC-mPEG350-10% (R4)	0.722
F10	GC-XP-7165 (R10)	Control

capacitance of F4 coatings than that of F1 and F2 coatings can be correlated to the higher extent of hydrophilic ether group in resin R4 than that in resins R1 and R2. Similarly, higher water uptake of coating F10 indicated by its higher capacitance than that of coatings F1 and F2 suggests that resin R10 may contain a higher extent of hydrophilic groups than that in resins R1 and R2 and that the extent of hydrophilic ether groups might be similar to that in resin R4.

4.3.10. Salt spray test

Salt spray tests were performed on the screened coatings on steel and aluminum substrates. The coatings on steel substrate were delaminated within 24 hrs of salt spray and the coatings on steel substrates were removed from the salt spray chamber. The coatings on aluminum substrate did not show delamination, blister, or creep over ten days of salt spray. However, the panels became reddish brown dark over 240 hrs of salt spray. Figure 4.13 shows the pictures of the coatings after ten days of salt spray test.

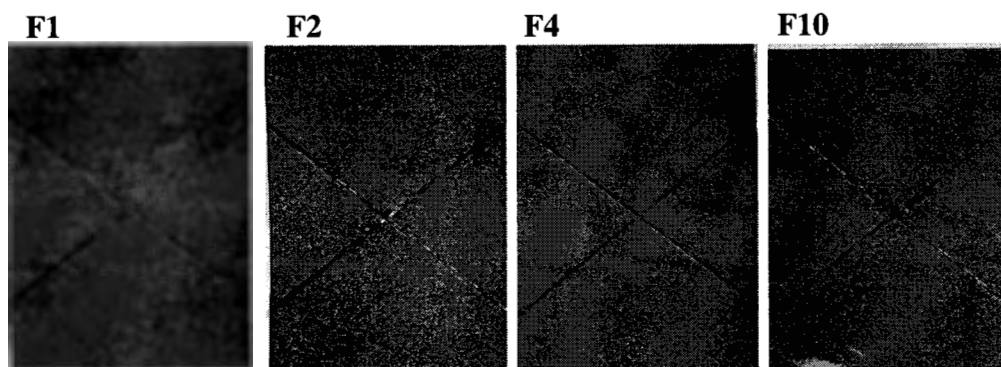


Figure 4.13. Salt spray on the coatings on aluminum substrate for ten days.

It should be noted that the aluminum panes were treated with Alodine 5700 before applying the coatings on them. Unlike for the coatings on steel substrate, the coatings on aluminum substrate did not delaminate. This could be due to surface treatment of the aluminum panels which improved the adhesion of the coatings.

4.4. **Conclusions**

Glycidyl carbamate resins can be made water dispersible by incorporating non-ionic hydrophilic groups such as mPEG into the resin structures. Chain length and mol % incorporation of mPEG in GC resins influence the water dispersibility. All of the resins except R1 and R10 were able to be dispersed in water without organic cosolvents or surfactants. The coatings crosslinked with anquamine 731 were transparent and had

smooth surface. Coatings F1, F2, F4, and F10 based on GC resins R1, R2, R4, and R10, respectively showed good water and solvent resistance in water drop, water double rubs, and MEK double rubs tests. The coatings had good impact strength, flexibility, adhesion, hardness, Young's modulus, and low elongation at break.

EIS experiments showed that the barrier properties of the coatings were influenced by the hydrophilic content of the coatings. Bode plots of the coatings on steel substrate after 2.5 hrs of immersion and the coatings on aluminum substrate after seven days of immersion showed capacitive, resistive, and capacitive behavior and indicated high interaction with water. Relatively, coatings F1 and F2 had higher impedance than coatings F4 and F10 and indicated higher resistance to water. Coating F4 based on R4 resins had a higher extent of hydrophilic ether group than that of coatings F1 and F2 based on resins R1 and R2, respectively. Higher capacitance of coatings F4 and F10 than that for coatings F1 and F2 indicated higher water uptake.

The salt spray tests indicated that substrate treatment had an influence on adhesion of the coatings. The coatings on steel substrates were delaminated in a day in salt spray chamber while the coatings on treated aluminum substrate remained intact and no blister or delamination was observed. The aluminum substrate became reddish brown over the period of exposure.

4.5. References

1. Edwards, PA, Striemer, G, Webster, DC, "Novel Polyurethane Technology Through Glycidyl Carbamate Chemistry". *J. Coat. Technol. Res.*, **2** (7) 517-527 (2005)
2. Chattopadhyay, DK, Raju, KVS, "Structural Engineering of Polyurethane Coatings for High Performance Applications". *Prog. Polym. Sci.*, **32** (3) 352-418 (2007)

3. Tarlas, HD, "Amine Cured Epoxy Resin Coatings for Resistance to Atmospheric Corrosion". *Mater. Prot.*, **9** (5) 37-42 (1970)
4. Edwards, PA, Striemer, G, Webster, DC, "Synthesis, Characterization and Self-crosslinking of Glycidyl Carbamate Functional Resins". *Prog. Org. Coat.*, **57** (2) 128-139 (2006)
5. Chattopadhyay, DK, Webster, DC, "Hybrid coatings from novel silane-modified glycidyl carbamate resins and amine crosslinkers". *Prog. Org. Coat.*, **66** (1) 73-85 (2009)
6. Chattopadhyay, DK, Zakula, AD, Webster, DC, "Organic-inorganic hybrid coatings prepared from glycidyl carbamate resin, 3-aminopropyl trimethoxy silane and tetraethoxyorthosilicate". *Prog. Org. Coat.*, **64** (2-3) 128-137 (2009)
7. de Meijer, M, "Review on the Durability of Exterior Wood Coatings With Reduced VOC-content". *Prog. Org. Coat.*, **43** (4) 217-225 (2001)
8. Geurink, PJA, Scherer, T, Buter, R, Steenbergen, A, Henderiks, H, "A Complete New Design for Waterborne 2-Pack PUR Coatings With Robust Application Properties". *Prog. Org. Coat.*, **55** (2) 119-127 (2006)
9. Tanabe, H, Ohsugi, H, "A New Resin System for Super High Solids Coating". *Prog. Org. Coat.*, **32** (1-4) 197-203 (1997)
10. Elmore, JD, Kincaid, DS, Komar, PC, Nielsen, JE, "Waterborne epoxy protective coatings for metal". *J. Coat. Technol.*, **74** (931) 63-72 (2002)
11. Galgoci, EC, Komar, PC, Elmore, JD, "High performance waterborne coatings based on dispersions of a solid epoxy resin and an amine-functional curing agent". *J. Coat. Technol.*, **71** (891) 45-52 (1999)

12. Marrion, AR, *The Chemistry and Physics of Coatings*. 2nd ed., The Royal Society of Chemistry, Cambridge (2004)
13. Melchior, M, Sonntag, M, Kobusch, C, Jurgens, E, "Recent developments in aqueous two-component polyurethane (2K-PUR) coatings". *Prog. Org. Coat.*, **40** (1-4) 99-109 (2000)
14. Mundstock, H, Pires, R, Richter, F, Schmitz, J, "New low viscous polyisocyanates for VOC compliant systems". *Macromol. Symp.*, **187** 281-292 (2002)
15. Overbeek, A, "Polymer heterogeneity in waterborne coatings". *J. Coat. Technol. Res.*, **7** (1) 1-21 (2010)
16. Schoff, CK, "Organic coatings: the paradoxical materials". *Prog. Org. Coat.*, **52** (1) 21-27 (2005)
17. Shaffer, M, Stewart, R, Allen, K, Wylie, A, Lockhart, A, "Two component polyurethane coatings: High performance crosslinkers meet the needs of demanding applications". *Journal of Coatings Technology CoatingsTech* January 2009, 2009, pp 50-55.
18. Taylor, JW, Winnik, MA, "Functional latex and thermoset latex films". *JCT Res.*, **1** (3) 163-190 (2004)
19. Wicks, ZW, Wicks, DA, Rosthauser, JW, "Two package waterborne urethane systems". *Prog. Org. Coat.*, **44** (2) 161-183 (2002)
20. Wicks (Jr), ZW, Jones, FN, Pappas, SP, Wicks, DA, *Organic Coatings: Science and Technology*. 3rd ed., John Wiley and Sons Inc., New Jersey (2007)
21. Back, GE, Wang, PC, Corley, LS, Elmore, KD, "Water dispersible epoxy resins." US 6,956,086 B2, 2005.

22. Corley LS, Kincaid DS, Young, GC, "Amine-terminated polyamide in oil-in-water emulsion." US 5,962,269, 1999.
23. Corley LS, Kincaid, DS, Young, GC, "Aqueous dispersion of polyamide-amine derived from aminoalkylpiperazine epoxy resin." US 5,998,508, 1999.
24. Matthias, L, Cook, M, Klippstein, A, "Method of preparation of a water based epoxy curing agent." US 7,615,584 B2, 2009.
25. Stark, CJ, Elmore, JD, Back, GE, Wang, PC, Galgoci, EC, "Aqueous dispersion of epoxy resins." US 6,221,934, 2001.
26. Edwards, PA. Glycidyl carbamate resins to achieve polyurethane properties and epoxide reactivity. Ph.D. Dissertation, North Dakota State University, Fargo, 2004.
27. Hill, LW, "Determination of Crosslink Density in Thermoset Coatings". *Polym. Mater. Sci. Eng.*, **77** 387-388 (1997)
28. Skaja, A, Fernando, D, Croll, S, "Mechanical Property Changes and Degradation During Accelerated Weathering of Polyester-Urethane Coatings". *J. Coat. Technol. Res.*, **3** (1) 41-51 (2006)
29. Wold, CR, Soucek, MD, "Viscoelastic and thermal properties of linseed oil-based ceramer coatings". *Macromol. Chem. Phys.*, **201** (3) 382-392 (2000)
30. Wadgaonkar, B, Ito, S, Svizero, N, Elrod, D, Foulger, S, Rodgers, R, Oshida, Y, Kirkland, K, Sword, J, Rueggeberg, F, Tay, F, Pashley, D, "Evaluation of the effect of water-uptake on the impedance of dental resins". *Biomaterials*, **27** (17) 3287-3294 (2006)

CHAPTER 5. UV CURABLE GLYCIDYL CARBAMATE RESINS

5.1. Introduction

UV-curing or radiation curing has gained interest due to its unique economic and ecological advantages. These unique advantages are ultrafast curing at ambient temperatures or lower and 100 % solids or low VOC coating formulations, as in most cases solventless liquid monomers, oligomers, or solid polymers are used.^{11, 58, 85, 86}

Radiation curing or photocrosslinking produces densely crosslinked polymeric materials within a very short time (seconds) from multifunctional monomers, oligomers or telechelic polymers upon exposure to radiation such as ultraviolet light (UV) or electron beam (EB).⁸⁷⁻⁸⁹ For more than three decades radiation curing has been successfully used for many applications such as coatings, adhesives, inks, optical waveguides, and microelectronics. UV curable coatings are widely used for furniture, plastic substrates, optical fibers, compact discs, headlight lenses, and metal substrates.^{85, 90} Photopolymerizable monomers, oligomers and polymers (based on acrylate, vinyl and epoxide groups) are widely used to produce UV curable coatings, inks, adhesives, composites, etc. Structure and functionality of UV curable oligomers, polymers and reactive diluents and type of photoinitiators governs speed of cure, extent of crosslinking and final performance of coatings (flexibility, hardness, adhesion, and scratch and chemical resistance).^{1, 85, 87, 92-94}

Glycidyl carbamate (GC) resins are obtained by the reaction of isocyanate functional compounds with glycidol. GC resins contain urethane (-NHCO-) and epoxy functional groups in their structure. Thus, an unique property of GC resins is that the performance of urethane and the reactivity of epoxide is combined in single resin

structure.^{45, 49} Polyurethane and epoxy resins are widely used in numerous commercial applications such as coatings, composites, high performance polymers, etc. Urethane coatings offer excellent toughness, adhesion, flexibility and chemical resistance. Epoxy coatings offer excellent corrosion and solvent resistance, adhesion and versatility of crosslinking (curing) mechanisms.^{13, 35} The combination of urethane and epoxy functional groups in GC resins imparts an excellent set of properties to GC-based coatings. Reactive epoxy groups in GC resins can be crosslinked using amines and by self crosslinking to produce high performance coating systems.^{45, 46, 48, 49} GC resins also produced organic-inorganic hybrid coatings with an excellent set of properties by sol-gel crosslinking.⁵²⁻⁵⁴

With the realization that the GC resins produce coatings with an excellent combination of properties when crosslinked by amines, self-crosslinking, and by hybrid sol-gel crosslinking, the technology of GC resins and coatings was extended for use in UV curing. The goal of the research presented in this chapter was to obtain UV curable resins and UV cured coatings. GC resins were reacted with acrylic acid to generate UV curable GC resins. BGC, IGC and modified IGC resins were used synthesized and reacted with acrylic acid to obtain a series of acrylated GC resins. Several reactive diluents were used to make UV curable coating formulations. UV cured GC coatings were produced and their properties were studied.

5.2. Experimental

5.2.1. *Materials*

Polyisocyanate resins used to obtain GC resins were hexamethylene diisocyanate isocyanurate (Desmodur N 3600) and hexamethylene diisocyanate biuret (Desmodur N 3200) provided by Bayer MaterialScience. Glycidol was supplied by Dixie Chemical.

Glycidol was stored refrigerated to minimize the formation of impurities. Dibutyltindilaurate (DBTDL), purchased from Aldrich, was used to catalyze the isocyanate and hydroxyl reactions to form the glycidyl carbamate (GC) resins. Acrylic acid (AA) was purchased from Sigma Aldrich. *p*-Toluenesulfonic acid (*p*TSA) purchased from Aldrich was used as a catalyst for transesterification reaction between AA and the epoxy group. Hydroquinone purchased from Sigma Aldrich was used as an inhibitor to avoid gelation by free radical polymerization during the esterification reaction. A modifier alcohol used was ethylene glycol propyl ether (EP) obtained from Fluka-Aldrich. All the reagents were used as received without any further purification. CN929, a trifunctional urethane acrylate resin obtained from Sartomer was used as a control. Reactive diluents used were 1,6 hexanediol diacrylate ester (SR 238), 2(2ethoxyethoxy)ethyl acrylate (SR 256), ethoxylated trimethylolpropane triacrylate (SR 454) provided by Sartomer. CN373, a reactive amine coinitiator obtained from Sartomer was used to improve surface cure. Photoinitiator Irgacure 184 (1-hydroxycyclohexyl phenyl ketone) was obtained from Ciba Chemicals.

5.2.2. Synthesis of acrylated glycidyl carbamate resin

The synthesis of acrylated GC resins was a two step reaction. In the first step, biuret glycidyl carbamate (BGC), isocyanurate glycidyl carbamate (IGC), and modified GC resins based on isocyanurate and EP were obtained. In the second step, the epoxy groups of the GC resins were reacted with AA to obtain the corresponding acrylated GC resins. Table 5.1 shows the recipes for the synthesis of the acrylated GC resins.

Table 5.1. Recipe for the synthesis of acrylated GC resins.

Synthesis of GC resin						Synthesis of acrylated GC resin			
GC resin	Desmodur N 3200 (gm)	Desmodur N 3600 (gm)	EP (gm)	Glycidol (gm)	EEW (g/eq)	Acrylated GC resin	GC resin (gm)	AA (gm)	Final acid value (mg KOH / gm)
BGC	100	--	--	40.50	273	ABGC	83.12	21.92	7
IGC	--	100	--	40.45	276	AIGC	75.26	19.70	7
IGC-EP 15%	--	150.65	12.87	51.80	338	AIGC-EP 15%	75.10	16.16	6
IGC-EP 33%	--	150	28.14	40.04	425	AIGC-EP 33%	95.30	16.13	7

A 500 ml four neck reaction vessel was used for the synthesis of acrylated GC resins. The vessel was fitted with a condenser, nitrogen inlet and Model 210 J-KEM temperature controller and mechanical stirrer. A water bath was used for heating and cooling the vessel. The stoichiometric equivalent amount of HDI polyisocyanate resin (biuret or isocyanurate) and glycidol based on $-NCO$ and $-OH$ groups used for the synthesis of BGC or IGC resin was 1:1 (NCO:glycidol). During the synthesis of BGC and IGC resins, the reaction vessel was charged with corresponding polyisocyanate resin followed by addition of the required amounts of glycidol. For the synthesis of modified IGC resins, the vessel was charged with the required amount of isocyanurate polyisocyanate, glycidol, and modifier EP. Two modified IGC resins IGC-EP 15% and IGC-EP 33% were obtained by using the stoichiometric equivalent amounts of NCO, glycidol, and EP as 1:0.85:0.15 and 1:0.66:0.33, respectively. Thus, for the synthesis of modified IGC resins a portion of glycidol was replaced by EP. Once the vessel was charged with required amount of polyisocyanate, glycidol, and modifier, the reaction mixture was stirred for about 45 – 60 min. at 40 – 45 °C to ensure a homogeneous mixture. The catalyst (DBTDL), in the form of a solution in tertiary butyl acetate (1 – 2 % by wt.), was added after the completion of mixing. The amount of catalyst added was 0.03 % by wt. (of the total reaction charge). After the addition of catalyst around at about 40 – 45 °C, all of the reactions showed an exotherm, bubble formation and an increase in viscosity. The reactions were continued until the $-NCO$ peak in FTIR spectra disappeared completely. Epoxy equivalent weight (EEW) of the synthesized GC resins were determined by epoxy titration method.

The acrylated GC resins were obtained by the reaction of GC resins with AA. The reaction was carried out in a similar four neck reactor assembly used for the synthesis of GC resins. The required amount of reactants, GC resin, and AA (1:1 epoxy:acid stoichiometric ratio), were added to the reactor. The reaction mixture was stirred for about 20 min. at 45 – 50 °C to obtain a homogeneous mixture. After completion of the mixing, the catalyst (*p*TSA) of about 0.03% by wt. (of the reactants) was added at 40 °C along with hydroquinone (0.02-0.09 % by wt. of the total reactants). The reaction was carried out at the temperature between 65 – 75 °C. The reaction progress was monitored by acid value titration. The reaction was continued until acid value reached to 8. Thus the acrylation of GC resins such as BGC, IGC, IGC-EP 15%, and IGC-EP 33% was carried out to obtain corresponding acrylated GC resins ABGC, AIGC, AIGC-EP 15%, and AIGC-EP 33%, respectively.

5.2.3. FTIR measurements

A Nicolet 8700 FTIR spectrometer from Thermo Scientific was used for the FTIR measurements. Sample aliquots were taken and coated on a potassium bromide salt plate. Spectra acquisitions were based on 32 scans with a data spacing of 1.98 cm⁻¹. The FTIR was set for auto gain to monitor spectral range of 4000 – 500 cm⁻¹. The change in band absorption of isocyanate (2272 cm⁻¹), -OH and -NH (3750 – 3000 cm⁻¹), amide (1244 cm⁻¹), epoxide (910 cm⁻¹ and 859 cm⁻¹), and acrylate (810 cm⁻¹) bands were used to follow the reaction progress.

5.2.4. Epoxy titration

Epoxy equivalent weight of the resins was determined by titration with hydrogen bromide (HBr) according to ASTM D1652. A required amount of resin (0.06 to 0.8 gm)

was dissolved in 5 – 10 ml of chloroform and was titrated against a standardized HBr solution prepared in glacial acetic acid. The indicator used was a solution of crystal violet in glacial acetic acid. End point of the titration was the appearance of permanent yellow-green color.

5.2.5. Acid value titration

Acid value of the resins was determined by titration with 0.1 N KOH solution according to ASTM D 1639. A required amount of resin (0.5 to 1.0 gm) was dissolved in isopropyl alcohol (10 to 15 ml) and titrated against 0.1 N KOH solution using phenolphthalein indicator. End point of the titration was the first persistent faint pink color.

5.2.6. Viscosity determination

An advanced Rheometric Expansion System (ARES, TA instruments) with parallel plate geometry (25.0 mm plate diameter) was used to determine the viscosity of the GC resins as a function of temperature. The experiments were performed in dynamic temperature ramp mode. The temperature was ramped from 25 °C to 50 °C at rate of 5 °C/min at the frequency of 5 rad/sec.

5.2.7. UV curable formulation and coating preparation

The UV curable coating formulations were prepared using acrylated GC resins, reactive diluents, and photoinitiator. The reactive diluents used were 2(ethoxyethoxy)ethyl acrylate (SR 256), 1,6 hexanediol diacrylate ester (SR 238), and ethoxylated trimethylolpropane triacrylate (SR 454). The photoinitiator and amine co-initiator used were Irgacure 184 and CN373, respectively. Figure 5.1 shows the structures of the reactive diluents and photoinitiator used in this study.

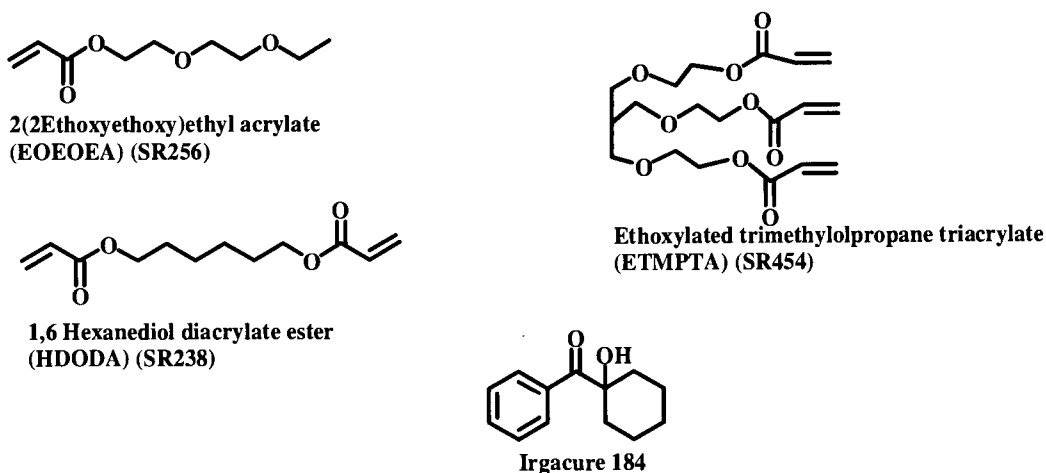


Figure 5.1. Reactive diluents and photoinitiator used.

Table 5.2. shows the recipe for the coating formulation. The resin was mixed with the required amount of reactive diluents, photoinitiator, and amine co-initiator. The formulations were warmed to 45 – 50 °C to ensure complete homogeneous mixing.

Table 5.2. Recipe for UV curable coating formulation.

Ingredients	Parts per weight
Resin	61.1
SR 238	12.2
SR256	16
SR 454	6.1
Irgacure 184	2.3
CN373	2.3

The films were drawdown at 6 mils wet thickness on steel panels (Q panels, QD 36). The coatings were cured in air using Fusion LC6B Benchtop Conveyor with an F300 UV lamp. Table 5.3 shows the intensity of UV lamp used for the curing. The UV-light intensity at the was measured using a UV Power Puck II from EIT Inc. The general curing protocol was to pass the coating through the lamp at the conveyer belt speed of 24 ft/min. (~ 5 sec. exposure) until a tack free through dry film was obtained. Thus, a low number of passes through the lamp to obtain a tack free through dry film indicated fast curing. The through dry time for the film formation was tested according to the ASTM D

1640. The coatings were kept at ambient overnight before the characterization of their performance. Thickness of the cured coatings was 70 to 80 μm .

Table 5.3. UV-lamp intensity used for curing.

UV-radiation type (Range)*	mW/cm ²
UVA (390-320 nm)	1300
UVB (320-280 nm)	450
UVC (260-250 nm)	70
UVV (395-445 nm)	1100

*(Range is reported according to the specification of UV Power Puck II measuring device)

5.2.8. Performance of coatings

König pendulum hardness of the coatings was measured following ASTM D 4366. The hardness test results are reported in seconds (sec). Reverse impact strength of the coatings was determined following ASTM D 2794 using a Gardener impact tester. The maximum drop height was 43 inches and the drop weight was 4 pounds. Cracking or loss of adhesion was noted and inch-pounds (in-lbs) were reported at film finish failure. The conical mandrel test was also used according to ASTM D 522 for the determination of flexibility the coatings. The results of flexibility test were reported as the length of a crack (cm) formed on the coating during the test. Methyl ethyl ketone (MEK) double rubs test was used according to ASTM D 5402 to assess the chemical resistance and development of cure. A 26-ounce hammer with three layers of cheesecloth wrapped around the hammerhead was soaked in MEK. The hammer head was rewet with MEK after 30 – 50 double rubs. Once mar was achieved, the number of double rubs was noted. Cross hatch adhesion of the coatings was evaluated using a Gardco cross hatch adhesion instrument following ASTM D 3359.

5.2.9. Kinetic experiments using real-time FTIR (RTIR)

Real-time Fourier transform infrared (RTIR) experiments were performed by using a Nicolet 8700 spectrometer from Thermo Scientific with detector type DTGS KBr, with a UV optic fiber mounted in a sample chamber. The light source was 100-Watt compact arc DC mercury vapor lamp. The UV-light intensity at the sample position was measured using a UV power Puck II from EIT Inc. and the result is shown in Table 5.4

This set up monitors the reaction insitu as the photopolymerization proceeds. The coating formulation was coated on the KBr window in thin films. The coating was then exposed to UV radiations for 222 sec. at 1 scan per second and all the experiments were performed in air. The decrease in the peak are of acrylated peak at 810 cm^{-1} was monitored to follow the photopolymerization.

Table 5.4. RTIR UV-lamp intensity.

UV-radiation type (Range)*	mW/cm ²
UVA (390-320 nm)	69
UVB (320-280 nm)	459
UVC (260-250 nm)	0
UVV (395-445 nm)	48

*(Range is reported according to the specification of UV Power Puck II measuring device)

5.2.10. Differential scanning calorimetry (DSC)

A TA Instruments Q1000 differential scanning calorimeter (DSC) with an auto sampler accessory was used to determine the glass transition temperature (T_g) of the coatings. DSC experiments were performed by placing a sample into the conventional aluminum pans. The samples were subjected to a heat-cool-heat cycle. The samples were heated to 200 °C and then cooled to -75 °C and held there for 5 min. DSC thermogram

were taken from -75 °C to 250 °C at a heating rate of 10 °C min⁻¹. Glass transition temperature was determined as the temperature of the inflection at the mid-point.

5.2.11. Dynamic mechanical analysis (DMA)

A TA Instruments Q800 Dynamic Mechanical Analysis system was used to determine viscoelastic properties of the cured coating films. The dimensions of free films used were of 23 to 26 mm in length, 5 mm in width and 0.09 to 0.1 mm in thickness. Poisson's ratio was assumed to be 0.4 for all of the coating films. The experiments were carried out within a temperature range of -20 °C to 200 °C with a temperature ramp rate of 5 °C min⁻¹ at a frequency of 1 Hz. The storage modulus values (E') in the rubbery plateau region (well above T_g) are used to calculate the crosslink density of the coatings. Equation (5.1) was used to calculate cross-link density (ν_c) of the coatings.^{112, 121}

$$E' = 3\nu_c RT \quad (5.1)$$

where, E' = storage modulus (Pa); ν_c = crosslink density (mol/lit); R = gas constant (8.3 J/K/mol); and T = temperature (K).

5.2.12 Tensile test

Tensile testing of the coatings was performed using Instron 5542 instrument. The test specimen were prepared according to ASTM D 638-5 method. The test was carried out at 10 mm/min at ambient conditions. Elongation at break and Young's modulus of the coatings were determined.

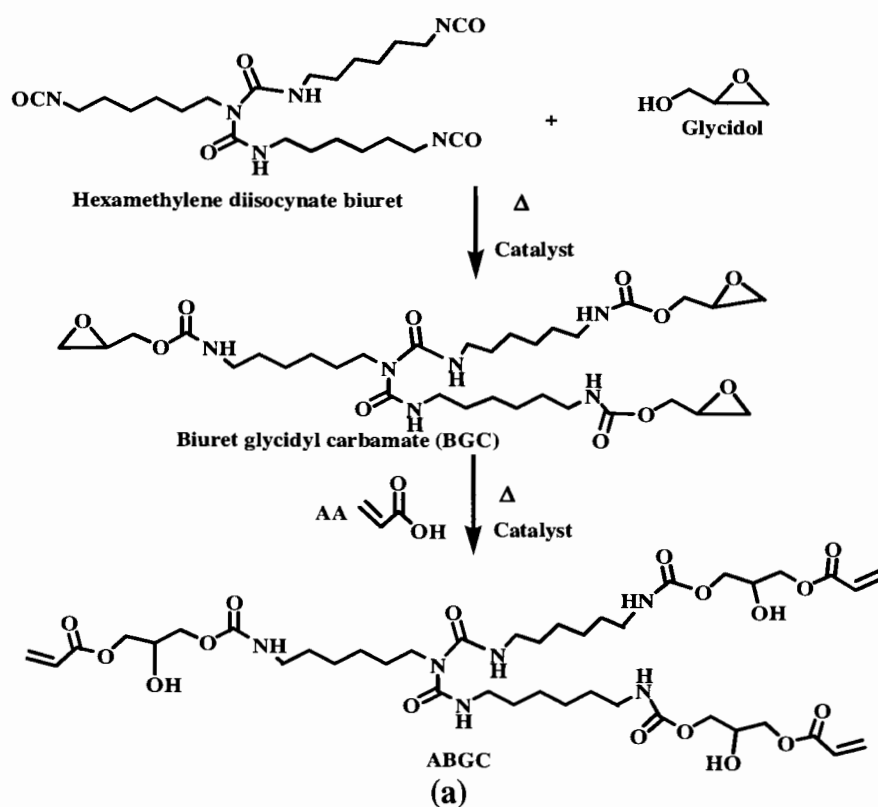
5.2.13. Thermogravimetric analysis (TGA)

TGA was performed using a TA Instruments Q500. Temperature was ramped from ambient to 800 °C with a ramp rate of 10 °C min⁻¹. A nitrogen atmosphere was used during the test. Weight retained was plotted as a function of temperature.

5.3. Results and discussion

5.3.1. *Synthesis of acrylated GC resins*

Acrylated GC resins were synthesized by reacting BGC, IGC, IGC-EP 15%, and IGC-EP 33% resins with acrylic acid and the corresponding acrylated GC resins obtained were labeled as ABGC, AIGC, AIGC-EP 15%, and AIGC-EP 33%, respectively. Figure 5.2 shows the synthesis scheme for ABGC, AIGC, and AIGC-EP 33%. BGC and IGC resins have higher epoxy functionality than modified IGC resins and required higher a amount of AA for the acrylation. Thus, ABGC and AIGC had higher acrylate functionality than the modified IGC resins. The synthesized acrylated GC resins have combination of functional groups such as urethane, hydroxyl, and acrylate.



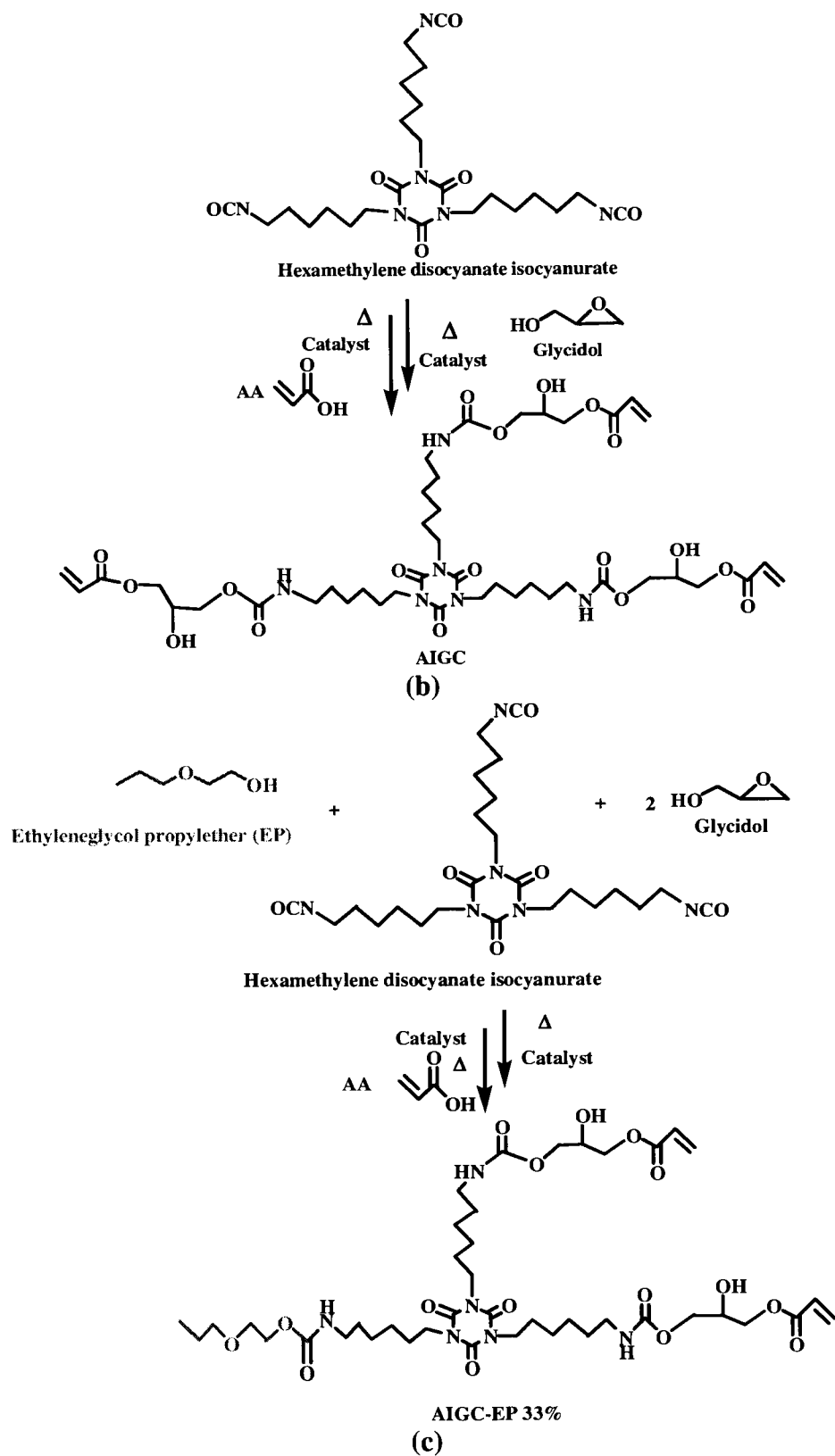


Figure 5.2. Schematic representation of the synthesis of (a) ABGC, (b) AIGC, and (c) AIGC-EP 33%.

The FTIR spectra show, the characteristic absorption bands for epoxide and acrylate groups observed between 913 to 840 cm^{-1} and at 810 cm^{-1} .^{106, 151} A comparison of the FTIR spectra for the GC resins with the acrylated GC resins showed the disappearance of the absorption band for epoxide (910 and 859 cm^{-1}) and the appearance of the absorption band for acrylate (810 cm^{-1}) in the acrylated GC resins. Figure 5.3 shows the FTIR spectra for GC resins and acrylated GC resins.

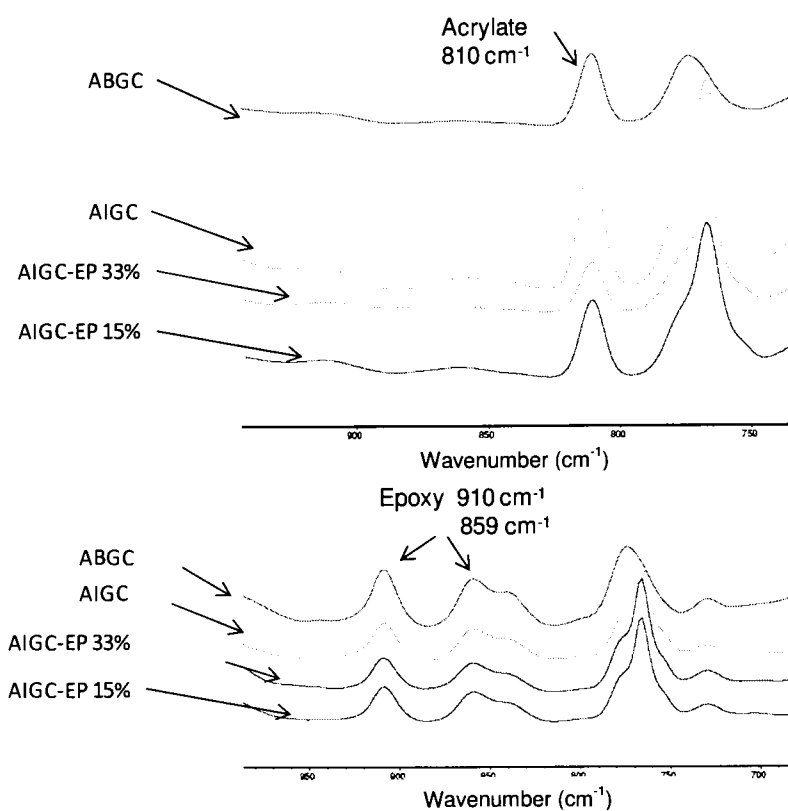


Figure 5.3. FTIR spectra for the GC resins and the acrylated GC resins.

5.3.2. Viscosity of acrylated GC resins

GC resins had very high viscosity due to hydrogen bonding groups in them. The viscosity of the GC resins was found to be reduced by modification of the resins by alcohols (Chapter 2). Acrylated GC resins contain hydroxyl group generated during the reaction of epoxy group of GC resin with acrylic acid. Acrylated GC resins had very high

viscosity. The control trifunctional urethane acrylate resin (CN929) had the lowest viscosity. ABGC had the highest viscosity. The generated hydroxyl groups and carbonyl groups of acrylate in the acrylated GC resin may contribute to the hydrogen bonding in the resin and increase their viscosity. The viscosity of acrylated resins was lower for the alcohol modified resins. The viscosity of the resins also reduced with the increase in temperature. Table 5.5 shows the viscosity of the acrylated GC resins as a function of temperature. The decrease in viscosity with increase in temperature was very significant in acrylated GC resins compared to that of the control resin.

Table 5.5. Viscosity of acrylated GC resins.

Acrylated GC resin (neat)	Complex viscosity (η^*) (mPa·s x 10 ³)					
	25°C	30°C	35°C	40°C	45°C	50°C
ABGC	80,000	53,000	30,000	13,000	7,000	3,200
AIGC	25,000	12,000	4600	2000	850	455
AIGC-EP 15%	8,000	5,100	2,800	1300	625	315
AIGC-EP 33%	3,000	1,900	1000	500	250	125
CN929 (Ctrl)	36	33	24	16	10	7

5.3.3. Degree of conversion in UV curing

Real time infrared (RTIR) spectroscopy was used to determine the degree of conversion during the UV crosslinking reaction. The absorption band at 810 cm⁻¹ due to the out of plane =C-H vibration in the acrylate group was monitored in RTIR to determine the degree of conversion. The degree of conversion was determined using the equation 5.2.¹⁵²

$$\text{Degree of conversion} = [(A_{810})_0 - (A_{810})_t] / (A_{810})_0 \times 100 \quad 5.2$$

where, $(A_{810})_0$ is the absorption before UV exposure and $(A_{810})_t$ absorption after UV exposure. Figure 5.4 shows the degree of conversion as the function of UV exposure time. The isocyanurate based acrylated GC resins (AIGC, AIGC-EP 15%, and AIGC-EP

33%) had a higher degree of conversion compared to that of the biuret based acrylated GC resin (ABGC). The control resin (CN929) had the lowest degree of conversion. Table 5.6 shows the degree of conversion in the coatings after 1 min. of exposure to UV radiation.

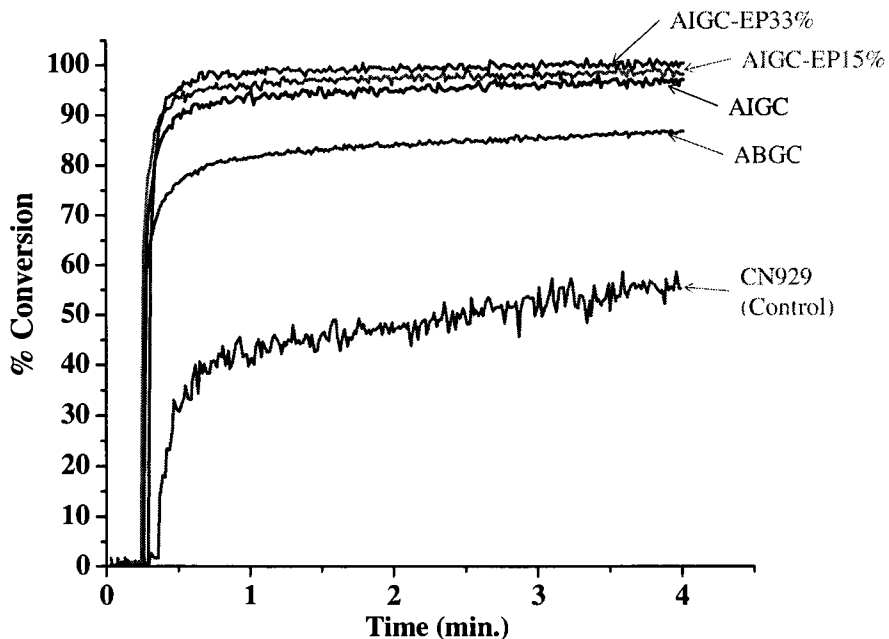


Figure 5.4. Degree of conversion of the acrylate double bonds determined using RTIR.

Table 5.6. Degree of conversion of the acrylate double bonds in the UV cured coatings.

Coating	Conversion (%)
ABGC	80±4
AIGC	94±2
AIGC-EP 15%	97±2
AIGC-EP 33%	99±0.6
CN929	44±8

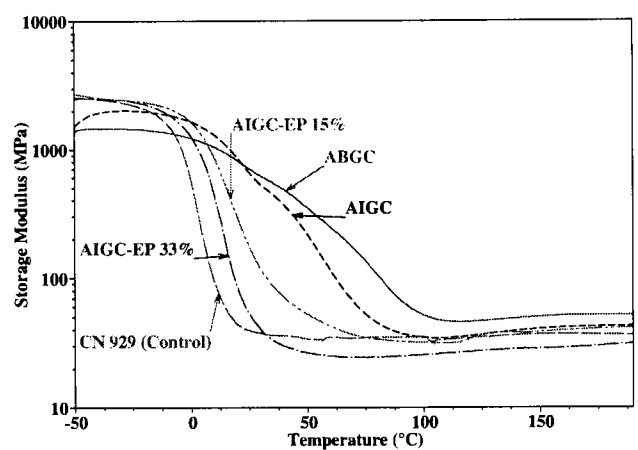
5.3.4. Coating properties

The UV curable coating formulations were prepared using the combination of reactive diluents, photoinitiator, and amine co-initiator. The coatings were cured by passing the coating through the lamp at the conveyer belt speed of 24 ft/min. (~ 5 sec

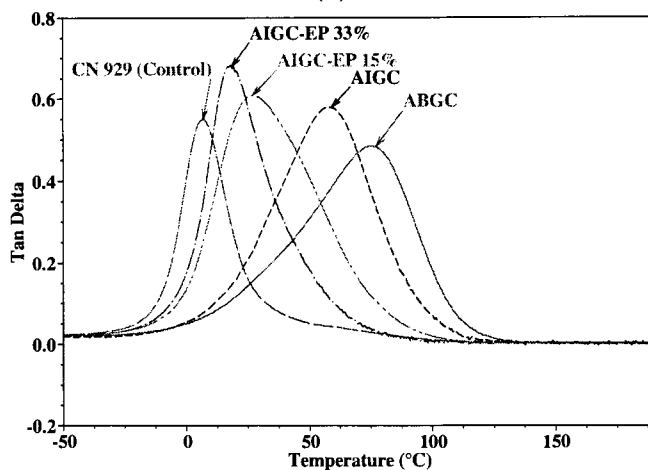
exposure) until a tack free through dry films are obtained. Thus, a lower number of passes indicates faster curing. All of the acrylated GC coating formulations produced tack free through dry films in 1 pass, while the control coating formulation required 3 passes. This indicated that acrylated GC resins cured faster than the control resin. This observation can be correlated to the degree of conversion determined using RTIR. RTIR experiments showed that the degree of conversion for acrylated GC coating formulation was higher compared to that for control coating formulation.

The properties of the UV cured coatings were influenced by the composition of the acrylated GC resins. Table 5.7 shows the properties of the UV cured coatings. The crosslink density of the coatings was determined from the value of storage modulus well above T_g . The storage modulus and $\tan \delta$ plots obtained in DMA experiments are shown in Figure 5.5 the ABGC coatings had the highest crosslink density which is reflected in their highest T_g , hardness, and Young's modulus and the lowest reverse impact strength, poor conical mandrel flexibility, and elongation at break. AIGC coatings had lower crosslink density than that for ABGC and had lower T_g , hardness, and Young's modulus than ABGC coatings. The AIGC coatings had higher elongation at break and impact strength than the ABGC coatings. The increase in modification of the resins decreased the crosslink density of the coatings and increased impact strength and elongation at break and decreased hardness, T_g , and Young's modulus. The GC coatings had good chemical resistance indicated by MEK double rubs values. The MEK double rubs decreased at 33% modification for AIGC-EP 33% coating. The control coatings had the crosslink density above AIGC-EP 33% and below that of AIGC-EP 15%. The control coatings had the lowest T_g and the highest impact strength.

The breadth of the $\tan \delta$ peaks can be correlated to heterogeneity and damping characteristics of the crosslinked network.^{117, 122} $\tan \delta$ plots for acrylated GC coatings were broader than the control coating and indicated a more heterogeneous network with more damping character in the GC coatings compared to the control coating. AIGC-EP 33% coating had relatively narrow $\tan \delta$ peak compared to the other GC coatings and indicated more homogeneous network compared to the other GC coatings.



(a)



(b)

Figure 5.5. (a) Storage modulus and (b) $\tan \delta$ curves for coatings ABGC, AIGC, AIGC-EP 15%, AIGC-EP 33%, and CN929.

Table 5.7. Properties of the UV cured GC coatings.

Coating	MEK double rubs	Conical mandrel flexibility (cm) (0 cm = best)	Reverse impact (in.lb)	Cross-hatch adhesion (5B = best)	Pendulum hardness (sec)	T _g (°C) (DSC)	Crosslink density (mol/L)	Elongation at break (mm)	Young's modulus (MPa)
ABGC	>400	Fail	<8	Brittle	151	52	4.7	1.2	2450
AIGC	>400	Fail	18	Brittle	121	41	3.8	2.9	2040
AIGC-EP 15%	>400	4 cm	34	Brittle	70	27	3.6	5.0	568
AIGC-EP 33%	360	0 cm	78	0B	30	13	2.7	5.3	103
Control	>400	0 cm	118	0B	35	3	3.3	4.3	106

5.3.5. Thermal stability

Figure 5.6 shows the thermal stability of the UV cured coatings determined by TGA. The onset temperature for the degradation of the coatings was around 255 °C. The control coatings had slightly lower weight loss compared to that of the acrylated GC coatings at 255 °C.

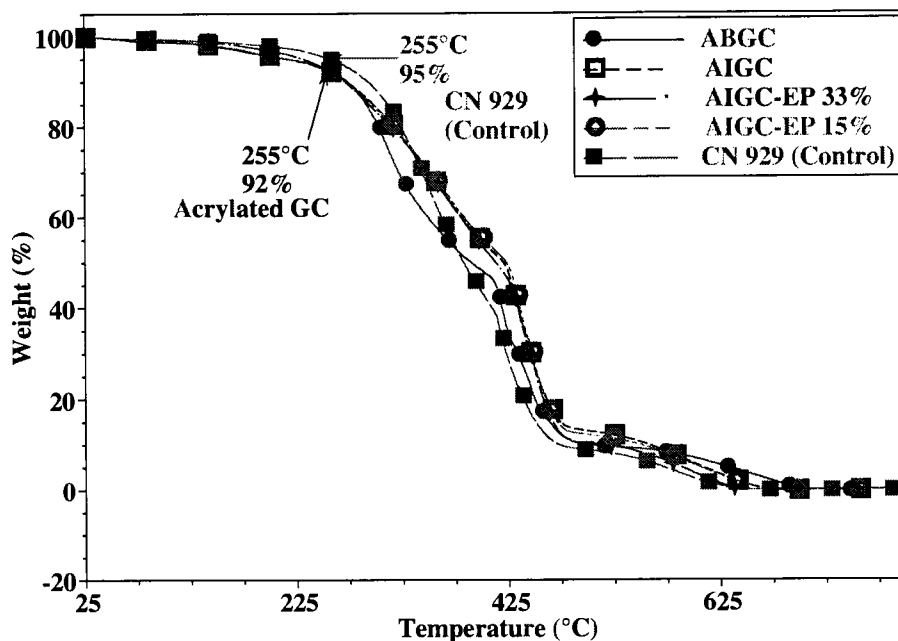


Figure 5.6. TGA of coatings ABGC, AIGC, AIGC-EP 15%, AIGC-EP 33%, and CN929 in nitrogen atmosphere.

5.4. Conclusions

GC resins can be acrylated and can be formulated with common reactive diluents to obtain UV curable GC coatings. The composition of the acrylated GC resins influenced the resin viscosity and the coating properties. Modification of the resins reduced the viscosity. The degree of conversion increased with the increase in the extent of modification. AIGC-EP 33% showed the highest degree of conversion. UV curable GC coating formulations produced tack free films faster (1 pass through the UV lamp

exposure unit) than the control formulation (3 passes). UV cured GC coatings had excellent solvent resistance, good hardness, and high modulus. The flexibility of the coatings increased with alcohol modification.

5.5. References

1. Decker, C, "Kinetic study and new applications of UV radiation curing". *Macromol. Rapid Commun.*, **23** (18) 1067-1093 (2002)
2. Schwalm, R, "Crosslinking effect on mechanical properties of UV curable coatings". *PPCJ, Polym. Paint Colour J.*, **189** (4421) 18-20, 22 (1999)
3. Yagci, Y, Jockusch, S, Turro, NJ, "Photoinitiated Polymerization: Advances, Challenges, and Opportunities". *Macromolecules (Washington, DC, U. S.)*, ACS ASAP (2010)
4. Schwalm, R, *UV Coatings - Basics, Recent Developments and New Applications*. Elsevier Science (2006)
5. Decker, C, "UV-radiation curing chemistry". *Pigm. Resin Technol.*, **30** (5) 278-286 (2001)
6. Decker, C, "Light-induced crosslinking polymerization". *Polym. Int.*, **51** (11) 1141-1150 (2002)
7. Mehnert, R, Pincus, A, Janorsky, I, Stowe, R, Berejka, A, *UV and EB Curing Technology and Equipment*. SITA Technology Ltd., London (1998) Vol. I,
8. Rao, AV, Kanitkar, DS, Parab, AK, "Some specialty coatings from radiation curable poly(acrylic) combinations". *Prog. Org. Coat.*, **25** (3) 221-33 (1995)

9. Chattopadhyay, DK,Panda, SS,Raju, KVSN, "Thermal and mechanical properties of epoxy acrylate/methacrylates UV cured coatings". *Prog. Org. Coat.*, **54** (1) 10-19 (2005)
10. Wicks (Jr), ZW,Jones, FN,Pappas, SP,Wicks, DA, *Organic Coatings: Science and Technology*. 3rd ed., John Wiley and Sons Inc., New Jersey (2007)
11. Crivello, JV,Dietliker, K,Bradley, G, *Photoinitiators for Free Radical, Cationic and Anionic Photopolymerization*. 2nd ed., SITA Technology Ltd., London (1998) Vol. III,
12. Webster, G, *Prepolymers and Reactive Diluents - Chemistry and Technology of UV and EB Formulation for Coatings, Inks and Paints*. SITA Technology Ltd., London (1996) Vol. II,
13. Edwards, PA. Glycidyl carbamate resins to achieve polyurethane properties and epoxide reactivity. Ph.D. Dissertation, North Dakota State University, Fargo, 2004.
14. Edwards, PA,Striemer, G,Webster, DC, "Novel Polyurethane Technology Through Glycidyl Carbamate Chemistry". *J. Coat. Technol. Res.*, **2** (7) 517-527 (2005)
15. Chattopadhyay, DK,Raju, KVSN, "Structural Engineering of Polyurethane Coatings for High Performance Applications". *Prog. Polym. Sci.*, **32** (3) 352-418 (2007)
16. Tarlas, HD, "Amine Cured Epoxy Resin Coatings for Resistance to Atmospheric Corrosion". *Mater. Prot.*, **9** (5) 37-42 (1970)
17. Edwards, PA,Erickson, J,Webster, DC, "Synthesis and Self-crosslinking of Glycidyl Carbamate Functional Oligomers". *Polym. Prepr. (Am. Chem. Soc., Div. Polym. Chem.)*, **44** (1) 54-55 (2003)

18. Edwards, PA, Striemer, G, Webster, DC, "Synthesis, Characterization and Self-crosslinking of Glycidyl Carbamate Functional Resins". *Prog. Org. Coat.*, **57** (2) 128-139 (2006)
19. Chattopadhyay, DK, Muehlberg, AJ, Webster, DC, "Organic-inorganic hybrid coatings prepared from glycidyl carbamate resins and amino-functional silanes". *Prog. Org. Coat.*, **63** (4) 405-415 (2008)
20. Chattopadhyay, DK, Webster, DC, "Hybrid coatings from novel silane-modified glycidyl carbamate resins and amine crosslinkers". *Prog. Org. Coat.*, **66** (1) 73-85 (2009)
21. Chattopadhyay, DK, Zakula, AD, Webster, DC, "Organic-inorganic hybrid coatings prepared from glycidyl carbamate resin, 3-aminopropyl trimethoxy silane and tetraethoxyorthosilicate". *Prog. Org. Coat.*, **64** (2-3) 128-137 (2009)
22. Hill, LW, "Determination of Crosslink Density in Thermoset Coatings". *Polym. Mater. Sci. Eng.*, **77** 387-388 (1997)
23. Skaja, A, Fernando, D, Croll, S, "Mechanical Property Changes and Degradation During Accelerated Weathering of Polyester-Urethane Coatings". *J. Coat. Technol. Res.*, **3** (1) 41-51 (2006)
24. Carrasco, F, Pagès, P, Lacorte, T, Briceño, K, "Fourier Transform IR and Differential Scanning Calorimetry Study of Curing of Trifunctional Amino-epoxy Resin". *J. Appl. Polym. Sci.*, **98** (4) 1524-1535 (2005)
25. Zhou, H, Li, Q, Lee, TY, Guymon, CA, Joensson, ES, Hoyle, CE, "Photopolymerization of Acid Containing Monomers: Real-Time Monitoring of Polymerization Rates". *Macromolecules*, **39** (24) 8269-8273 (2006)

26. Uhl, FM, Davuluri, SP, Wong, S-C, Webster, DC, "Organically modified montmorillonite in UV curable urethane acrylate films". *Polymer*, **45** (18) 6175-6187 (2004)
27. Higginbottom, HP, Bowers, GR, Ferrell, PE, "Cure of Secondary Carbamate Groups by Melamine-Formaldehyde Resins". *J. Coat. Technol.*, **71** (894) 49-60 (1999)
28. Sorathia, UA, Yeager, WL, Dapp, TL, "Interpenetrating Polymer Network Acoustic Damping Material." US Patent 5,225,498, 1993.

CHAPTER 6. AIR DRYING GLYCIDYL CARBAMATE RESIN AND COATINGS

6.1. Introduction

One of the oldest binders for coatings are drying oils such as linseed, tung, soybean, castor, safflower, etc. obtained from renewable sources (plants). Conventional binders used in air-drying coatings are based on alkyd resins (obtained by the polycondensation reaction of polycarboxylic acids, polyhydric alcohols, with oils or unsaturated fatty acids) and are widely used for exterior and interior coatings on wood, metal, and architectures.¹⁻³

Glycidyl carbamate (GC) resins are obtained by the reaction of isocyanate functional compounds with glycidol. GC resins contain urethane (-NHCO-) and epoxy functional groups in their structure.⁴ Polyurethane and epoxy resins are widely used in numerous commercial applications such as coatings, composites, high performance polymers, etc. Urethane coatings offer excellent toughness, adhesion, flexibility and chemical resistance. Epoxy coatings offer excellent corrosion and solvent resistance, adhesion and versatility of crosslinking (curing) mechanisms.^{5,6} The combination of urethane and epoxy functional groups in GC resins imparts an excellent set of properties to GC-based coatings. Reactive epoxy groups in GC resins can be crosslinked using amines and by self crosslinking to produce high performance coating systems.^{4,7-9} The development of GC resin technology carried out has produced promising results. GC resins can also be modified or crosslinked with amine terminated alkoxy silane group to produce organic-inorganic hybrid coatings by a sol-gel mechanism.¹⁰⁻¹² With the realization that GC resins produce coatings with an excellent combination of properties

when crosslinked by amines, self-crosslinking, and by hybrid sol-gel crosslinking, the technology of GC resins and coatings was further explored for air-drying.

In this research work, GC resin was reacted with linseed oil fatty acid (LOFA) to introduce unsaturated fatty acid groups in the resin. Formulations of the LOFA functionalized GC resin (GC-LOFA) were developed to produce air drying coatings. Air drying coatings made from GC-LOFA resin showed good film formation by autoxidation mechanism and exhibited good coating performance.

6.2. Experimental

6.2.1. *Materials*

Hexamethylene diisocyanate biuret, a biuret resin condensate derived from hexamethylene diisocyanate (Desmodur N 3200), was provided by Bayer Material Science AG, has an NCO equivalent weight of 183 g/eq. Glycidol was supplied by Dixie Chemical. Glycidol was stored under refrigeration to minimize the formation of impurities. Dibutyltindilaurate (DBTDL), purchased from Aldrich, was used to catalyze the isocyanate and hydroxyl reactions to form the glycidyl carbamate (GC) resins. Tertiary butyl acetate (TBA) was obtained from Aldrich and was used to make catalyst solution. Linseed oil fatty acid (LOFA), Industrene 120, supplied by PMC Group, Inc., has an acid value of 200 mg KOH/gm. *p*-Toluenesulfonic acid (*p*TSA) purchased from Aldrich was used as a catalyst for transesterification reaction between LOFA and the epoxy group. Several driers were used for autoxidation of GC coatings such as cobalt (12% Cobalt HEX-CEM supplied by OMG), zinc (Nuxtra Zinc 8%, supplied by Dura Chemicals, Inc.), zirconium (18% Zirconium HEX-CEM supplied by OMG), calcium (Duroct Calcium 8%, supplied by Dura Chemicals, Inc.) and manganese (12%

Manganese CEM-ALL, supplied by OMG). Ascinin Anti Skin 0446 was used as anti skinning agent during air drying formulations. TBA, xylene (Aldrich) and toluene (Aldrich) were used as solvents for coating formulations. Tung oil obtained from Aldrich was used in several coating formulations to explore its compatibility with the air drying of GC coatings. Uralkyd resins obtained from Reichhold were used to prepare control coatings. The uralkyd resins were UROTUF F48-M50 and UROTUS F77-M60 based on soybean oil and linseed oil, respectively. All reagents were used as received without any further purification.

6.2.2. Synthesis of air drying GC resin

A 500 ml four neck reaction vessel was used for the synthesis of GC and GC-LOFA resins. The vessel was fitted with a condenser, nitrogen inlet and Model 210 J-KEM temperature controller and mechanical stirrer. A water bath was used for heating and cooling the vessel. The stoichiometric equivalent amount of isocyanates and glycidol based on $-NCO$ and $-OH$ groups used for the synthesis of GC resin was 1:1 (NCO:glycidol).

For the synthesis of the base GC resin, the reaction vessel was charged with Desmodur N 3200 followed by addition of the required amount of glycidol. The reaction mixture was stirred for about 45 – 60 min. at 40 – 45 °C to ensure a homogeneous mixture. The catalyst (DBTDL), in the form of a solution in tertiary butyl acetate (1 – 2 % by wt.), was added after the completion of mixing. The amount of catalyst added was 0.03 % by wt. (of the total reaction charge). After the addition of catalyst around at about 40 – 45 °C, the reaction showed an exotherm, bubble formation, and an increase in viscosity. The reaction was continued until the $-NCO$ peak in FTIR spectrum disappeared

completely. Epoxy equivalent weight of GC resin was determined by titration with hydrogen bromide (HBr) according to ASTM D1652.

GC-LOFA resin was obtained by reacting the GC resin with LOFA. The reaction was carried out in the same four neck reactor assembly used for the synthesis of GC resin.

Figure 6.1 is a schematic representation of the synthesis of GC-LOFA. The required

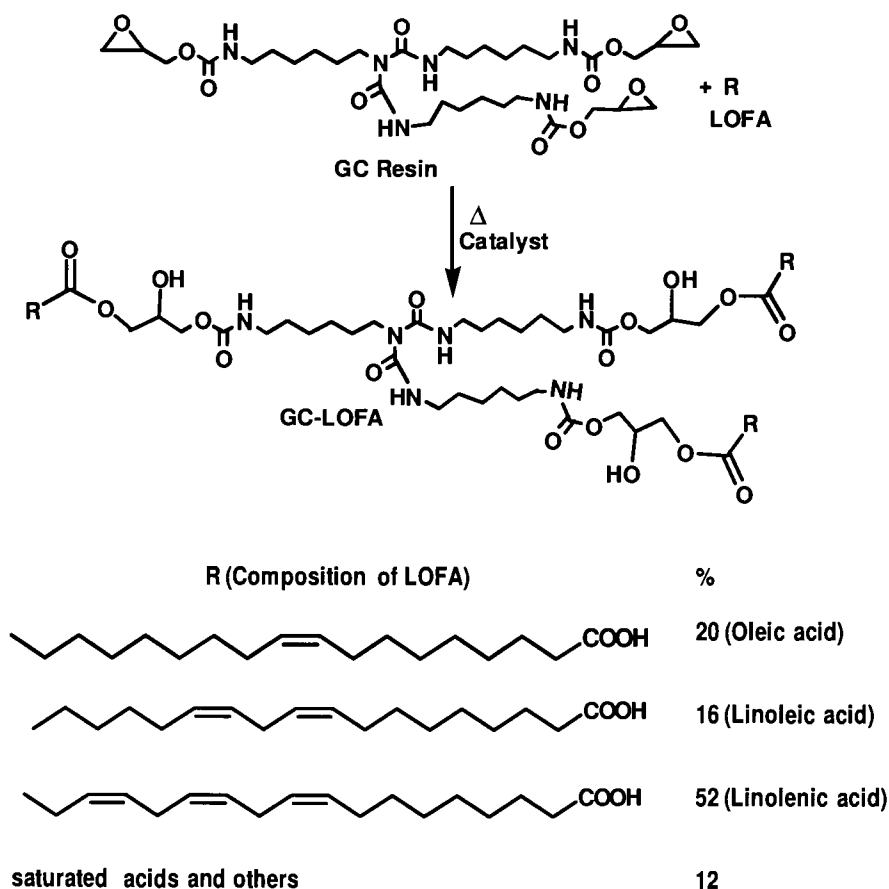


Figure 6.1. Schematic representation of the synthesis of GC-LOFA.

amount of the reactants, GC resin and LOFA (1:0.9 molar ratio), were added to the reactor followed by the addition of solvent mixture consisting of TBA, toluene and xylene (1:1:0.8 wt. ratio). The total amount of the solvent mixture added was 10 % by wt. of the reactants. The reaction mixture was stirred for about 30 min. at 45 – 50 °C to obtain a homogeneous mixture. After completion of mixing, the catalyst (*p*TSA), in the

form of solution in TBA (1 – 2% by wt.) was added to the reactor. The amount of catalyst added was 0.03% by wt. (of the reactants). The reaction was carried out at the temperature between 55 – 65 °C. The reaction progress was monitored by acid value titration. The reaction was continued until acid value reached 4 and became constant. The resin was collected in a glass jar.

6.2.3. FTIR measurements

A Nicolet 8700 FTIR spectrometer from Thermo Scientific was used for FTIR measurements. Sample aliquots were taken and coated on a potassium bromide salt plate. Spectra acquisitions were based on 32 scans with a data spacing of 1.98 cm^{-1} .

6.2.4. Epoxy titration

Epoxy equivalent weight of the resins was determined by titration with hydrogen bromide (HBr) according to ASTM D1652. A required amount of resin (0.06 to 0.8 gm) was dissolved in 5 – 10 ml of chloroform and was titrated against a standardized HBr solution prepared in glacial acetic acid. The indicator used was a solution of crystal violet in glacial acetic acid. End point of the titration was the appearance of permanent yellow-green color.

6.2.5. Acid value titration

Acid value of the resins was determined by titration with 0.1 N KOH solution according to ASTM D 1639. A required amount of resin (0.5 to 1.0 gm) was dissolved in isopropyl alcohol (10 to 15 ml) and titrated against 0.1 N KOH solution using phenolphthalein indicator. End point of the titration was the first persistent faint pink color.

Table 6.1. Recipe for the synthesis of air drying GC resin.

Synthesis of GC resin				Synthesis of air drying GC resin			
GC resin	Desmodur N 3200 (gm)	Glycid ol (gm)	EEW (g/eq)	Air drying GC resin	GC resin (gm)	LOFA (gm)	Final acid value (mg KOH / gm)
BGC	200	81.57	269	BGC-LOFA	100	94.45	4

6.2.6. NMR characterization

^{13}C NMR was done for BGC and modified GC resins using a JEOL-ECA (400 MHz) NMR spectrometer coupled with an auto-sampler accessory. The spectra were run at 24 °C with 1000 scans. The samples were prepared by dissolving 50 to 70 mg samples in 0.7 ml CDCl_3 . The spectra were analyzed using Delta NMR processing and control software (Version 4.3.5).

6.2.7. Air drying coating formulations

Several combinations of driers, solvents, and anti skinning agents were tested to obtain defect (wrinkle) free smooth coatings. The successful formulations were used to make coatings and study their performance. Table 6.2 shows the air drying coating formulations prepared using GC-LOFA and control uralkyd resins. Six formulations were prepared with a combination of driers and reactive diluent (tung oil). The coatings prepared using the GC-LOFA were labeled as F1 to F6 corresponding to the formulations from 1 to 6. The coatings prepared from control uralkyd resins, UROTUF F48-M50 and UROTUS F77-M60, were labeled as M-50-1 to M-50-6 and M-60-1 to M-60-6, respectively corresponding to the formulations 1 to 6.

Table 6.2. Air Drying coating formulations.

Ingredients (% wt.)	Formulation code					
	1	2	3	4	5	6
Resin	62	64	62	59	62	59
Xylene	12	11	12	12	10	12
Toluene	12	11	12	12	10	12
Cobalt 12% HEX-CEM	1	0	0	1	0	0
Nuxtra Zinc 8%	5	5	5	5	5	5
Zirconium 18% HEX-CEM	5	5	5	5	5	5
Duroct Calcium 8%	0	0	0	6	3	6
Manganese 12% CEM-ALL	0	0	1	0	0	1
Tung Oil	0	2	0	0	2	0
Ascini 0446	2	2	2	2	2	2

6.2.8. Study of coating performance

Coatings were made on smooth finished cold rolled steel panels (Q panels, QD 36) at 6 mils wet thickness. All coatings showed dry to touch and through dry within two days. Coatings were aged for 15 days at ambient before studying their properties. The dry film thickness of the coatings was between 30 – 40 μm . König pendulum hardness of the coatings was measured following ASTM D 4366. Pencil hardness test was also carried out according to ASTM D 3363 to determine the hardness of the coatings. The hardness test results are reported in seconds (sec). Reverse impact strength of the coatings was determined following ASTM D 2794 using a Gardener impact tester. The maximum drop height was 43 inches and the drop weight was 4 pounds. Crazeing or loss of adhesion was noted and inch-pounds (in-lbs) were reported at film finish failure. Samples that did not fail at the maximum drop height were noted as having an impact strength of >172 in-lbs. The conical mandrel test was also used according to ASTM D 522 for the determination of flexibility the coatings. The results of flexibility test were reported as the length of a crack (cm) formed on the coating during the test. Methyl ethyl ketone (MEK) double rubs

test was used according to ASTM D 5402 to assess the chemical resistance and development of cure. A 26-ounce hammer with three layers of cheesecloth wrapped around the hammerhead was soaked in MEK. The hammer head was rewet with MEK after 30 – 50 double rubs. Once mar was achieved, a number of double rubs was noted. Cross hatch adhesion of the coatings was evaluated using a Gardco cross hatch adhesion instrument following ASTM D 3359.

6.2.9. Differential scanning calorimetry (DSC)

A TA Instruments Q1000 differential scanning calorimeter (DSC) coupled with an auto sampler accessory was used to determine the glass transition temperature (T_g) of the coatings. DSC experiments were performed by placing a sample into the conventional aluminum pans. The samples were subjected to a heat-cool-heat cycle. The samples were heated to 200 °C and then cooled to -75 °C and held there for 5 min. DSC thermogram were taken from -75 °C to 250 °C at a heating rate of 10 °C min⁻¹. Glass transition temperature was determined as the temperature of the inflection at the mid-point.

6.2.10. Thermogravimetric analysis (TGA)

TGA was performed using a TA Instruments Q500. Temperature was ramped from ambient to 800 °C with a ramp rate of 10 °C min⁻¹. A nitrogen atmosphere was used during the test. Weight retained was plotted as a function of temperature.

6.3. **Results and discussion**

6.3.1. Synthesis of air drying GC resin

Figure 6.2 shows the ¹³C NMR spectra of the GC-LOFA resin. The GC-LOFA resin was synthesized from the reaction of linseed oil fatty acid with GC functional resin.

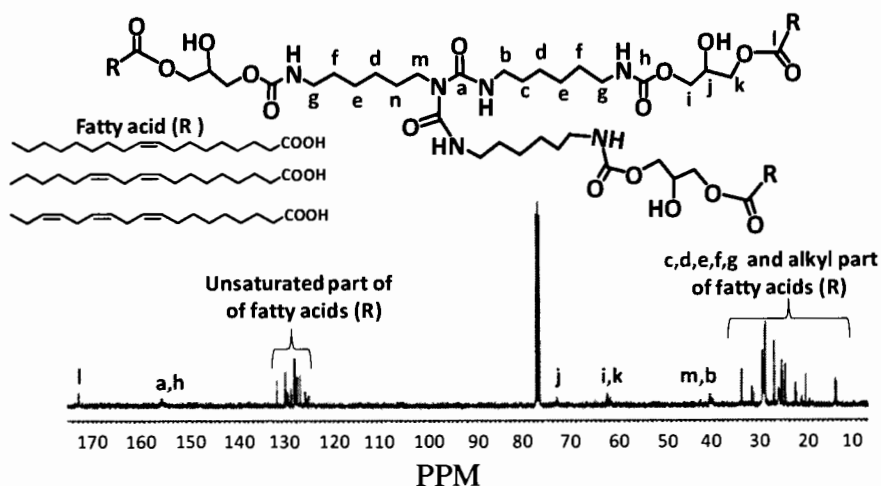


Figure 6.2. ^{13}C NMR spectra of the GC-LOFA resin.

The resin was highly viscous. NMR spectra shows the disappearance of GC epoxy peaks at 45 and 50 ppm while appearance of characteristic fatty acid peaks for carbon in unsaturated part (125 to 135 ppm) and carbon in saturated alkyl part (15 to 35 ppm).

6.3.2. *Performance of the coatings*

The coating formulations were prepared using driers commonly used for alkyd-based coatings. The coatings were kept at ambient for aging before their properties were studied. Table 6.3 shows the coating properties of the GC coatings and control coatings. Air dried GC coatings showed good adhesion and flexibility compared to the control coatings. T_g values of the coatings were between 20 - 22 °C. The T_g values for the selected control coatings were higher than that of the GC coatings. Solvent resistance of the coatings was moderate. Table 6.4 shows the hardness development in the GC coating. Hardness of the coatings was found to increase over a period of time and indicated that the autoxidation process was continuing. Tables 6.5 and 6.6 show the hardness development of the UROTUF F48-M50 coatings and UROTUF F77-M60 coatings, respectively. GC coatings had higher pencil hardness compared to that of UROTUF F48-

M50 coatings. König pendulum hardness of GC coatings was lower than the control coatings.

Table 6.3. Coating properties after two weeks of air drying.

GC Coating	Conical mandrel flexibility (0 cm=Best)	Cross-hatch adhesion (5B=Best)	Reverse impact (in-lb)	MEK double rubs	T _g (°C) by DSC
F1	0	2B	>172	20	20
F2	0	2B	>172	30	22
F3	0	4B	>172	30	20
F4	0	2B	>172	30	22
F5	0	5B	>172	30	21
F6	0	2B	>172	20	22
M-50-1	Fail	0B	18	110	57
M-50-2	Fail	0B	22	140	--
M-50-3	Fail	0B	10	100	53
M-50-4	Fail	0B	14	140	--
M-50-5	Fail	0B	18	150	57
M-50-6	Fail	0B	26	140	--
M-60-1	0	0B	42	170	55
M-60-2	0	0B	58	160	--
M-60-3	1	0B	42	170	52
M-60-4	3	0B	42	170	--
M-60-5	1	0B	46	160	57
M-60-6	3	0B	46	150	--

-- experiment was not performed.

Table 6.4. Hardness development in air drying GC-LOFA coatings.

Weeks	F1		F2		F3		F4		F5		F6	
	P*	K*	P	K	P	K	P	K	P	K	P	K
1	B	20	B	16	B	18	B	15	B	17	B	18
2	B	18	B	16	B	19	B	22	B	20	B	21
3	B	21	B	21	B	21	B	26	B	24	B	25
4	HB	26	HB	21	HB	21	HB	37	HB	21	HB	29
5	HB	22	F	20	HB	20	F	33	F	30	F	27
6	F	28	F	22	F	20	F	32	F	26	F	27
7	F	29	F	25	F	22	F	36	F	31	F	18
8	F	37	F	29	F	26	F	40	F	35	F	30
15	F	72	F	69	F	52	F	79	F	75	F	58

*P=Pencil hardness, and K=König hardness

Table 6.5. Hardness development in air drying UROTUF F48-M50 coatings.

Weeks	M-50-1		M-50-2		M-50-3		M-50-4		M-50-5		M-50-6	
	P*	K*	P	K	P	K	P	K	P	K	P	K
1	6B	95	6B	86	5B	83	5B	136	5B	145	5B	140
2	6B	119	6B	119	5B	100	5B	161	5B	159	5B	153
3	4B	157	4B	138	4B	115	4B	194	2B	190	3B	175
4	3B	181	3B	157	4B	123	3B	190	2B	189	3B	180
5	3B	195	3B	178	4B	137	3B	220	2B	184	3B	172
7	2B	199	2B	171	3B	138	3B	205	B	179	3B	182
8	B	195	2B	195	3B	156	2B	207	B	192	3B	184
11	B	196	2B	190	3B	175	2B	193	B	192	2B	188

*P=Pencil hardness, and K=König hardness

Table 6.6. Hardness development in air drying UROTUF F77-M60 coatings.

Weeks	M-60-1		M-60-2		M-60-3		M-60-4		M-60-5		M-60-6	
	P*	K*	P	K	P	K	P	K	P	K	P	K
1	6B	47	6B	45	4B	47	4B	85	4B	64	4B	84
2	2B	99	2B	98	2B	107	B	152	2B	136	2B	142
3	B	171	B	159	B	141	B	170	B	155	B	171
4	B	172	B	157	B	135	B	180	B	159	B	169
5	HB	187	HB	175	B	153	HB	200	B	170	HB	177
7	H	182	H	164	B	144	2H	183	2H	165	H	165
8	H	194	H	179	B	162	2H	193	2H	171	H	182
10	H	182	H	159	B	145	2H	177	2H	170	H	182

*P=Pencil hardness, and K=König hardness

6.3.3. *Thermal stability*

Thermal stability of the GC coating and selected control coatings was determined using TGA. Figure 6.3 and Figure 6.4 show the results of TGA experiments. The onset temperature for the thermal degradation of the GC coatings and the control coatings was around 230 °C.

6.4. Conclusions

Air drying glycidyl carbamate resin can be synthesized by reacting GC resin with LOFA. GC-LOFA resin can produce air drying coatings using common driers. GC coating formulations containing tung oil and with no cobalt drier had good hardness and

adhesion. The coatings were stable around 230 °C. The increase in hardness values of the coatings over a period of time indicated continuing autoxidation process.

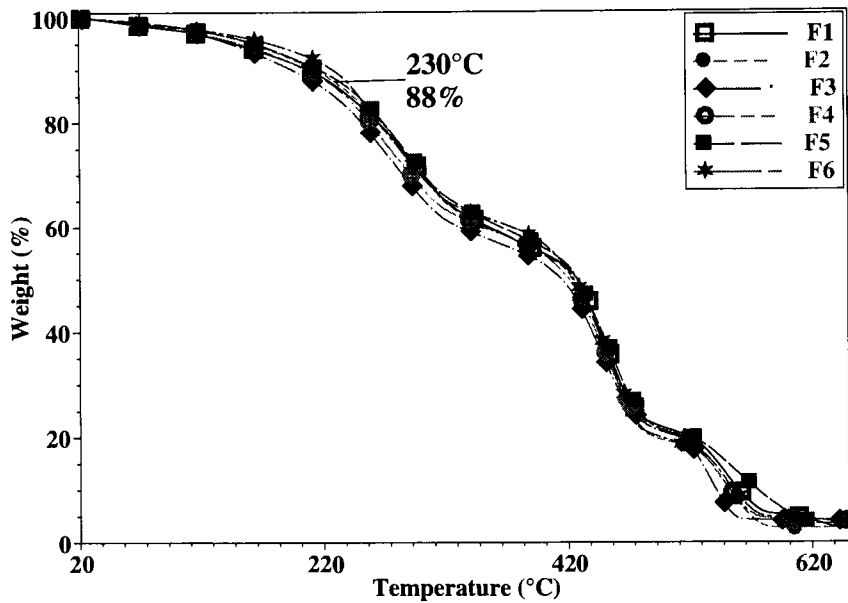


Figure 6.3. TGA of GC-LOFA coatings in nitrogen atmosphere.

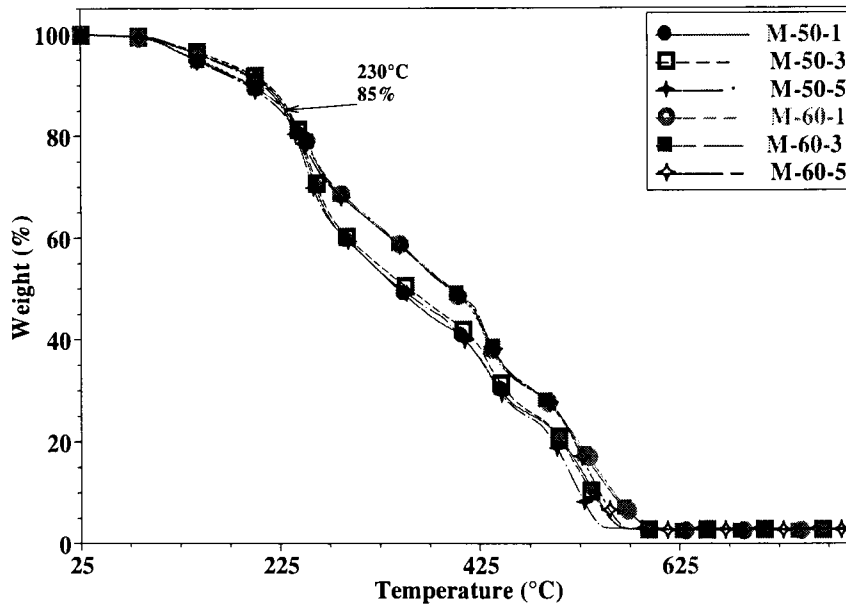


Figure 6.4. TGA of control coatings in nitrogen atmosphere.

6.5. References

1. van, GR, Bouwman, E, "The oxidative drying of alkyd paint catalysed by metal complexes". *Coord. Chem. Rev.*, **249** (17-18) 1709-1728 (2005).

2. van, HJ, Oostveen, EA, Micciche, F, Noordover, BAJ, Koning, CE, van, BRATM, Frissen, AE, Weijnen, JGJ, "Resins and additives for powder coatings and alkyd paints based on renewable resources". *J. Coat. Technol. Res.*, **4** (2) 177-186 (2007).
3. Wicks (Jr), ZW, Jones, FN, Pappas, SP, Wicks, DA, *Organic Coatings: Science and Technology*. 3rd ed., John Wiley and Sons Inc., New Jersey (2007).
4. Edwards, PA, Striemer, G, Webster, DC, "Novel Polyurethane Technology Through Glycidyl Carbamate Chemistry". *J. Coat. Technol. Res.*, **2** (7) 517-527 (2005).
5. Chattopadhyay, DK, Raju, KVSAN, "Structural Engineering of Polyurethane Coatings for High Performance Applications". *Prog. Polym. Sci.*, **32** (3) 352-418 (2007).
6. May, CA, *Epoxy Resins - Chemistry and Technology*. 2nd ed., Marcel Dekker, Inc., New York (1988).
7. Edwards, PA. Glycidyl carbamate resins to achieve polyurethane properties and epoxide reactivity. Ph.D. Dissertation, North Dakota State University, Fargo, 2004.
8. Edwards, PA, Erickson, J, Webster, DC, "Synthesis and Self-crosslinking of Glycidyl Carbamate Functional Oligomers". *Polym. Prepr. (Am. Chem. Soc., Div. Polym. Chem.)*, **44** (1) 54-55 (2003).
9. Edwards, PA, Striemer, G, Webster, DC, "Synthesis, Characterization and Self-crosslinking of Glycidyl Carbamate Functional Resins". *Prog. Org. Coat.*, **57** (2) 128-139 (2006).
10. Chattopadhyay, DK, Muehlberg, AJ, Webster, DC, "Organic-inorganic hybrid coatings prepared from glycidyl carbamate resins and amino-functional silanes". *Prog. Org. Coat.*, **63** (4) 405-415 (2008).

11. Chattopadhyay, DK, Webster, DC, "Hybrid coatings from novel silane-modified glycidyl carbamate resins and amine crosslinkers". *Prog. Org. Coat.*, **66** (1) 73-85 (2009).
12. Chattopadhyay, DK, Zakula, AD, Webster, DC, "Organic-inorganic hybrid coatings prepared from glycidyl carbamate resin, 3-aminopropyl trimethoxy silane and tetraethoxyorthosilicate". *Prog. Org. Coat.*, **64** (2-3) 128-137 (2009).

OVERALL CONCLUSIONS

A variation in the composition of GC resins was found to be a viable technique to alter the properties of the GC resins and the GC coatings. Extremely high viscosity of polyisocyanate based GC resins was reduced dramatically -up to 90 %- by modification of the resins with alcohol. The type of alcohol and extent of alcohol used to replace a portion of the glycidol influenced the resin and coating properties. DB was found to be the most effective in viscosity reduction. Viscosity of the GC resin decreased with increase in the extent of modification and was found to level off after 33 % mol of modification. The modification of the resin at only 15 % mol by EP reduced the resin viscosity significantly. The reactive epoxy functional groups in the resins decreased with the alcohol modification. With a higher extent of modification, the crosslink density, T_g , and hardness were lowered while the flexibility and $\tan \delta$ broadening increased. PACM crosslinked coatings had higher T_g , lower elongation at break, and higher modulus compared to the A-2353 crosslinked coatings. The modification with non-polar hydrophobic alcohol such as 2EHA resulted in coatings with the highest impedance and the lowest capacitance values while the modification with hydrophilic DB resulted in coatings with the lowest impedance and the highest capacitance values. BGC coatings show lower impedance and higher capacitance than that of BGC-2EHA, BGC-EP 15%, and BGC-EP 33% coatings.

GC resins based on linear diisocyanates and diols show a good combination of properties such as high flexibility, high solvent resistance, good barrier properties, and corrosion resistance. The composition of diisocyanate and diols in the resin composition influenced the coating properties. The coatings based on the GC resin composed of HDI,

BEPD, and NPG had the highest elongation at break while the coatings based on the GC resin composed of H₁₂MDI and BEPD had the lowest elongation at break. The coatings based on GC resin composed of H₁₂MDI and BEPD had showed capacitance behavior with the highest impedance and the lowest capacitance values. This trend indicated that the H₁₂MDI based coatings had higher protective properties and less interaction with water compared to the other coatings. This effect can be correlated to the higher amount of non-polar hydrophobic groups in H₁₂MDI based coatings than that in the other coatings. Flexibility of the TMDI and BEPD based coatings was improved by the incorporation of NPG and DG in the resin compositions however, solvent resistance decreased with the incorporation of NPG and DG.

Glycidyl carbamate resins can be made water dispersible by incorporating non-ionic hydrophilic groups such as mPEG into the resin structures. Chain length and % mol incorporation of mPEG in GC resins influenced the water dispersibility. All of the GC resins except R1 (containing 5 % by mol mPEG350) and R10 (control) were able to be dispersed in water without organic cosolvents or surfactants. The coatings crosslinked with Anquamine 731 were transparent and had smooth and glossy surfaces. Coatings based on GC resins R1, R2 (containing 5 % by mol mPEG550), R4 (containing 10 % by mol mPEG 350), and R10, showed good water and solvent resistance in water drop, water double rubs, and MEK double rubs tests. The coatings had good impact strength, flexibility, adhesion, hardness, modulus, and low elongation at break. In EIS testing coatings based on resins R1, R2, R4, and R10 had capacitive behavior in high frequency region, resistive behavior in mid-frequency region, and capacitive behavior in low frequency region and indicated the interaction of the coatings with water. Salt spray tests

showed the influence of substrate pretreatment on adhesion and corrosion performance. Waterborne coatings on untreated steel panels delaminated within 24 hrs of salt spray exposure while the coatings on the treated aluminum panels remained adhered to the panels during 240 hrs of salt spray testing.

GC resins can be acrylated and can be formulated with common reactive diluents to obtain UV curable GC coatings. The composition of the acrylated GC resins influenced the resin viscosity and the coating properties. The alcohol modification of the acrylated GC resins reduced the resin viscosity. The degree of conversion of acrylate double bonds during UV curing increased with the increase in the extent of modification. AIGC-EP 33% showed the highest degree of conversion. Acrylated IGC resin had a higher degree of conversion than acrylated BGC. UV curable GC coating formulations produced tack free films faster (1 pass through the UV lamp exposure unit) than the control formulation (3 passes). UV cured GC coatings had excellent solvent resistance, good hardness, and high modulus. The flexibility of the coatings increased with alcohol modification.

Air drying GC resins can be synthesized by reacting BGC resin with LOFA. BGC-LOFA resins can result in air drying coatings using common driers. Air drying coating formulations containing tung oil and with no cobalt drier had good hardness and adhesion. The increase in hardness values of the coatings over a period of time indicated continuing autoxidation process.

FUTURE WORK

GC resins based on HDI polyisocyanate resins (HDI biuret and HDI isocyanurate) have very high viscosity. Modification of BGC with alcohol reduced the viscosity dramatically. It was observed that the modification by 15 % mol, reduced the resin viscosity significantly. The reactive epoxy groups in the resins and crosslink density of the coatings also reduce with the modification. Optimum crosslink density is desired to attain the balance of properties such as T_g , hardness, flexibility, solvent resistance, and barrier properties. The starting HDI polyisocyanate used for the synthesis of GC resins contain trimer, pentamer, heptamer, and higher molecular weight oligomers. The starting NCO functionality can be varied by selecting the HDI polyisocyanate resin with different composition of oligomer compositions. Thus the reactive epoxy groups in resulting GC resin can also be varied. The composition of the modified GC resins based on different grades of HDI polyisocyanate resins can be expected have low viscosity and increased reactive epoxy functional groups.

GC resins for flexible primer application were obtained using diisocyanates such as HDI, H_{12} MDI, and TMDI diisocyanates and combinations of diols and triol. HDI based GC coatings had higher flexibility than the other diisocyanate based coatings. However, H_{12} MDI based coatings had the highest barrier properties compared to the other coatings. The balance of the flexibility and barrier properties of the coatings can be expected to obtain using a GC resin having a composition of two diisocyanates (HDI and H_{12} MDI). The composition of diols (BEPD and NPG) that resulted in good flexibility and solvent resistance can be used to obtain such GC resins.

Waterborne GC coatings were found to have low barrier properties. It was observed in this research that lower the polar hydrophilic groups in the resins and in the coatings higher was the barrier properties of the coatings. In waterborne coatings, a hydrophilic water-based amine crosslinker (Anquamine 731) was used which could contribute to the hydrophilicity of the coatings. The other water-based crosslinker such as Anquawhite 100 and Anquamine 721 can be explored to determine their influence of hydrophilicity of the coatings. Another way to reduce hydrophilic groups in the waterborne GC coatings would be to design a GC resin containing both hydrophobic as well as hydrophilic groups. For instance, a GC resin containing 2EHA and mPEG350 or mPEG550 may give balanced properties such as good dispersibility of resin and low hydrophilicity and high barrier properties of coating.

Structure, functionality, and extent of reactive diluents and photoinitiators used in UV curable coatings govern the degree of conversion, speed of cure, extent of crosslinking, and final performance of UV cured coatings. An experiment using a statistical experimental design approach can be used to determine the influence of reactive diluents and photoinitiators on the performance of the UV cured GC coatings.